DISCLAIMER

This report was prepared as an account of work sponsored by an agency of the United States Government. Neither the United States Government nor any agency thereof, nor any of their employees, makes any warranty, express or implied, or assumes any legal liability or responsibility for the accuracy, completeness, or usefulness of any information, apparatus, product, or process disclosed, or represents that its use would not infringe privately owned rights. Reference herein to any specific commercial product, process, or service by trade name, trademark, manufacturer, or otherwise does not necessarily constitute or imply its endorsement, recommendation, or favoring by the United States Government or any agency thereof. The views and opinions of authors expressed herein do not necessarily state or reflect those of the United States Government or any agency thereof.

DOE/ET/26225-1
GA-A16713
UC-94d

THERMOCHEMICAL WATER-SPLITTING CYCLE, BENCH-SCALE INVESTIGATIONS, AND PROCESS ENGINEERING

FINAL REPORT FOR THE PERIOD FEBRUARY 1977 THROUGH DECEMBER 31, 1981

by
J. H. NORMAN, G. E. BESENBRUCH, L. C. BROWN,
D. R. O'KEEFE, and C. L. ALLEN

General Atomic Company
P.O. Box 81608
San Diego, California 92138

DOE/ET/26225--1

DE86 001139

Prepared for the
U. S. Department of Energy
Assistant Secretary, Conservation & Renewable Energy
Office of Energy Systems Research
under Contract DE-AC02-80ET26225

GENERAL ATOMIC PROJECT 3332
DATE PUBLISHED: MAY 1982

GENERAL ATOMIC COMPANY

DISTRIBUTION OF THIS DOCUMENT IS UNLIMITED

DISCLAIMER

This report was prepared as an account of work sponsored by an agency of the United States Government. Neither the United States Government nor any agency Thereof, nor any of their employees, makes any warranty, express or implied, or assumes any legal liability or responsibility for the accuracy, completeness, or usefulness of any information, apparatus, product, or process disclosed, or represents that its use would not infringe privately owned rights. Reference herein to any specific commercial product, process, or service by trade name, trademark, manufacturer, or otherwise does not necessarily constitute or imply its endorsement, recommendation, or favoring by the United States Government or any agency thereof. The views and opinions of authors expressed herein do not necessarily state or reflect those of the United States Government or any agency thereof.

DISCLAIMER

Portions of this document may be illegible in electronic image products. Images are produced from the best available original document.

CONTENTS

FIGURES

FIGURES

FIGURES

TABLES

TABLES

EXECUTIVE SUMMARY

BACKGROUND

THE HYDROGEN ECONOMY

The fossil energy reserves of the world are limited and will be severely depleted in the next few hundred years. This depletion period will be characterized by increasing production costs and shortages. These events portend a grave danger to our society since fossil fuels constitute the backbone of our energy supply. Energy supplies, however, are not truly limited as our present usage might imply. Nuclear fission fuels, solar energy, and fusion fuels have the potential to fully replace fossil fuels at a considerably higher energy utilization level for a time period consistent with the life of our planet. Thus, energy shortages do not constitute an insoluble problem.

In spite of this favorable finding, energy carriers will undergo a considerable transition, particularly in the chemical fuel sector, which at present produces the lion's share of the energy we use. Probably electrification will increase. That is, battery-operated vehicles will become much more prevalent, house heating and cooling will tend toward electrical, etc. However, the demand for chemical fuels will remain. Electrifying the transportation sector appears to be limited. Aircraft and ships need fuel that will be difficult to supply through batteries or high-tension lines. Automobiles will probably continue to use a chemical fuel.

As shortages in petroleum products increase, a shift to a more basic chemical fuel is expected to occur. This more basic fuel appears to be hydrogen. Since it does not occur in quantity in a free state on the earth, it will have to be manufactured. The only logical long-range source of hydrogen is water. To release hydrogen from water requires energy. Thus, hydrogen, like

electricity, is manufactured from other prime energy sources, such as thermal energy, electrolytic energy, or photoenergy.

HYDROGEN FROM THERMAL ENERGY

The production of hydrogen from thermal energy supplied by nuclear or solar sources appears to be the most practical applicable technique with our present-day knowledge and ability. This can be done in a number of ways. The simplest technical concept to most of us is the application of electricity generated from thermal energies in an electrolysis process to decompose H_2O into H_2 and O_2. This, however, is not the only way; moreover, it is not necessarily the most economical way.

During the last two decades, a method of applying high-temperature process heat directly in certain chemical processing schemes has been recognized and studied. This is the beginning of the determination of the most economical method of producing hydrogen. These methods are categorized as thermochemical water-splitting techniques. The currently favored chemical cycles utilize process heat at up to ~1200°C in forcing endothermic chemical reactions to occur. A classical example of this type of reaction is the decomposition of H_2SO_4 into H_2O, SO_2, and O_2. This particular reaction is utilized by all three of the major thermochemical H_2 cycles undergoing engineering development at this time.

WATER SPLITTING AT GENERAL ATOMIC

The sulfur-iodine water-splitting cycle is characterized by the following three reactions:

$$2H_2O + SO_2 + I_2 \rightarrow H_2SO_4 + 2HI$$
$$H_2SO_4 \rightarrow H_2O + SO_2 + 1/2\ O_2$$
$$2HI \rightarrow H_2 + I_2.$$

This cycle was developed at General Atomic after several critical features in the above reactions were discovered. These involved phase separations, catalytic reactions, etc. At a point when these reactions were reasonably well characterized in the laboratory, estimates of the energy efficiency of this economically reasonable advanced state-of-the-art processing unit produced sufficiently high values (to ~47%) to warrant cycle development effort by DOE along with GA and its sponsors, at that time the American Gas Association and the Gas Research Institute. The DOE contract was largely directed toward the engineering development of this cycle, including a small demonstration unit (CLCD), a bench-scale unit, engineering design, and costing. Some laboratory development of the cycle has also been done as part of this contract. This effort since 1977 is presented in the body of this report. The work has resulted in a design that is projected to produce H_2 at prices not yet generally competitive with fossil-fuel-produced H_2 but are projected to be favorably competitive with respect to H_2 from fossil fuels in the future. Also, large thermochemical plants project to be competitive with electrolytic processes because of favorable plant size scaling relationships. Thus, while H_2-producing technologies have not been developed to their ultimate capabilities, present projections are quite favorable for water splitting, and in particular the GA sulfur-iodine cycle as discussed by Ekman (Ref. I). At present the cycle is being developed for high-temperature heat sources such as the HTGR, solar power tower technology, and the LLNL Tandem Mirror Fusion Reactor.

OVERVIEW OF THE HYDROGEN PRODUCTION PROCESSES

Fossil Sources of Hydrogen

The major source of H_2 at present is natural gas reforming. An anticipated major future supply is coal gasification. As long as these fossil supplies are inexpensive and by-product gas (principally CO_2) formation is acceptable, hydrogen will most

economically be produced from fossil sources. This situation, however, is clearly limited because of the very nature of fossil energy. The rate of usage is of the order of millions of years of deposited fossil fuel per year. This can be possible mathematically for only a few centuries at best, and a cost crossover will occur long before fossil fuels are exhausted.

ELECTROLYTIC PROCESSES FOR HYDROGEN PRODUCTION

There are a number of electrolytic processes for producing H_2 from H_2O. These take some form of aqueous electrolysis (usually from an alkaline solution), special electrolytes such as GE's solid polymer electrolyte, and high-temperature electrolysis usually employing a doped ZrO_2 electrolyte. These processes are subjects of development efforts with the goal of establishing their costs. All of these processes depend on generated electricity to a greater or lesser extent (e.g., high-temperature electrolysis uses less electricity and more process heat) and thus are subject to the generation costs. Electrical generation at present is less than 40% efficient and more often nearer 30%. It is not expected that electrolytic processes will approach 100% efficiency (120% is possible); thus, a considerable efficiency gap exists in which a more efficient process may be developed. The gap may be closed in two ways: by more efficient (1) electricity generation and (2) electrolysis. However, the cost of the generated hydrogen is the real factor which should be minimized in any production scheme and not the efficiency of the process. It is unlikely that electricity generation costs have truly been minimized, and efforts to minimize such generation are still warranted. Process heat, however, being the precursor to electrical energy, is expected to be a less expensive form of energy.

Alkaline electrolysis is a seasoned, well-established form of H_2 production. Nevertheless, it has not been optimized for a hydrogen economy. Techniques to increase current densities

(rates) are very important. A portion of this increase will come by operating at higher temperatures (and pressures). Materials problems (cell construction, electrodes, membranes) are paramount in developing this technology.

Solid polymer electrolyte electrolysis is being developed by General Electric. The electrolyte (Nafion) is very expensive. The Nafion membrane serves as the separator membrane and the electrolyte. Catalytic electrodes contact the electrolyte. Water is supplied to the electrolyte while H_2 and O_2 are ducted out. The cell is operated up to 150°C. GE is attempting to scale up the concept as a method of reducing the cost of H_2 produced.

High-temperature electrolysis is closely related to high-temperature fuel cells. In the electrolysis case H_2O is fed in and H_2 and O_2 are the products of electrolysis, while the opposite is true for an H_2-O_2 fuel cell. High temperatures reduce the electrical energy required due to decreasing free energy requirements for decomposing water and reduce the oxide ion transfer resistance in the ZrO_2 electrolyte. The problems here are the same as those of the fuel cell--cost and reliability of the ZrO_2 membranes. The system is simple and, if sufficient flux of products can be achieved at reasonable capital and maintenance costs, the concept could be economically viable.

Photoelectrochemical water splitting is an emerging technology. Potentials are generated by the interaction of light on high-band gap semiconductors. While current densities are not apt to be high, the major problem still remains the cost of the required device surface area to collect the solar energy.

HYBRID THERMOCHEMICAL WATER-SPLITTING PROCESSES

The hybrid thermochemical sulfur cycle at Westinghouse combines H_2SO_4 decomposition with the electrolysis of SO_2-H_2O mix-

tures. The potentials required by this electrolysis are greatly reduced from those of conventional electrolysis. However, achieving comparable current densities with H_2O electrolysis is a distant goal. This means that the electrolysis capital cost is high but the power requirement is low. The system also requires considerable high-quality process heat to decompose the H_2SO_4.

The hybrid bromine-sulfur cycle of the Commission of European Communities JRC Ispra Establishment avoids to a degree the major portion of the current density problem with electrolyzing SO_2 by electrolyzing the product of a $Br\text{-}SO_2\text{-}H_2O$ reaction--that is, HBr. Electrode kinetics are generally better for this electrolysis. It is also true that the theoretical potential is somewhat higher. The reaction between Br_2, SO_2, and H_2O can produce quite concentrated reactants, which means that less process heat is required to decompose the H_2SO_4, while the HBr is produced at a very high activity. The process has the same comparative requirements as the sulfur cycle with respect to direct water electrolysis in having a higher capital cost than the direct electrolysis and having to make this up by lower energy costs.

PURE THERMOCHEMICAL WATER-SPLITTING PROCESSES

While the same capital versus energy arguments appear to be in order for a pure thermochemical cycle such as the GA sulfur-iodine cycle, the comparison is far less obvious. This is because electrolytic cells do not scale favorably with the size of the hydrogen-producing system after a very nominal size. Electrode surface areas cannot be made cheaper as they are made larger than this nominal size. Unit repetition is the only technique for increasing capacity. On the other hand, the production of chemical reactor vessels is dependent upon the volume of the reactor. Costs of reactor volumes scale quite favorably up to very large sizes. Thus, a more complicated pure thermochemi-

cal cycle has the possibility in large sizes of overcoming capital cost advantages of the simpler electrolytic processes in small systems. Thus, pure thermochemical water-splitting cycles have distinct properties that set them apart from other processes, and a much deeper analysis is required before a judgement on economic competition can be made.

THE SULFUR-IODINE CYCLE

The sulfur-iodine cycle, developed at GA, is a fully thermochemical water-splitting cycle which utilizes process heat at qualities consistent with the temperatures readily deliverable by HTGRs, some fusion reactors, and solar CRTs. It uses the high temperatures from these sources to decompose H_2SO_4. Lower temperatures are used to process moderately concentrated H_2SO_4 solutions (57%) to azeotropic H_2SO_4 (98%) and to process H_2O-HI-I_2 solutions and decompose HI to H_2 and I_2. In the course of processing these solutions, energy is required to separate H_2O and HI. This is done, at present, using a concentrated H_3PO_4. Other processing schemes are being developed that may require less energy and less capital equipment. The remaining subprocess is the formation of the H_2SO_4 and HI-H_2O-I_2 solutions. This is done in an exothermic reaction at ~120°C, and the considerable heat must be removed from the products of reaction and utilized as economically feasible. The processing scheme for this cycle where the reactants and products are fluids only is shown in Fig. I-1.

The cycle has been under development during the last decade and has shown considerable promise of being economical. A major portion of the needed technical data has been derived from this effort. The cycle has been bench-tested in a small unit designed for the production of 1 liter of H_2 per minute. Although the unit was operated in a series of unit operations, it has not been operated as a single unit.

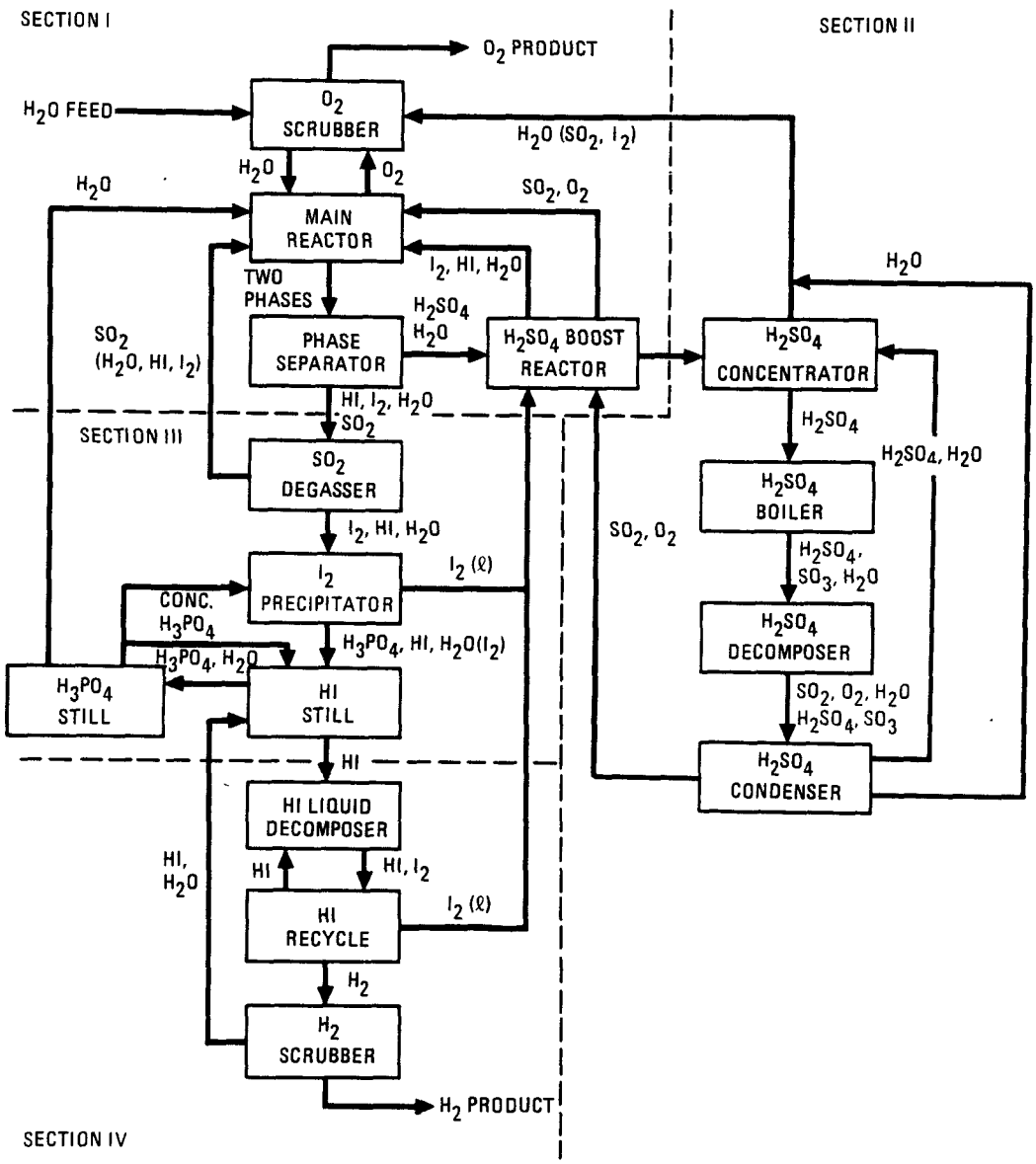

Fig. I-1. Flow diagram for the sulfur-iodine cycle

Another effort has involved the estimation of efficiency of the cycle and cost of the hydrogen produced in a major production facility. Design efforts have involved coupling the cycle to both fusion and solar heat sources. In these cases the cycle promises to produce hydrogen at future prices that are attractive. The cost estimates for a 3000-MW fusion reactor are about 11$/MBtu H_2.

The goals of the development work on the sulfur-iodine cycle are to bring this concept to a stage where it can be compared with other hydrogen-producing technologies so that engineering economics can be used to determine whether it deserves to be developed as the sole method or one of the methods of choice for the hydrogen economy. During the present efforts, much shorter goals must be pursued. These are:

1. Uncover and develop the technical features of the cycle in a scientific sense.
2. Develop engineering evaluations of the performance of the cycle.
3. Uncover the weaknesses of the cycle to determine if any one of these is so limiting as to disqualify the cycle as a future production scheme.

The work at GA has continually strived toward these goals.

PROCESS DESCRIPTION

The overall process for the sulfur-iodine cycle has been divided into five sections to facilitate the flowsheeting effort. Four of the sections pertain to the chemical process, and the fifth describes the heat and energy transport systems. Insofar as practical, the four process sections are designed as independent units with a minimum of energy and process flow interconnections. A generalized flow diagram for the process is presented in Fig. I-1.

Section I contains all equipment associated with the prime chemical reaction, which produces the two separate acid phases from water, sulfur dioxide, and liquid iodine. since the sulfur dioxide occurs initially as a mixture with oxygen, or in the solar flowsheet with nitrogen, Section I also contains facilities for cleaning the diluent gas prior to disposal. The chemical reaction of Section I is exothermic, so no heat input is required. Significant heat transfer is involved in removing the excess heat of reaction to the waste heat recovery system.

The most recent Section I flowsheet was produced in 1981. This design was based upon minimizing the hydrogen production cost rather than maximizing process efficiency, which had been the goal in previous design efforts. The design is characterized by standard chemical engineering unit operations such as packed columns for mass transfer operations and shell and tube heat exchangers for the heat transfer operations. Temperatures in this section are low enough that fluorocarbon-lined mild steel may be used for all vessels. The only unusual material requirement is the specification of niobium for the tubes of the exchanger which removes the exothermic heat of reaction.

Section II encompasses all the equipment required to concentrate, vaporize, and decompose the sulfuric acid product from Section I. Included are considerable heat transfer facilities for reuse of the waste heat from the high-temperature processes at lower temperatures. Since the sulfuric acid decomposition process requires a great deal of thermal energy at the highest temperatures encountered in the process, Section II must be tailored to the specific heat availability curve of each proposed heat source.

The latest Section II developed under this project was issued in 1979. This Section II was matched to an HTGR heat source. Since that time, Section II designs have been produced

for solar heat sources and fusion heat sources under separate funding. The 1979 flowsheet was developed during the time when maximization of thermal efficiency was the guiding rule for water-splitting process development. The multistage flash evaporation with multiply interconnected vaporizers and condensers for each stage and vapor recompression heat reuse of the 1979 flowsheet has been replaced with a simpler, albeit less efficient, evaporation scheme in the latest Section II design (Ref. II) produced by Lawrence Livermore National Laboratory as part of a joint GA-LLNL design of a fusion-powered water-splitting plant.

In Section III, pure liquid HI is produced from the I_2-H_2O-HI reaction product of the prime reaction. The I_2 is first separated from H_2O-HI; then the HI is separated from the water. Conceptually, the latter separation is the more difficult since HI and water form an azeotrope and thus they cannot be separated by distillation. Both of these separations are accomplished by the same agent, i.e., H_3PO_4. The phosphoric acid acts both to extract the HI and water from the iodine phase and to complex the water so that the HI can be distilled away from the H_3PO_4-H_2O solution.

The most energy and capital intensive part of Section III is the separation of the H_3PO_4-H_2O solution. This is accomplished in the very efficient though capital intensive method of multistage flash evaporation with vapor recompression.

The latest version of Section III was produced in 1981. This version was both more efficient and less expensive than the previous version. The major difference was that the HI distillation was accomplished at a pressure high enough to produce liquid rather than gaseous HI. Production of liquid HI lowered the maximum required H_3PO_4 concentration from 100% to 96%, thus eliminating one stage of evaporation and vapor recompression.

The final process step occurs in Section IV where the liquid HI is decomposed and the H_2 product is separated from the reaction medium. The 1981 design is a minor upgrading of the 1979 version. A slight efficiency improvement occurred through a refinement of the previous design, but the major change was specification of a method of removing impurity H_2S from the hydrogen plant, which had not been defined in the previous flowsheet.

Since Section V specifies the interconnection between the process and the heat source, it must be tailored specifically to each heat source. Section V was specified for an HTGR heat source in 1979. Since that time, new Section Vs have been specified for solar and fusion heat sources under separate funding. Section V designs also provide for the generation of any electricity or shaft power required for process pumps or compressors. Insofar as possible, this is obtained via waste heat reuse in power bottoming cycles.

PROCESS COST AND ECONOMICS

Based on the solar adaptation of the latest flowsheet, a 500-MWt GA sulfur-iodine water-splitting plant was designed to the extent that preliminary cost estimates could be made. At this level of design, the size and materials of construction are specified for the major pieces of process equipment. Standard costing techniques can then be used to estimate the installed capital cost and the yearly operating cost.

As specified in this report, capital charges were included for the complete chemical plant and for the solar energy transport and conversion facilities. The mirror field and power tower structures were not designed. The cost of the solar facilities was included in the cost estimate as an operating cost. It is assumed that in time solar energy will become competitive with nuclear energy. Thus, a cost typical of a process heat HTGR, $2.50/GW, was used as the basic solar energy cost.

Estimating the basic capital and operating costs is reasonably straightforward, but converting these numbers into a final hydrogen cost requires financing assumptions. Constant dollar (July 1980) public utility financing was assumed. Public utility financing assumes that the total capital is financed by debt. This gives a higher production cost than if equity financing were involved but a lower sales price since no provision is made for profit. Constant dollar financing eliminates the vagaries of inflation and in essence gives the cost that would be characteristic if the plant were already in operation. In the analysis, a July 1980 dollar was assumed as a basis, and a 5% real cost of money superimposed upon the unspecified variable inflation rate was further assumed.

Under the stated assumptions, the cost of hydrogen from a solar-powered, 500-MWt GA sulfur-iodine water-splitting plant is conservatively estimated to be 17.96 to 21.58 $/GJ. Under sponsorship of the Office of Fusion Energy, using the same assumptions, the cost of hydrogen from a fusion-powered 3000-MWt GA sulfur-iodine water-splitting plant was found to be 10.32 to 11.53 $/GJ (Ref. II). These hydrogen costs may be compared with the predictions of Karl Ekman of JPL (Ref. I) for the projected cost of hydrogen from various sources versus time. Figure I-2 shows Ekman's predictions together with the GA cost estimates. To facilitate the comparison, Ekman's costs have been rescaled to reflect a change in the base dollar from 1979 to July 1980 (15%) and the energy unit converted from MBtu to GJ.

It should be noted that, because future improvements reducing the cost of solar heat were assumed, the exact placement in time of the solar cost estimate is not possible since it will occur only when this cost reduction has been accomplished.

Thermochemical water-splitting is capital intensive and so are the candidate heat sources: solar, fusion, and HTGR. The resultant cost of hydrogen is thus sensitive to the capital cost

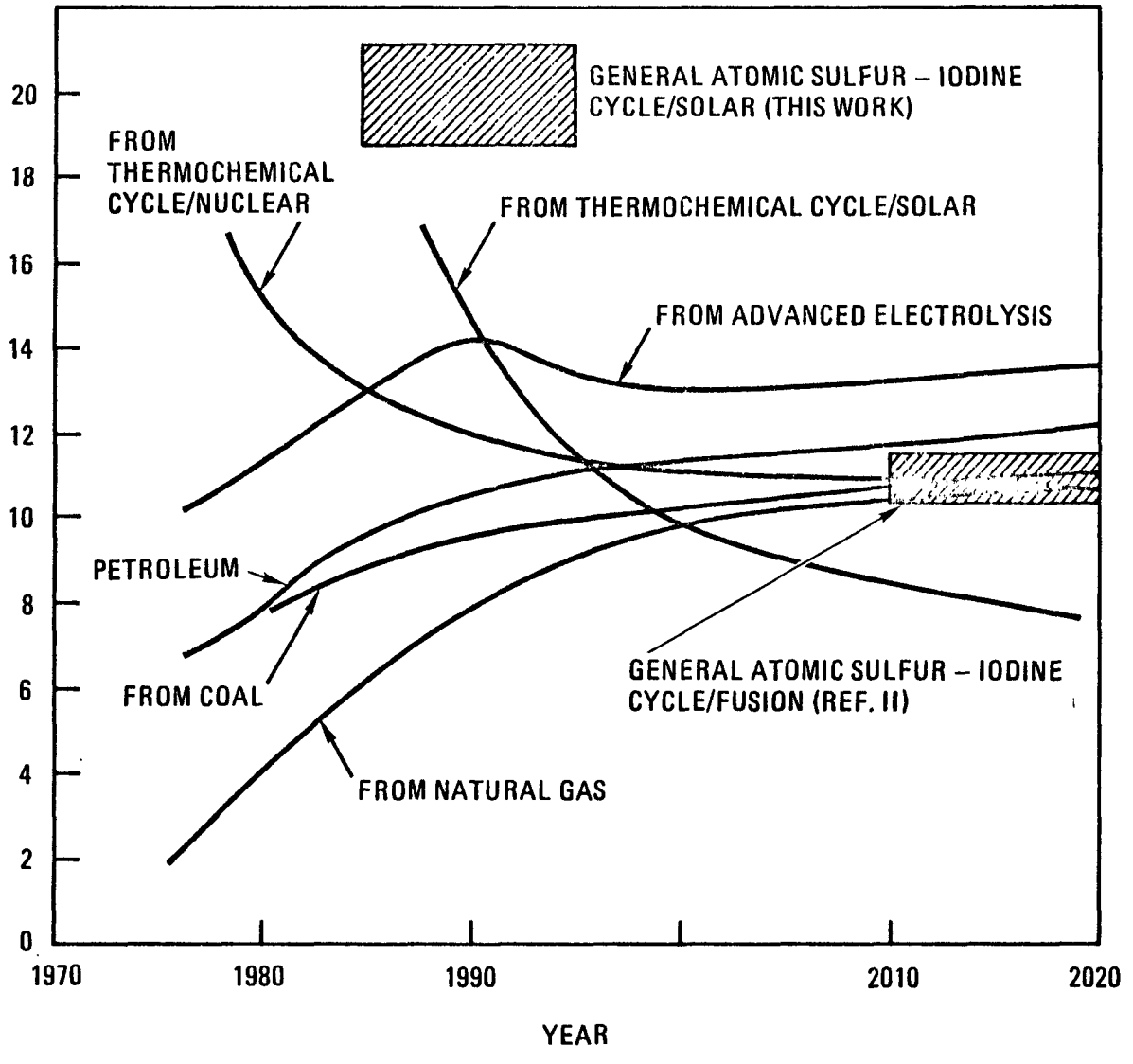

Fig. I-2. Estimated hydrogen production costs (1980$) updated from Ref. I.

of the water-splitting plant, the capital cost of the heat source, and the thermal efficiency of the water-splitting plant. The effect of these variables is discussed in Appendix E, but the results may be generalized as follows: the optimum plant efficiency decreases as the ratio of thermochemical plant cost to heat source cost increases. Decreasing the cost of the heat source will thus permit a lower efficiency and less complex design for the thermochemical plant. Decreasing the thermochemical plant cost, at constant thermal efficiency, will have a significant effect on the capital cost.

This report indicates that the Section II sulfuric acid processing capital costs are major in the chemical plant capital costs for solar-powered water-splitting. This is in contrast to the fusion-powered water-splitting case (Ref. II) where the Section III, H_2 Purification, capital costs dominate.

Future work to reduce the capital cost should emphasize most costly parts of the process. These then will depend upon the heat source being considered.

CONCLUSIONS AND RECOMMENDATIONS

ACCOMPLISHMENTS

Most of the technological developments which established the credibility of the sulfur-iodine cycle were achieved on GA's privately funded program. The two-phase separation of the products of the H_2O-SO_2-I_2 Bunsen reaction wherein the H_2SO_4 phase is nearly devoid of HI and the HI phase is similarly devoid of H_2SO_4 was discovered early in GA's efforts and is the cornerstone of the cycle.

The thermal decomposition of H_2SO_4 was also studied. This reaction was found to be slow at temperatures below 900°C and needed to be catalyzed. In an extensive effort at GA, catalysts

were identified that very greatly accelerated this decomposition at temperatures as low as 500°C where the equilibrium (at atmospheric pressures) highly favors undecomposed SO_3.

It was also found that SO_2 need not be separated from O_2 before it is used in the Bunsen (H_2O-SO_2-I_2) reaction and that this reaction can be used to clean up the oxygen for discharge.

The use of H_3PO_4 to free the HI from the phase in which it is manufactured was also developed. The HI is freed from the H_2O and I_2 contaminants by this reagent. The I_2 is recovered as a second phase, while the H_2O is left as a residue in the H_3PO_4 when the HI is distilled. Finally, the water is distilled from the H_3PO_4.

Catalysts were developed for the decomposition of HI. During this work it was discovered that active catalysts could decompose HI present as a liquid. This allows a considerably enhanced conversion of the HI to be achieved, thus minimizing recycle and making pipeline quality H_2 (50 Bar).

A phase separation which allows the attainment of a nearly dry HI liquid phase in the presence of H_2O and I_2 was discovered. This separation presents an opportunity to achieve dry HI liquid with a lesser expenditure of energy.

The use of HBr in place of H_3PO_4 as an agent to separate the H_2O-HI-I_2 product solution was discovered. This process was later partially developed under the DOE program.

Materials of containment were established for all of the process fluids under projected process conditions. The cycle chemicals are quite corrosive and therefore ordinary materials were often found to be inappropriate, but certain materials used for commercial corrosive systems were found to contain these chemicals satisfactorily.

A continuation of the development effort has been carried out under DOE programs. This effort has been directed toward the improvement of certain of the cycle's operations or toward matching the process to available process heat. The continued effort on the HBr resolution of $HI-H_2O-I_2$ solutions has been studied to determine the efficacy of the HI extraction with HBr, the ability to recover HBr and the energy requirement to do so, and the fate of HBr not recovered but sent back to the Bunsen reactor for enrichment in HI. These questions have been sufficiently resolved so that an engineering estimate on the process can and is being made.

A better operational catalyst for decomposing HI(ℓ) has been found in the field of homogeneous catalysis. High conversions of HI(ℓ) to H_2 and I_2 are retained while the catalyst remains totally unaffected by the process and can easily be recycled to the catalytic reactor.

Efforts on fitting the sulfur-iodine cycle to solar systems have required the consideration of heat storage systems. In this area, a potential seasonal storage system as well as a diurnal system has been discovered. The process makes S and H_2SO_4 from SO_2 and H_2O and later burns it to SO_2 to release stored chemical energy of high quality. The produced SO_2 can be used directly in the sulfur-iodine cycle and can be converted to more S and H_2SO_4.

Direct heat exchange systems have been devised in which fluids are directly contacted to accomplish transfer of heat. Such a process saves heat exchange surfaces and makes the recovery of low-temperature heat more economical for, e.g., the heat generated in the $H_2O-SO_2-I_2$ reaction.

The major task of the DOE-supported work at GA has been the engineering development of the sulfur-iodine cycle. This has included at least two stages of cycle design and efficiency exam-

ination. Evaluation has been addressed for HTGR, solar, and fusion heat sources. The efficiency evaluations have provided values from 47 to 40% depending on the heat source, with solar being the lowest because of requirements for solar energy storage.

Capital cost studies for the various designs have been made. The results of these studies provide credibility to the cycle as a developing method of producing H_2.

Early in the DOE contractural studies a chemical demonstration unit was built and operated. The unit was operated on recycle materials and was shown to produce H_2 and O_2 in a continual manner. The operation of the unit was filmed and copies of the film were distributed to DOE and other sponsors.

A 1-liter H_2/minute bench-scale unit was constructed as part of an engineering evaluation of the process. The individual unit operations of the sulfur-iodine cycle have been tested in this unit. The solution reaction and the H_2SO_4 processing was brought to cycle integration readiness. The HI processing units were all operated, redesigned where necessary, and rebuilt. The bench-scale unit has not been tested as an integrated unit. This unified operation was not programmed for this early in the effort.

The development effort on the GA cycle has demonstrated good prospects for engineering viability of the cycle. Moreover, the R&D effort has provided new methods which promise to improve this viability. This is recognized in an analysis by Ekman (Ref. 1). Development of the GA sulfur-iodine cycle is continuing through DOE sponsorship in efforts to adapt it to solar energy sources and fusion reactors.

Major accomplishments of the work on the sulfur-iodine cycle at GA are summarized as follows:

1. Phase separation for H_2SO_4 and HI solutions.
2. Catalysts for H_2SO_4 decomposition.
3. Azeotrope breaking for HI-H_2O solutions using H_3PO_4.
4. Catalytic decomposition for liquid HI.
5. Direct utilization of SO_2-O_2 gases in the H_2O-SO_2-I_2 reaction.
6. Balanced scrubbing of SO_2 and I_2 from O_2 effluent.
7. Identification of viable materials of containment.
8. Identification of HBr as a substitute for H_3PO_4 in HI-H_2O azeotrope breaking.
9. Phase separations for H_2O-HI solutions from HI( ).
10. HBr use as a substitute for H_3PO_4 in HI-H_2O azeotrope.
11. Homogeneous catalysis system for HI( ) decompostiin.
12. Identification of a solar durnal and seasonal energy storage system utilizing sulfur, which on demand is capable of creating high-quality heat.
13. Identification of direct heat exchange systems for minimizing heat exchange surfaces.
14. Design and efficiency evaluation of the sulfur-iodine cycle for HTGRs, the Tandem Mirror Reactor for fusion and solar CRT systems.
15. Capital cost studies for these designs.
16. Design, construction, and operation of a demonstration unit for the cycle.
17. Design, construction, and operation of the individual units of a 1-liter/min H_2 bench-scale unit for the cycle.

COST BENEFIT ANALYSIS

The Hydrogen Economy

Use of hydrogen as an energy transport medium enables non-fossil energy sources to replace fossil fuels for applications where electricity is impractical or too costly. In a hydrogen

economy, demand for transportation fuels, residential and commercial heating, and industrial process heat can all be met with hydrogen by using nonfossil energy sources such as nuclear fission, fusion, or solar.

There are presently of the order of 10 competing techniques for producing hydrogen. It is too early in the state of technology development to know which technique will be least costly, but it is reasonable to assume that one of these will be at least 10% less costly than any of the others. An R&D program to identify the least costly technique could conceivably cost $1 billion over the next 30 years. As information is obtained, the more promising techniques would be developed further, while the less promising ones would be dropped or retained as backup technologies.

Using present value analysis, it can be shown that the present value of future cost savings greatly exceeds the present value of R&D costs. Assuming first that the present value of R&D costs is $1 billion, the average annual R&D expenditures over the next 30 years would be $65 million, using a 5 real discount factor:

$$\text{Present value of cost} = 10^9 = \frac{65 \times 10^6}{0.05} [1 - (1.05)^{-30}] \quad .$$

The future benefit resulting from this R&D expenditure is estimated to be $30 billion per year starting at the time the lowest-cost hydrogen technology is fully deployed. This deployment could occur within the next 30 to 50 years. This estimate assumes that future U.S. non-electric energy expenditures are equal to the present $300 billion per year level and that non-electric energy demands are not met using a hydrogen production process that is 10% less costly than alternative processes.

Assuming that the technology is fully deployed in 30 years and that the 10% benefit continues indefinitely, the present

value of the benefit equals $140 billion. This follows from the relationship:

$$\text{Present value of benefit} = \frac{3 \times 10^{10}}{0.05} (1.05)^{-30} = 1.4 \times 10^{11} \quad .$$

If the technology is not deployed until 50 years from now, the present value of the benefit is reduced to $50 billion.

The benefit-to-cost ratio for the hydrogen technology development program is seen to be in the range 50:1 to 140:1, indicating that the value of the program greatly exceeds its costs.

Another way of viewing benefit versus cost is to determine the number of years of benefit needed to break even on costs in present value terms. This breakeven time is 0.15 to 0.40 years for deployment starting in 30 to 50 years, respectively. The result for deployment in 30 years is obtained by solving the following equation for N:

$$10^{9} = \frac{3 \times 10^{10}}{0.05} (1.05)^{-30} \left[1 - (1.05)^{-N}\right] \quad .$$

Both approaches show that the potential benefits of a sizable R&D program to develop the lowest-cost hydrogen production technology is justified. Annual R&D funding of $65 million per year for the next 30 years could pay for itself in considerably less than a year after technology deployment and have a benefit-to-cost ratio in the range 50:1 to 140:1. Without the R&D program, the lowest-cost hydrogen production technology would not be identified, and future hydrogen costs would likely be considerably higher than necessary.

The Sulfur-Iodine Cycle

Water-splitting, in particular the sulfur-iodine cycle, is one of the more promising low-cost hydrogen-producing processes. As a result, R&D funding of at least $10 million per year for this particular technology is warranted on the basis of the extremely large future benefits of identifying and deploying the lowest-cost process.

The stage of development of the sulfur-iodine cycle is one of preliminary evaluation. Chemistry and engineering development needs considerable progress before proper comparisons with more developed technologies can be made. There are, however, a number of known favorable characteristics of the cycle. For example, it effectively uses process heat from HTGRs, fusion reactors, and solar CRTs, the process scales well with size, and reactions are fast, indicating relatively small production equipment requirements and chemical inventory. Some items of concern are the corrosiveness of the system, indicating expensive containment materials and a large requirement for heat transfer surface.

Certain modifications to the process are now being studied and are discussed in this report. These have a reasonable probability of markedly improving the process.

DEVELOPMENT PLAN

Introduction

All unit operations of the basic GA sulfur-iodine thermochemical water-splitting process were tested at the laboratory scale and have been verified in flow systems at bench-scale level. All experimental work, but for some high-pressure HI decomposition, was carried out in glass apparatus. During the latter part of the effort, however, significant potential improvements to the process were identified. Insufficient time was

available to carry out an organized development effort that could fully verify the concepts and provide engineering data for the incorporation of these new concepts into the engineering flowsheet. These improvements could significantly lower the overall cost of the GA process, and these need to be studied further.

Future effort on the GA process must address combined efforts in the area of research and process development.

R&D Priorities

A number of processes are insufficiently defined and could be developed to the benefit of the sulfur-iodine cycle. One of these is developing a better method of recovering HI from HI-H_2O-I_2 solutions. The use of H_3PO_4 for this purpose forces the recovery of H_2O from H_3PO_4 solutions. The best design developed so far involves vapor recompression. By this means this process can be done very efficiently, but it requires expensive capital equipment. At the present time HBr treatment appears to be a viable alternative to the H_3PO_4 treatment. There are a number of areas in this treatment that are not yet defined. These are (1) the result of treating HBr-H_2SO_4-H_2O solutions countercurrently with I_2 and SO_2 similar to the H_2SO_4 boost reactor, (2) the vapor-liquid equilibria data in the high-pressure, high-temperature H_2O-HBr system that are necessary to define number of plates, reflux ratios, etc., and (3) further data on the behavior of HBr in the SO_2-H_2O-I_2 reaction. Other alternative ideas to H_3PO_4 processing should also be studied. There are some identified candidates that deserve study.

A second process for study would be the evaluation of the catalytic decomposition of liquid HI using a homogeneous catalyst and liquid-liquid phase separation. Rate measurements at elevated temperatures and pressures have been insufficient to fully evaluate the process. The catalyst recovery scheme needs to be further developed.

The development of the sulfur storage system for solar systems appears to be valuable. This system brings seasonal energy storage from a dream to a real possibility. Moreover, the heat derived from the energy storage plan is of such a quality that Brayton cycles can be considered. The storage plan links very well with the sulfur-iodine cycle but also can stand alone as a heat storage system.

Process Development Program

A general need for accurate flowsheeting is the availability of accurate physical and chemical properties that pertain to the processes being flowsheeted. The technical requirements for the processes are often unusual, for instance high-pressure vapor-liquid equilibrium data or thermodynamic data on unusual mixes of interacting chemicals. A portion of the development program must be devoted to obtaining data applicable to the design of pilot-plants.

Unit operations studied at the bench-scale have provided considerable information for pilot-plant design. There is, however, a considerable gap in many areas between the unit operations that have been studied and those necessary for pilot-plant design. It is appropriate to reduce that gap by further unit-operations studies as a part of the development program.

As a portion of the unit-operations studies, a renewed effort on materials testing is required. Where possible, candidate materials for pilot-plant operation should be used in unit-operations equipment. The influence that corrosion products have on the chemical cycle should also be determined as a part of these studies. Detailed materials studies become of greater and greater importance as the pilot plant stage is approached.

The flow sheeting and costing efforts to evaluate and optimize the process are increasing in importance. These efforts provide the basis for the decision making about whether chemical operations truly augment the process and thus guide the R&D effort. These decisions become more difficult as the optimum is approached, but by the time the pilot plant is on the drawing boards this effort should have discerned as clearly as economically possible that the best process design will result and that all questionable areas have been fully evaluated.

Summary

In order to address these issues, a set of near-term recommendations and a 10-year development program have been prepared. A schedule for the development program is shown in Table I-1, and recommendations for action items that would further enhance and/or evaluate the sulfur-iodine cycle follow:

1. Further investigate the whole cycle effects of the HBr treatment of the HI bearing phase.

2. Construct a preliminary flowsheet and cost analysis for the HBr treatment version of the cycle.

3. Investigate other alternative treatments to the H_3PO_4 treatment of the HI bearing phase.

4. Further define the H_2SO_4 processing system and the sulfur storage system for solar applications.

5. Test the homogeneous catalyst system for liquid HI decomposition at temperature and pressure.

6. Bring to unit operations testing more of the parts of the process, e.g., the H_2SO_4 boost reaction, liquid HI decompo-

TABLE I-1. PROCESS DEVELOPMENT PROGRAM

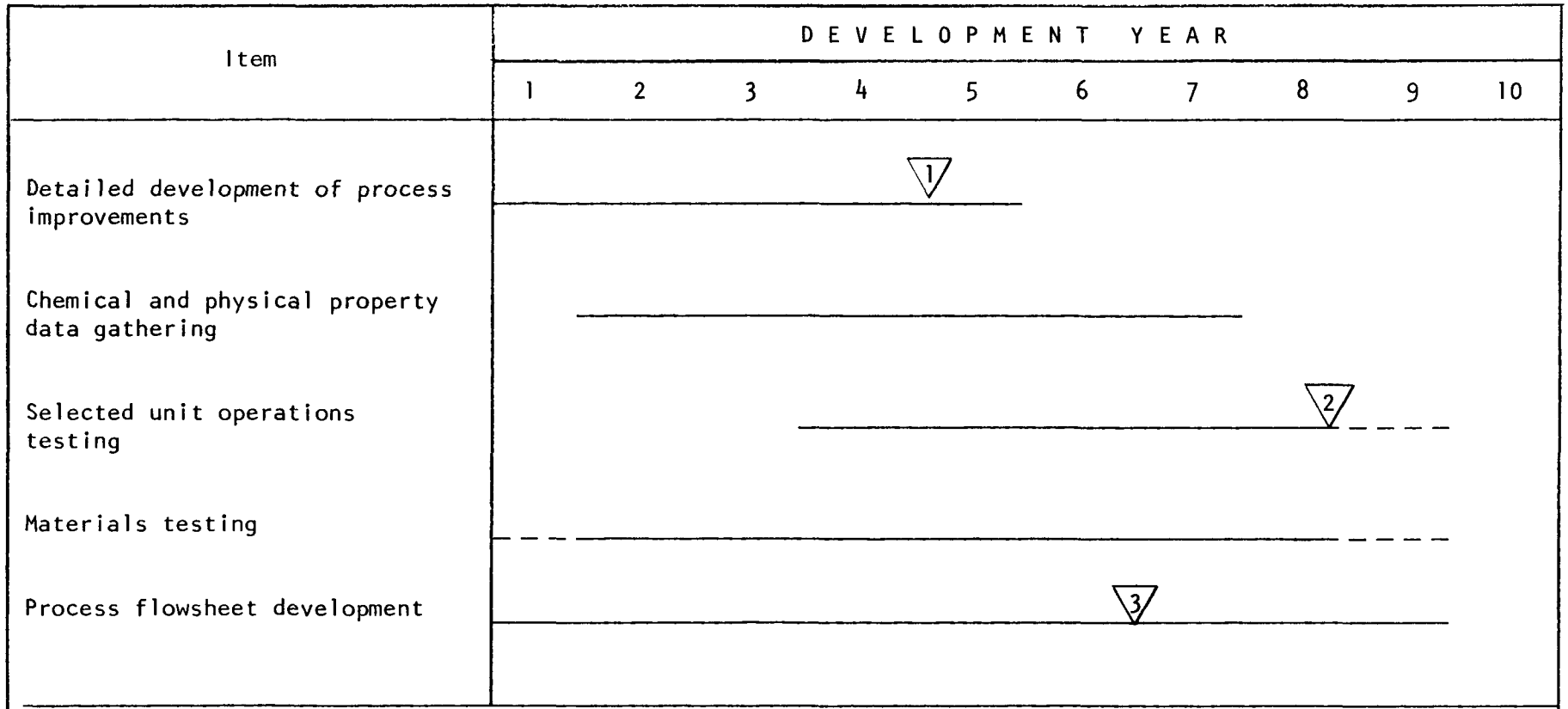

1) Complete development of major process improvements.
2) Complete unit operations testing → data are now available for pilot plant scaleup.
3) Incorporate process improvements into flowsheet.

sition, Bunsen reaction operation with boost reaction I_2 products, etc.

7. Expose real containment materials in unit operations testing.

8. Develop computerized engineering design codes sufficient to allow process optimization techniques to be used.

9. Develop costing models so that optimization of the cost of producing H_2 can be performed.

Emphasis in the process development program is placed on (1) development of process improvements because they potentially lead to a more attractive process, (2) the gathering of basic physical, chemical, and materials of construction properties data because pilot plant design is impossible without basic data due to the chemical nature of the process, and (3) the testing of selected process unit operations at a scale beyond the laboratory effort but not at pilot scale.

After completion of this development program, all data and technology will be at hand to allow the design and construction of a pilot plant to demonstrate the process.

REFERENCES

I. Ekman, K., "Cost of Hydrogen from Fossil and Nuclear Fuels," Jet Propulsion Laboratory Report JPL 5030-416, July 15, 1980.

II. Werner, R. W., O. H. Krikorian, and S. L. Ribe, "Conceptual Design Study FY 1981, Synfuels from Fusion Using the Tandem Mirror Reactor and a Thermochemical Cycle to Produce Hydrogen," Lawrence Livermore National Laboratory Report UCID-19311, February 9, 1982.

1. INTRODUCTION

1.1. BACKGROUND

Thermochemical water splitting potentially provides a non-fossil renewable source of hydrogen. It characteristically requires high-temperature heat input to achieve the necessary conditions for at least one of the chemical reactions to take place and appears to be compatible with the deliverable heat qualities projected for three important heat sources: gas-cooled fission reactions, fusion reactors, and systems for concentrating solar energy.

General Atomic Company (GA) has been working on the development of the cycle for all three of these heat sources, beginning investigations of thermochemical water splitting in October 1972. The result of this initial work was the discovery of a promising cycle (called the sulfur-iodine cycle) that requires no solids handling. General Atomic has cooperated with the Department of Energy (DOE) and the Gas Research Institute (GRI) to develop the thermochemical water-splitting process to the point where it has been demonstrated by flowsheeting and costing techniques as a commercially viable source of hydrogen. Other participants in this effort have included the American Gas Association (whose sponsorship was assumed by GRI), Northeast Utilities Service Company, Southern California Edison Company, the University of California Los Alamos National Laboratory (LANL), and the University of California Lawrence Livermore National Laboratory (LLNL).

The process can be described by the following three chemical equations:

$$2H_2O + I_2 + SO_2 \rightarrow H_2SO_4(sol) + 2HI_x(sol) \quad \sim 370\ K \qquad (1)$$

$$H_2SO_4(sol) \rightarrow H_2O + SO_2 + 1/2\ O_2 \quad \text{up to } \sim 1150\ K \qquad (2)$$

$$2HI_x(sol) \rightarrow H_2 + xI_2 \qquad \sim 500\ K \qquad (3)$$

where the x in the reactions represents the average of several polyiodides (hydrated) formed in the initial solution reaction. Although the cycle can be represented by the three above reactions, several processing steps are necessary to accomplish these reactions.

In February 1977, DOE [then Energy Research and Development Administration (ERDA)] began sponsoring process engineering design studies, some R&D efforts, and laboratory bench-scale investigations under Contract EY-C-03-0167, Project Agreement 63 and later DE-AT03-76SF90351 and DE-AC02-80ET26225. The general objective of the bench-scale work is to obtain better insight into the actual processing steps and their interaction by conducting key continuous flow reactions and separation steps that had previously been done on a batch basis. Bench-scale investigations also give information on the handling of fluids involved, on the operational behavior of key pieces of equipment, and on the effects of incomplete physical separations and possible side reactions. In the later stages of the studies, the three subunits of the bench-scale system were to be operated integrated as one unit. While this has not been done, the work has provided much valuable information for pilot plant design and operation. Process engineering efforts have shown the energy efficiency that can be obtained, have given guidance to further chemical and bench-scale investigations, and have become a basis for realistic cost estimates. Research and development efforts have provided improved methods of closing the cycle and promise better cycle economy.

This document is a report on the DOE-sponsored work for the period February 1, 1977, through December 31, 1981. Section 2 presents the closed-loop cycle demonstration effort, Section 3 describes the bench-scale investigations, Section 4 presents

the process engineering effort, and Section 5 presents research efforts to further elucidate and to improve the cycle.

1.2. THE SULFUR-IODINE CYCLE

Several thermochemical cycles were studied in early work at GA. One of these, the sulfur-iodine cycle, was investigated with the idea of overcoming the acid-separation bottleneck and is described in Refs. 1 through 11. This cycle, though known, had not been developed due to the inability to separate the products, H_2SO_4 and HI. These products coexisted in a water solution. The product solution is dilute if significant amounts of unreacted I_2, SO_2, and H_2O were not all present. When somewhat more concentrated solutions were achieved by having an excess of all reactants present in an equilibrium mixture, attempts to separate HI and H_2SO_2 failed. For instance, to distill HI out of H_2SO_4, SO_2 is distilled first. The products then begin to be consumed in a back-reaction. Such a back-reaction between H_2SO_4 and HI is well documented in the literature (Ref. 12).

With respect to the cycle, the key feature of the Bunsen reaction found by the task group was that at certain reactant concentrations, a phase separation occurs with H_2SO_4 principally in one phase and HI principally in the other. This finding about the Bunsen reaction (also designated as the SO_2-I_2-H_2O reaction or the main or prime reaction by GA) has been developed to derive separated products for the best energy efficiency and cost effectiveness during the course of this and other contracts.

The GA sulfur-iodine cycle, represented by Eqs. (1) through (3), promises to be one of the most efficient and simplest water-splitting cycles. One of the best high-temperature reactions for cycles is the decomposition of H_2SO_4. The H_2SO_4 can accept heat at varying temperatures such as that available from the helium coolant of an HTGR. It will accept sufficient heat so that cycle-

closing reactions need not be particularly energetic. The decomposition products of H_2SO_4 (SO_2 and O_2) do not recombine unless appropriately catalyzed. Thus, sensible heat present in these decomposition product gases can be efficiently heat exchanged without recombination. Within the conditions utilized, this process requires only fluids handling. This provides the cycle with significant engineering advantages.

Hydrogen iodide is another unique material. Its stability is low enough so that it can be decomposed to hydrogen and iodine at quite low temperatures (150° to 300°C) sufficiently (≥20%, depending on conditions) while creating pipeline-quality H_2 (5.0 MPa). The decomposition products are fully fluid in this cycle.

The Bunsen reaction creates product solutions of these two particularly well-suited materials for water splitting. These two solutions must be processed in endothermic steps to derive purified H_2SO_4 and HI. Most of the chemical efforts of this program have been devoted to creating the most tractable product solutions from the Bunsen reaction and to learning how to most effectively process them back into Bunsen reactants and O_2 and H_2 products.

The sulfur-iodine cycle described by Eqs. (1), (2), and (3) appears to be very simple. In reality, the mode of accomplishing this cycle is considerably more complex than the three equations would indicate. The presently preferred mode for completing this cycle is presented in the set of transformations given below, the block diagram of Fig. 1, and the step and diagram explanation that follows:

Step

1 $2H_2O(\ell) + SO_2(g) + xI_2(\ell) \rightarrow H_2SO_4(sol) + 2HI_x(sol)$

2 $H_2SO_4(sol) \rightarrow H_2SO_4(\ell)$

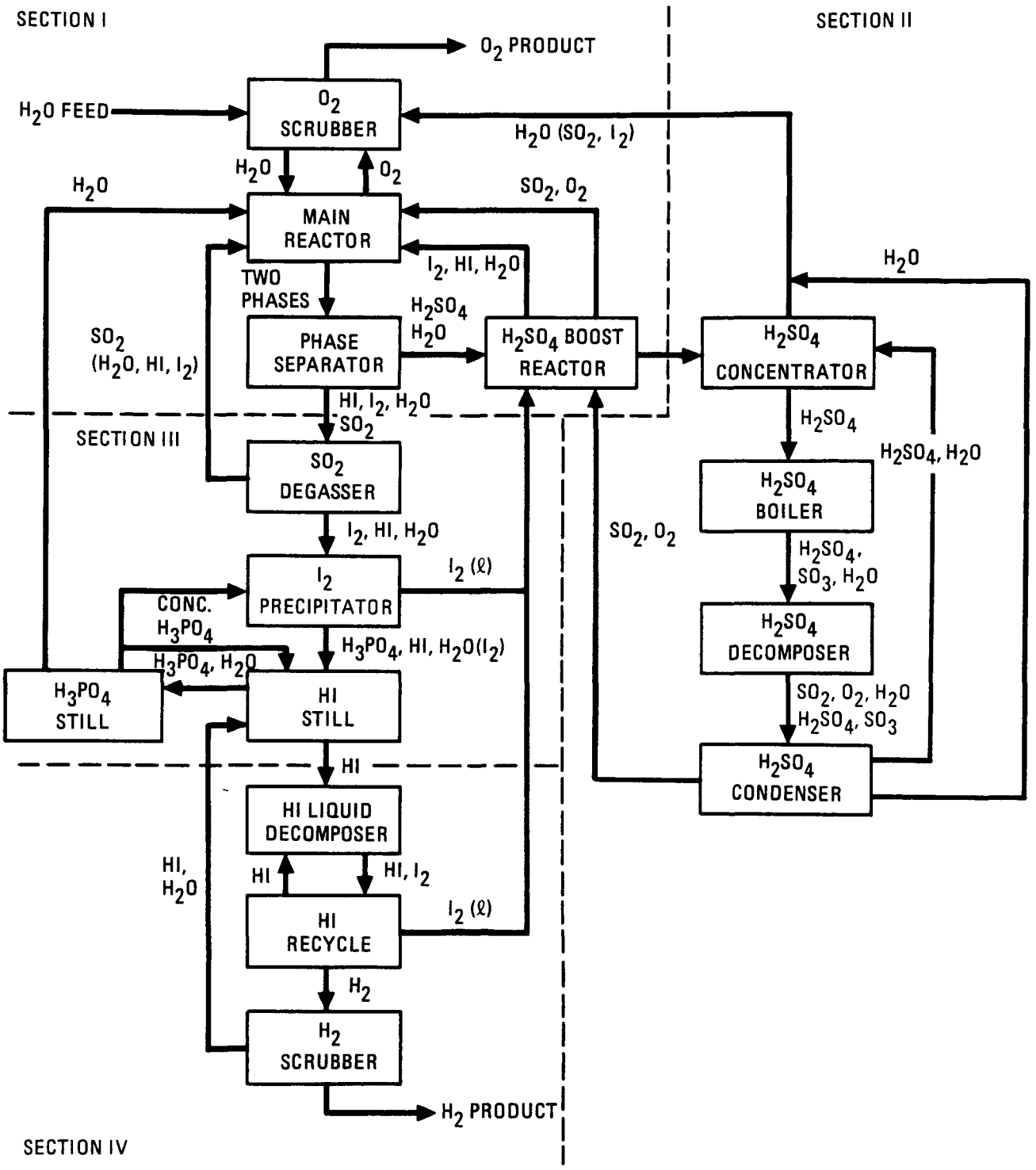

Fig. 1. Flow diagram for the sulfur-iodine cycle

3 $H_2SO_4(\ell) \rightarrow H_2SO_4(g)$

4 $H_2SO_4(g) \rightarrow H_2O(g) + SO_3(g)$

5 $SO_3(g) \rightarrow SO_2(g) + 1/2\ O_2(g)$

6 $2HI_x(sol) \rightarrow 2HI(g) + (x-1)\ I_2(\ell) + H_2O(\ell)$

7 $2HI(g) \rightarrow 2HI(\ell)$

8 $2HI(\ell) \rightarrow H_2 + I_2(sol)$

9 $I_2(sol) \rightarrow I_2(\ell)$

Step 1 is the prime reaction where the acid solutions are made. This step is described in the four unit operations of Section I in the diagram. The SO_2-O_2 product gas from Section 2 is contacted in the main reactor with the iodine from the H_2SO_4 boost reactor to upgrade its HI content as well as make the bulk of the H_2SO_4. This reaction scrubs the SO_2 out of the O_2, which is later purified in the O_2 balanced scrubber. The balanced scrubber accepts a portion of the recycle H_2O where the vapor transported I_2 and SO_2 are reacted with H_2O stoichiometrically. The scrubber is balanced by adding an amount of whichever reactant is required to bring the scrubber to stoichiometric with respect to the Bunsen reaction. In this dilute acid concentration, the products of this reaction are fully scrubbable and the reactants, except for H_2O, are exceptionally well scrubbed according to equilibrium considerations. The product is a wet, but otherwise pure, oxygen.

The remaining unit operation of Section I is the H_2SO_4 boost reactor, where advantage is taken of the driving force of pure $I_2(\ell)$ in a countercurrent reactor to produce additional Bunsen reaction products. The product H_2SO_4 solution from the main reactor is fed with SO_2 into one end of the countercurrent reac-

tor and I_2 is fed into the other end. The products of this reactor are H_2SO_4 boosted in concentrations from ~50% to ~57%--a tenfold increase in H_2SO_4 activity--and an I_2 that has the produced HI dissolved in it along with a small amount of H_2O. This stream is fed to the main reactor for upgrading. The products of Section I are, thus, oxygen, an ~57% H_2SO_4 solution, and a solution of HI and H_2O in I_2 contaminated with SO_2.

Section II involves the purification, boiling, and decomposition of the sulfuric acid as covered by Steps 2 through 5 and the four unit operations appropriately labeled in Fig. 1. Product from the H_2SO_4 boost reactor is concentrated by boiling away H_2O, I_2, and SO_2 and destroying dissolved HI through reversing Eq.(1). By the time that the H_2SO_4 is beginning to approach azeotropic concentrations, H_2O is the only contaminant left. After the final H_2O is removed in the distillation column, the remaining azeotrope is sent to the boiler where it is first vaporized to mainly $H_2SO_4(g)$ and then, as the temperature is raised, decomposes more and more into $SO_3 + H_2O$. Upon further heating, the SO_3 is, according to equilibrium considerations, partially decomposed in the catalytic decomposer to $SO_2 + 1/2\ O_2$. The hot gases are disentrained from the catalyst and heat-exchange-cooled whereby, first, undecomposed H_2SO_4 is condensed, and, later, H_2O is condensed leaving a wet SO_2-O_2 product which is returned to Section I.

Section III, as described in Steps 6 and 7 and the four unit operations of Fig. 1, accepts the main reactor HI_x product. It is necessary to remove dissolved SO_2. The HI in this product during further treatment will become susceptible to oxidation by certain oxidizing agents. Both SO_2 and H_2SO_4 are such agents. The H_2SO_4 cannot easily be removed, and it is present in very small amounts such that its oxidation of HI is accepted while that of SO_2 is not. After SO_2 degassing, Steps 6 and 7 can be carried out. In the present design Step 6 is carried out using H_3PO_4 as the separation agent. The countercurrent treatment of

the degassed HI_x at temperatures above the melting point of I_2 creates two phases--one, a solution of HI, H_2O, and some I_2 in H_3PO_4, and the other, I_2 with contaminant levels of the other phase species. After cleaning, the I_2 is returned to Section I.

The H_3PO_4 treatment not only separates most of the iodine but also decreases the H_2O activity by H_3PO_4 hydration. This results in an increase in the HI activity such that it can be distilled readily out of the H_3PO_4 solution with little H_2O contamination; that is, the H_2O, HI azeotrope is broken. This distillation is done under pressure so that HI can be recovered as a liquid without refrigeration techniques.

Within Section III, the H_3PO_4-H_2O mixture, resulting from the treatment followed by HI distillation, must be recovered. In an energy conservative process, such as vapor recompression, water is removed from the H_3PO_4 solution. This regenerates the capability of the H_3PO_4 to treat more HI_x product and creates recycle H_2O to return to Section I.

The liquid HI from Section III is directed to Section IV - Steps 8 and 9 and the three unit operations shown in Fig. 1. Within this section the HI(ℓ) is exposed to catalyst at temperatures around 200°C where H_2 and I_2 are produced. This process causes about 50% of the HI to be decomposed. The separated H_2 is then treated to remove and recycle most of the HI directly and is later washed to remove the last traces of HI before exporting. In this process the H_2 is produced at >5.0 MPa as needed to introduce into pipelines. The iodine product solution is rectified, returning the HI to the decomposer while the purified I_2 is sent to Section I.

The bench-scale engineering efforts and the flowsheeting and costing of the sulfur-iodine process are based upon this description of the cycle and will be discussed in greater detail in later portions of this report.

2. CLOSED-LOOP CYCLE DEMONSTRATOR

During the latter part of FY-78, DOE requested that GA demonstrate the sulfur-iodine cycle in a closed loop using recycled materials. Work on design of such a system [the Closed-Loop Cycle Demonstrator (CLCD)] started in September 1978 and construction was completed in December.

2.1. DESIGN AND CONSTRUCTION

The CLCD was not designed to duplicate the conditions of the process engineering flowsheet, but rather to provide an early demonstration of the feasibility of the cycle under recycle conditions. A schematic diagram of the system is shown in Fig. 2.

The reactants H_2O, I_2, and SO_2 are fed into a main reaction vessel (R-1) and continuously recirculated, by means of a pump (P-1), in a loop where temperature control can be obtained by heating or cooling through the cooler (C-1). Some of the products are intermittently fed to the liquid-liquid separator (R-2), where the two acid phases are separated. The upper H_2SO_4 phase is purified by boiling in R-3 and then decomposed in a quartz tube furnace containing Fe_2O_3 catalyst (H-1,R-4). The product gas is first cooled in a condenser (C-3, R-5), the condensed phase (unreacted H_2SO_4) is recycled to R-3, and the gas phase (SO_2 and O_2) is first vented and later recycled. The lower phase from R-2 (HI-I2-H_2O containing SO_2) goes to an off-gas reactor (R-6), where SO_2 is extracted under vacuum at 370 K and trapped in the liquid nitrogen traps (TR-3 and TR-4). Again, intermittently, the degassed lower phase is sent to a furnace (H-2, R-7), where some of the HI is thermally decomposed into H_2 and I_2. The product gases are first cooled in C-4 and then fed to a series of separators and condensers (R-8, R-9, and C-5 and/or C-6), where H_2O, HI, and I_2 are separated and sent to the main reaction vessel (R-1) for recycle. The H_2 gas is purified

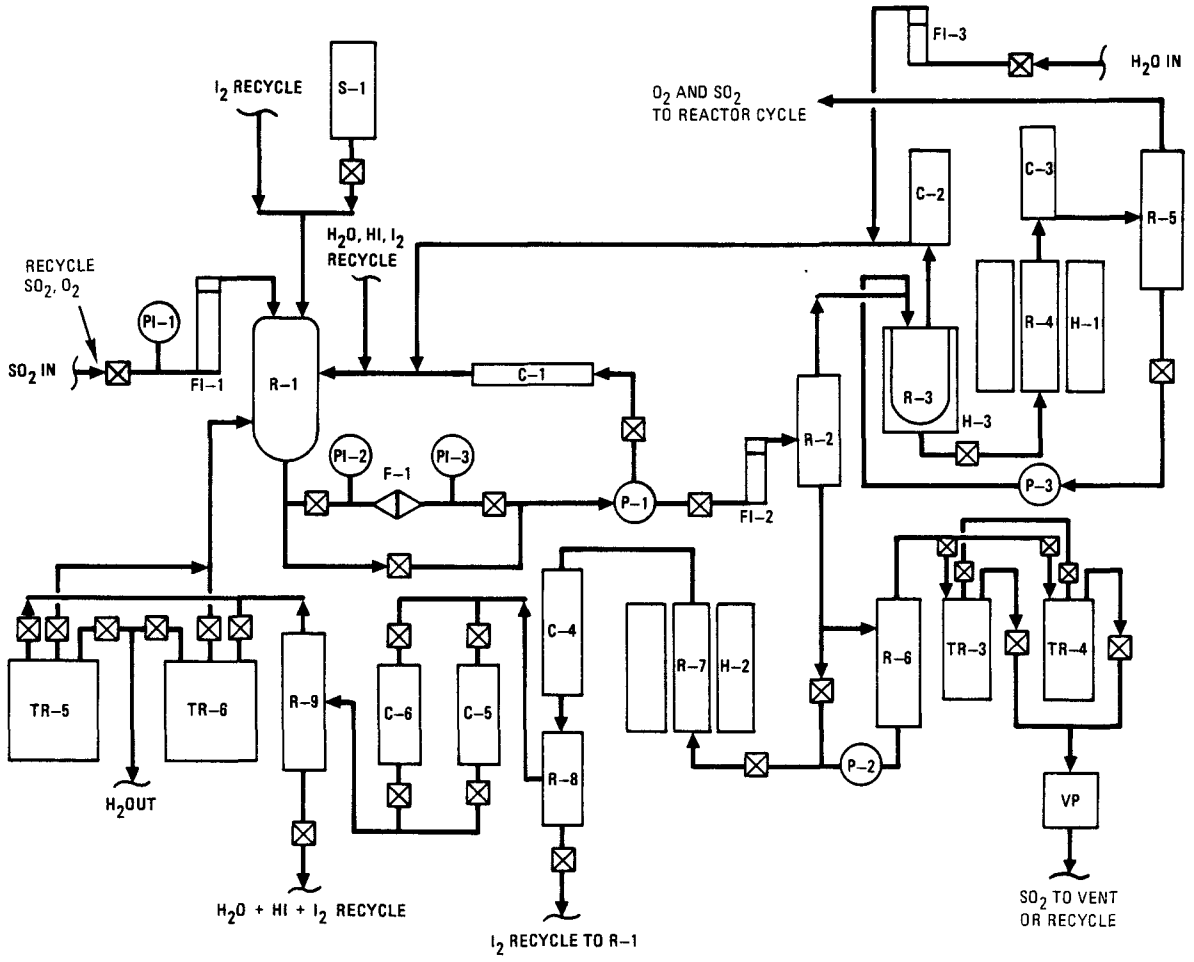

COMPONENT DESIGNATION

C-1	PRIME REACTION RECIRCULATING PRODUCT COOLER
C-2	UPPER PHASE OFF GAS COOLER
C-3	H_2SO_4 POST-CRACK PRODUCT COOLER
C-4	HI POST-CRACK PRODUCT COOLER
C-5	HYDROGEN PURIFICATION LOOP PRE-COOLER
C-6	HYDROGEN PURIFICATION LOOP PRE-COOLER
F-1	PRIME REACTION MAIN-LOOP FILTER
FI-1	SO_2 INPUT FLOW INDICATOR
FI-2	MAIN LOOP OUTPUT FLOW INDICATOR
FI-3	WATER SUPPLY INPUT FLOW INDICATOR
H-1	H_2SO_4 CRACKING FURNACE
H-2	HI DECOMPOSITION FURNACE
H-3	UPPER PHASE PURIFICATION HEATER
P-1	MAIN LOOP CIRCULATING PUMP
P-2	LOWER PHASE CIRCULATING AND FEED PUMP
P-3	H_2SO_4 RECYCLE PUMP
R-1	MAIN REACTION VESSEL
R-2	MAIN REACTION PRODUCT LIQUID-LIQUID SEPARATOR
R-3	H_2SO_4 PURIFICATION BOILER
R-4	H_2SO_4 DECOMPOSITION REACTOR
R-5	UPPER PHASE POST-DECOMPOSITION GAS-LIQUID SEPARATOR
R-6	LOWER PHASE OFF-GAS REACTOR
R-7	LOWER PHASE DECOMPOSITION REACTOR
R-8	LOWER PHASE POST-DECOMPOSITION GAS-LIQUID SEPARATOR
R-9	HYDROGEN PURIFICATION LOOP GAS-LIQUID SEPARATOR
S-1	IODINE SUPPLY VESSEL
TR-3	LOWER PHASE SO_2 OFF-GAS LN_2 TRAP
TR-4	LOWER PHASE SO_2 OFF-GAS LN_2 TRAP
TR-5	HYDROGEN PURIFICATION LOOP LN_2 TRAP
TR 6	HYDROGEN PURIFICATION LOOP LN_2 TRAP
VP	LOWER PHASE OFF-GAS SYSTEM VACUUM PUMP

Fig. 2. Closed-loop cycle demonstrator

in the liquid nitrogen traps (TR-5 and TR-6) before metering and collecting.

Construction and assembly of the CLCD took place between October and December 1978. Glass was used throughout the system, with the exception of the high-temperature portions [the two cracker-cooler units (R-4/C-3 and R-7/C-4)], which were made of quartz. Figure 3 shows the CLCD as it was installed.

2.2. OPERATION

Operation of the CLCD took place during the first weeks of January 1979. As a result of the experience gained during testing of bench-scale Subunit I, no operational problems were encountered. All valves, joints, pumps, and temperature and flow controls worked as designed. For simplicity of operation, it was found convenient to add a small displacement pump to feed the HI cracker; this allowed independent operation of the degassing loop (P-2/R-6) from operation of the decomposer (R-7).

Operation of the CLCD started by introducing 3 kg of iodine and 1 kg of water at room temperature into the main reaction vessel (R-1). SO_2 was bubbled through at a rate of 3 liters/min until there was evidence of formation of two separate liquid phases (20 min). The prime reaction products were kept circulating through the filter (F-1) and the cooler (C-1) by means of the pump (P-1). Since the temperature had risen to only 45°C, no cooling was necessary. Intermittently, the liquid was fed to the phase separator (R-2) and allowed to rest up to 5 min to complete the separation; the upper phase was then sent to the H_2SO_4 purification boiler (R-3) and the lower phase to the degasser (R-6).

The H_2SO_4 was concentrated from an initial 30+% to approximately 95%, and all of the water and traces of SO_2, I_2, and HI were condensed in C-2 and recycled into the main loop. The concentrated, purified liquid H_2SO_4 was fed to the decomposer

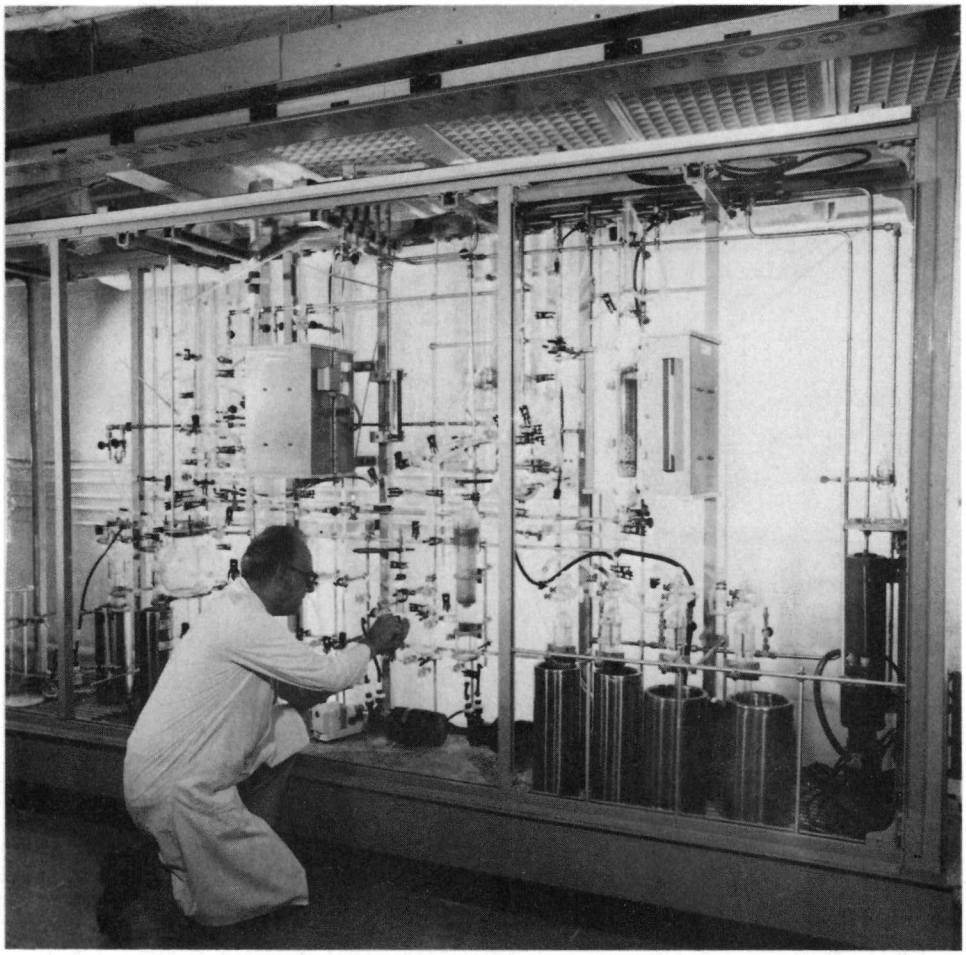

Fig. 3. Installation of CLCD

(R-4), filled with pellets of Fe_2O_3 catalyst kept at 850°C, at a rate of approximately 5 cm^3/min. The product gases were condensed in C-3, with the uncracked H_2SO_4 recycled to the boiler and the resulting SO_2-O_2 mixture sent directly to the main loop for recycle or a sampling and/or venting system. The lower phase was degassed (SO_2 removal) under vacuum in R-6 for 10 min before it was sent to the HI cracking step.

Since, for simplicity, the CLCD was designed without the HI purification step, the lower phase (HI-I_2-H_2O) was fed directly to the HI cracker and no catalyst was used.

The liquid feed rate was approximately 4 cm^3/min, and the decomposer temperature was held at 900°C. Before operating the HI decomposer, the system was flushed with HI.

The product gases from the decomposer (R-7) were cooled and the condensed liquid (H_2O, I_2, and unreacted HI) was recycled to the main loop. The cooled gas was purified in the liquid nitrogen traps (TR-5 and TR-6), and the product H_2 was collected under water in a graduated cylinder for analysis or utilized as desired. The rate of H_2 production was approximately 20 cm^3/min.

Operation of the loop was accomplished subsequently in a complete recycle mode: the main reaction products were formed by reacting the recycled H_2O and I_2 (and some HI as well) from the HI decomposition system with the SO_2 and H_2O obtained from the H_2SO_4 decomposition system. No differences were observed.

During the operation of the small loop, small quantities of sulfur were observed in the recycled liquids after the HI condensers (particularly C-4) and small amounts of H_2S collected in the H_2 purification traps. This was due to incomplete separation of the sulfur-containing species (SO_2 and H_2SO_4) from the lower phase prior to decomposition. The lower phase concentration and purification step (H_3PO_4 treatment), which is an integral part of

the cycle, will minimize this recognized problem. This treatment will be tested in bench-scale Subunit III.

Operation of the CLCD has confirmed the feasibility of the GA water-splitting cycle and provided laboratory personnel with information useful for the detailed construction and operation of the bench-scale unit.

A motion picture was made of the operating CLCD and distributed to funding agencies supporting sulfur-iodine cycle efforts.

3. BENCH-SCALE INVESTIGATIONS

After extensive studies of the chemistry of the sulfur-iodine cycle, a bench-scale system study was initiated with the goal of studying the cycle under continuous operation conditions. This section describes the design, construction, and operation of the units of the system, which consists of three subunits corresponding to the three basic reactions of the cycle.

Subunit I ($HI-H_2SO_4$ production and separation) supplies I_2, H_2O, and SO_2 to a reactor where these ingredients are mixed and equilibrated, forming two liquid product phases which are later separated. Included in Subunit I is the removal of unreacted SO_2 from the HI_x solution phase.

Subunit II (H_2SO_4 concentration and decomposition) concentrates and purifies H_2SO_4 solution by removal of iodine-containing species, H_2O, and dissolved SO_2. This is followed by vaporization and decomposition of H_2SO_4 to equilibrium concentrations at ~1100 K. The products of the decomposition are separated from unreacted acid, and they themselves are separated, providing SO_2 and H_2 for recycle and product O_2. The O_2 is cleaned up before discharge.

Subunit III (HI concentration and decomposition) separates I_2 and H_2O from the HI_x phase by first contacting the degassed HI_x solution with H_3PO_4 solution followed by a column distillation of HI out of the H_3PO_4 solution. The H_3PO_4 solution is reconcentrated for recycle by boiling out H_2O. The formed HI is decomposed to H_2 and I_2 at near equilibrium conditions. The product H_2 and I_2 and the unreacted HI are separated for recycle (I_2 and HI) or discharge (H_2) after appropriate cleanup.

All three sections have been operated. The design, construction, and operation of these units are described in the

following sections.

3.1. SUBUNIT I

3.1.1. Design and Construction

Work was first begun on this Bunsen reactor unit in 1977. A unit to perform the main reaction was designed (Ref. 10), and the necessary equipment and apparatus were procured. The unit was built to the initial design except for a few changes to improve its operability and was cold tested late in 1977. Early in 1978 the unit was operated producing product solutions at concentrations expected from the earlier chemical laboratory batch type experiments. This unit was operated in a hood within the chemical laboratory with the intention of transferring the operation to a chemical engineering laboratory which would be capable of housing all three sections of the cycle's bench-scale unit.

After these successful tests, the chemical engineering laboratory was ready to accept this and the other two units. This bench-scale Subunit I was disassembled and reassembled with a few planned changes which were expected to improve the operation. The main changes made at that time were (1) the repackaging of the I_2 delivery vessel to facilitate heating and to allow the use of a load cell which could measure, in an integrated fashion, the delivery rate of iodine from the vessel, (2) a pump system for I_2 delivery, (3) the installation of SO_2 degassing equipment for lower phase, and (4) an SO_2 off-gas cleanup system which returns condensable vapors. Also, a gravity overflow separator system was invented and incorporated into the unit. Details of the final design are represented in Fig. 4.

Section 1 operates by delivering known rates of flow of I_2, H_2O, and SO_2 into the finned reactor vessel. The iodine is

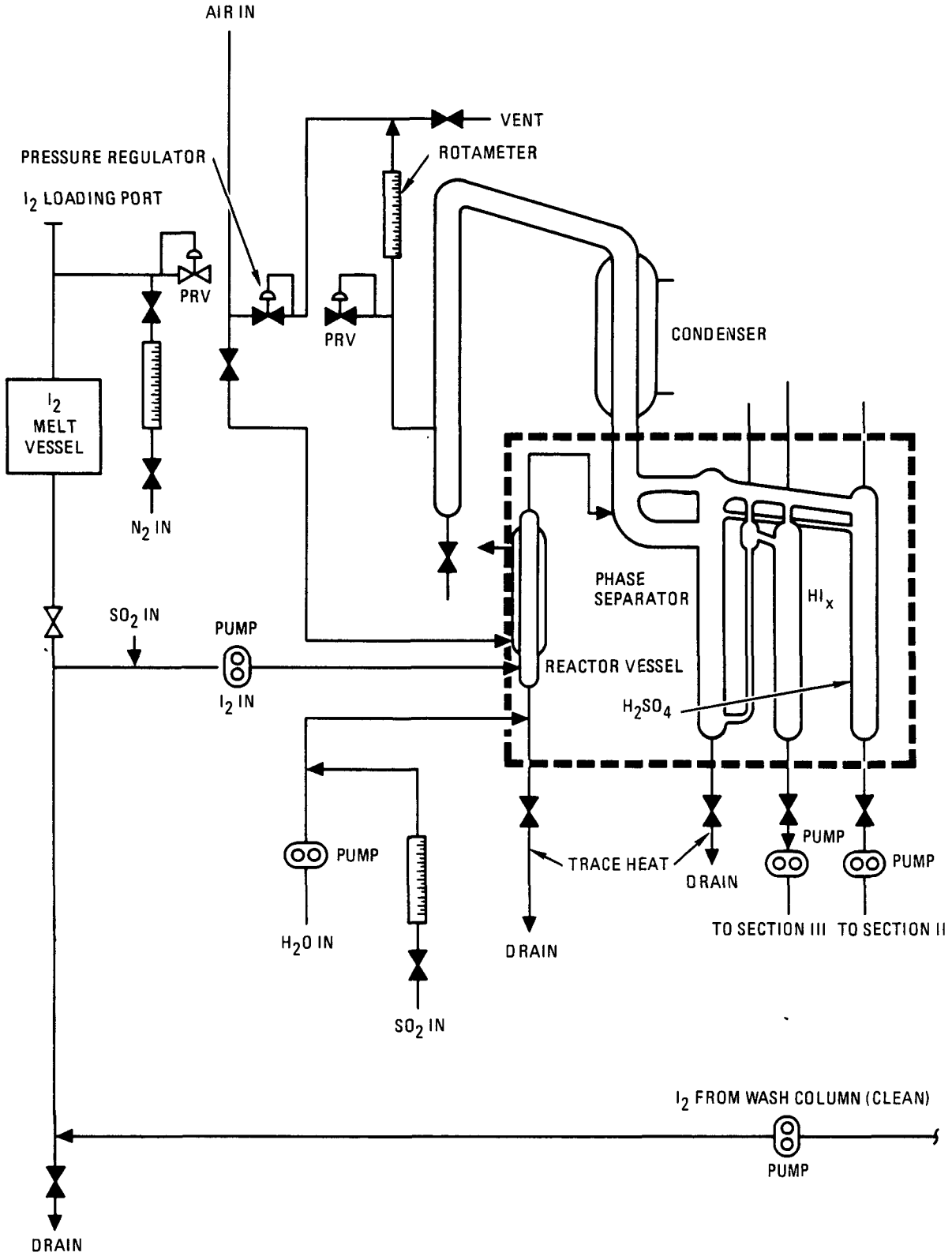

Fig. 4. Subunit I bench-scale design

delivered as a melt from the jacketed I_2 melt vessel. Preliminary to operating Section 1, iodine loaded into the I_2 melt vessel is heated. It takes about 0.5 hr to melt the contents of fresh fill and somewhat longer for remelting a charge. This difference is accounted for by the poor thermal conductivity of a solid block of iodine. A desired iodine flow rate is established by a positive displacement ceramic metering pump whose operation is monitored by the load cell. This iodine is delivered through heat-traced lines to the base of the finned reactor vessel. Water is delivered through a metering pump, combined with the SO_2 flow, and preheated. This mixture is brought into the finned reactor, which is shown in Fig. 5, below the iodine entry point. The SO_2 flow is delivered from a pressurized gas cylinder through a metering valve and appropriate flow meters.

The alternating-direction finned reactor operates at about 200 kPa pressure. A significant excess (beyond stoichiometric) flow of SO_2 is utilized to propel the mixing liquids through the finned reactor in order to provide adequate mixing. The excess SO_2 gas has a residence time of <1 sec in the reactor versus a number of seconds for the liquids. The fluids, so reacted, exit from the finned reactor into the phase separator diagrammed in Fig. 6 where gas and liquid liquid separation take place. The finned reactor and the phase separator are thermostatted in a glass-fronted forced convection oven. The reactor itself is jacketed for temperature adjustment during the exothermic Bunsen reaction. The front glass window allows the operator to observe the flows in the reactor and separator vessels so that he can establish and maintain control of the operation of this unit. The temperature of the fluid flowing from the reactor vessel and the oven temperature are measured and associated with the delivered phases.

The separator accepts the fluids from the finned reactor vessel. In the first chamber the gases are separated from the liquids. The gases are passed through a condenser to knock out

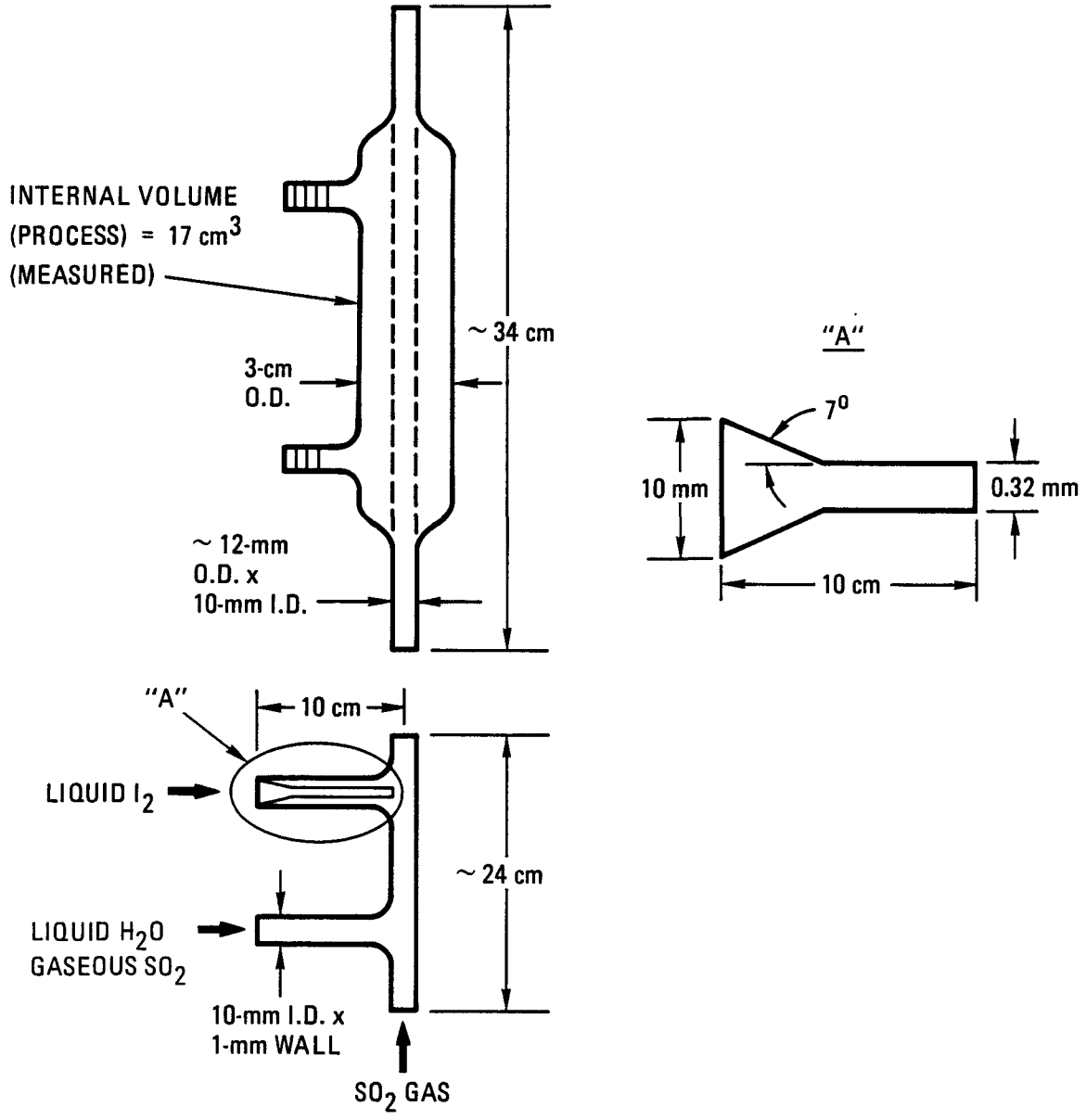

Fig. 5. Subunit I main reaction vessel mixing entry

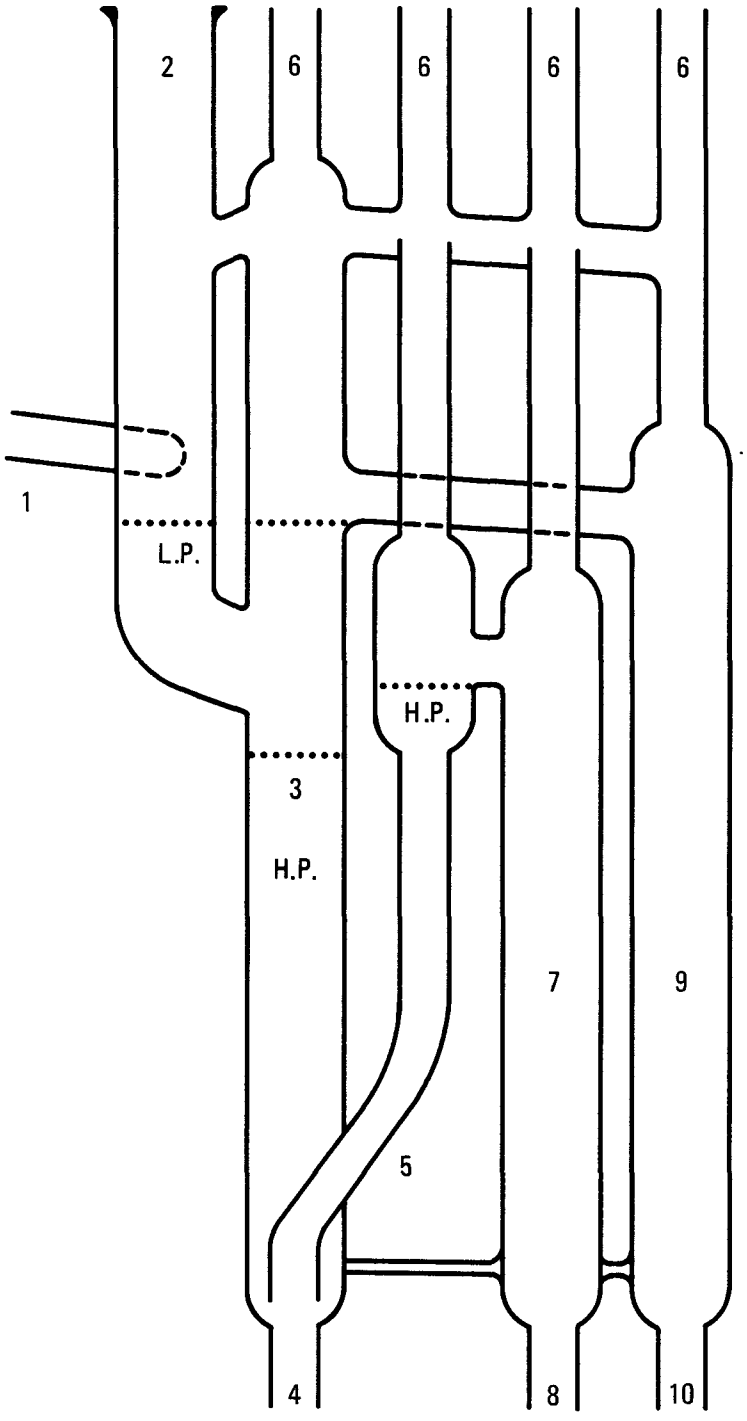

1. PRODUCT INLET
2. GAS EXIT
3. PHASE SEPARATION
4. WASTE EXIT
5. HI_x DELIVERY TUBE
6. MATERIAL TESTING PORT
7. HI_x RESERVOIR
8. TO SUBUNIT III
9. H_2SO_4 RESERVOIR
10. TO SUBUNIT II

Fig. 6. Subunit I phase separation apparatus

most of the water and iodine vapors in the exiting SO_2, which can be recycled. These condensed products are returned to the separator. The liquids from the reactor vessel and the condenser are delivered to the lower portion of the separator. In this section the heavier HI_x phase falls through the lighter H_2SO_4 phase. The separator is designed so that the heavier phase will flow up a tube from the bottom of this separator into an overflow leading to an HI_x holding chamber, and the lighter H_2SO_4 will overflow from the top of the separator into an H_2SO_4 holding chamber. These products can be pumped on demand or continuously to Section II and Section III. Samples of these product streams can be withdrawn through penetrations in the top of the separator which can also be used as material testing ports.

The apparatus in this section is made of Pyrex glass using corrosion-resistant Teflon fittings and valves to join glass parts. Some Hastelloy B tubes and Hastelloy C valves are used in the I_2 feed system. A Teflon pressure relief valve located downstream of the condenser controls the pressure in the apparatus. An auxiliary exit valve is available to fine tune the SO_2 flow. The as-constructed unit is shown in Fig. 7.

3.1.2. Operation

Several experiments yielding useful data were conducted in earlier versions of Subunit I. The first experiment produced separable light and heavy acid phases over a 90-min period. Analysis of 73 g of light phase after degassing indicated an H_2SO_4 concentration of ~42 wt %, whereas the design concentration is 50 wt % without a "boost" reaction. Approximately 3.8 kg of heavy phase was also collected but not analyzed. These quantities resulted from the reaction of approximately 3 kg of purified liquid iodine with 1.2 liters of water. The average I_2/H_2O ratio was 2.5/1 (weight basis) as compared to 7/1 (design). A later experiment produced approximately 34 g of light phase with an H_2SO_4 concentration of approximately 48 wt % after degassing.

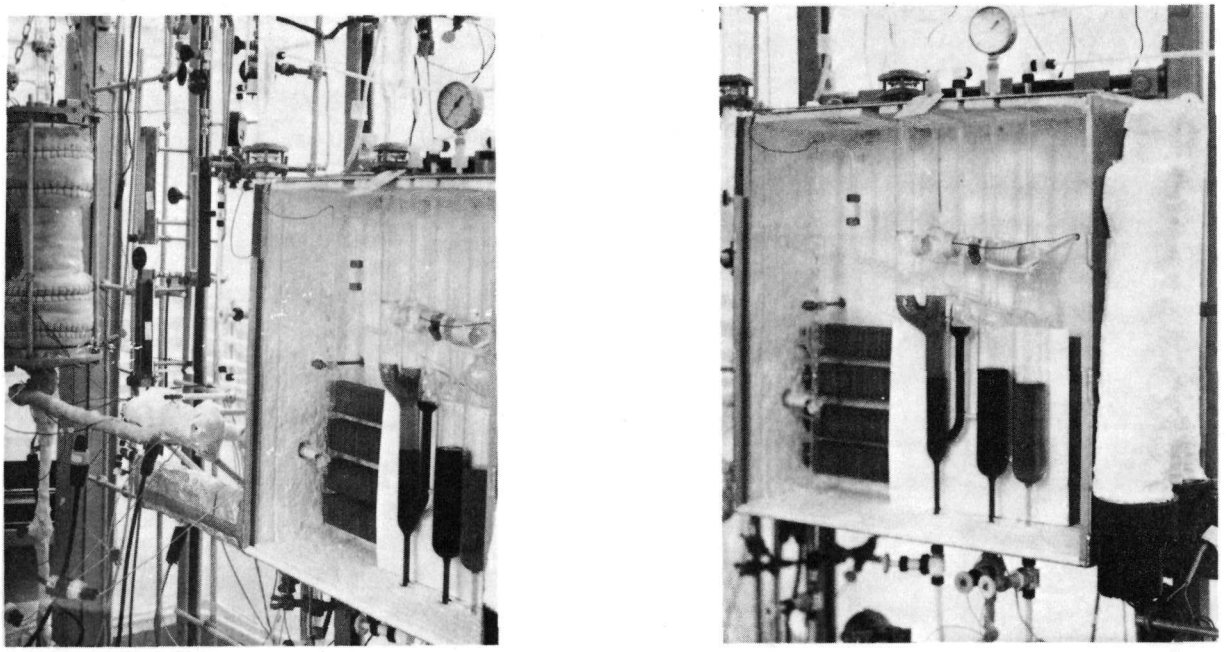

(a) (b)

Fig. 7. Photographs of Subunit I: (a) reactor-separation plus the iodine supply and delivery system; (b) enlargement of reactor-separator

This is very close to flowsheet design conditions. Approximately 3 kg of resublimed iodine reacted with 160 ml of water in a 40-min period, giving an average I_2/H_2O weight ratio of 19/1.

Initially two tests were conducted with the redesigned equipment. One was run with a relatively low weight ratio of I_2 to H_2O of 2.5. Analysis of the light phase after degassing indicated H_2SO_4 concentrations of between 42 and 44 wt %, whereas the design concentration is 50 wt %. The other test was then run employing a weight ratio of I_2 to H_2O of 5.3, and the concentration of the H_2SO_4 product phase increased to 49 wt %, which is close to design value.

A series of experiments was then conducted using the design weight ratio of I_2 to H_2O of 7.0. The data are presented in Table 1. It is to be noted that the results are all near or over design levels.

The bench-scale system was designed to produce H_2 at a rate of 1 liter/min. With the exception of the last point, the data in Table 1 indicate that nominally, except for the 2-6 condition, this design level was being achieved. This last 2-6 condition was performing at a level of 2 liters H_2/min. There seems to be no reason to believe that this production rate represents the limit of the as-designed unit.

These experiments have verified the concept of a cocurrent reactor for the main solution reaction and, in general, the operability of the components of Subunit I. In addition, the experiments indicate that flowsheet design conditions can be met without great difficulty.

TABLE 1
EXPERIMENTAL RESULTS ON OPERATION OF SUBUNIT I

SAMPLE NO.	I^2 FLOWRATE (G/MIN)	H_2O FLOWRATE (G/MIN)	SO_2 FLOWRATE (G/MIN)	% H_2SO_4 IN LIGHT PHASE
3332-1 - 1	112	16	>3.2	40.60*
1 - 2	112	16	>3.2	48.20
1 - 3	112	16	>3.2	52.64
1 - 4	112	16	>3.2	51.57
1 - 5	112	16	>3.2	46.12
2 - 1	112	16	>3.2	46.10
2 - 2	112	16	>3.2	47.75
2 - 3	112	16	>3.2	49.54
2 - 4	112	16	>3.2	48.46
2 - 5	112	16	>3.2	48.78
2 - 6	224	32	>6.4	46.20

* I_2 flowrate not stabilized.

3.2. SUBUNIT II

3.2.1. Design and Construction

The design and construction of the H_2SO_4 processing unit was completed in May 1979. The overall criteria for Subunit II H_2SO_4 concentration and decomposition are:

1. The unit shall reproduce the individual process operating steps of the large-plant conceptual flowsheet.

2. The process operating steps shall occur at the temperatures used for the large-plant conceptual flowsheet.

3. The bench-scale equipment shall be designed and instrumented to facilitate the gathering of performance data useful for guiding scaleup and detailed design of pilot-plant-scale equipment.

Limitations of time and resources made it infeasible to meet all the foregoing criteria strictly, and some of their particular aspects are conflicting. The strictness with which the particular processing steps of the large-plant conceptual flowsheet are reproduced in the bench-scale system has been somewhat relaxed to facilitate the taking of data on the behavior of the materials as they undergo processing; for example, the SO_2, HI, and I_2 are removed from the H_2SO_4 solution in a single step of the large-plant conceptual flowsheet, but the removals are done in two steps in the bench-scale design. The design is presented in Fig 8.

The feed system for Subunit II provides flow metering of the light phase liquid effluent from Subunit I. The light phase flow from Subunit I is 50 wt % H_2SO_4 aqueous solution at an absolute pressure from ambient to 3.1×10^2 kPa and at a temperature from

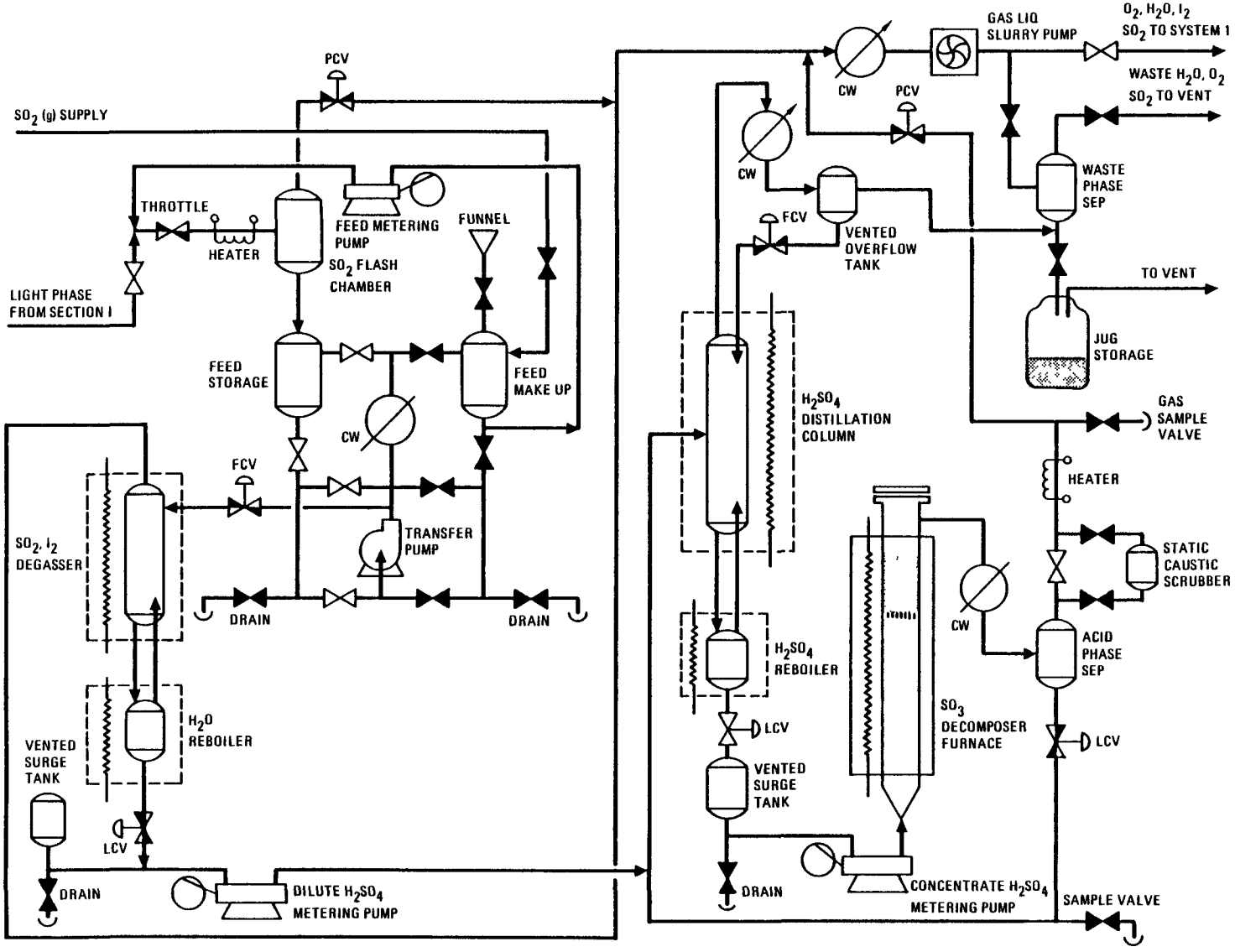

Fig. 8. Simplified bench-scale flowsheet for Subunit II (H_2SO_4-H_2O separation and decomposition)

ambient to 115°C. Variable amounts of SO_2, HI, and I_2 on the order of 0.5 to 1.5 wt % each are dissolved in the solution with some of the I_2 possibly occurring as a solid phase.

Removal of I_2 from the sulfuric acid is effected by countercurrently contacting the input liquid against heated water vapor at temperatures and times adequate to vaporize substantially all the I_2 from the liquid. The heated water vapor is generated from the liquid effluent of the countercurrent contacting operation. Figure 9 shows a diagram of the I_2 stripping column. The countercurrent contact time and temperature, which control the H_2SO_4 concentration, are used to effect the substantially complete conversion of any HI present to I_2,H_2O and SO_2 by back-reaction with H_2SO_4. After cooling, the acid solution is metered at a controlled flowrate into a fractionation still (Fig. 10). The still produces 96 wt % aqueous H_2SO_4 and H_2O vapor substantially free of H_2SO_4 in separate streams. Azeotropic H_2SO_4-H_2O is 98.4% H_2SO_4.

The H_2SO_4 decomposition system cools the 96 wt % H_2SO_4 effluent of the H_2SO_4 concentration system from its normal boiling point to 42°C. After cooling, the acid is metered at a controlled flowrate into a vertical-tube decomposition chamber in the lower portion of which vaporization of the liquid takes place. In the upper portion catalytic decomposition of the vapor occurs to within a few percent of equilibrium decomposition. The system provides decomposition temperatures from 500 to 1000°C at ambient pressure for varying catalyst bed volumes having empty tube nominal slug flow contact times of up to 10 sec for the gas. The catalyst employed during these studies has been Pt-deposited on a commercial ZrO_2 1/8 in. pellet. The preparation and performance of this catalyst are described in Ref. 1.

The system provides controllable cooling of the effluent from the decomposition chamber such that undecomposed H_2SO_4 solution may be condensed at a temperature effecting a virtually

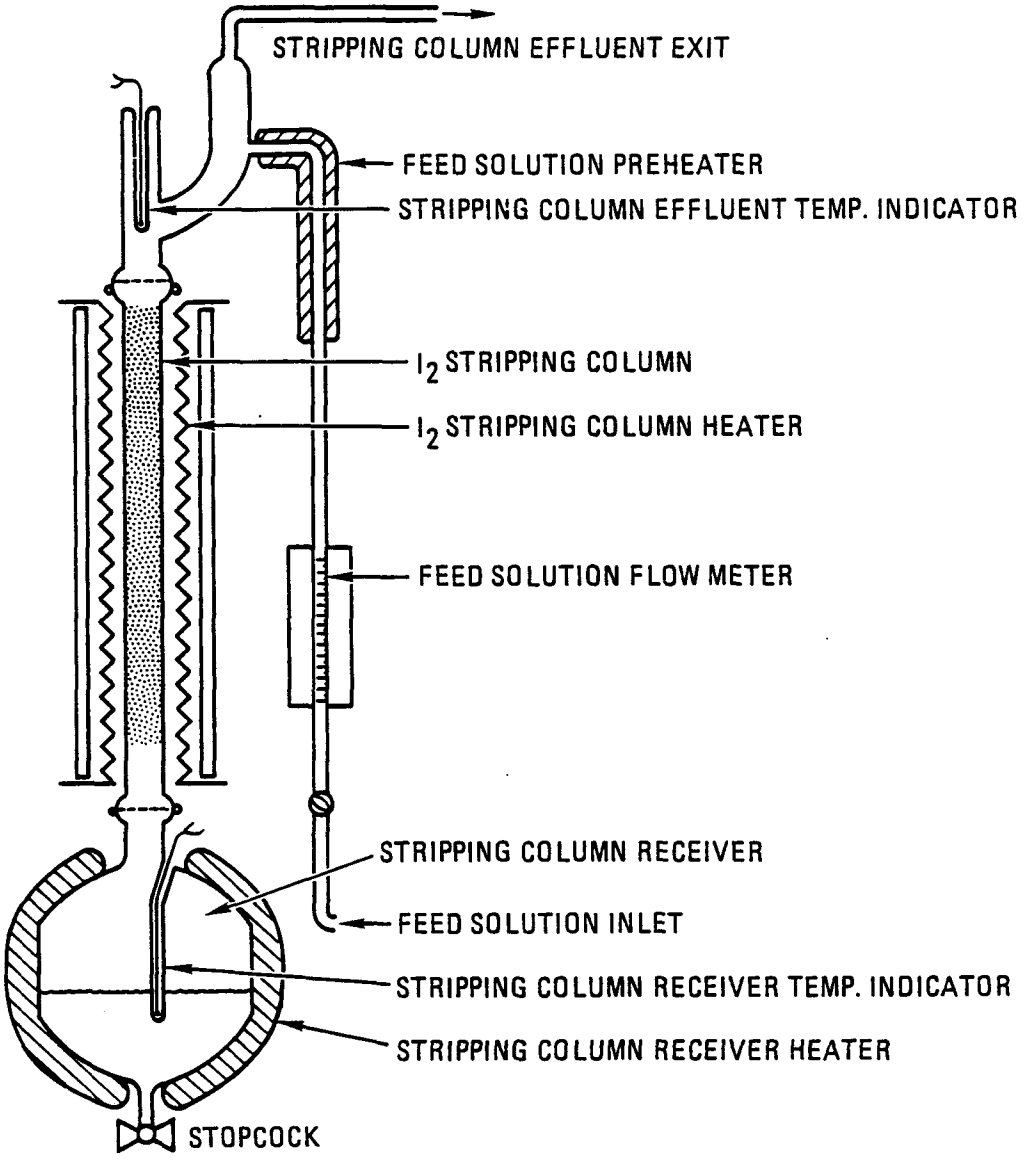

Fig. 9. Schematic of iodine stripping column in Subunit II

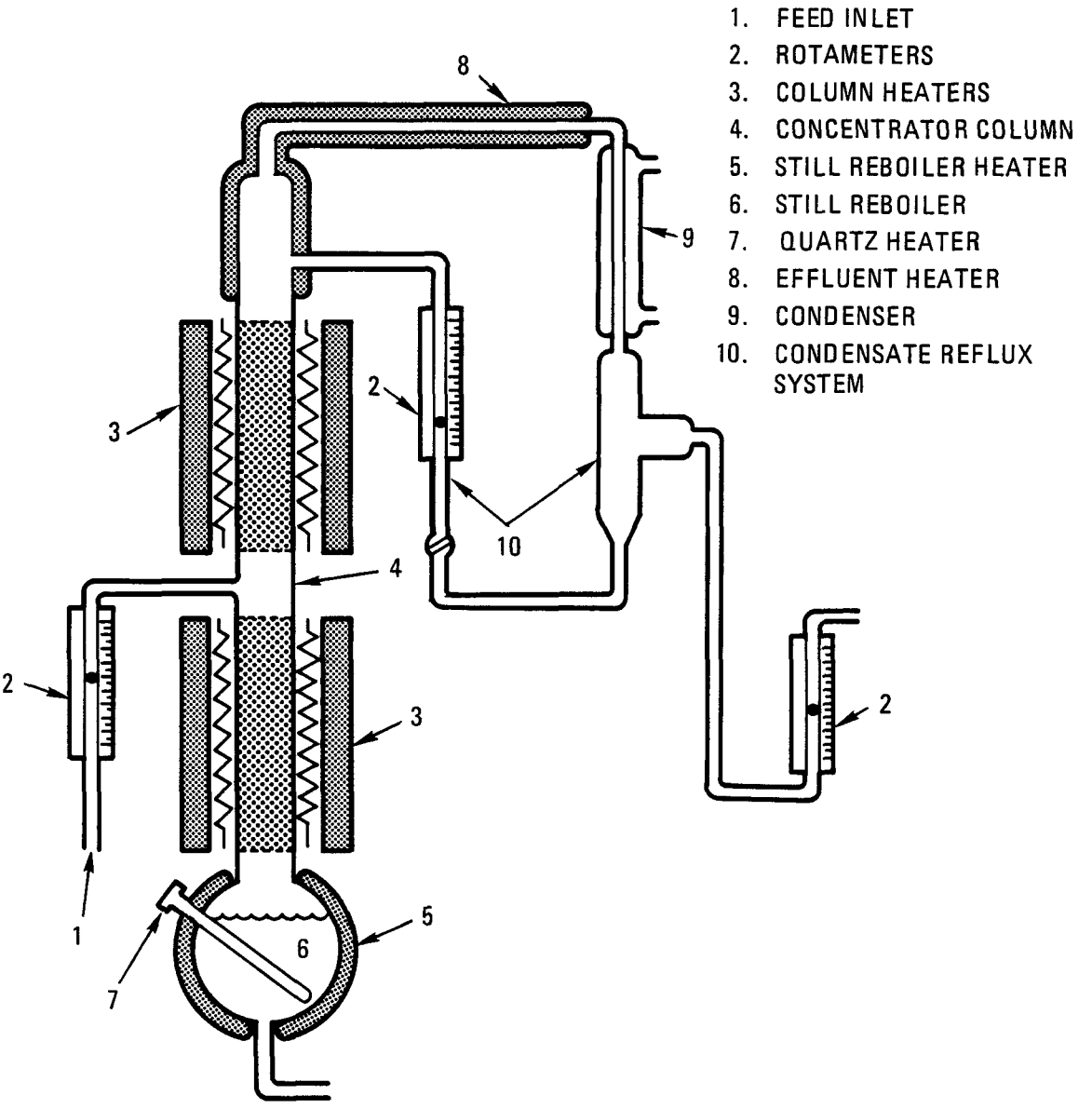

Fig. 10. Subunit II sulfuric acid concentration still

complete partitioning between H_2SO_4 and H_2O versus SO_2 and O_2. The H_2SO_4 solution and the uncondensed gases are separated. The solution can be returned as part of the still feed stream of the H_2SO_4 concentration system.

The off-gas system collects gas from the SO_2 removal step, the HI-I_2 removal system, and the H_2SO_4 decomposition system through control valves which permit regulating the pressure differential between the off-gas system and the other subsections of the overall unit. The system can discharge these mixed gases (mainly SO_2 and O_2) to the Subunit I feed inlet SO_2 stream or to a gaseous waste vent.

For the gaseous effluent of the H_2SO_4 decomposition system, the off-gas system removes substantially all SO_2 from the O_2 in a form amenable to subsequent quantitative chemical analysis, and it meters the flow of the SO_2 free gaseous effluent or the whole gaseous effluent of the H_2SO_4 decomposition system when the SO_2 removal capability is by-passed.

The materials of construction of Subunit II which contact the process materials are glass, quartz, an alumina ceramic, Teflon, polypropylene, Kynar, Hypalon, and 316 stainless steel. The foregoing selection of materials is conditioned by the commercial availability of the various equipment components at reasonable cost and with reasonable delivery times. Glass and Teflon have been preferred unless some specific consideration supervened. Quartz is used for the H_2SO_4 decomposition chamber to withstand temperatures up to 1000°C and the strong thermal gradients which will exist in the chamber. The metering pumps which seem most suited to the precise-flow feed service for the H_2SO_4 concentration still and the H_2SO_4 decomposer are commercially supplied with alumina ceramic plungers. The rotameters commercially available in the very low flow rate ranges required have Kynar end-fitting pieces. The off-gas pump capable of withstanding the corrosive action of HI and I_2 for gas-liquid-solid

flow is available with a variety of plastic body-elastomeric impeller combinations, of which a Teflon body and a Hypalon impeller seem likely to be most resistant to chemical attack. The pressure snubbers, which are incorporated with the intent of ensuring accurate instantaneous flow measurements of the H_2SO_4 concentration and H_2SO_4 decomposition feeds, are commercially available with 316 stainless steel end fittings. The feed makeup and transfer pump wetted parts are Ryton. The cooling of some streams is an adaptation to the limits on the service conditions of those materials other than glass, Teflon, and quartz instead of adhering to strict modeling of the large-plant conceptual flowsheet.

Construction of Subunit II alongside of Subunit I in the engineering laboratory was started in March 1979 and was completed in May. Equipment shakedown, including leak testing, instrument calibration, and verification of functional operability with water and inert gas, was completed in June. Subunit II is shown in Fig. 11.

As with Subunit I, no fundamental process design problems were discovered during shakedown. Several minor equipment design problems, such as pump air locks and inoperable flow indicators, were uncovered. The changes recommended to resolve these problems were implemented.

3.2.2. Operation

Operation of Subunit II was broken down naturally into three distinct phases--I_2 stripping, H_2SO_4 concentration, and H_2SO_4 decomposition. These will be individually discussed.

3.2.2.1. I_2 Stripping Experiments.

Experiments were carried out in Subunit II to establish design parameters for the iodine removal from the upper phase

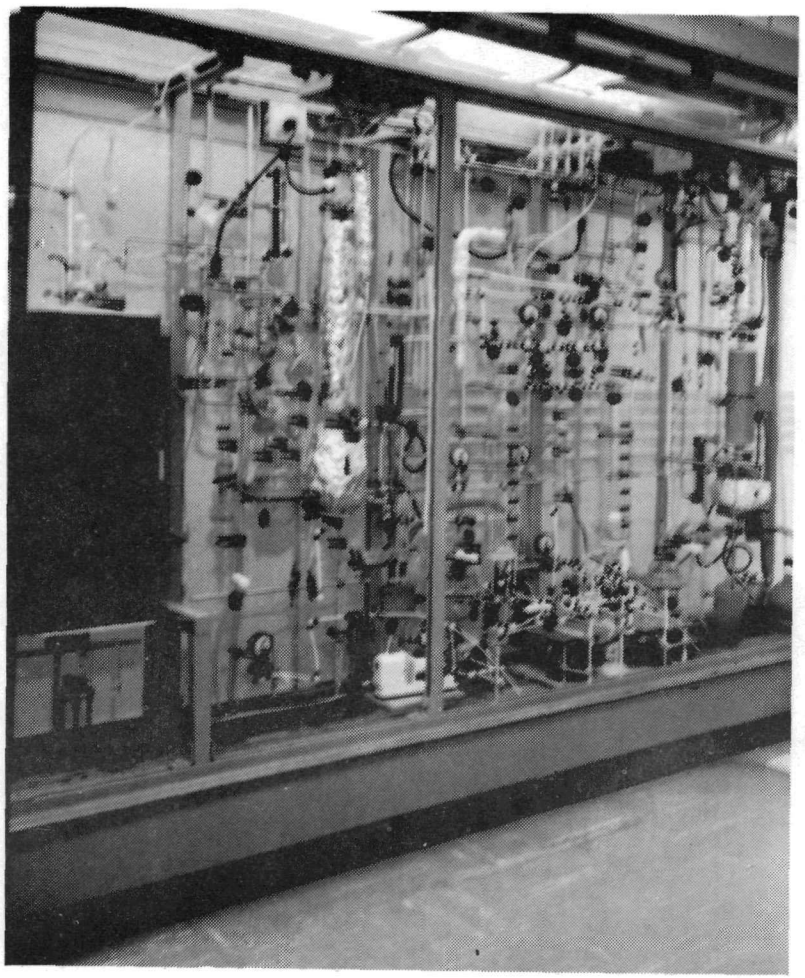

(a)

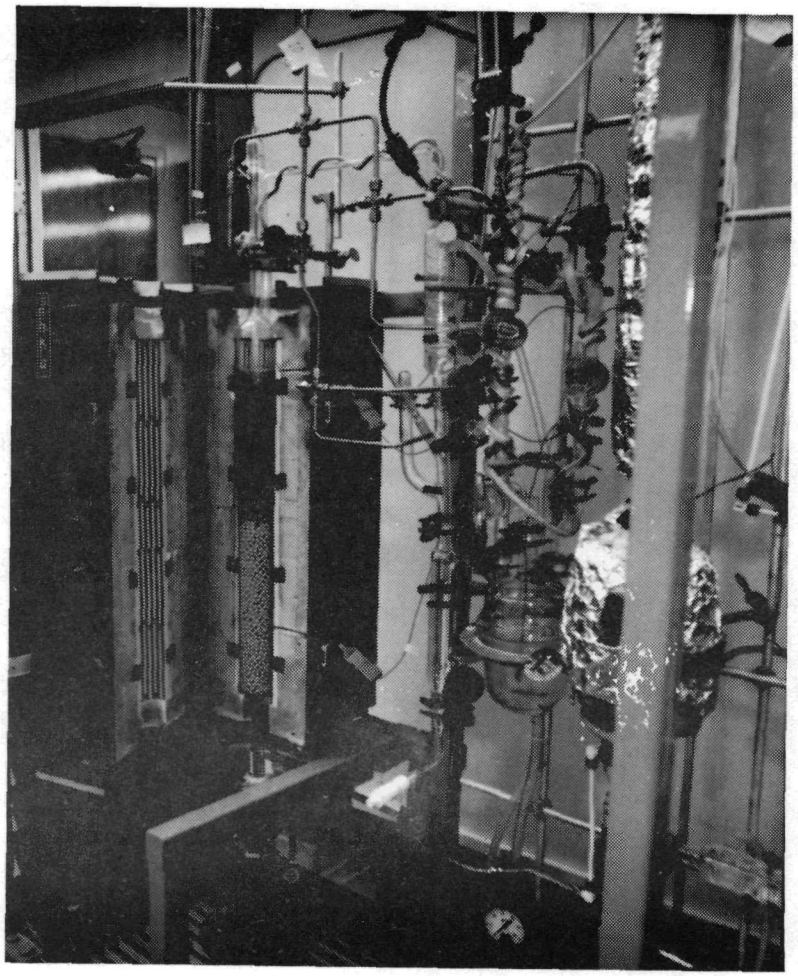

(b)

Fig. 11. Bench-scale Subunit II: (a) overview, (b) SO_3 decomposer with catalyst in place

sulfuric acid. Removal of the iodine from the upper phase will reduce potential corrosion problems during final concentration of the acid and allow the use of lower cost system construction materials.

Before these experiments could get underway, a problem had to be faced with the feed to this equipment. The centrifugal pumps had to be replaced with inert gas pressurization to initiate system flows. Through what appears to be a nucleation controlled process, the centrifugal pumps caused precipitation of I_2 crystals and possibly sulfur from the fluids with concomitant problems of partial flow blockage and feed concentration changes. This problem occurred when the synthetic feed solutions were stored a relatively long time (1 hr or more). Apparently, storage for these lengths of time results in a supersaturation of I_2 and sulfur due to slow back reaction of the H_2SO_4 and HI in solution. In light of this problem, a series of tests was conducted to determine the highest levels of I_2 concentration that could be obtained in a 50 wt % solution of H_2SO_4 and a 1.2 wt % solution of HI. The I_2 concentration levels that were tested were 0.2, 0.4, 0.6, and 0.8 wt % in the above H_2SO_4,HI feed solution.

The I_2 crystals were weighed and dissolved in the HI. This solution was then added to the 50 wt % H_2SO_4 in small aliquots while the H_2SO_4 solution was being agitated. The four different solutions containing the various concentrations of I_2 were allowed to sit until precipitation of I_2 crystals was observed. Results are as follows:

1. 0.2 wt % - no precipitation in 18 hr.
2. 0.4 wt % - no precipitation in 18 hr.
3. 0.6 wt % - I_2 precipitation occurred overnight.
4. 0.8 wt % - immediate precipitation.

All feed solutions prepared in the laboratory for use in Subunit II contained 50 wt % H_2SO_4, 1.2 wt % HI, and 0.6 wt % I_2.

All data presented for Subunit II are based on the above formula unless otherwise noted.

Three long-term experiments (3260-79, 3260-83, and 3260-90) utilizing the I_2 stripping column (Fig. 9) were completed. Experiment 3260-79 was for a duration of 390 min (6.5 hr), experiment 3260-83 was for a duration of 542 min (9.0 hr), and experiment 3260-90 was for a duration of 690 min (11.5 hr). Figures 12, 13, and 14 show the temperatures for the various components versus time for all three runs.

The I_2 stripping column (Fig. 9) consists of a quartz tube 60 cm in length by 3 cm in diameter filled with glass beads (3 mm dia). It is resistance heated externally (heating tape) and insulated with fiber fray. In its present setup, utilizing the highest flowrate tested (17 cc/min), a maximum internal temperature of 185°C can be achieved.

Table 2 shows the internal temperatures along with the data collected. As can be observed from the table, very low concentrations were achieved, but at the present time exact permissible levels of I_2 concentrations are not known. Figure 15 shows I_2 concentration versus internal column temperature (since no thermocouple exists inside the column, temperatures were calculated using measured H_2SO_4 concentration at the exit of the column), and it can be seen that higher temperatures at the flowrates used would not appreciably decrease the I_2 content of the cleaned feed solution.

The results indicate that, with flowrates of 10 and 17 cm^3 feed solution/min, very good stripping of the iodine can be achieved at relatively low temperatures. At a flowrate of 5 cm^3/min, bypass flow occurs in the column, and the results are somewhat erratic.

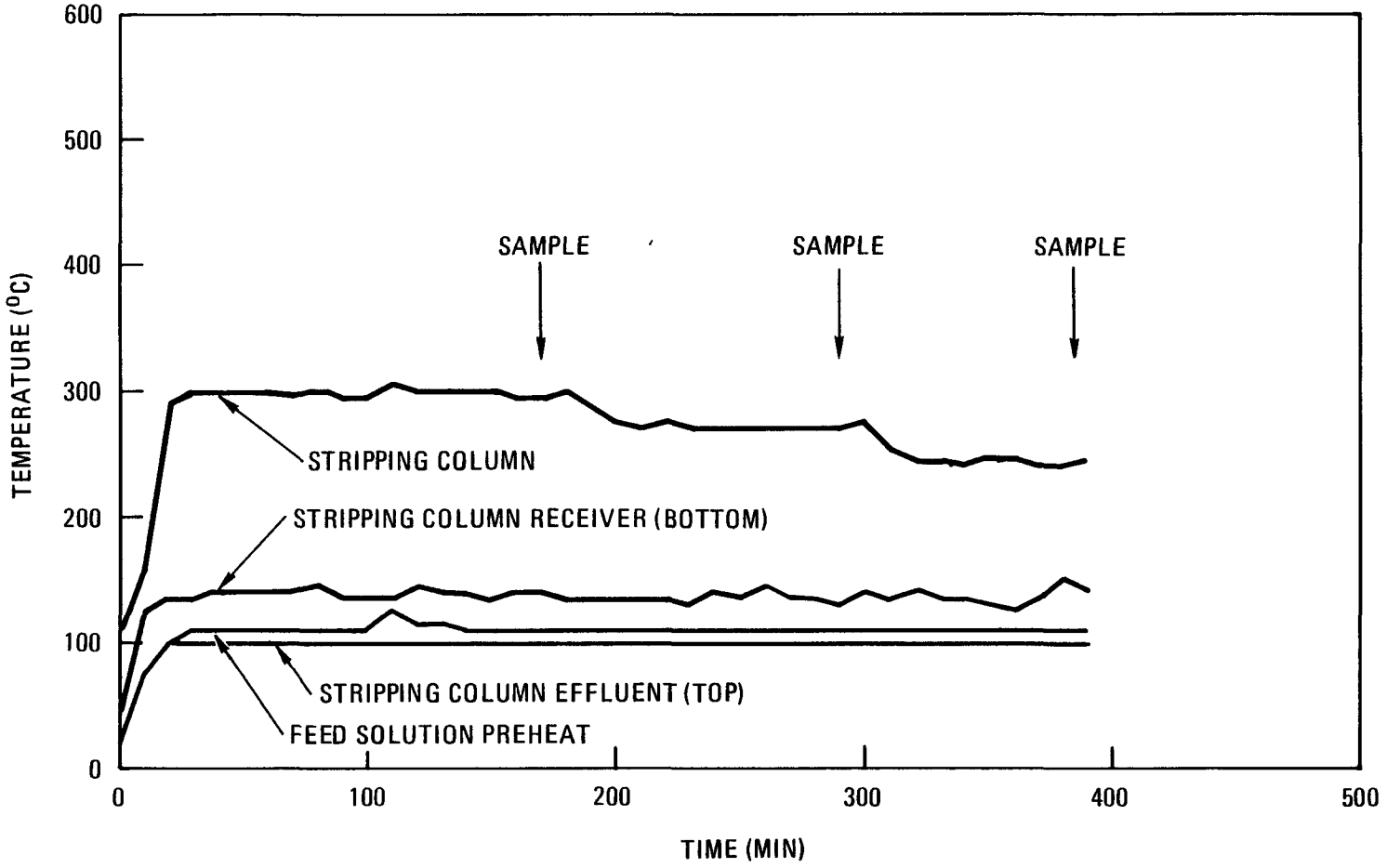

Fig. 12. Subunit II experiment 3260-79

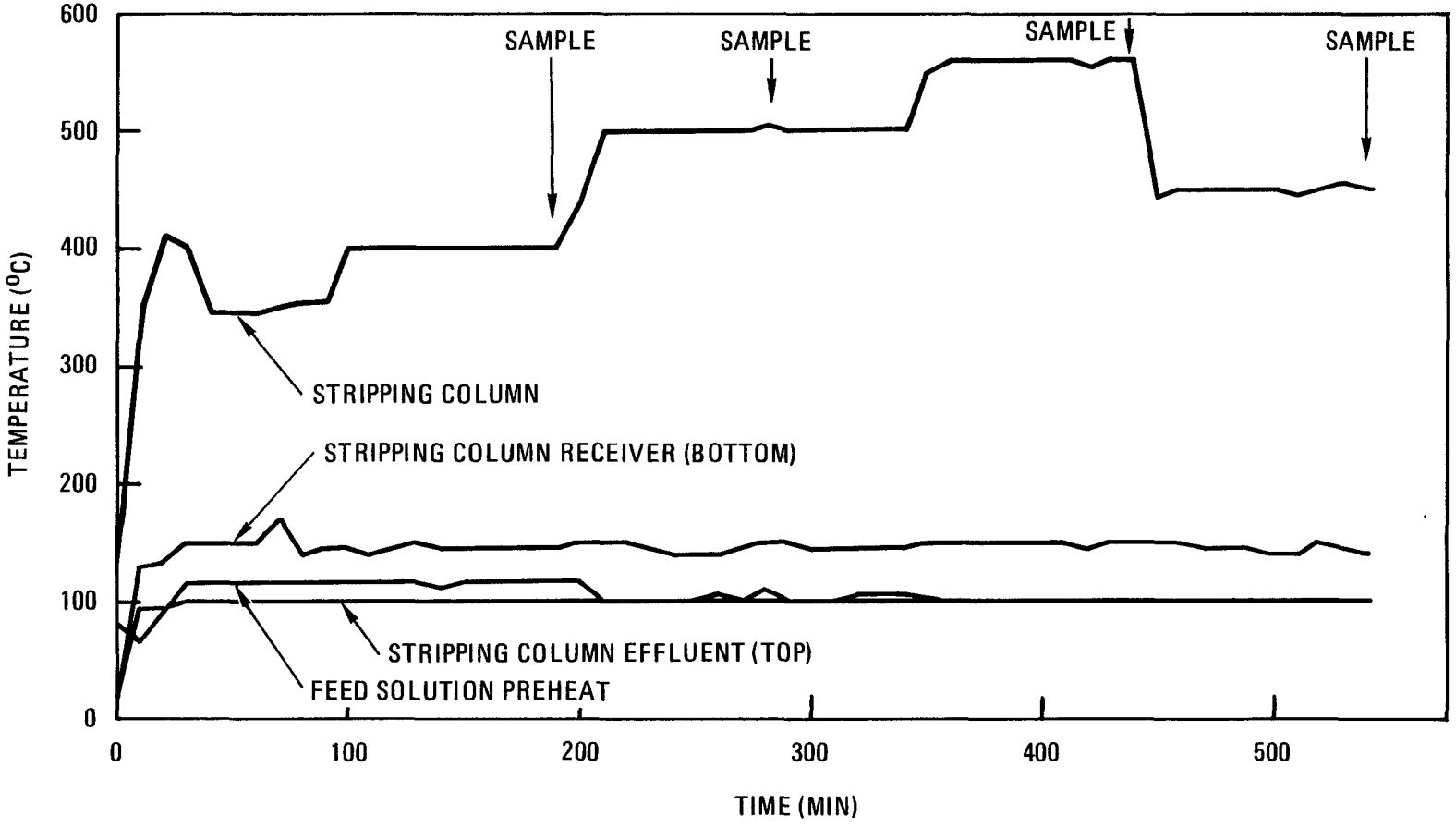

Fig. 13. Subunit II experiment 3260-83

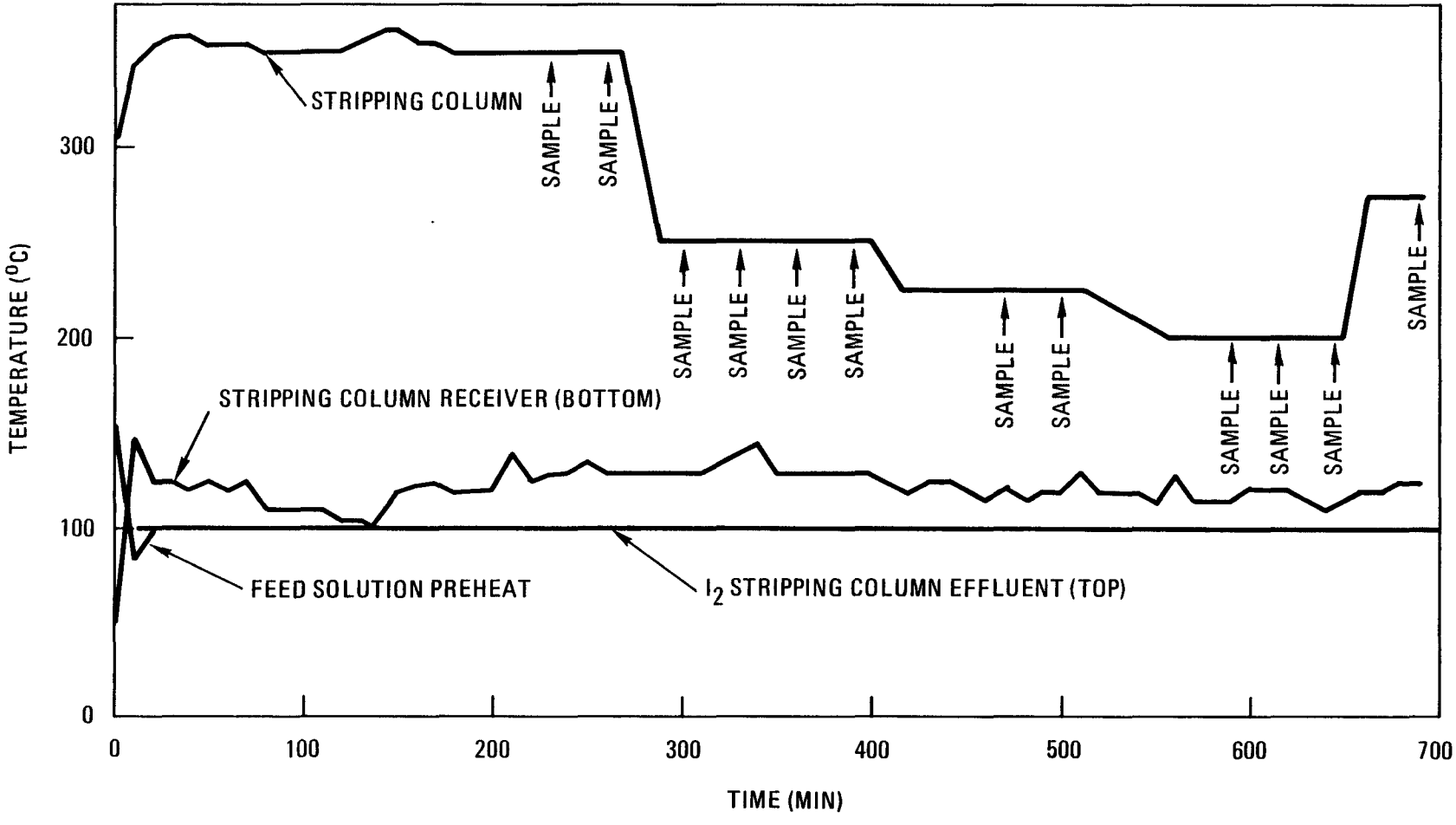

Fig. 14. Subunit II experiment 3260-90

TABLE 2
RESULTS OF I_2 STRIPPING EXPERIMENTS

SAMPLE NO.	COLUMN TEMPERATURE (°C)	FEED FLOWRATE (cm^3/MIN)	H_2SO_4 CONCENTRATION (WT %)	I_2 CONCENTRATION(a) (ppm)
3260-79-1030	148	10	63.9	1.86
3260-79-1230	141	10	60.6	4.82
3260-79-1407	133	10	56.9	14.35
3260-83-1058	160	10	68.3	0.66
3260-83-1326	164	17	69.6	3.26
3260-83-1508	185	17	75.9	1.15
3260-83-1645	150	17	64.2	7.88
3260-90-1750	135	5.0	57.9	23.54
3260-90-1815	141	5.0	60.5	15.13
3260-90-1895	132	5.0	56.4	15.33
3260-90-1550	138	5.0	59.5	---
3260-90-1620	140	5.0	60.0	14.86
3260-90-1303	152	5.0	65.7	---
3260-90-1333	158	5.0	67.5	---
3260-90-1403	148	5.0	64.0	2.89
3260-90-1430	143	5.0	62.5	0.76
3260-90-1930	197	5.0	78.9	0.99
3260-90-1053	228	5.0	93.3	---
3260-90-1123	228	5.0	93.4	0.0

(a) I_2 concentration includes I_2 in the form I_2 and HI.

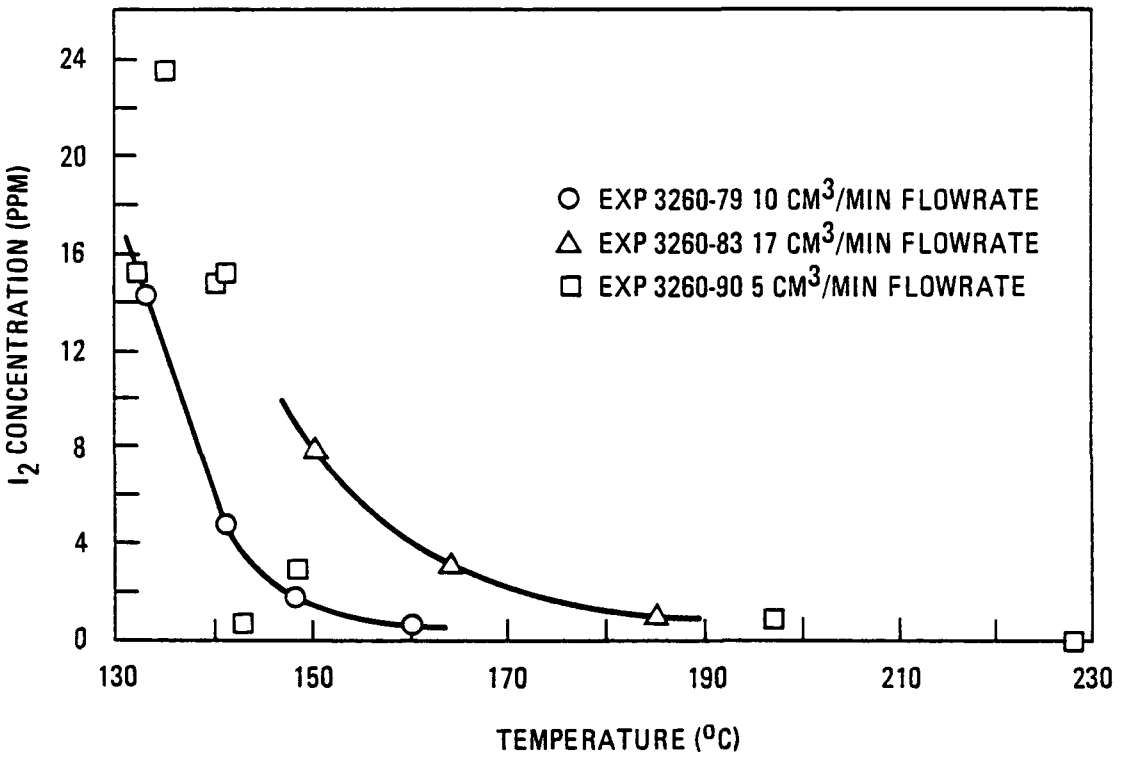

Fig. 15. I_2 concentration versus column temperature for Subunit II for 5, 10, and 17 cm^3/min feed flowrates

When the 10 cm^3/min and the 17 cm^3/min feed flow curves of Fig. 15 are compared, the concentration of changed I_2 in the effluent increases by a factor of 3.5 when the flowrate is increased by a region factor of 1.7 with constant temperature at the bottom of the column. Since the constant temperature is a boiling condition, the column bottom concentration is the same at both flowrates; and the liquid-to-vapor flowrate mole ratio of the column is practically unchanged. With constant feed input composition at the top, the operating vapor equilibrium line behavior on a mole fraction plot should be nearly unchanged for the observed large shift in the bottom liquid concentration with flowrate. That simple interphase diffusion is the dominant mass transfer resistance mechanism is unlikely. The effect of gas flowrate on the height of a transfer unit is, in general, small, as is the effect of liquid flowrate.

Probably, the I_2 concentration in the liquid effluent is controlled by the rate of reaction between HI and H_2SO_4 to generate free, volatile I_2. Also, probably, the average residence time of the fluid flowing through the column and the rate of steam flow are important parameters with respect to this reaction.

Analysis of the above experiments (the I_2 stripped feed solutions) was by conventional methods. H_2SO_4 analysis was by titration with 1.0 M NaOH, and total I_2 analysis was by activation analysis.

3.2.2.2. H_2SO_4 Concentration Experiments.

The H_2SO_4 concentration process provides 96 wt % H_2SO_4 to the SO_3 decomposer. Since extensive vapor-liquid equilibria data already exist for the H_2SO_4-H_2O system, the only data taken in these bench-scale studies were operational with respect to accepting the upstream output rate and meeting the downstream input concentration specification.

For a feed rate of 5 cm^3/min of 60 wt % H_2SO_4 (equivalent to 1 standard liter/min H_2), the equipment was able to supply H_2SO_4 in excess of 96 wt % without the originally specified feed preheater. With an Inconel feed preheater installed, the concentrated H_2SO_4 output rate (equivalent to 2 standard liters/min H_2) could be doubled; but the metal contamination of the product, judged qualitatively by color change, was deemed unacceptable. As a practical solution, the required additional heat was supplied via a quartz immersion heater in the still pot. This arrangement operated satisfactorily for 10 cm^3/min feed rates of 60 wt % H_2SO_4. Figure 10 shows the H_2SO_4 concentration still with the immersion heater.

Four complete runs proved attainment of satisfactory operation at initial design levels.

Experiment 3260-94 was run 410 min (6.8 hr) at a feed flowrate of 10 cc/min of 60 wt % H_2SO_4. In this experiment, shown in Fig. 16, temperatures of the various still components were brought to operating levels before introduction of flow. As can be seen from Fig. 16 (temperature of still components versus time), the still reboiler temperature could not be maintained at 330°C, the temperature necessary to produce H_2SO_4 concentration levels of greater than 96 wt %. The 10 cc/min flowrate on experiment 3260-94 is approximately twice the initial design limit. A feed preheater was not used during this run.

Experiment 3260-95 was run 180 minutes (3 hr) at design flowrate of 5 cc/min. The flow of feed solution was started before operating temperatures were reached (Fig. 17). The still reboiler temperature climbed to normal operating levels, and samples taken at this point showed H_2SO_4 concentration to be 96.4 wt %. At this point feed flowrate was increased to 12.5 cc/min with immediate temperature drop in the still reboiler.

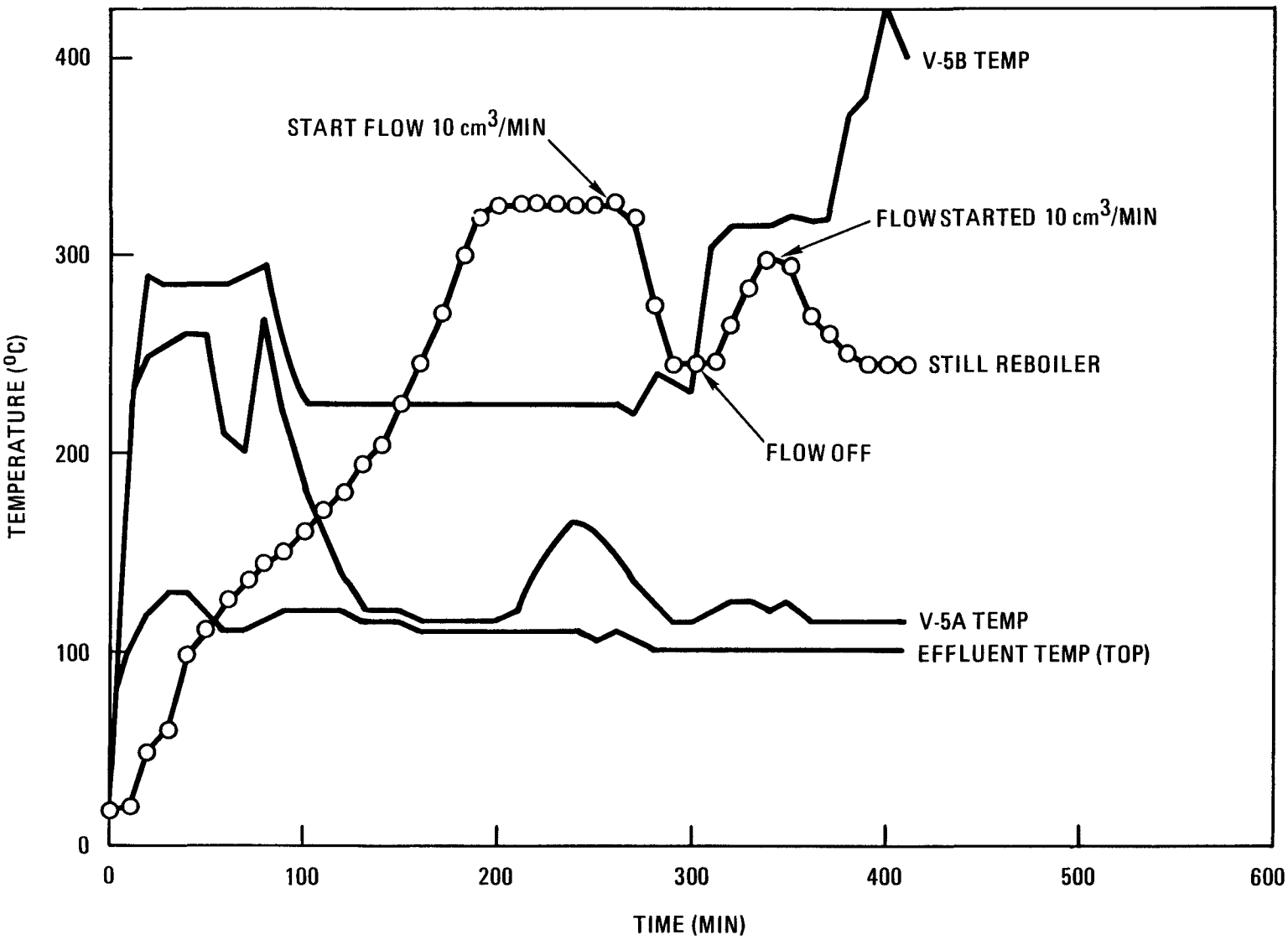

Fig. 16. Subunit II experiment 3260-94

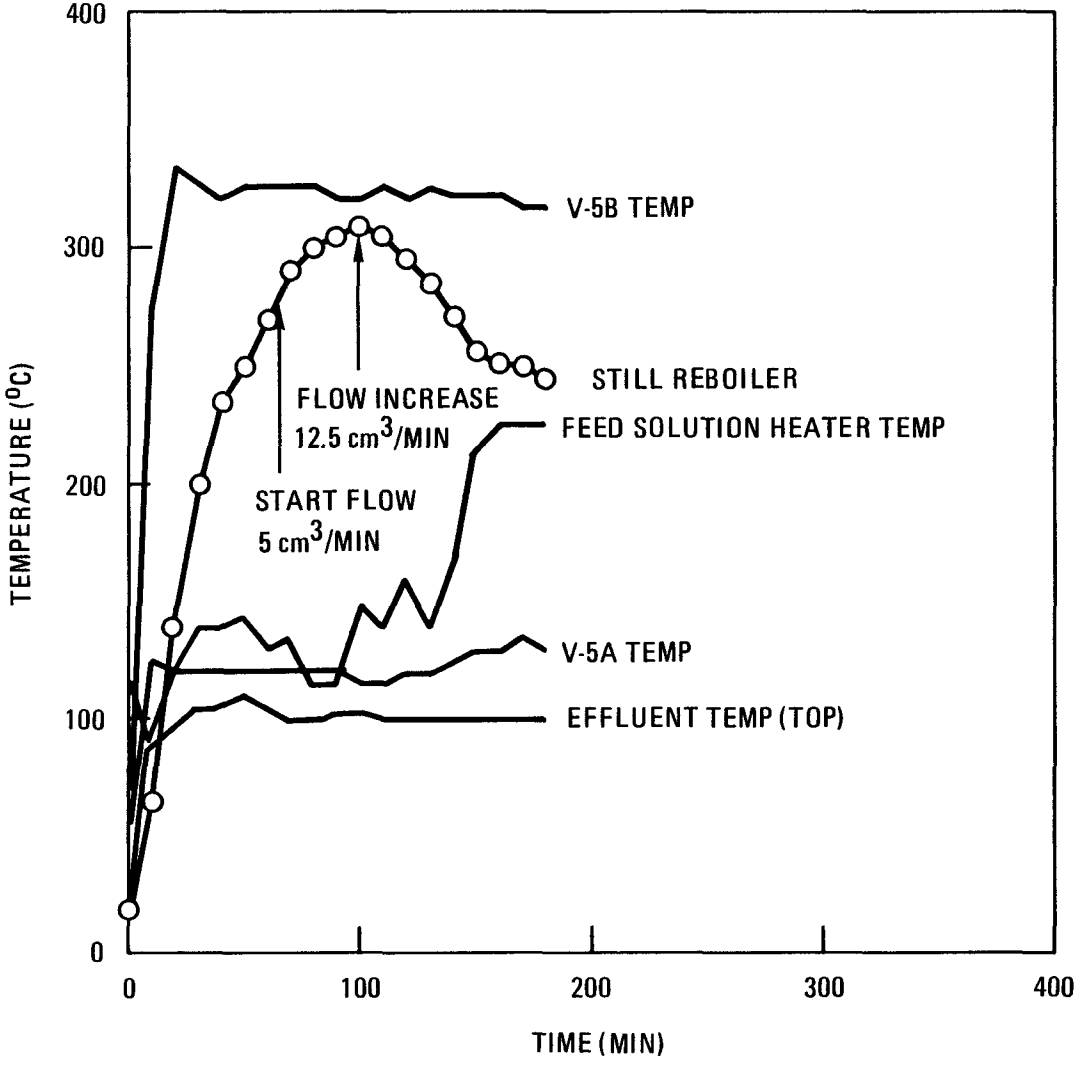

Fig. 17. Subunit II experiment 3260-95

Experiment 3260-96 was run for 280 min (4.7 hr) at a feed flowrate of 10 cc/min. As can be seen from Fig. 18, immediate decay in still reboiler temperature occurred upon introduction of feed flow. A design change was required on the still reboiler.

At flowrates higher than design limit (5 cc/min 60 wt % H_2SO_4), still reboiler temperature could not be maintained at an acceptable level (320 to 330°C) and modification was necessary if higher flowrates (greater than 5 cc/min) were to be used. A quartz immersion heater was fabricated into the reboiler still so additional heat could be added when necessary.

Experiment 3260-103 was run for a total of 3 hr. The H_2SO_4 concentrator section was heated to normal operating temperatures (still reboiler at 325°C) before introducing flow. Flow was started at 5 cc/min of 60 wt % H_2SO_4 and temperature was allowed to equilibrate. At 5 cc/min flow the still reboiler maintained its initial starting temperature of 325°C. Flowrate was then increased to 10 cc/min, and still reboiler temperature decayed to 300°C. At this point the quartz immersion heater was turned on and temperature in the still reboiler recovered to initial 325°C in 15 min. The system was allowed to run until equilibrium was obtained (constant still reboiler temperature); then the system was shut down. The data for this experiment are shown in Fig. 19. The introduction of the quartz immersion heater to the system now allows increasing H_2SO_4 flowrates to greater than twice design limits. The operation of this apparatus is considered to exceed design limits and awaits utilization in the integrated Subunit II.

3.2.2.3. H_2SO_4 Decomposition Experiments.

Experiments were run which had the goals of evaluating the decomposition of H_2SO_4 into SO_2, H_2O, and O_2 and observing any catalyst changes in the bench-scale apparatus as shown in Fig. 20. A platinum-on-commercial-zirconia substrate, 0.3175 cm (1/8

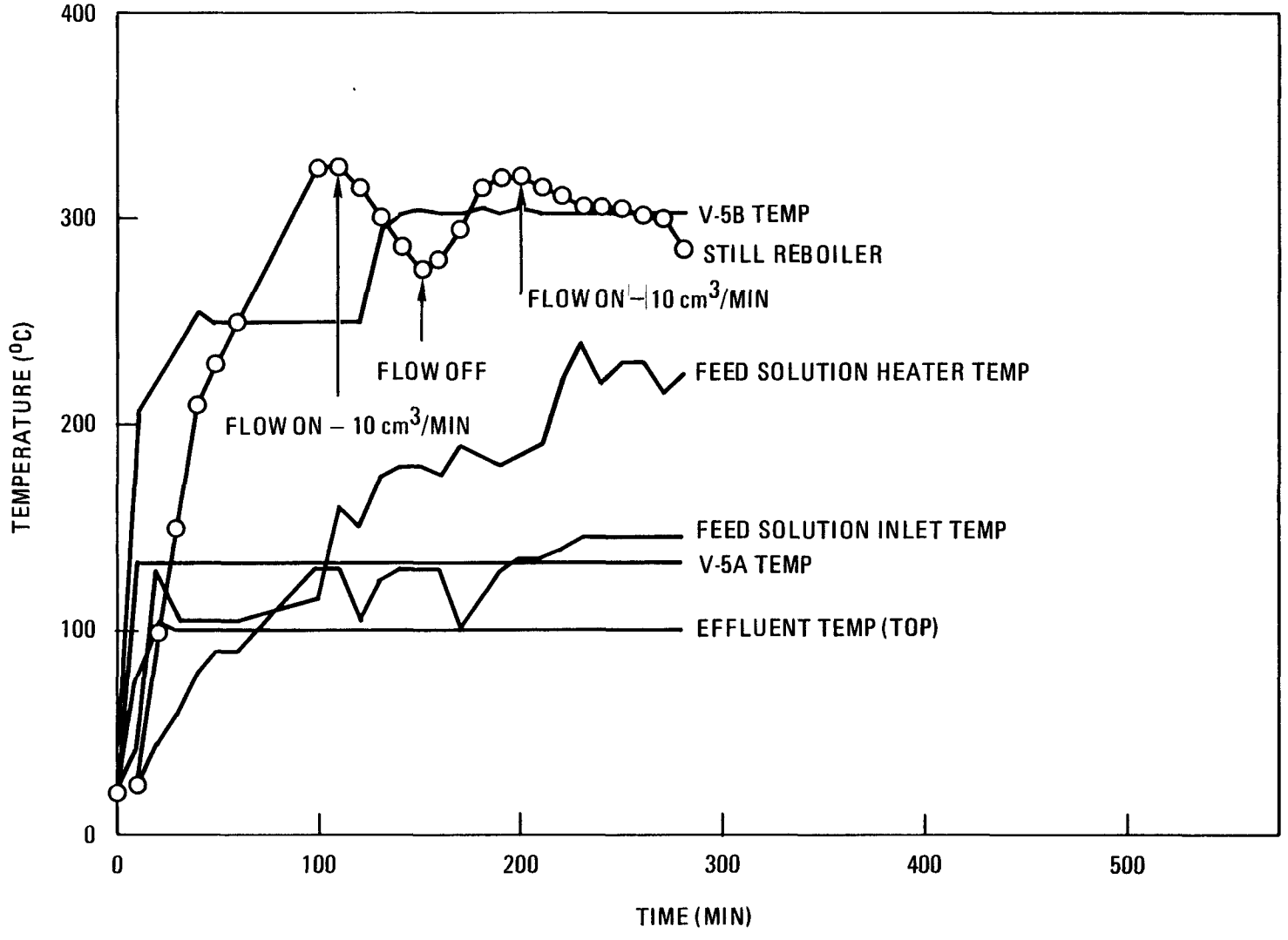

Fig. 18. Subunit II experiment 3260-96

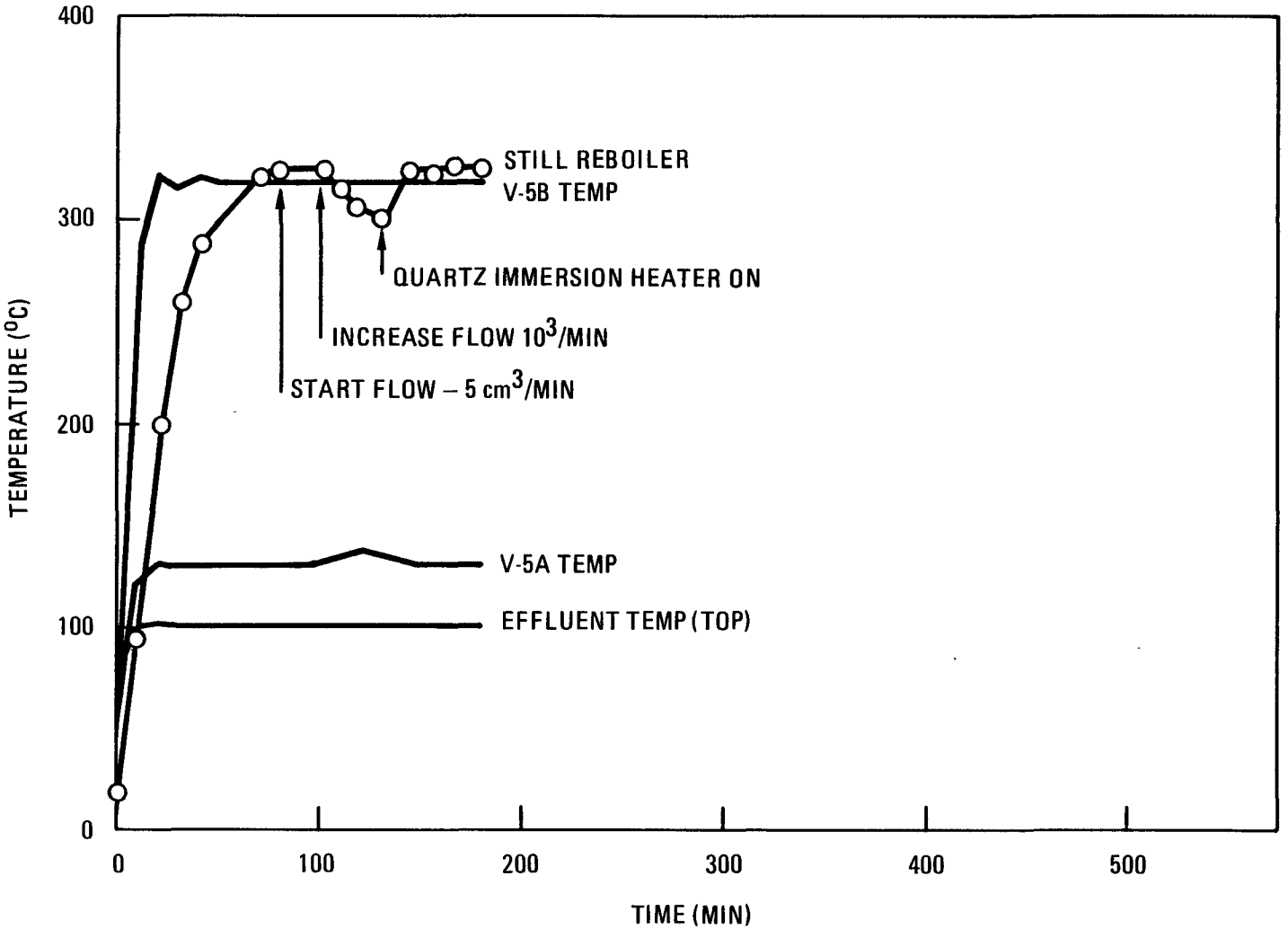

Fig. 19. Subunit II experiment 3260-103

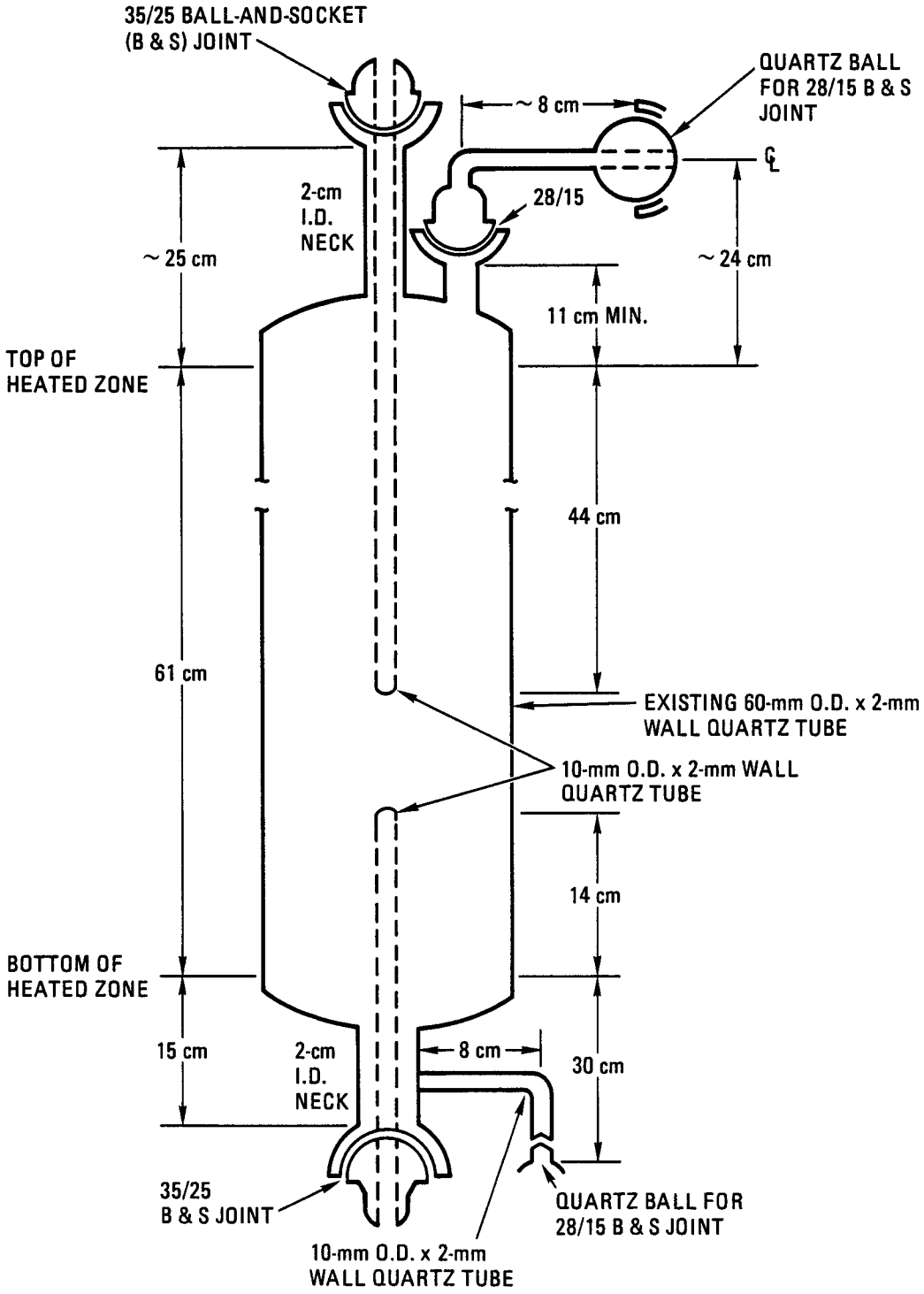

Fig. 20. Decomposer furnace tube

in. diameter), right cylinder pellets loaded at GA with 0.2 wt % platinum, was used at temperatures between 800° and 900°C. The gas slugflow residence time in the reactor was between 0.3 and 1 s.

As a preliminary to bench-scale evaluation experimentation, furnace operation as a combination boiler and decomposer was investigated. Mapping temperatures while the reactor was running was an important test procedure. Temperatures were mapped using a thermocouple in the central penetrations in the reactor. The temperature maps are presented in Fig. 21. Two maps are shown. One is for a no-flow circumstance and basically charts the heat supply and leakage effects. One observes distinct heat leakage from the ends of the reactor as evidenced by the temperature gradients toward the ends. This, of course, represents only a maintenance load. The flow circumstance represents a process load and greatly modifies the temperature pattern. At the inlet end one observes a gradient representing heating of liquid H_2SO_4. The first plateau represents the boiling of the H_2SO_4. The following sharp temperature rise represents dissociating $H_2SO_4(g)$ to SO_3 and H_2O. This process is seen to level out forming a plateau just before catalyst contact. The actual plateau region is caused by the large heat demand at the catalyst interface for this very fast catalytic reaction where most of the decomposition of SO_3 to SO_2 takes place. The slow rise corresponds to the continued SO_3 decomposition and gas heatup until the point in the furnace where the final equilibrium is attained. One should note that the natural heat leakage at the end of the furnace causes the temperature to fall. If, in this falling temperature region, catalyst resides, recombination will occur such that the product will be characteristic of these lower temperatures rather than the high plateau temperature. For this reason catalyst is only loaded to the 50.8-cm (20-in.) position.

For the furnace and catalyst configuration described above, Fig. 22 presents the conversion of the furnace as anticipated

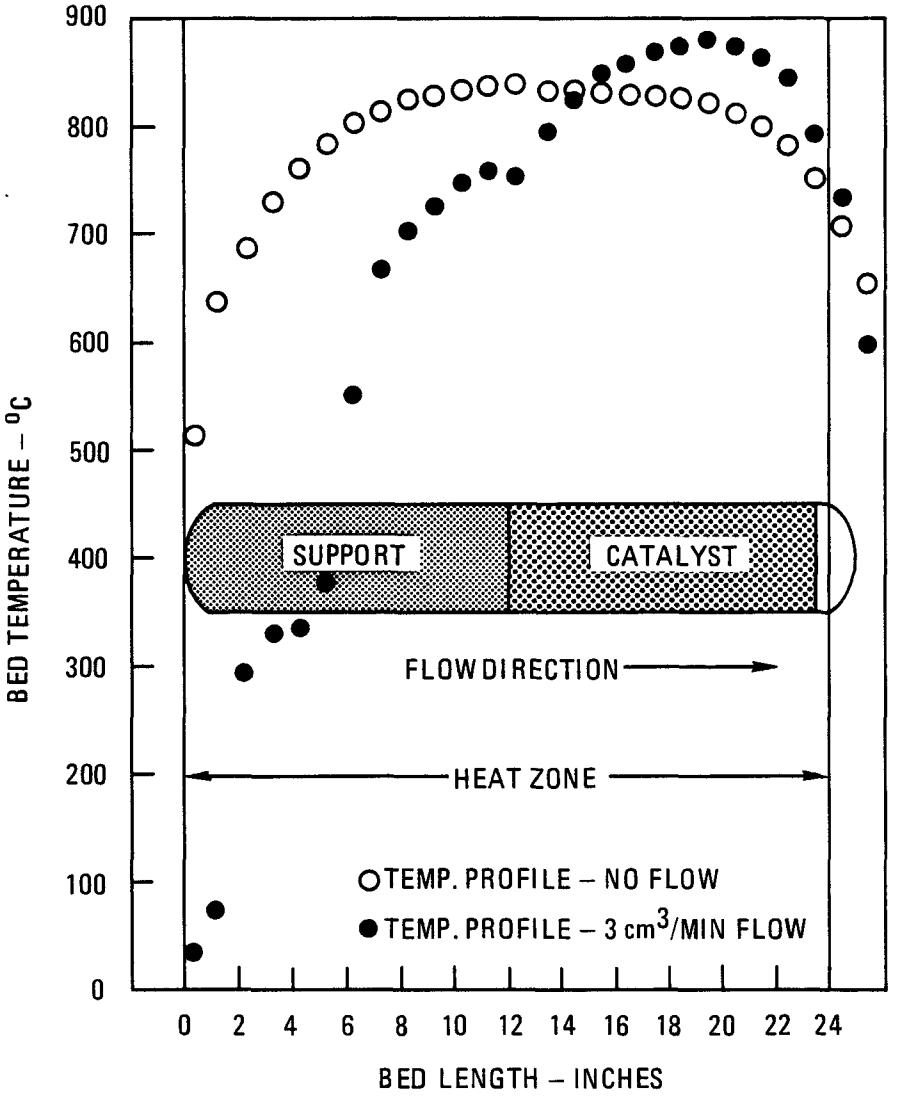

Fig. 21. Subunit II experiment 3260-97

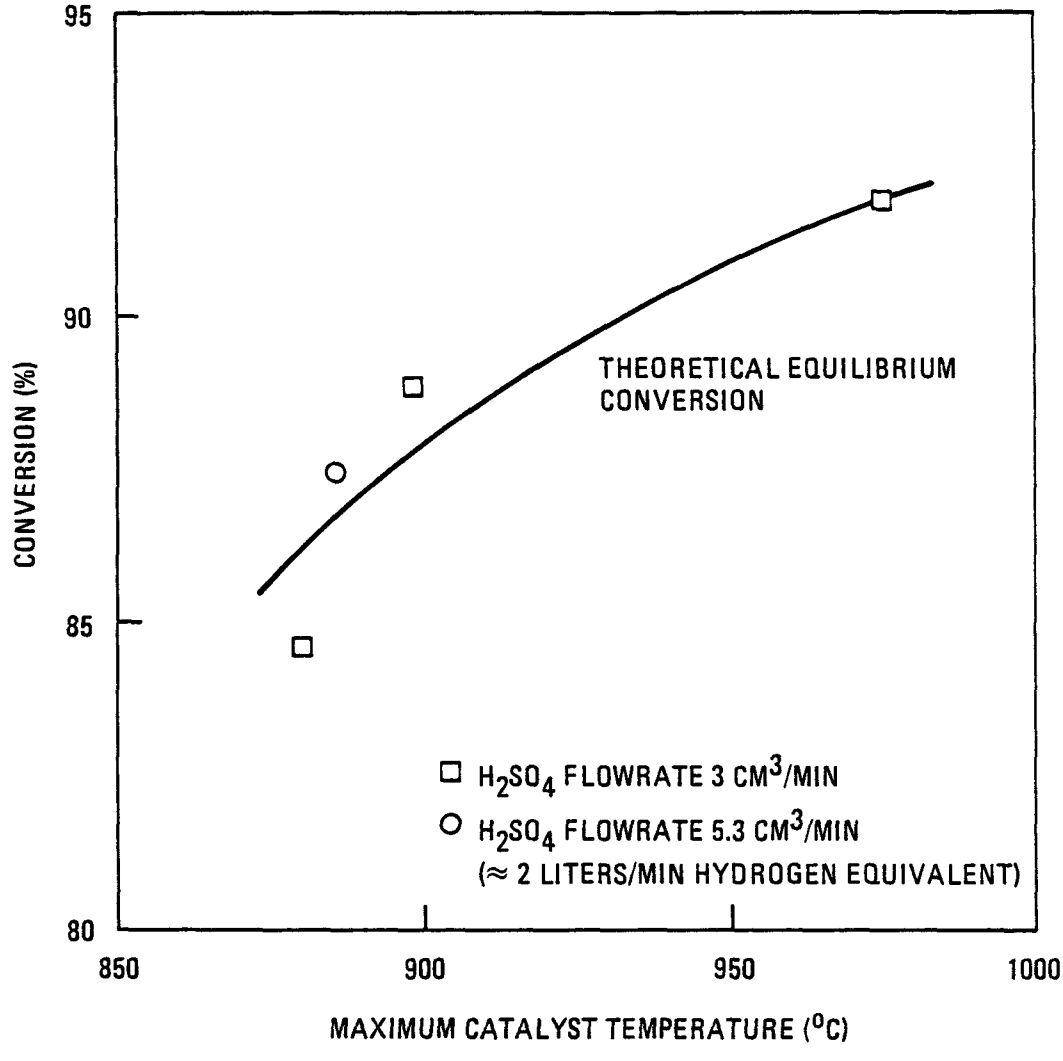

Fig. 22. Performance of bench-scale H_2SO_4 decomposition equipment

using thermodynamic data for the maximum temperature of the furnace for the four runs obtained thus far. These data points were calculated by measuring both (1) the amount of unreacted H_2SO_4 which condensed in the decomposer effluent and the amount of SO_2 absorbed in caustic solution, and (2) the oxygen output flowrate after the caustic absorption of SO_2. The two methods agree to within 5%, with the first method being preferred as the more accurate; this method is the basis for the Fig. 22 data. Catalyst bed temperature was taken to be the maximum reading of an axial temperature traverse of the bed taken during steady-state operation.

Liquid sulfuric acid flowrates of 3.0 and 5.3 cm^3/min (equivalent to 1.1 and 2.0 standard liters/min H_2, respectively) were employed. The experimental results are within 2% of the theoretical prediction using the maximum catalyst temperature and the equilibrium composition calculated from the JANAF tables (Ref. 13). The low point at 875°C in Fig. 22 was obtained in a loading of the catalyst bed for which a significant portion of the bed was in a region near the exit where the temperature had substantially fallen off from the maximum near the axial center of the decomposer. This resulted in the significant back reaction of the decomposition products from the hotter region and thus the low conversion compared to theoretical. This problem was rectified as described by shortening the catalyst bed. The other data points in Fig. 22 were taken using such a configuration. Table 3 reports the H_2SO_4 decomposition run data. Flow rate effects on conversion appeared to be unobservable.

In the first decomposition run, zirconia pellets without platinum were used to support the catalyst in the hottest zone of the vertical furnace. The zirconia bed support at the boiling interface of the concentrated H_2SO_4 feed was chemically attacked sufficiently to make desirable replacement with some other support material. The zirconia support pellets were replaced by a high silica (53 wt % SiO_2) aluminosilicate ceramic, 1.27 cm (0.5

TABLE 3
H_2SO_4 DECOMPOSITION RUN DATA

RUN NO.	H_2SO_4 FEED RATE (CC/MIN)	PERCENT H_2SO_4 DECOMPOSED	MAX. CATALYST TEMP. (°C)	TOP-OF-BED CATALYST TEMP. (°C)	WT % H_2SO_4 ACID CONDENSATE
3260-97	3	84.6	880*	795*	49.7
3260-98	3	88.9	897	882	40.5
3260-98	3	91.9	973	942	32.4
3260-100	6	87.4	885	870	43.9

* Length of catalyst bed was 2 inches longer on this run than for all the others, and extended 2 inches closer to further outlet.

in.) diameter spheres, with the trade name Denstone (a product of Norton Company). This support material showed only slight color change and surface roughening at the boiling interface after the first run and no discernible further change in subsequent runs. Additionally, a rust-pink band was seen deposited on the reactor tube wall after the first run with the Denstone support, although it was not discernible on the catalyst itself, and no change in catalyst activity was detected in any of the runs. The band might be associated with some iron extraction from the Denstone balls.

This portion of Subunit II performed up to expectations in the final experiments and is considered operational.

3.2.2.4. Joint Operation of the Components of Subunit II.

The overall simultaneous operation of all Subunit II components was demonstrated at a flowrate equivalent to 2 standard liters/min H_2. All process steps functioned as designed until after 12 to 14 hr operation, when apparent cyclic thermal ratcheting of the large rough-surfaced spherical Denstone support pellets against the quartz reaction tube of the decomposer caused tube breakage. Use of smaller particles of irregular shape (possibly cracked Denstone spheroids) is expected to eliminate this problem, which in the projected metal tube reactors would not even have been observed.

3.3. SUBUNIT III

3.3.1. Introduction

Processing of the lower phase product of the main reaction to produce H_2 is accomplished in this unit. The unit operations performed are (1) the removal of dissolved SO_2 from the lower phase product, (2) the countercurrent treatment of the degassed solution with a concentrated H_3PO_4, resulting in stripping the HI

and H_2O from the lower phase, (3) washing the resultant I_2( ) for recycle to the main reaction in Subunit I, (4) distilling the HI out of the H_3PO_4 solution, (5) reconcentrating the H_3PO_4, (6) catalytically decomposing HI, and (7) recovering for recycle or distribution reactant HI and products I_2 and H_2. The first three unit operations take place in a single hot box process. The fourth unit operation takes place in a distillation column, the fifth in another distillation unit, and the sixth and seventh operations in yet another section of the bench-scale unit. The operation of Subunit III will be discussed in terms of this listing--that is, unit operations 1, 2, and 3 in the lower phase treatment section, 4 in HI distillation, 5 in H_3PO_4 recovery, and 6 and 7 in HI decomposition. This subunit design is shown in Figs. 23 and 24.

3.3.2. Lower Phase Processing

The removal of SO_2 from lower phase is accomplished in a hot box operation as illustrated in Fig. 25. The upper portion of one of the two packed columns in this figure represents a countercurrent inert gas purging system in which the SO_2 is removed from lower phase. This unit, along with the rest of the hot box operation, has been tested with lower phase made in Subunit I. The success of this gas purge is evidenced by the apparent lack of appearance of sulfur downstream. Analytical results on the iodine for determining its sulfur content have not yet been obtained in this operation, but it has been experienced that moderate quantities of sulfur generation are easily apparent as well as generated H_2S. Neither were detected. Thus, one can project that the SO_2 removal system was working.

The I_2 knockout columns, redesigned by replacing the three original columns by two longer columns, are also in the hot box. The first column, after gas purging the SO_2, is used to countercurrently contact lower phase with concentrated H_3PO_4 in a Raschig ring packed column.

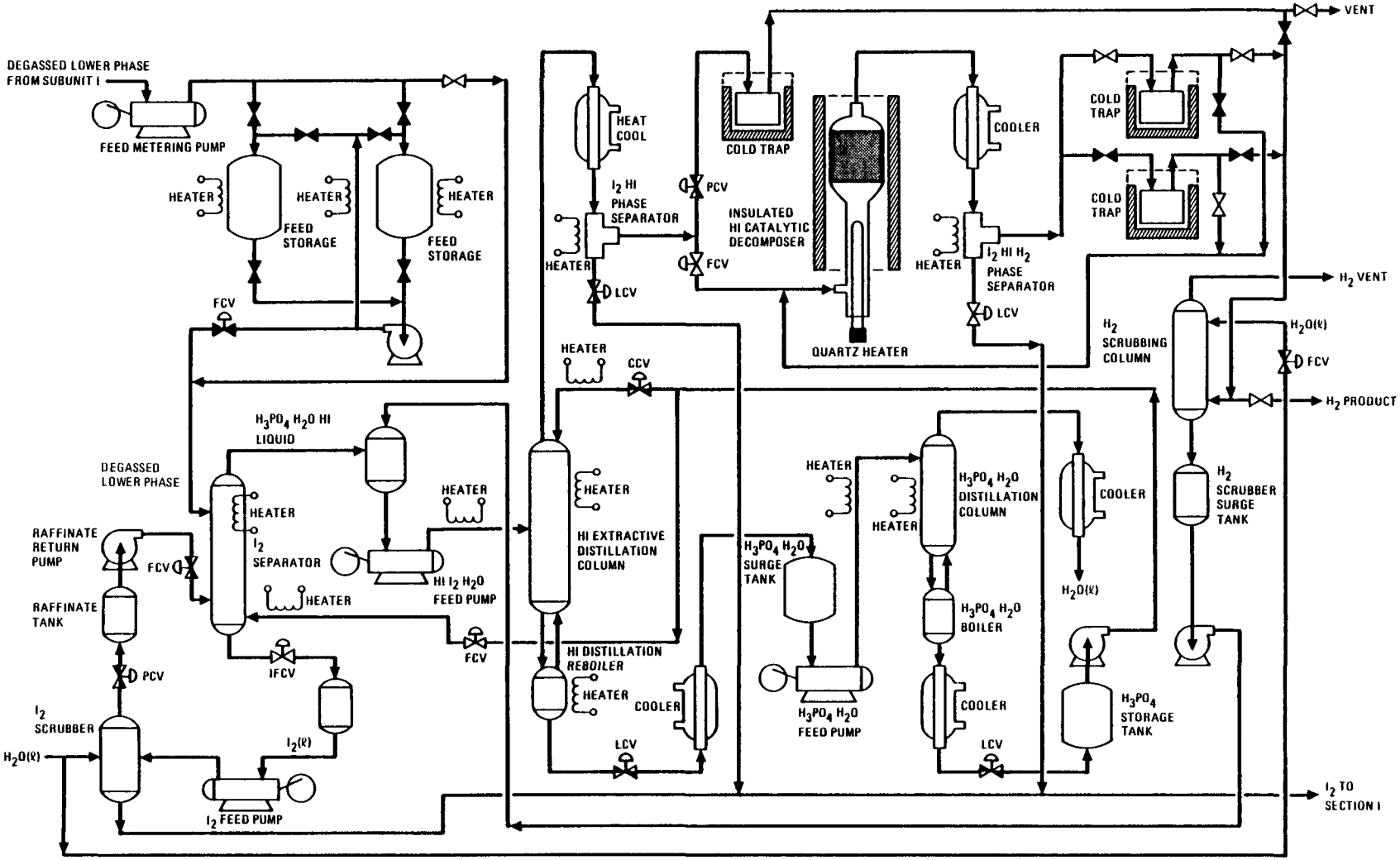

Fig. 23. Simplified bench-scale flowsheet for Subunit III (HI concentration and decomposition)

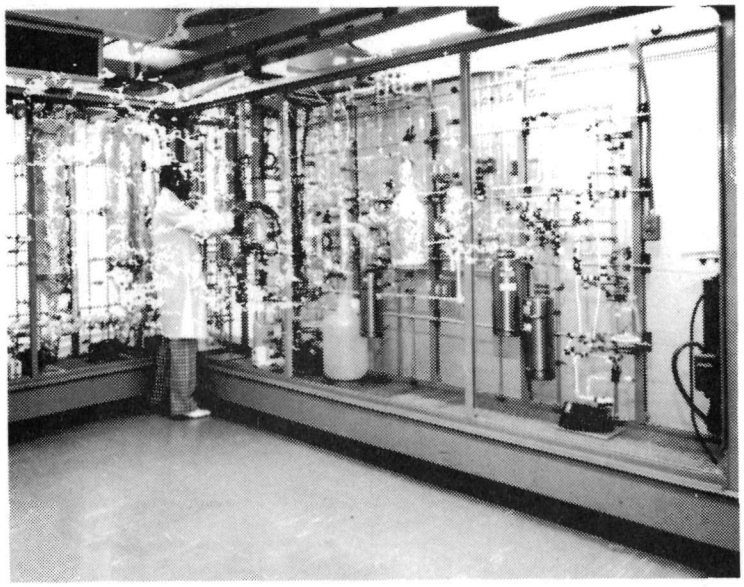

(a)

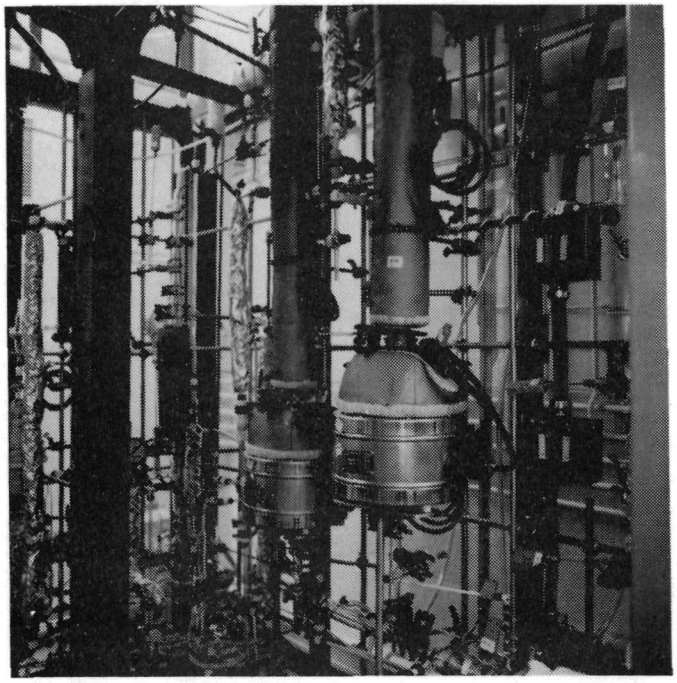

(b)

Fig. 24. Bench-scale Subunit III: (a) overview, (b) HI extractive distillation column and H_3PO_4-H_2O distillation column

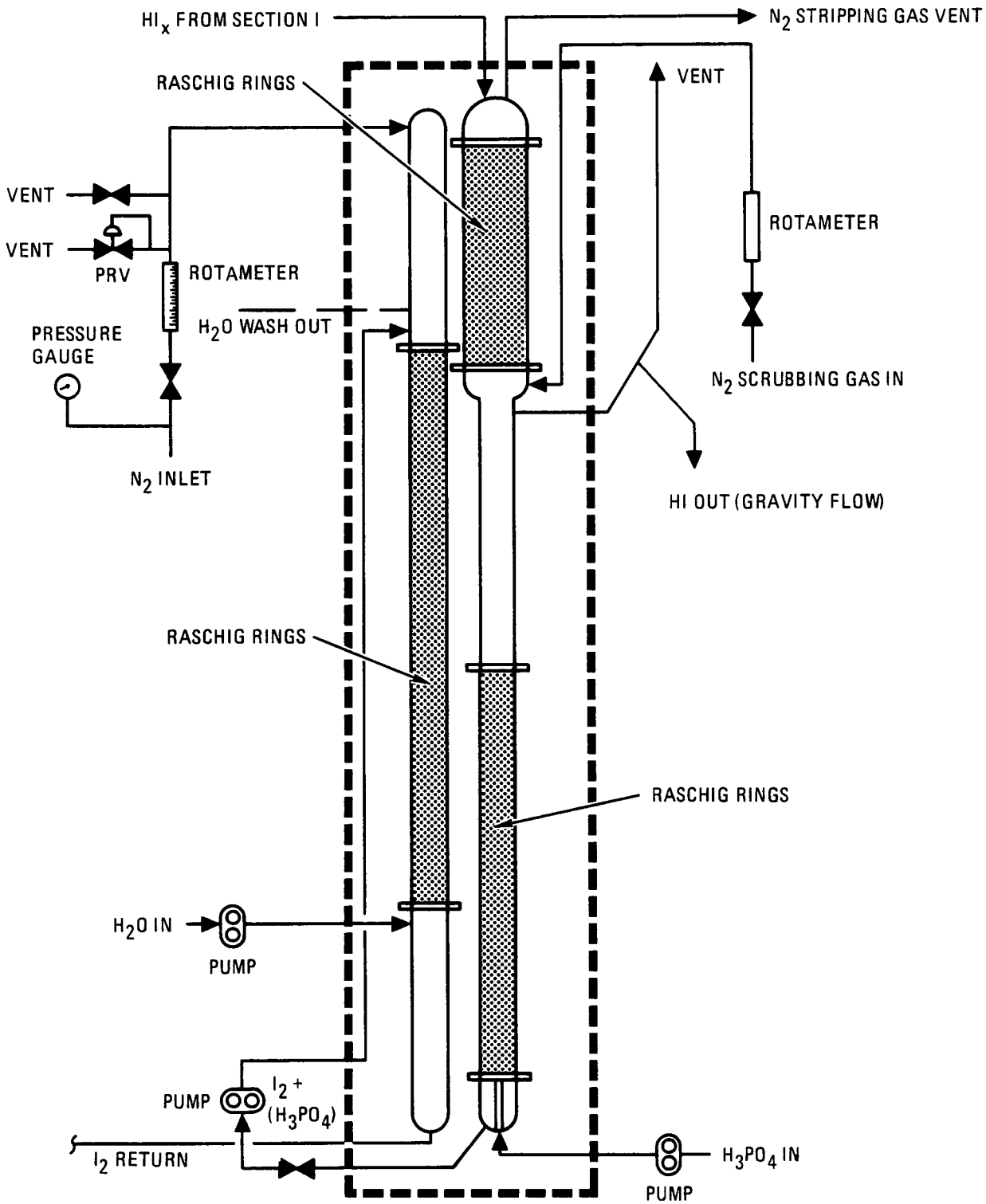

Fig. 25. Bench-scale design - Section III degassing and H_3PO_4 treatment of HI_x solutions

The exiting impure I_2 stream is pumped to the second column where it is washed with water to remove a small amount of dissolved H_3PO_4. This second column is run at 2 atm to keep the water from vaporizing at the operating temperature of 115°C. Pressure is applied to the column with nitrogen gas and is controlled by a pressure regulator valve. The distributions and packing supports in this column were fabricated from Teflon sheets, which also serve as gaskets between column sections. Ball-and-socket ports and thermocouple wells were added to the glass columns that were purchased. Other ports were also included for future installation of pressure transmitters, which will ultimately control liquid levels via the pumps.

The hot box, which houses the two columns, was made out of a welded metal framework and insulated. Three glass panels front the box and can be removed easily. Heaters were placed along the walls near the bottom of the box.

The system was run in conjunction with Subunit I and performed as expected, although the test was shortened by an HI_x pump malfunction. The system appeared to operate well with the exception of this pump. It is expected that as soon as adequate pumps are available to move I_2 and HI_x, this system will operate with a minimum of attention. Nevertheless, this unit has not at this point in time fully confirmed the laboratory data concerning these unit operations.

3.3.3. HI Separation

This subunit separates HI from the H_3PO_4 solution from the I_2 knockout columns. In the first tests of this portion of the cycle, a column packed with small Raschig rings was utilized. This column performed the task of separating HI from the H_2O and H_3PO_4 very well at low flow rates, but the throughput of the column was quite limited. As the flow rate was increased to

approach design limits, flooding occurred and of course the separation was lost.

In an attempt to increase throughput, a larger packing material was used. This larger packing material did improve flow for this relatively viscous working fluid such that flooding did not occur up to design levels. Nevertheless, column efficiency was decreased by this change, and the HI was delivered wet even with design flow of concentrated H_3PO_4 against the gas flow.

It is clear that a distillation column will be able to separate the HI as projected, but still other solutions are necessary. For this purpose two glass bubble-cap vacuum insulated columns, 10 stages apiece, were purchased and installed. Two columns were needed to provide a central entry point for the HI pregnant HI-H_3PO_4-H_2O phase. At this point in time this column is still to be tested, but design performance and throughput are expected from this unit.

During this work several other design problems were solved. One was the method of delivery of dilute H_3PO_4 to the concentration column. For this purpose a jack leg product draw off was employed. Another problem was the heating of the pot. Quartz immersion heaters were used to solve this problem. A third problem was the freezing of the concentrated H_3PO_4 in lead lines. This was solved by always keeping the lead lines, holding vessels, and pumps hot.

The resulting system appears operable. An initial attempt at mass balancing over the operation indicated that this was possible and that behavior was roughly as desired. The system has been operated in conjunction with the H_3PO_4 concentration system. It is believed that it is capable of working in a combined Subunit III test.

3.3.4. H_3PO_4 Concentration

In the H_3PO_4 concentration column, the 85 wt % H_3PO_4 effluent of the HI distillation step is heated to sufficient temperature, 222°C, to substantially remove water from the H_3PO_4. The distilled water is then available for recycle to Subunit I, and 96% H_3PO_4 is recycled to the I_2 separation system and to the HI distillation step at the metered rates specified in the design criteria for those subsections of bench-scale Subunit III.

The phosphoric acid concentrator was modified to provide total heat input via quartz immersion heaters and jack leg take-off similar to the HI separation column. The previous design, which employed both immersion heaters and a heating mantle, did not provide sufficient room for total immersion of the quartz heater. A very dehydrated high-temperature phosphoric acid (HPO_3?) formed in the vapor space from contact of H_3PO_4 with the heating element. This attacked both the heater and the glass vessel in the vapor region. The new vessel is sufficiently deep to accept the full immersion heater below the liquid line, precluding this problem.

There were also packing difficulties in the H_3PO_4 distillation column. However, they were much more easily solved since one of the products is basically nonvolatile. The column operates quite well without any packing. This redesigned system has been run many hours and produces 96 wt % H_3PO_4 at design level rates.

3.3.5. HI Decomposition

Bench-scale testing of HI decomposition has been planned for two or more stages. One version of the sulfur-iodine cycle includes catalytic gas phase decomposition of HI and a second more advanced version includes catalytic liquid phase decomposition. In either case, final versions of these processes would

produce ~50 atm H_2. Pipeline quality H_2 is expected to be the product of the cycle. Nevertheless, for initial bench-scale tests simple systems have been selected to initially close the cycle. For these initial bench-scale studies, 1 atm catalytic decomposition has been selected. Product HI from the HI distillation system has been represented in the tests performed to date by commercial cylinder HI.

The operation of this test in the cyclic version includes cooling the HI and I_2 vapor effluent from the HI distillation step in a condenser to a temperature slightly exceeding the melting point of iodine, and separating condensable iodine from the residual vapor before the vapor is metered and sent to the vertical tubular heated chamber. Thermal decomposition of the HI vapor occurs in the heated chamber at a controlled temperature in the range of 177° to 440°C at substantially ambient atmospheric pressure. The controlled temperature volume for HI decomposition is 4×10^{-3} m^3, including catalyst volume, if any. The present integrated bench-scale system employs gaseous HI decomposition.

In these initial studies, the HI decomposition gaseous products were first cooled to a temperature below the melting point of iodine (114°C) and condensed iodine was separated from the residual gas vapor. The iodine fell to a collection pot where it was held until remelting and recycle. The residual gas vapor from the I_2 condensation was then chilled with liquid nitrogen or dry ice to a sufficiently low temperature to remove substantially all condensable vapors from the H_2 product gas. Provision was also made to revaporize the condensed HI for recycle at metered rates to the HI decomposition step.

The H_2 purification step provides countercurrent scrubbing with water to remove low concentrations of HI from the effluent H_2 of the HI recycle system.

This unit was operated with no major engineering problem from the beginning. A conversion ($2HI \rightarrow H_2+I_2$) of 22% per pass has been routinely obtained. The predicted equilibrium conversion at the measured reactor outlet temperature is 16% (Ref. 13). This discrepancy has not been fully explained yet, but the observed conversion is either characteristic of higher temperature than actually measured in the activated charcoal catalyst bed or of a system which is removing a product as it is formed, as charcoal is prone to do.

Efficient iodine removal from the product stream was achieved by increasing the heat transfer area of the iodine trap and by lowering the temperature. Glass HI traps were replaced with stainless-steel pressure vessels allowing longer run times and better control of the recycle HI flow.

As a test, the HI decomposition reactor was operated with no catalyst in an attempt to determine the source of the super equilibrium decomposition previously observed. Greater than equilibrium decomposition was obtained, but not as high as with the catalyst. This indicates that some of the decomposition reaction is taking place in the boundary layer of the preheater and does not equilibrate. It may also be in line with the charcoal being an excellent adsorbant for iodine, which at nonsteady state conditions shifts the reaction toward higher conversions. Laboratory studies have indicated rather long periods are necessary for steady state to be achieved.

A liquid phase decomposition unit that operates at pressures consistent with pipeline quality H_2 has been developed on another program (Ref. 6). This unit has been operated under conditions consistent with the bench-scale unit H_2 production rates. Thus, the independent test of liquid HI decomposition has been performed. With some effort this system could be integrated into the bench-scale system of the sulfur-iodine cycle.

3.4. SUMMARY OF BENCH-SCALE OPERATIONS

The operations of each of the subunits have all been tested. At least one of the unit operations has not been tested in its redesigned form (HI distillation from H_3PO_4 solutions). Nevertheless, the system is basically considered operational for an integrated test of the sulfur-iodine cycle. There would be some minor requirements for developing recycling methods for some of the chemicals, but these would be done by more or less standard practice.

A number of improvements in the engineering operation of the cycle have resulted from this effort. For instance, liquid-liquid separation techniques in the main reactor have been devised, the use of packed columns in several other operations has been improved by finding operationally effective systems, metering and pumping of iodine solutions at higher temperatures have been developed, and in general other techniques have been proved out. The work has been very valuable in developing the sulfur-iodine cycle.

4. PROCESS ENGINEERING DESIGN

4.1. INTRODUCTION

The engineering flowsheet for the General Atomic sulfur-iodine thermochemical water-splitting cycle has progressed through several revisions under the dual objectives of maximizing the process efficiency and minimizing the resultant hydrogen cost. Although a plant cannot be cost effective unless it is efficient, in the limit of maximum efficiency a plant would have to operate reversibly at zero production rate and infinite product cost. The 1979 flowsheet (Ref. 11) was prepared with the goal of maximizing process efficiency subject to the constraints of good engineering practice as a first approximation of a plant with minimum cost. The details of this flowsheet are presented in Appendix D and discussed in Section 4.2. During 1981 this flowsheet was selectively revised with the goal of reducing the product hydrogen cost while maintaining the high efficiency (47%) of the 1979 flowsheet. The goal was met, and the results are presented in Appendix C and discussed in Section 4.3.

Originally the process heat HTGR was considered to be the heat source of choice for thermochemical water splitting, but fusion reactors and concentrated solar sources are also being investigated. The 1979 flowsheet was designed to match an HTGR heat source. Solar and fusion based funding sources have begun to fund the matching of these heat sources to the water-splitting cycle. Therefore, the 1981 design effort concentrated on Sections I, III, and IV, which are less directly dependent on the heat source.

4.2. 1979 FLOWSHEET

A simplified schematic flow diagram of the 1979 version of the sulfur-iodine process conceptually showing product mass flows and recycle streams is given in Fig. 26. Figures 27 through 31 are simplified versions of the five detailed engineering flowsheets.

A description of the 1979 version of the sulfur-iodine process flowsheet Sections I through V is given below. For reasons of simplicity, the descriptions are keyed to the simplified flow diagrams (Figs. 27 through 31). Detailed flowsheets for Sections I through V, including mass and energy balances, are included as Appendix D.

4.2.1. 1979 Flowsheet Section I: H_2SO_4-HI Production and Separation; O_2 Separation

The main solution reaction is carried out in Section I of the flowsheet together with the purification of the product oxygen. Figure 27 shows a simplified version of the detailed flowsheet for this section.

In the main reaction, recycle iodine from Sections III and IV reacts with water from SO_2 from a mixture of gaseous SO_2-O_2 in a countercurrent reactor (C-101). The reaction results in the formation of the two acids, H_2SO_4 and HI, in solution. The discovery of the formation of two phases and the natural separation of these phases made the sulfur-iodine cycle feasible. The lower density phase (upper phase) contains all the H_2SO_4 at a concentration of approximately 50 wt % with traces of iodine and a small amount of dissolved SO_2. The higher density phase (lower phase) contains all the HI with considerable amounts of iodine in an H_2O solution. A small quantity of SO_2 and a trace of H_2SO_4 are also present.

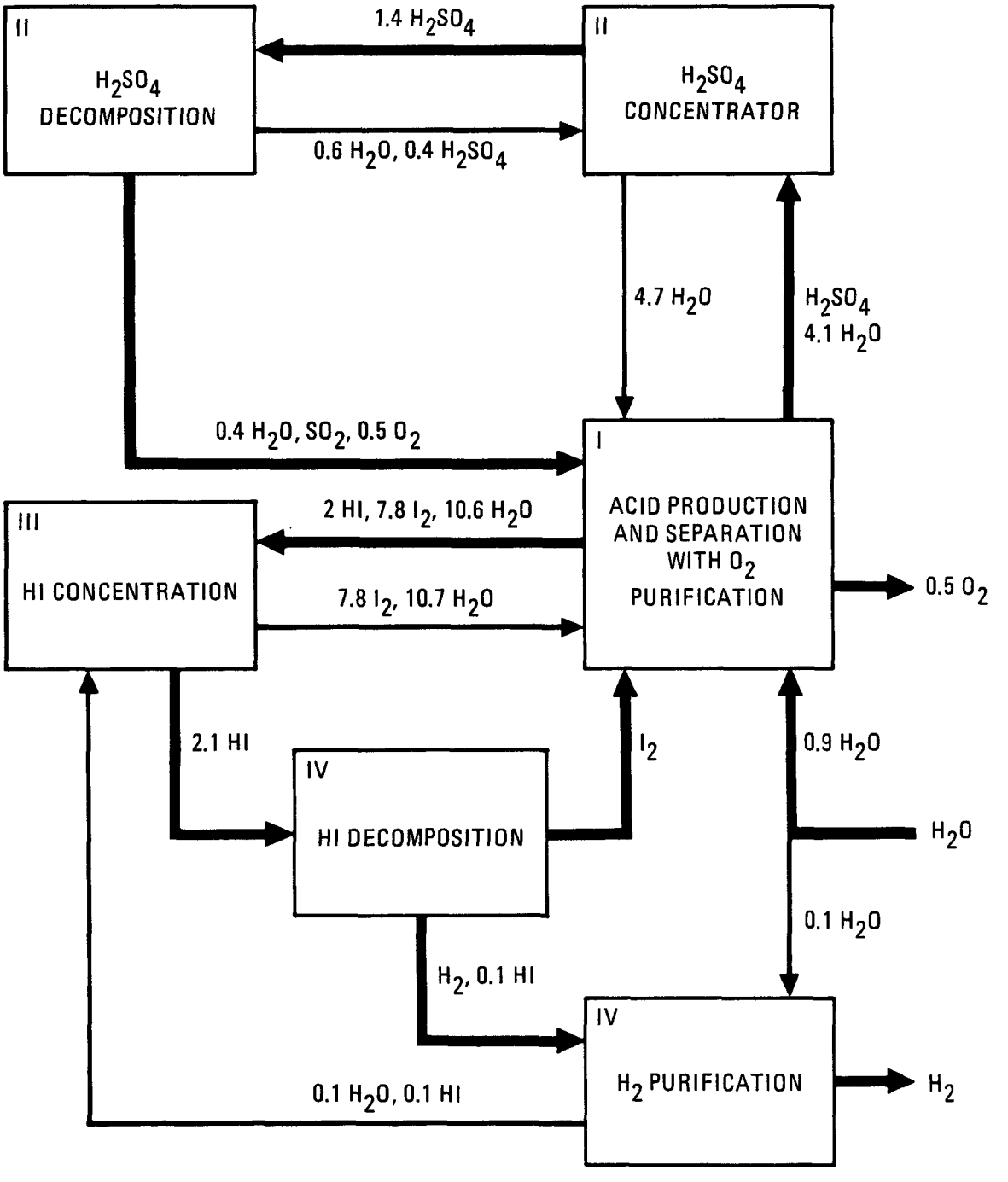

Fig. 26. Simplified schematic flow diagram of the 1979 version of the sulfur-iodine cycle

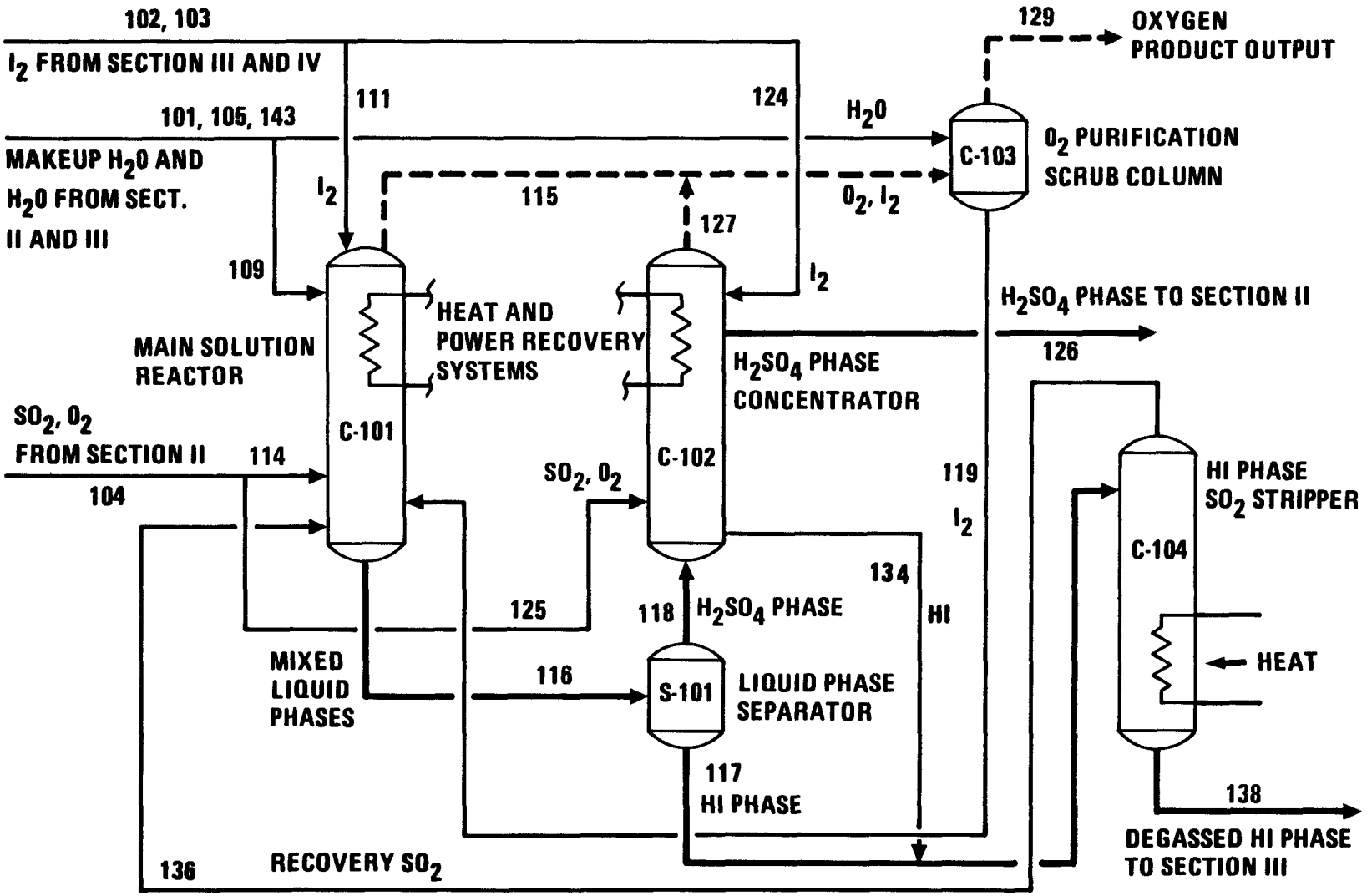

Fig. 27. Simplified flowsheet for Section I: H_2SO_4-HI production and separation; O_2 separation (1979 version

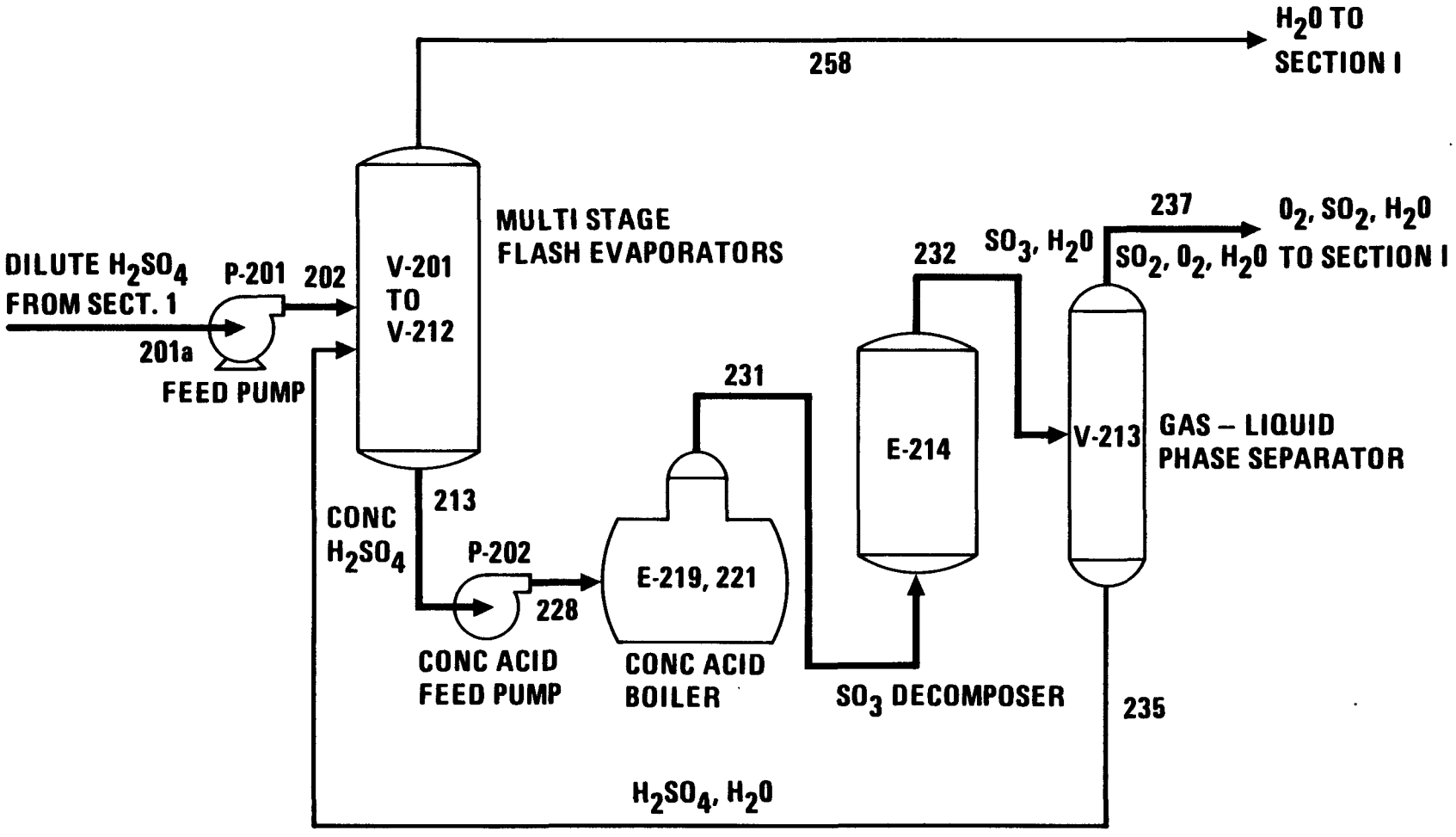

Fig. 28. Simplified flowsheet for Section II: H_2SO_4 concentration and decomposition (1979 version)

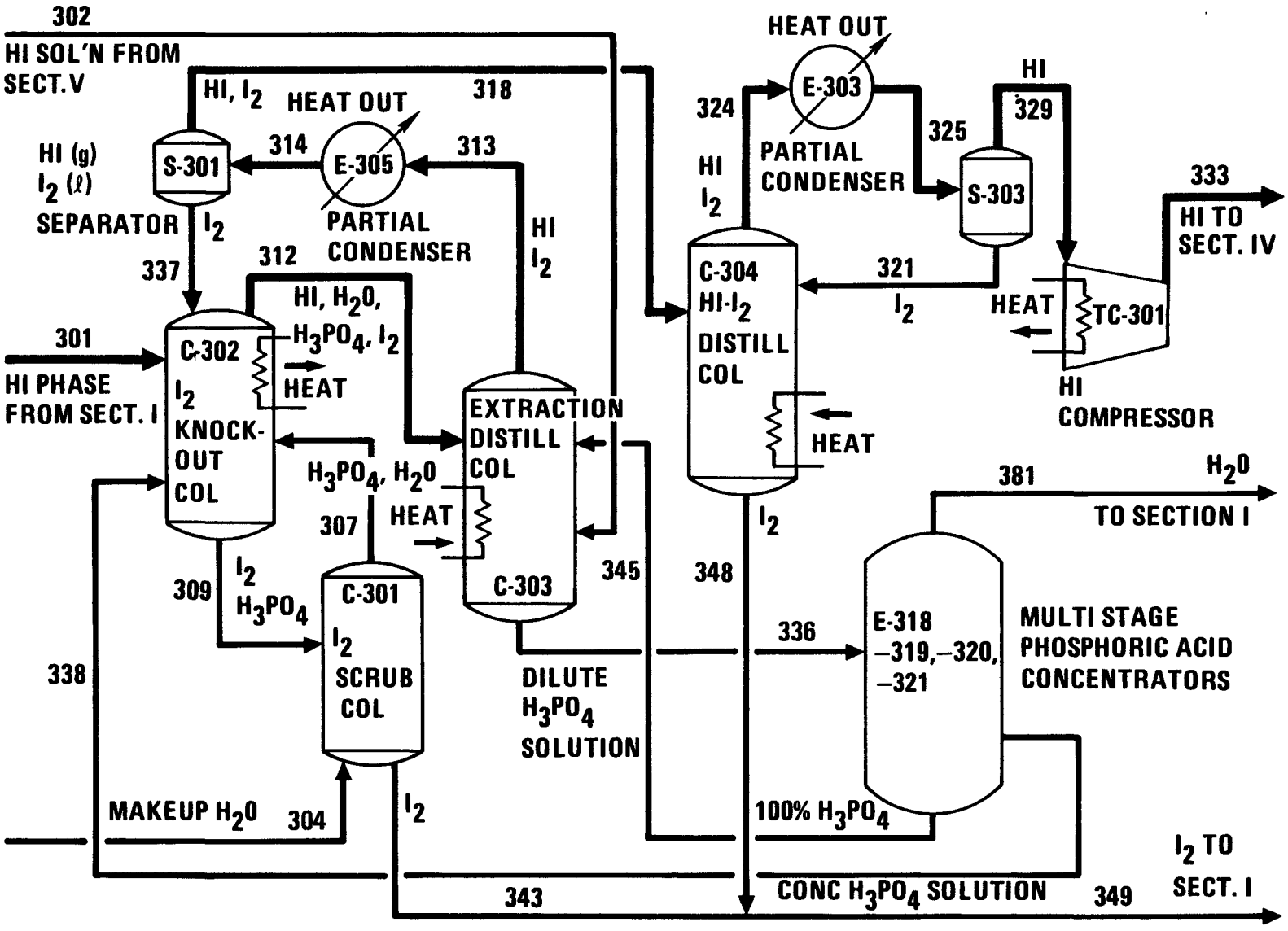

Fig. 29. Simplified flowsheet for Section III: HI separation (1979 version)

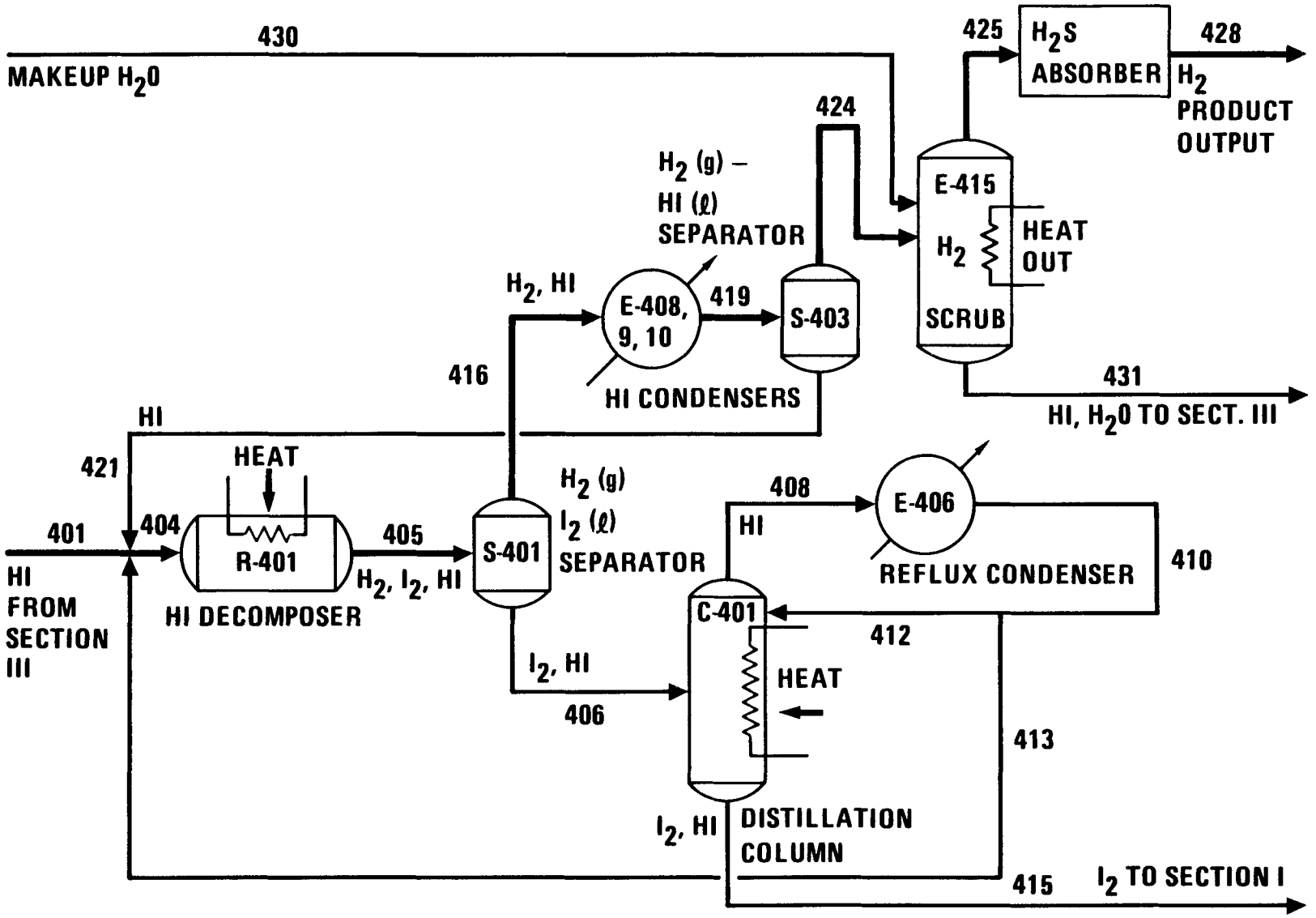

Fig. 30. Simplified flowsheet for Section IV: HI decomposition (1979 version)

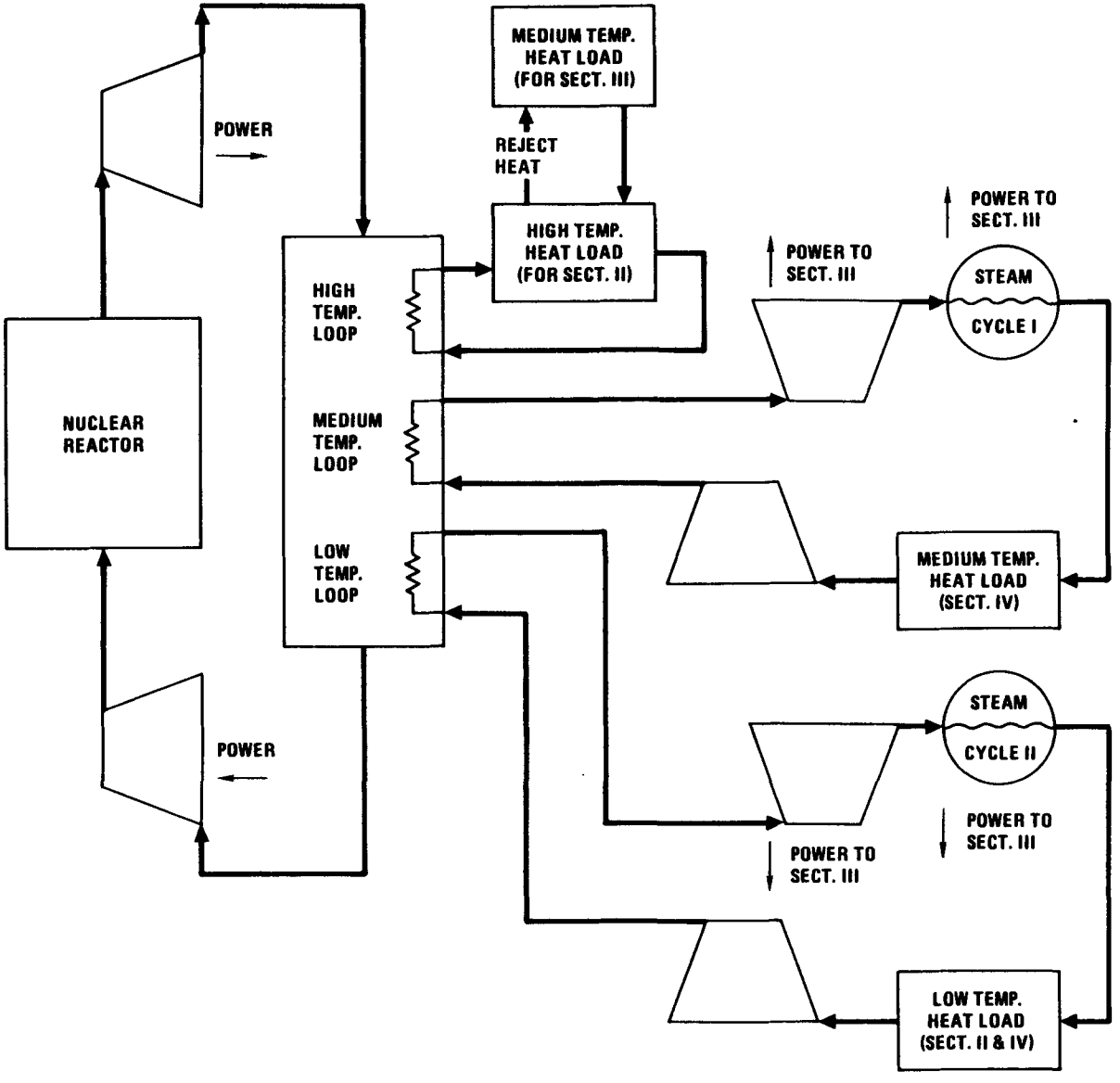

Fig. 31. Simplified flowsheet for Section V

The phases are separated (S-101), and the sulfuric acid phase is reacted with molten iodine and SO_2. This increases the H_2SO_4 concentration to approximately 57 wt % and generates reaction product HI. The 57% sulfuric acid is transferred to Section II for concentration and decomposition. The lower phase goes through a degassing step, which removes practically all the SO_2 (C-104). This lower phase containing HI, H_2O, and I_2 is then transferred to Section III for purification and HI separation.

The SO_2 entering the main reaction (C-101) and the H_2SO_4 boost reaction (C-102) is a mixture of SO_2 and O_2 coming directly from the SO_3 decomposition reaction of Section II. As this gas mixture passes through the reactor, SO_2 is removed by reaction with I_2 and H_2O, and the gas leaving the top of the main solution reactor is practically pure oxygen with small amounts of iodine. The iodine is removed in a scrub column (C-103), and pure oxygen leaves the system as a product.

All reactions in Section I have been demonstrated in the laboratory, and the yields quoted in the material balance sheets of Appendix D are based on actual experimental data. The engineering design of Section I is based on GA experiments and available thermodynamic literature data.

4.2.2. 1979 Flowsheet Section II: H_2SO_4 Concentration and Decomposition

Concentration and decomposition of sulfuric acid are carried out in this section, which fulfills one part of the recycle requirement by generating the needed SO_2 for the main reaction from the H_2SO_4 decomposition. Figure 28 shows a simplified version of the detailed flowsheet for this section.

Dilute sulfuric acid (57 wt %) from Section I is concentrated in a series of flash evaporators (V-201 through V-212). The concentrated H_2SO_4 is decomposed (E-221) to H_2O and SO_3, and

the sulfur trioxide is decomposed (E-214) to sulfur dioxide and oxygen. The SO_3 decomposition is the highest temperature step in the total process, with operating temperatures of up to 870°C. The gaseous mixture of SO_2 and O_2 is separated from the water and unreacted H_2SO_4 and transferred to the main solution reaction in Section I. The condensate from this separation is recycled to the first flash evaporator.

The concentration and decomposition of H_2SO_4 are common to a number of water-splitting cycles and have been evaluated in several laboratories. General Atomic has developed proprietary catalysts and processes which have been demonstrated at the quoted temperature. The engineering design of Section II is based on GA experimental data and available thermodynamic literature data.

4.2.3. 1979 Flowsheet Section III: HI Separation

Hydrogen iodide is separated from the components of the $HI-I_2-H_2O$ solution (lower phase) in this section. Figure 29 shows a simplified version of the detailed flowsheet for this section.

Lower phase from Section I containing approximately 4 moles of iodine and 5 moles of water for each mole of HI is treated with concentrated phosphoric acid (C-302), and a major portion of the iodine (~95%) is separated from the solution. This iodine is scrubbed with water to remove small amounts of HI and H_3PO_4 (C-301) and returned to the main solution reaction of Section I. The overhead solution containing HI, H_2O, H_3PO_4, and some I_2 is subjected to an extractive distillation (C-303), where most of the water (99%) remains with the phosphoric acid and the HI and I_2 are removed as overhead vapor. Minor amounts of H_2S may be formed in three steps from a reaction of trace quantities of H_2SO_4 with HI. The dilute phosphoric acid is concentrated in a series of concentrators (E-318 through E-321) and reused for the

iodine separation as discussed above. The overhead containing HI, some I_2, and a very small amount of water is cooled (E-305) to condense and separate (S-301) some of the iodine and then subjected to another distillation (C-313). Here the HI is purified to a level where it can be sent to Section IV for decomposition after compression to 5.065 MPa (50 atm).

The engineering design of the HI purification system is based on laboratory data collected at GA. Design of the phosphoric acid concentration section is based on available thermodynamic data from the literature.

4.2.4. 1979 Flowsheet Section IV: HI Decomposition

The decomposition of hydrogen iodide is carried out in this section. Figure 30 shows a simplified version of the detailed flowsheet for this section.

Purified liquid HI [5.065 MPa (50 atm)] from Section III is catalytically decomposed at approximately 120°C (R-401). The degree of decomposition is only approximately 30% in one pass. Therefore, the recycle step has to be used in this section. The hydrogen product is separated from most of the I_2 and some HI in a liquid gas separator (S-401). This gas is then cooled (E-408, E-409, and E-410) to condense out most of the HI, which is recycled to the HI decomposer (R-401). The gaseous H_2 product is scrubbed with H_2O. and pure hydrogen is the resulting end product. The liquid from the gas-liquid separator (S-401) contains mostly iodine and HI. The HI is removed by distillation (C-401) and returned to the HI decomposer (R-401). The iodine is returned to the main solution reaction in Section I.

The engineering design of Section IV is based on experimental laboratory data collected at GA. The catalysts for the liquid HI decomposition have been developed and demonstrated. General Atomic has filed for a patent for the decomposition of

liquid HI. The decision to design the system for 5.065 MPa (50 atm) pressure was based on existing pipeline pressures for natural gas transmission.

4.2.5. 1979 Flowsheet Section V: Power Generation and Heat Transfer

Section V of the flowsheet describes the generation of heat and power needed in some of the processing sections. The basic assumption has been that a high-temperature gas-cooled nuclear reactor, similar to the one designed by GA, would be available. Figure 31 shows a simplified block diagram of the detailed flowsheet for this section.

Helium from the primary loop transfers its heat to three secondary helium loops through heat exchangers that operate at high, intermediate, and low temperatures. The high-temperature loop provides the heat for the sulfuric acid decomposition reaction of flowsheet Section II. Recovered heat from Section II is utilized to provide heat for the HI distillation and phosphoric acid concentration of flowsheet Section III. The intermediate-temperature loop provides the heat for flowsheet Section IV, HI decomposition. Power for flowsheet Section III is generated through a helium turbine and a steam cycle. The low-temperature loop provides low value heat to flowsheet Sections II and IV, sulfuric acid concentration and HI distillation. Additional power for flowsheet Section III is generated through a helium turbine and a second low-temperature steam cycle. Section I is heat self-sufficient and exports power to other sections.

The design of Section V is based on available thermodynamic data and good engineering practice.

4.3. 1981 FLOWSHEET

A simplified schematic of the 1981 flowsheet is presented in Fig. 32. At this level of detail the flowsheet is basically the same as the 1979 flowsheet, except that the iodine recycle between Sections I and III is significantly increased.

The main objective of the 1981 flowsheeting effort was to refine the 1979 flowsheet so as to reduce the hydrogen product cost. This required that equipment sizing and costing be included in the effort. The basic design assumed a 3000 MWT power source such as an HTGR or fusion reactor. A second version assumed a 500 MWT solar powered plant.

Although the main emphasis was on reducing capital cost, a few improvements in efficiency were also made. To a large degree these efficiency improvements were traded for reduced capital cost and the overall efficiency remained at 47%. Although details of the flowsheet are given in Appendix C, a simplified mass flow diagram is given in Fig. 32, and simplified schematics of Sections I, III, and IV are given in Figs. 33 through 35 to aid the process description.

4.3.1. 1981 Flowsheet Section I: H_2SO_4-HI Production

Although functionally similar to the previous version, the Section I flowsheet has undergone significant revision in reaching the present form indicated. The prime impetus toward the new design was the realization that the only metals compatible with the HI_x solutions are expensive and exotic metals such as niobium. Section I was redesigned to minimize heat transfer involving HI_x streams. Additionally, heat transfer surfaces were removed from packed columns to simplify construction.

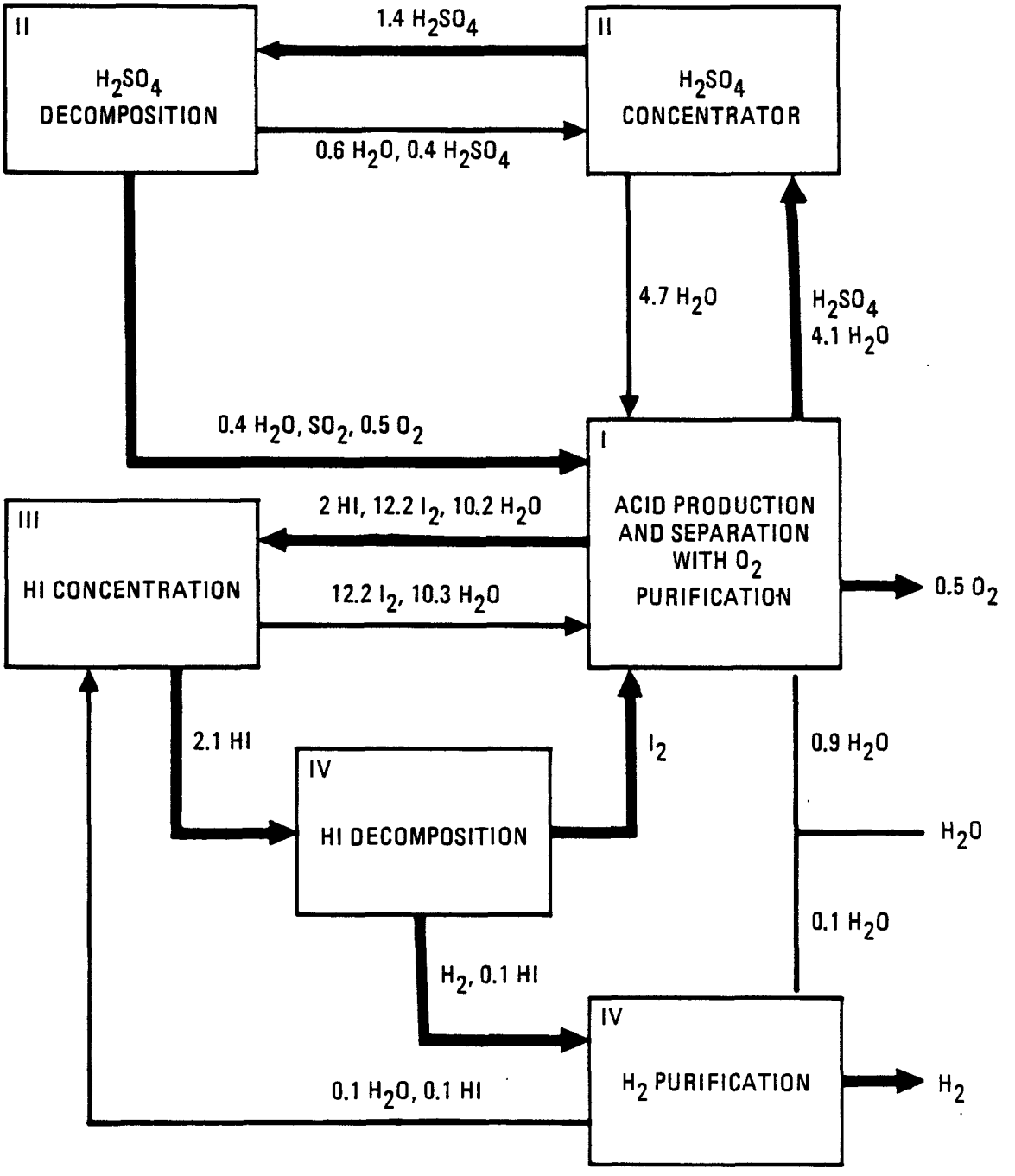

Fig. 32. Simplified schematic flow diagram of the 1981 version of the sulfur-iodine cycle

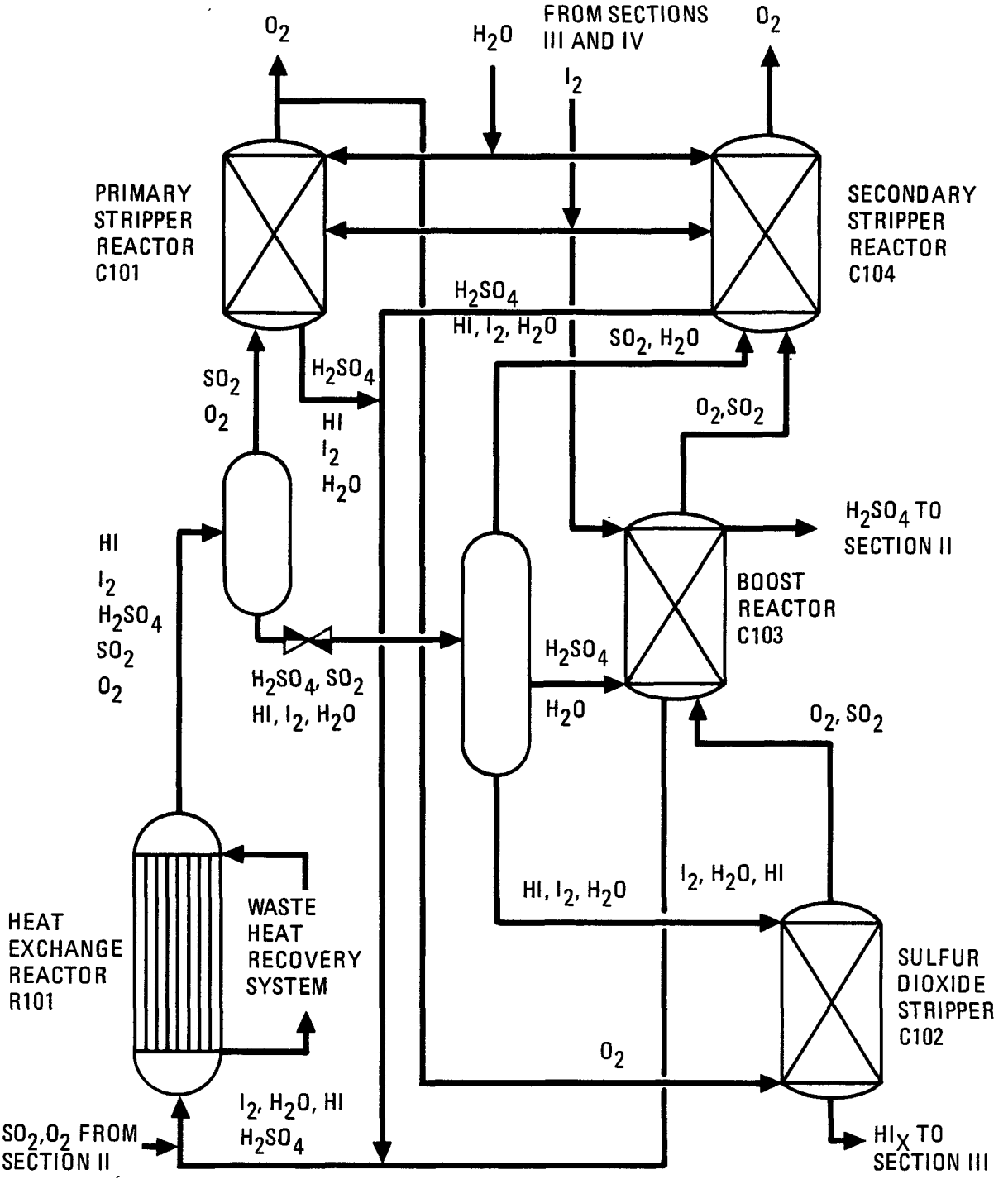

Fig. 33. Simplified flowsheet for Section I: H_2SO_4-HI_x production (1981 version)

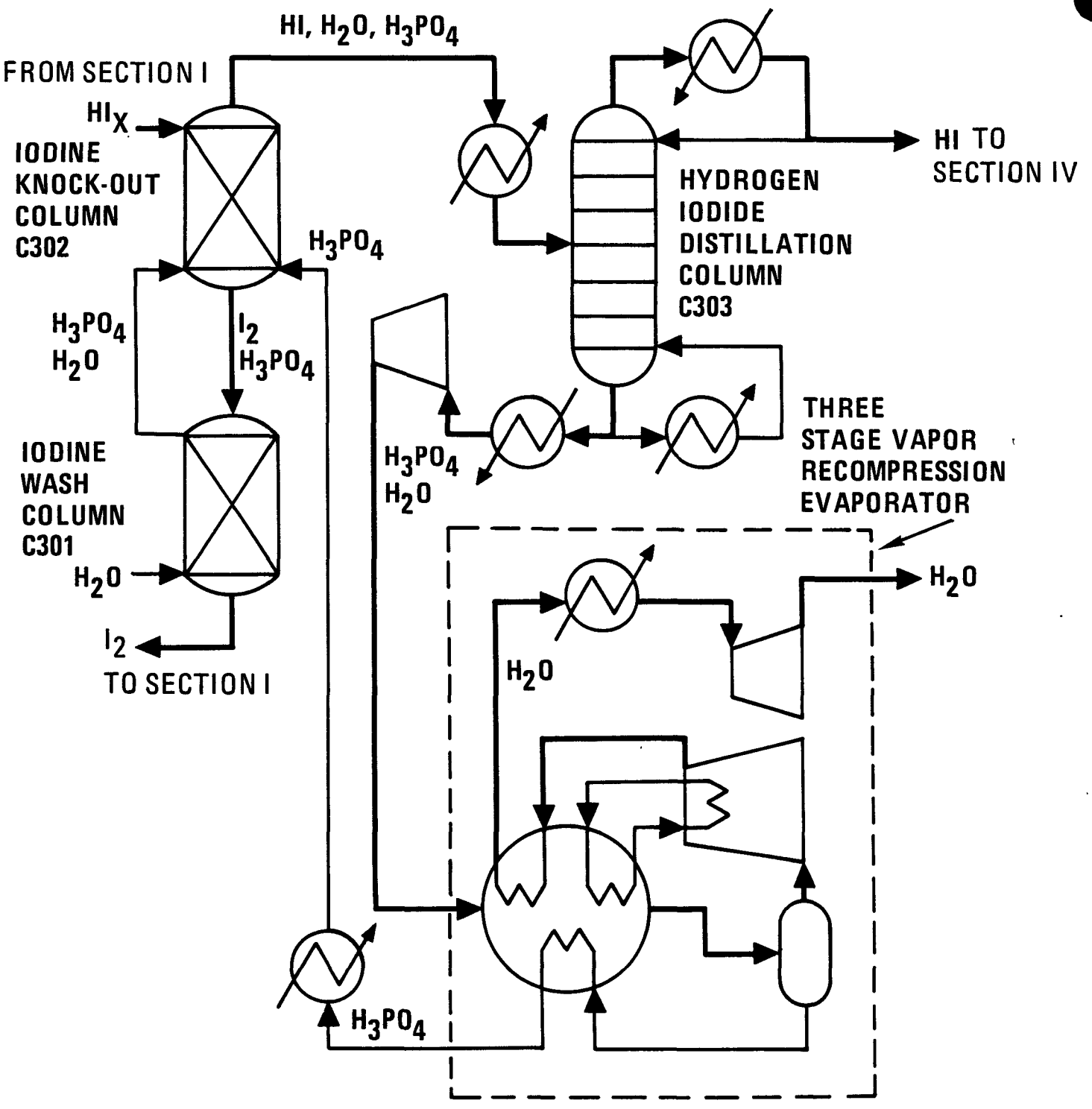

Fig. 34. Simplified flowsheet for Section III: separation of aqueous HI_x into HI, I_2, and H_2O (1981 version)

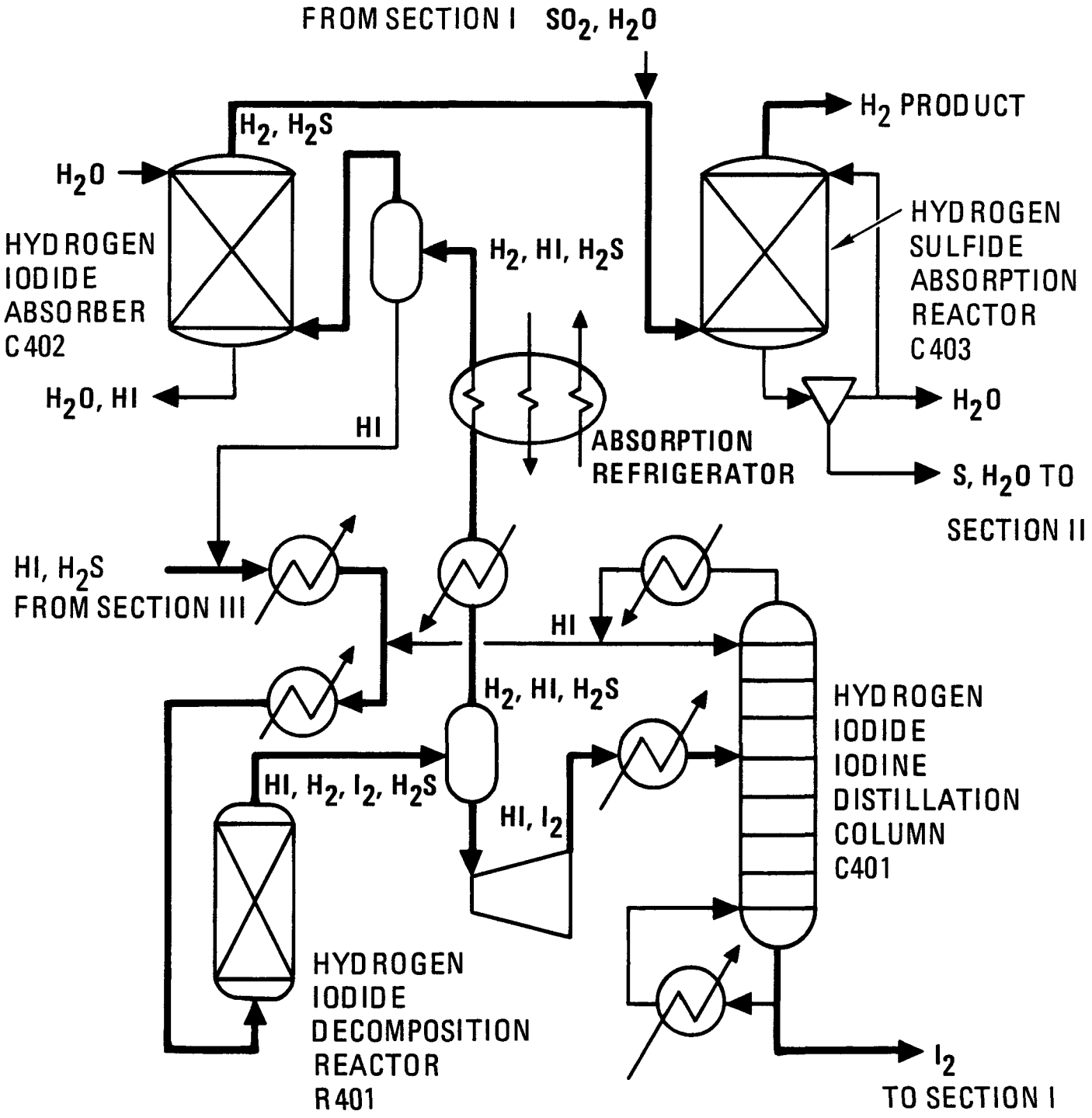

Fig. 35. Simplified flowsheet for Section III: HI decomposition (1981 version)

The main solution reaction is exothermic, and Section I requires no heat input from the heat source but exports a significant quality of low grade heat to the power bottoming cycle. The Section I process is shown schematically in Fig. 33.

Even though Section I requires no heat input from the heat source, the design of the main solution reaction step has a major influence on the overall process efficiency and thus upon the reactor size and the hydrogen production cost. Although decisions on heat and power recovery within Section I have an effect on efficiency, the composition and temperature of the light phase flowing to process Section II (the H_2SO_4 processing step) and the heavy phase flowing to Section III (the HI concentration step) strongly influence the overall efficiency of the process. In the interest of efficiency, both streams should leave Section I at as high a temperature as possible and at the highest acid concentration possible. Since the equilibrium of an exothermic reaction shifts towards the reactants as temperature is raised, a compromise must be made between high temperature and high product acid concentrations. In deciding the operating conditions for Section I some economic trade-off calculations were made, but a full-scale process optimization was not in the scope of this work. The basis the resulting decisions, as well as those for the rest of this study, may best be termed "engineering judgment." When trade-off calculations were not definitive, the decision was usually made on the side of "high efficiency" not "low capital cost."

Consideration of two factors dominates the design of Section I: (1) the large quantity of heat produced by the main solution reaction must be removed, and (2) the combination of hydrogen iodide and iodine in an aqueous phase (referred to as HI_x) is extremely corrosive to materials normally employed for heat transfer surfaces. The only metals known to resist HI_x are the refractory metals, such as zirconium, niobium, tantalum, and molybdenum. The present design employs niobium for heat transfer

surfaces contacting HI_x, which permits the reaction energy to be used in the power bottoming cycle.

Niobium is relatively expensive. Therefore, to reduce the capital cost of Section I, a number of design techniques have been employed which improve heat transfer and decrease the amount of Nb required. Some of these are:

1. Cool feed streams to Section I. Prior to carrying out the main solution reaction, heat from the Section I feed streams is transferred to the power bottoming cycle. This involves less expensive heat transfer materials than Nb and reduces the amount of heat transferred from the reaction products of the main solution reaction.

2. Operate adiabatically. Instead of cooling the reaction products from 393 to 368 K (to shift the equilibrium towards the products) and then reheating the separated products, the desired production rate of the main solution reaction is maintained, operating adiabatically, by increasing the iodine concentration to provide the needed shift in the equilibrium.

3. Use direct-contact heat exchange. Where possible, direct contact heat exchange between immissible liquid phases or gas and liquid phases is employed.

4. Apply enhanced heat transfer techniques. Utilizing two-phase gas-liquid flow through the heat exchanger gives higher than normal corrective heat transfer coefficients. Spiral-fluted tubing provides enhanced heat transfer and, due to the wall stiffening effect, permits thinner tube walls.

4.3.1.1. Heat Exchanger Reactor.

Almost 52% of the chemical reaction forming HI and H_2SO_4 takes place in the heat exchange reactor (R-101 in the flow diagram of Fig. 33) and in the piping immediately preceding the reactor. The reactor selected is a shell and tube heat exchanger with fixed tube sheets. The vessel, tube sheets, and heads are fabricated from mild steel. The heads are lined with fluorocarbon and the spiral fluted niobium tubes are welded to a niobium tube sheet liner. The process fluid is on the tube side of the exchanger and the shell side is part of the power bottoming cycle.

Upstream of the exchanger, the SO_2/O_2 from Section II (sulfuric acid processing) is mixed with the predominantly iodine stream from the boost reactor (C-103) and aqueous streams from the scrubbing reactors (C-101 and C-104). The combined streams react exothermically as they flow through fluorocarbon-lined pipe and into the heat exchange reactor. The pressure drop through the exchanger reduces the system pressure from an initial 0.50 MPa to 0.44 MPa, at which point the temperature reaches 393 K. At the exit of the exchanger the O_2 is removed from the stream in the first of two separators (S-101). In the second separator (S-102), operating at 0.11 MPa, three phases separate: the heavy liquid phase (HI_x), the light liquid phase (H_2/H_2SO_4), and a gas phase consisting of SO_2 and steam. The vaporization of water and SO_2 results in the temperature decreasing from 393 K to 385 K.

4.3.1.2. Lower Phase SO_2 Stripper.

The lower phase solution (HI_x) is saturated with SO_2 which, when allowed to remain, forms sulfur and H_2S via tramp reactions. An oxygen recycle stream strips most of the SO_2 in a packed bed stripper (C-102), thus minimizing the tramp reactions. A minimum amount of oxygen is employed for this operation as the evaporation of water into the oxygen cools the HI_x, requiring more heat

input in Section III (HI purification). With a 10% O_2 recycle, the HI_x is cooled from 385 K to 381 K.

The stripper, sized for operation at 70% of flooding, is a standard packed column design. The fluorocarbon-lined, mild steel vessel is packed with 50 mm ceramic Raschig rings. Since the operating pressure is near atmospheric, a glass-lined steel vessel is a viable option but would require fluorocarbon packing to avoid liner damage.

4.3.1.3. Boost Reactor.

In the boost reactor, the sulfuric acid concentration of the light phase increases from 50% to 57% by contacting with molten iodine in the presence of sulfur dioxide. The increased H_2SO_4 concentration is realized through the action of the main solution reaction. Water is used up by reaction with SO_2 and I_2 to form H_2SO_4 and HI. Over 7% of the total chemical reaction of Section I occurs in the boost reactor. Since the contact is performed in a countercurrent manner, the reactor also acts as a direct contact heat exchanger, raising the temperature of the sulfuric acid stream from 383 K to 393 K.

Although the mechanical design of the boost reactor is straightforward, i.e., a fluorocarbon-lined mild steel vessel packed with 50 mm ceramic Raschig rings, the sizing calculations are not. Common packed columns operate with either a gas rising through a descending liquid phase or a light liquid phase rising through a descending heavy liquid phase. The boost reactor has both a gas phase (SO_2 in O_2) and a light liquid phase (H_2SO_4 and water) rising through the descending heavy liquid phase (I_2). The present design is based on adding the cross sectional areas required if the gas and light liquid separately contacted the heavy liquid. This is a very conservative approach. General Atomic believes that a design based upon information gained in a pilot plant would result in a smaller boost reactor vessel.

4.3.1.4. Scrubbing Reactors.

The oxygen is purified before discharge to the atmosphere in the scrubbing reactors. The packed column reactors operate in a titration mode in which sufficient iodine is added to the scrub water in the lower part of the column to react stoichiometrically with the sulfur dioxide present in the oxygen. In the upper part of the column the oxygen is washed with pure water. The primary scrubbing reactor (C-101) operates at 0.44 MPa, purifying the gaseous product of the heat exchange reactor (R-101). Over 19% of the Section I reaction takes place in the primary scrubbing reactor. Almost 22% of the total reaction takes place in the secondary scrubbing reactor at 0.10 MPa. The secondary scrubber cleans up the oxygen stream exiting the boost reactor as well as the steam/SO_2 stream produced during depressurization of the liquid reaction product of the heat exchange reactor.

Both scrubbing reactors perform a second function as direct contact heat exchangers. Oxygen leaving the process is cooled to near ambient conditions while preheating the water entering the process. The scrubber vessels are fluorocarbon-lined mild steel and the packing is 50 mm ceramic Raschig rings. Pilot plant tests may demonstrate reduced vessel costs. The upper portions of the scrubber contain only water and oxygen, so no lining should be required in this area. Depending upon the temperatures reached in the lower portions of the scrubber, less expensive linings may be possible.

4.3.1.5. Heat and Power Recovery.

The heat transferred to the power bottoming cycle from Section I totals 160 kJ/mole of H_2. The majority of this is transferred via the heat exchange reactor, but significant quantities of heat are also transferred from the hot water products of Sections II and III and from the SO_2/O_2 product of Section II.

Since the heat transfer materials used for water and SO_2 are much less expensive than the niobium used in the heat exchange reactor, there is the potential for further cost reduction by performing more of the cooling on water and SO_2 streams. Ultimately an economic optimization must determine the split in heat transfer duties on the basis of minimum hydrogen production cost.

A total of 27 kJ/mole of H_2 is recovered as work in Section I using turbines for pressure reduction. Preliminary indications are that the turbines are economic, but a final determination must await an analysis based on hydrogen cost resulting from this study.

4.3.2. 1981 Flowsheet Section II: H_2SO_4 Processing

The Section II flowsheet was not revised as part of the base program. Under separate funding the process was adapted to a solar heat source (Refs. 14 and 15); but since the process is enormously complicated by variation in the heat source, an integrated flowsheet did not result from that work.

Also, under subcontract to LLNL (Ref. 16), design and cost estimates were produced for connecting the GA process to a fusion reactor. In this work two different methods of coupling the water-splitting plant to the fusion reactor were explored. LLNL provided the Section II design for both methods, and the results are reported elsewhere (Ref. 16).

4.3.3. 1981 Flowsheet Section III: HI Concentration

The hydrogen iodide concentration step, Section III of the process, entails separation of a mixture of hydrogen iodide, iodine, and water (HI_x) into its component parts. A simplified flow diagram of Section III is presented in Fig. 34. The use of phosphoric acid as an extractive distillation agent remains as the reference process for HI purification, although operating

conditions have been altered to decrease capital cost and increase the efficiency of certain operations.

The system HI-H_2O forms a maximum boiling azeotrope at a composition of 57 wt % HI, which is approximately the composition of HI_x on an iodine-free basis. Iodine is held in the HI-H_2O solution through the formation of polyiodides such as HI_3, HI_5, HI_7, etc., which are formed only in the presence of water. Addition of H_3PO_4 lowers the activity of water, which performs two functions; first, it destabilizes the polyiodide complexes, permitting iodine to form a separate liquid phase; secondly, it breaks the azeotrope, which allows the HI to be distilled from the mixture. The HI distillation is performed under pressure so that liquid HI is available for decomposition in Section IV. Water is removed from the phosphoric acid by evaporation, and the phosphoric acid is recycled back into the process.

4.3.3.1. Iodine Separation.

The liquid iodine is separated from the HI_x in two steps. Both operations are performed in fluorocarbon-lined mild steel vessels packed with 20-mm ceramic saddles. In the iodine knockout column (C-302), the HI_x is contacted countercurrently with 96 wt % H_3PO_4. The HI and H_2O are extracted into the H_3PO_4, leaving molten iodine saturated with H_3PO_4. H_3PO_4 is washed from the iodine with water in the iodine wash column (C-301). The wash column is operated at 0.3 MPa and 393 K so as to maintain both iodine and water in the liquid state.

4.3.3.2. Hydrogen Iodide Distillation Column.

The HI is distilled from the H_3PO_4 solution in a plate column operating at 0.9 MPa. Operation at this pressure, instead of the 0.1 MPa used in the 1979 flowsheet, requires a higher temperature in the bottoms than employed at low pressure; but an expensive HI liquefaction step is eliminated. The column now

operates with a normal reflux instead of the 100% phosphoric acid pseudo reflux. Moreover, the overhead product is now pure HI and a HI/I_2 distillation column is eliminated. The in-column heat exchange used in the 1979 flowsheet was eliminated to simplify construction, but an intermediate condenser was added external to the column which allows part of the condensing heat to be withdrawn from the column at a useful temperature. Although a majority of the heat required to preheat the feed to operate the column is obtained by heat recovery within Section III, 72.4 kJ/mole of H_2 is required from Section V at 523 K.

Design of the column entailed a trade-off between capital and operating costs. Use of the intermediate condenser and operation at a relatively low reflux ratio reduce thermal energy requirements but require more trays in the column for adequate chemical separation. The final design included 50 Hastelloy-C trays in the Hastelloy-C clad mild steel tower. The trays selected were the trough type, being a reasonable compromise between the high efficiency of bubble cap trays and the low cost of sieve trays.

An additional small design complication arises because the feed to the HI distillation column is saturated with iodine. Liquid iodine must be removed continuously as HI is distilled away from the column at an intermediate point to avoid buildup. A stream, containing two liquid phases consisting of phosphoric acid and liquid iodine, is withdrawn from the iodine buildup region. The phosphoric acid returns to the column from the top of a liquid-liquid separator, and the bottom iodine phase passes to the iodine wash column for phosphoric acid removal before returning to Section I.

The small quantities of H_2SO_4 and SO_2, remaining in the lower phase product from Section I, react chemically with HI in the feed preheater for the HI distillation column. The products of the reactions are H_2O, I_2, H_2S, and S. The quantities

involved are so small that the relative amounts of S and H_2S have not been determined. For flowsheeting and cost estimating purposes, it has been assumed that one-half the sulfur in H_2SO_4 and SO_2 ends up as H_2S and one-half as S. The H_2S will leave the column in the overhead product, and the S is assumed to exit the column with the H_3PO_4. The liquid S is separated from the H_3PO_4 and oxidized back to SO_2 in Section II.

4.3.3.3. Phosphoric Acid Concentration.

Removal of water from the phosphoric acid is accomplished in three stages of vapor-recompression-driven flash evaporation. This is one less stage than used in the 1979 flowsheet because 100% H_3PO_4 is no longer required. Only the last stage requires any heat input from the heat source, but all three stages require significant quantities of power for vapor recompression. A total of 131 kJ of shaft power per mole of H_2 is required to operate the compressors, whereas only an additional 21 kJ of thermal power at 484 K per mole of H_2 is required from Section V to heat the high temperature evaporator. Heat is recovered within each evaporation stage from interstage cooling of the six-stage compressor, from the condensation of the compressed steam, and from the concentrated phosphoric acid product.

The phosphoric acid concentration step is simple in concept, but capital costs of the turbine compressors and heat exchangers are significant in the overall hydrogen production cost. Even though methods have been identified for making a considerable reduction in the cost of H_3PO_4 concentration, alternative chemical systems are under investigation with the goal of eliminating H_3PO_4 from the process.

4.3.4. 1981 Flowsheet Section IV: HI Decomposition

The HI decomposition step (Section IV of the process) must perform the following operations:

- o Decompose HI(l) to H_2(g) and I_2(l).
- o Separate HI from the I_2 and recycle to the decomposer.
- o Separate HI from the H_2 and recycle to the decomposer.
- o Scrub the H_2 product in preparation for distribution.

A simplified flow diagram of Section IV is presented in Fig. 35. As in Sections I and III, heat exchange has been moved external to the columns.

Three process variables dominate the design of Section IV and have a direct impact on Section V. The temperature and pressure of the decomposition reactor govern the equipment size and amount of recycle through the reactor. The HI-I_2 distillation column pressure determines the maximum process temperature of this section, and in the overall process, this temperature is second only to the SO_3 decomposer of Section II. Variables governing the cleanup of the hydrogen product have a smaller, but still significant, impact on the hydrogen production cost.

4.3.4.1. HI Decomposition.

Hydrogen iodide decomposition is accomplished in the HI decomposition reactor (R-401). The extent of the decomposition reaction is limited by thermodynamic equilibrium. Therefore, to limit the amount of recycle of HI back through the reactor, process conditions must be chosen so as to give a high conversion per pass through the reactor. Previous studies at GA (Ref. 6) have demonstrated that, when decomposition is carried out under high pressures so that HI and I_2 are present as liquids, a much higher decomposition yield is obtained than with the analogous gas phase decomposition. Selection of the temperature and pressure involves a number of trade-offs. The critical temperature of HI places an approximate upper limit upon the initial reaction temperature of an adiabatic flow reactor, while the required hydrogen delivery pressure places a lower bound upon the system

pressure. The reactor finally selected for HI decomposition is an adiabatic flow reactor with a 4-min residence time employing activated charcoal as a catalyst. The mild steel vessel is lined with fluorocarbon to protect it from the HI and iodine. The reactor operates at 8.3 MPa. (The 1979 flowsheet indicated 5.0 MPa, but there is some question whether the stream will remain liquid throughout the length of the flow reactor at that pressure.) The reaction temperature increases from 415 K at the inlet to 424 K at the outlet due to the slightly exothermic nature of the reaction under these conditions. The majority of the energy required to bring the HI to reaction temperature is supplied by heat refuse within Section IV. Only 6% of the energy (2 kJ/mole of H_2) must be supplied from Section V.

A design based upon a continuous stirred tank reactor deserves future consideration. It would require a considerably longer residence time than the adiabatic flow reactor, but the system pressure could be lowered to 5 MPa, which may lead to reduced capital costs.

4.3.4.2. $HI-I_2$ Distillation.

The liquid product from the HI decomposition reactor passes through a pressure-reducing turbine to the $HI-I_2$ distillation column (C-401). The pressure of the still (5.1 MPa) sets the temperature of the still bottoms at 713 K, which is the highest temperature required for the Section V helium. The still pressure and temperature may be decreased further, thus decreasing the high temperature heat load on Section V, but at the expense of increased low temperature heat requirements to reheat the still overhead product for recycle to the HI cracker. In addition, the heat now supplied from the overhead condenser to the evaporative refrigerator and from the bottoms product to the liquid HI heat exchangers would instead have to be supplied from other sources.

In addition to the 7 kJ/mole of H_2 required at 713 K, an additional 1.7 kJ is required at 616 K and 7.1 kJ at 522 K. This additional heat may be used at this lower temperature because the distillation column is designed with intermediate reboilers. The use of intermediate reboilers increases the capital cost due to the cost of both the boilers and additional trays in the column, but the overall thermal efficiency is improved significantly.

Each distillation column, constructed from Hastelloy-B clad mild steel, is 2.7 m in diameter for the bottom 12 m and expands to 4.7 m in diameter for the upper 3 m. There are 25 Hastelloy-B trough type trays in the bottom section and 6 in the top. The expanded top section is required by both the higher flow rates and lower density encountered in this section of the column.

4.3.4.3. Hydrogen Cleanup.

The hydrogen from the decomposer is cleaned in three operations. First, the bulk of the hydrogen iodide is removed by condensation. Second, remaining HI is removed with a water wash. Finally, the trace of H_2S is removed by a combination of chemical reaction and water wash. The H_2S removal step was not defined in the 1979 flowsheet.

The gaseous product of the HI decomposition reactor is cooled in three stages. A heat exchanger removes the high temperature portion of the heat to the power bottoming cycle and dumps the low temperature heat to cooling water. The stream is further cooled from 303 K to 291 K via an absorption refrigeration system. The LiBr-based refrigeration (Ref. 17) is driven by waste heat from the condenser of the HI-I_2 distillation column. After condensate separation, only a small quantity of HI and possibly H_2S remains in the hydrogen.

The remaining HI is easily removed via a water wash (C-402). A minimum amount of water is employed because any water added at

this point must be removed by distillation in Section III. In the absence of iodine, HI is not corrosive to nonmetallics; therefore, hydrocarbon-based lined mild steel is sufficient for this application. Since traces of iodine could enter the HI scrub column due to process upsets in the HI condensation system, the lower portions of the column are lined with fluorocarbon. The column is packed with 25-mm ceramic Raschig rings.

Due to the high acidity in the lower portions of the column, H_2S cannot be absorbed. H_2S builds up slightly in the upper section of the column until at steady state, H_2S passes on to the H_2S removal column (C-403) at the same rate it enters the HI scrub column. Since H_2S has a relatively low solubility in water, a simple water scrub would require that an excessive amount of water be processed through Section II to reconvert the H_2S to SO_2. The problem is solved by adding a small amount of SO_2 to the H_2S absorber. H_2S reacts with SO_2 in the presence of water to produce a sulfur slurry. The slurry is concentrated via a filter with backflush, so only a small amount of water accompanies the S back to Section II where it is converted to SO_2 via reaction with SO_3. The mild steel column, packed with 25-mm ceramic Raschig rings, is hydrocarbon lined to prevent corrosion.

The H_2 pressure is dropped to the distribution pressure of 5.1 MPa via a power recovery turbine and thus exits the process.

4.3.5. 1981 Flowsheet Section V: Heat and Power Interfacing

As in the case of Section II, further development of Section V has been left to other projects which match the cycle to particular heat sources. No work on Section V has been included in the base program since 1979.

4.4. COST OF HYDROGEN FROM A SOLAR-POWERED THERMOCHEMICAL WATER-SPLITTING PLANT

4.4.1. Capital Costs

The preliminary estimate of the cost of hydrogen from a solar-powered version of the GA sulfur-iodine thermochemical water-splitting cycle is 17.96 to 21.58 $/GJ (constant dollars, July 1980). This cost is based on utility financing of a 500 MWT hydrogen plant. The plant design was not optimized and this cost estimate is considered to be conservative.

This cost estimate assumes that the plant operates as an independent entity. Solar energy and water are the only inputs to the cycle and hydrogen is assumed to be the only salable product. No credit is assumed for the oxygen product, nor is any value placed upon the waste heat from the process. It would be improper to call any plant "solar" which receives a significant fraction of its energy input from nonsolar sources, but co-production of hydrogen and either electricity or process heat from an integrated solar plant may be economic. The sulfur energy storage scheme (Ref. 15) used to provide both diurnal and seasonal storage of solar energy for this hydrogen plant could produce peaking and evening power from a solar source using a hydrogen plant to recycle the sulfur dioxide combustion product. Sale of waste heat from the plant may also be possible in special circumstances where a suitable customer is located adjacent to the solar hydrogen plant.

Although a final cost estimate will require a detailed consideration of the daily and seasonal variations in insolation, use of the sulfur energy storage system permits effective decoupling of the diurnally operated sulfuric acid concentration and decomposition processes from the continuously operated hydrogen production processes. Figure 36 indicates how, with long-term

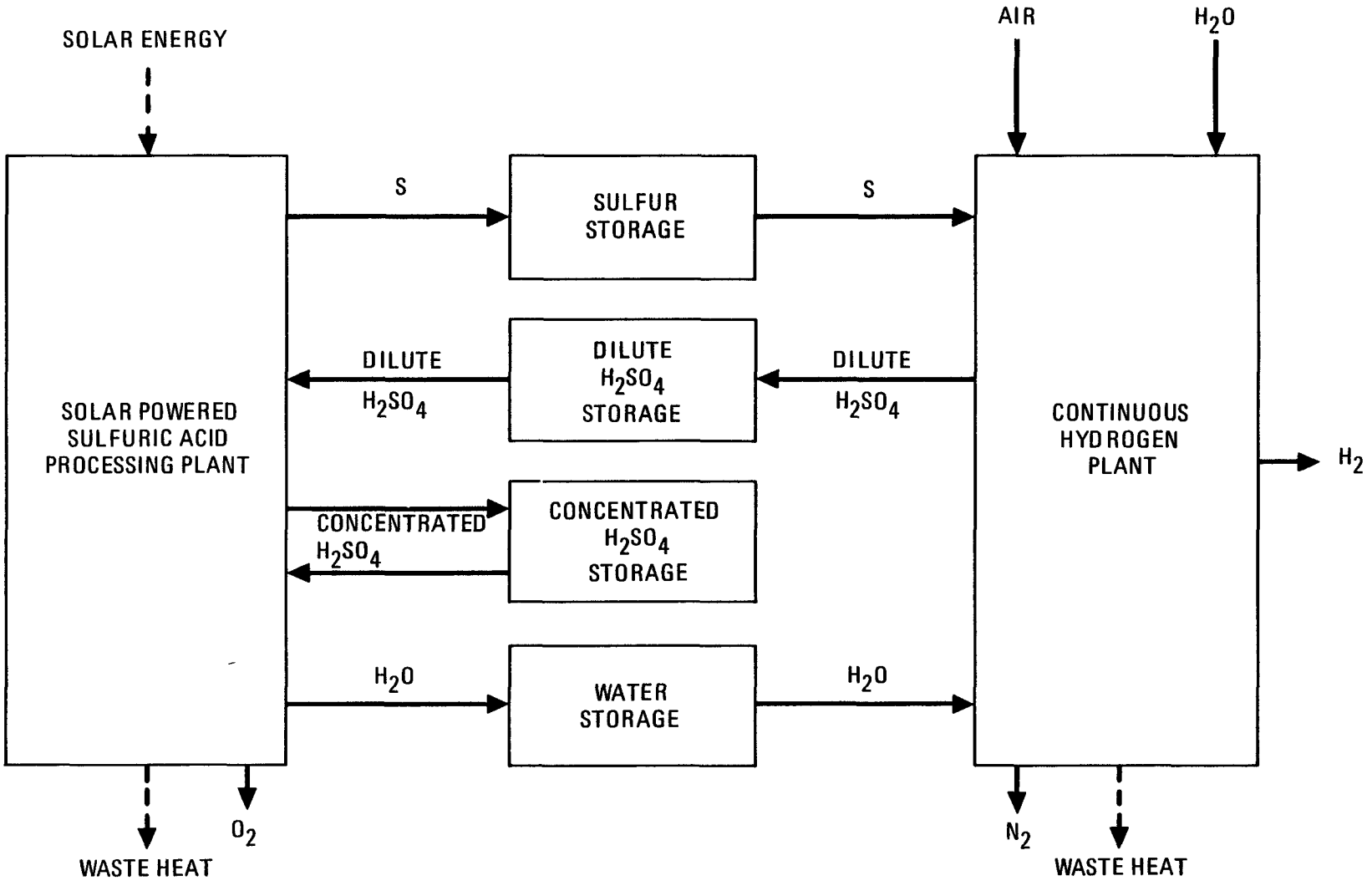

Fig. 36. Simplified diagram of the solar version of the sulfur-iodine cycle using sulfur storage

storage of sulfur, water, and concentrated sulfuric acid and with short-term storage of dilute sulfuric acid, the two portions of the process may be effectively operated independently. An actual plant would make use of solar energy and solar-produced SO_2 during daylight hours; thus the assumption of a decoupled plant produces a conservative cost estimate.

Portions of the following capital cost estimate are based on the cost for a fusion-powered water-splitting plant as estimated by GA and the LLNL (Ref. 16). Equipment has been resized to account for the smaller scale of the solar-powered plant and the nitrogen dilution of the sulfur dioxide in Section I. The sulfur combustion section including power production and heat transfer equipment was flowsheeted, and the equipment was sized and costed as part of this effort. Additional costs were included in the appropriate sections to account for the sulfur disproportionation equipment and the long-term chemical storage.

The capital costs for the chemical plants and the energy transport and conversion systems are given in Table 4. Also included is the cost of the process equipment, if made from carbon steel instead of the corrosion-resistant materials actually specified. The carbon-steel equipment costs are used in estimating the operating costs. Not included are the costs for the strictly solar portions of the facility, such as the power tower and the mirrors. The solar equipment costs are included in the final cost estimate as an equivalent operating cost.

The only costs not completely revised from the fusion version are those of Sections II and Va. The cost of Section II was modified from the more costly of the two fusion versions only by the addition of the costs for the sulfur dioxide disproportionation equipment and sulfuric acid storage. The size of the sulfuric acid processing section is identical for the solar and fusion plants considering that the solar plant operates only during daylight hours and that it has the additional load to

TABLE 4
CAPITAL COST OF A SOLAR-POWERED THERMOCHEMICAL HYDROGEN PLANT

Section		Carbon Steel Equivalent Equipment Cost (M$-July 1980)	Total Capital Cost (M$-July 1980)
I	Main Reaction (C)	2.5	15.8
II	Sulfuric Acid Processing (D)	39.6	133.6
III	HI Purification (C)	15.9	97.9
IV	HI Decomposition (C)	2.3	13.0
Va	Solar Energy Transport and Conversion (D)	-	119.0 - 297.4
Vb	Sulfur Combustion, Energy Transport and Conversion (C)	-	54.3
		60.3	433.6 - 612.0
	3% Contractor's Fee		13.0 - 18.4
			446.6 - 630.4
	Interest During Construction		35.2
			481.8 - 680.1

(C) Continuously Operated
(D) Diurnally Operated

provide sulfur storage. The sulfuric acid plant would be significantly smaller if decoupling of the diurnal and continuous plants had not been assumed.

It is difficult to estimate the cost of Section Va, which interfaces the thermal and electrical requirements of the diurnal plant with the solar heat source. Certainly the cost of Section V for the fusion plant sets an upper bound, since the solar plant does not have to meet the nuclear containment criteria nor does it have the large electrical loads of the fusion plant. A more reasonable estimate is that the solar Section Va is 40% of the fusion Section V. For completeness, the higher value is also carried through the cost estimating exercise.

The final entry in Table 4 is the contractor's fee of 3%. All other direct and indirect costs are included in the estimates from the individual sections.

4.4.2. Hydrogen Production Costs

Hydrogen production costs include the yearly capital charges and the costs of plant operation and maintenance. Since costs have not been provided for the solar portions of the plant, they are included separately as a cost of energy input to the process.

The capital costs will be a function of interest rates, the particular form of financing employed, the type of accounting employed, the construction time, and the operating life of the plant. Public utility financing and constant dollar accounting have been assumed. For public utility financing, the total capital is provided by debt, and there is no provision for profit. Constant dollar accounting assumes that all costs are expressed in terms of the value of money during the base year. Interest rates are then expressed as the increment by which actual interest rates exceed the inflation rate. Typically, the 5% of interest used expresses the true cost of borrowing money. The cost of

hydrogen expressed in constant dollars is then not an estimate of what hydrogen will cost in the future from a plant that is being built now, but rather an estimate of what hydrogen would cost now from a plant that had been built in the past. Since constant dollar financing is the method which best compares costs from future plants with today's costs, it is a standard for fusion cost studies (Ref. 18). All costs in this section are thus quoted in constant dollars.

The debt at the time plant construction is complete will be greater than the capital investment given in Table 4 because construction funds must be borrowed. Assuming continuous compounding and that the rate of borrowing is linear over the 3-year construction period, the capital to be recovered is 481.8-680.1 M$. Assuming a 30-year plant life and pay-back period, the yearly fixed cost due to capital charges is 30.0-43.8M$.

Standard techniques are available in the chemical engineering literature for estimating operating costs of chemical plants based on the capital cost of the plant as constructed from carbon steel equipment. Guthrie (Refs. 19 and 20) provides the factor (2.482) for converting the carbon steel equipment cost from Table 4 into a total plant cost and the factor (0.20) for estimating the total annual operating costs from the total plant cost. Applying both these factors, the operating cost of the chemical sections of the plant is obtained.

Sections Va and Vb are similar to power plants rather than chemical plants; therefore, the Battelle methods have been used (Ref. 18) for calculating operating costs for these sections. Operation, maintenance, and other fixed charges total 3.8% of the capital cost for public utility financing and constant dollar accounting.

The solar-powered hydrogen plant will produce 5.68×10^6 GJ equivalent of hydrogen per year. This assumes that the require-

ment for overnight energy storage reduces the plant efficiency to 40% (Ref. 1) from the 47% typical of a plant with a constant heat source. Table 5 shows that the yearly costs distributed over the yearly hydrogen production yields a hydrogen cost (neglecting the cost of solar energy) of 11.71 - 15.33 $/GJ.

It is not yet apparent what concentrated solar heat will cost from a plant of the proposed scale. On a constant dollar basis, the cost of solar energy is expected to decrease relative to the cost of fuel-based energy. When solar energy becomes truly competitive, its cost will approximate the constant dollar cost of present nuclear energy. On this basis $2.50/GJ has been used as the constant dollar cost of net solar energy delivered to the receiver. Since 40% of this energy ends up in the product hydrogen, the added cost for solar energy is $6.25/GJ. Adding this to the other costs in Table 5 gives a final hydrogen cost of $17.96 - 21.58/GJ.

There is substantial belief that efforts to improve the unit operations of the cycle will reduce the capital costs and thus the cost of manufacturing the hydrogen. While the above cost reflects future technology in the solar heat source, it does not reflect future hydrogen production technology.

4.5. THE FUNK PANEL REVIEW

During the course of development of the GA sulfur-iodine cycle, a number of external reviews have taken place. One of these was performed in the cycle development by Lummis and is now essentially outdated. Another more recent review was done by Ekman at JPL when he costed several methods of H_2 production. The fusion work managed by LLNL, adapting the sulfur-iodine cycle to their Tandem Mirror Fusion Reactor, constitutes still another review. These investigations of the GA cycle have generally portrayed this cycle in a most favorable light.

TABLE 5

HYDROGEN PRODUCTION COST

	Yearly Cost (M$ - July 1980)
Capital Charges	30.0 - 43.8
Annual Total Operating Cost Sections I - IV	29.9
Annual Total Operating Cost Sections Va and Vb	6.6 - 13.4
	66.5 - 87.1
Yearly Hydrogen Production 5.68×10^6 GJ	
Hydrogen Cost Excluding Solar Facilities	11.71 - 15.33 $/GJ
Hydrogen Cost due to Solar Facilities	6.25 $/GJ
Total Cost of Hydrogen	17.96 - 21.58 $/GJ (July 1980)

Perhaps the Funk panel constitutes the most in-depth critical review of the GA cycle and for that reason will be considered in more detail in this report. This panel produced, in a draft report dated July 30, 1980 and amended September 26, 1980, a list of the findings with respect to this cycle. This report was prepared after due consideration of the cycle in both their own deliberations and at least one investigative meeting at GA. In summary, their report states that there is enough data to say the "process is technically feasible as described by GA." The committee recognized the formidable material problems associated both with H_2SO_4 boiling and HI_x and I_2 handling but stated these "problems appear amenable to solution with known engineering materials." Further bench-scale testing was urged to verify results. The committee pointed out that "process economic data are lacking for the GA process" and recommended preparation of a "first cut economic analysis." They believe that such analyses will "clearly indicate areas requiring maximum improvement." A sensitivity analysis was suggested as possibly the only feasible means of costing accurately. Heat penalty analyses were also proposed.

Water retention was called out as a major problem in the GA cycle. It was, however, recognized that this water is being processed efficiently but at a relatively high cost. The committee recommended that "alternatives to circumvent the phosphoric acid dehydration step be considered on a priority basis." The committee noted that GA appears to be making good technical progress in "chemical and bench-scale studies" and quoted an example. They lauded the cycle for its near absence of side reactions and for its short reaction times as minimizing inventory and capital costs.

Efforts at GA have generally taken into consideration this review. An alternative to H_3PO_4 has been sought, and indeed at least two promising possibilities have been uncovered as reported in other sections of this report. Costing has been done and is

also presented in this report. Materials investigations were continued, however, for the most part in another program. General Atomic believes that the program shows ever-improving promise of providing H_2 from process heat sources at competitive costs.

4.6. PROCESS SIMULATOR COMPUTER CODES

During the course of the thermochemical water-splitting project at GA, it has been clear that flowsheeting and costing, to be done in a manner that will allow optimization techniques permitting selection of superior unit operations, must be computerized. During the course of these studies and studies at LLNL on a related program (Ref. 16), initial application of such codes to the GA sulfur-iodine cycle has been made. Other workers have also been of the same opinion. For instance, the Ispra facility has developed OPTIMO (Ref. 21), and the University of Aachen is working on such codes (Ref. 22). General Atomic's efforts in this area are described in Appendix A.

5. RESEARCH DEVELOPMENT EFFORTS

5.1. INTRODUCTION

The present GA sulfur-iodine water-splitting cycle is the cumulative result of a number of findings established during the course of R&D effort. Some of these include the phase separation in the Bunsen reaction, the H_2SO_4 boost reaction, advanced catalytic decomposition of H_2SO_4, direct SO_2,O_2 mixture utilization in the Bunsen reaction, catalytic liquid phase HI decomposition, and H_3PO_4 treatment to recover HI from HI-I_2-H_2O solutions. As shown in this section, R&D discoveries have not been exhausted in this field. This section reports two methods of circumventing the H_3PO_4 treatment--one as a new idea and the second as a partially developed scheme. In addition, some characterization of the H_3PO_4 treatment of HI_x solutions is reported. Finally, a better way to catalyze the HI( ) decomposition is presented. Much profitable work still lies in the future.

5.2. HBr TREATMENT OF HI_x SOLUTIONS

In the sulfur-iodine cycle a solution of HI, I_2, and H_2O is produced. This solution is the latent source of H_2 from the cycle. The HI and the H_2O are present in this solution at partial molar free energies of -6.2 and -0.6 kcal/mole, respectively (Ref. 5). In order to separate these components, at least these energies must be supplied. The cycle, in its current embodiment, uses concentrated H_3PO_4 to act on the solution in such a way that most of the iodine separates into a second phase, and more importantly the chemical potential of the H_2O is lowered by binding H_2O in the influence sphere of the H_3PO_4. This results in enhancement of the chemical potential of HI to the degree that it can be separated from the H_2O-H_3PO_4 solution by fractional distillation. Most of the energy associated with the HI-H_2O-I_2 solution separation is required during the separation of H_2O from

H_3PO_4 to prepare the H_3PO_4 for recycle. In the present engineering design of this portion of the process, this energy is supplied as work in the form of vapor recompression by turbines which take H_2O vapor from the H_3PO_4 distillation and compress it, causing condensation and the concomitant release of the heat of vaporization at temperatures slightly higher than the heat used to evaporate the H_2O in the first place. This vapor-recompression scheme saves considerable heat energy but uses expensive work energy generated in expensive equipment.

Because of the costs of processing and not because of energy efficiency considerations, other techniques for HI recovery from $HI-H_2O-I_2$ solutions have been investigated. Finding other competitive methods to rectify this solution is not any easy task. The energies involved are those of chemical reactions not usually encountered in solution separations. A simple extraction agent for HI must react with HI with greater energies than HI has with H_2O-I_2 systems. While one may find appropriate agents, the problem then becomes how to get the HI out of the extraction agent. A number of organic reagents which may extract HI reasonably well fail at this later stage. Nevertheless, success has been achieved in the search for alternate methods of processing $HI-I_2-H_2O$ solutions.

In an earlier publication (Ref. 6), HI and H_2O mixtures were reported to form two liquid phases: (1) a nearly dry liquid HI, and (2) a strong superazeotropic solution of HI in H_2O. Mixtures of $HCl-H_2O$ were also reported to phase separate (Ref. 23). This liquid-phase formation was concluded to have considerable value in separating HI from $HI-I_2-H_2O$ product solutions from the $H_2O-SO_2-I_2$ reaction. However, to achieve separation conditions, the HI content of these product solutions needs to be considerably increased. Up to now, this seemed possible only by techniques already in use, such as H_3PO_4 treatment.

Still earlier, a high-pressure distillation to break the $HI-H_2O-I_2$ pseudoazeotrope was investigated (Ref. 1) as an alternative to the H_3PO_4 treatment. This distillation process was found to be considerably less efficient than breaking the azeotrope of $HCl-H_2O$ (Ref. 24). Thus, the pursuit of this technique was temporarily abandoned. However, some engineering evaluations of the small azeotrope shifting, found to occur in the $HI-H_2O$ system (57% HI to ~45%), indicated that this process is basically similar in efficiency to the H_3PO_4 treatment.

A process has been conceived which combines high-pressure azeotrope shifting, two-phase formation, solvent extraction using a hydrogen halide (HCl or HBr) for HI separation, and some other features to sharply reduce the amount of H_2O distilled in processing HI_x solutions. To establish the feasibility of this process, laboratory experiments were undertaken to study (1) the distribution of HI between a dry hydrogen halide phase and the wet phase, (2) the behavior of I_2 in these phases, (3) the high-pressure distillation to separate H_2O and HBr, (4) the fate of the HBr and the degree of reaction of the reactants in the $H_2O-SO_2-I_2$ reaction, and (5) the recovery of HBr from these product solutions. These studies will be considered in this section.

5.2.1. Hydrogen Halide-Water System

During the course of investigating the catalytic decomposition of liquid HI, systems that were wet were studied to find the H_2O effect on catalysis. Surprisingly it was found that only a very limited amount of water could be added to a liquid $HI-I_2$ system without separation of a second phase, high in water content (Ref. 6). This separation was found to take place whether or not I_2 was present and persisted up through the condition where solid I_2 was present. The phase boundaries are presented in Fig. 37 for two temperature levels. A parallel to this unusual separation and coexistence of two so very interactive species was encountered in the $HCl-H_2O$ system (Ref. 23). As a

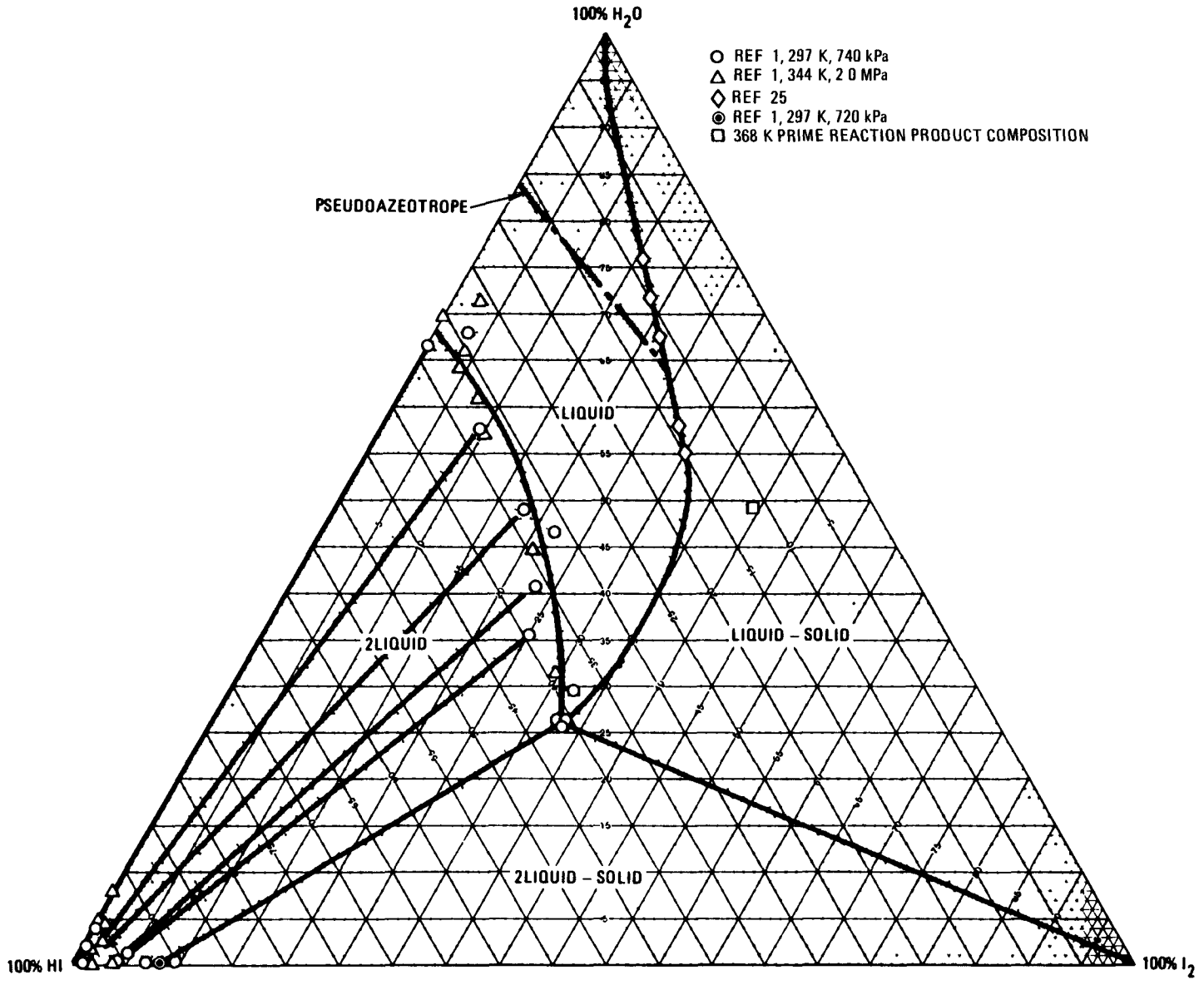

Fig. 37. Mole percent phase diagram for HI-I_2-H_2O mixtures

portion of the work done on this program, the phase separation in the HBr-H_2O water system was determined to result in coexisting equilibrium phases of a rather dry HBr solution and a 41 mole % solution of HBr in H_2O at 273 K. Thus, all three hydrogen halides tested (HF does not exhibit this phase separation) exhibit phase separation which may be best characterized by indicating that dry liquid hydrogen halides and hydrated hydrogen halides do not mix. This finding has been extended to hydrogen halide mixtures and water. These mixtures became a subject for investigation as a separation system for hydrogen halides and water. These studies have included investigations of HCl-HI-H_2O and HBr-HI-H_2O mixtures to determine the position of the tie lines in these systems in the presence of I_2.

In order to define these tie lines, a distribution coefficient approach was developed. This distribution coefficient is defined as

$$D = \frac{HI_{Dry} \cdot HX_{Wet}}{HI_{Wet} \cdot HX_{Dry}}$$

where the ratio of concentrations of the two hydrogen halides (in mole fractions) in the two phases are ratioed. This distribution coefficient has been found to be reasonably constant over a wide range of HI mole fractions when compared to one of the other hydrogen halides. Temperature variation studies have not revealed much sensitivity of the distribution coefficient, while at high temperature, iodine (when present in massive quantities) has shown a significant effect on this coefficient.

The most desirable occurrence would be to find a large value for the defined coefficient because this would mean that HI could be extracted efficiently in the dry phase with minimal amounts of the other hydrogen halide.

Hydrogen chloride was tested with rather discouraging results. The measured distribution coefficient with no I_2 present at ~260 K was 0.32. It would have been fortunate if HCl had worked better since the HCl-H_2O azeotrope can be broken in high-pressure distillations (Ref. 24) such that H_2O alone is left in the pot of the high-pressure distillation. This would have meant that HCl could be completely recovered by boiling it out of HCl-H_2O mixtures. The 0.3 distribution coefficient means, however, that about 12 times as much HCl must be distilled as there is HI present. This appears to be excessively energetic.

In contrast, HBr exhibits a much more favorable distribution coefficient of about 5. Tie lines which define this distribution coefficient are shown in Fig. 38. These were measured at different temperatures (273 to 356 K), pressures, and iodine contents (up to 8%). The distribution coefficients varied from 4.7 to 6.1 for these measurements--basically a constant. The phase boundary of the wet phase is depicted as a line connecting an HI-free value to an HBr-free value. The data, to a reasonable approximation, fit this line. There appears to be some small trend for the higher temperature points to have higher H_2O concentrations.

Using these data in a countercurrent extractor model, one can predict that 1 mole of HI can be extracted by 2.4 moles of HBr. When this is done, one obtains as one product solution a 70 mole % solution of HI in HBr on an I_2- and H_2O-free basis. The remaining solution contains essentially all of the original water and 2 moles HBr/initial mole of HI. The iodine appears in both solutions according to its solubilities and may appear as a solid under certain circumstances. However, it appears that, at a high enough temperature in the countercurrent column, the HBr will also extract the I_2. This is based on previous work on HI-I_2 solubilities (Ref. 26) and the similarities of liquid HBr and liquid HI. There needs to be little said about the dry HI-HBr phase. One can distill the HBr and HI out of it to purify the HI, or one could directly decompose HBr-HI mixtures in liquid

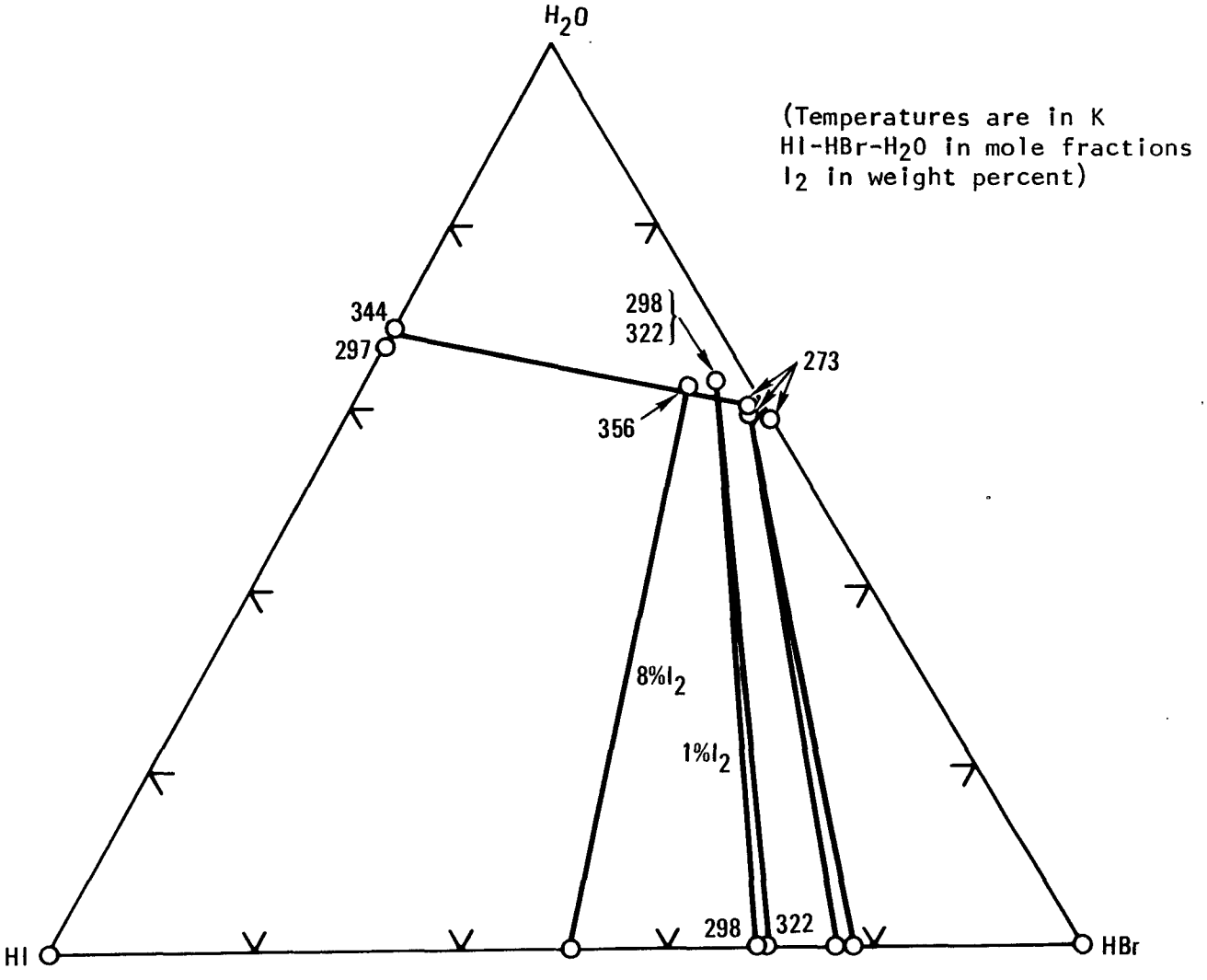

Fig. 38. Iodine-free tie lines for the two-phase HI-HBr-H_2O (I_2) system

decomposition processes already a part of the sulfur-iodine cycle (Ref. 6). In either case, processing the 70 mole % HI does not appear to be much of a problem. Processing the HBr-H_2O product solution does appear to be more of a problem and has been the object of study.

5.2.2. Experimental Procedures - High-Pressure Distillation Studies

A portion of the GA development program on the water-splitting cycle has been high-pressure (up to ~300 bars) distillation studies. An apparatus has been constructed that allows for supplying heat to a quartz still which operates inside of a pressure vessel. This apparatus is shown in Fig. 39 and is further described in Refs. 1 and 2. Its features include (1) a circulating boiler section which is heated by a bayonette heater located in a well at the bottom of the apparatus, (2) a vapor section which is insulated so that essentially no refluxing occurs in this section, (3) a vapor annulus surrounding and insulating the vapor section, (4) a condenser section through which a cooling fluid is pumped from the bottom of the pressure vessel, (5) a delivery tip equipped with a drop counter system to measure liquid flow from the still, and (6) a lazy susan collector system where successively each of six collection tubes can be positioned to accept the flow from the still. The still temperatures are measured by thermocouples located in an improved (since that discussed in the references) tube penetration ending in the insulated vapor section at the top of the boiler. In some previous work H_2O was used as the condenser coolant liquid, but in this work low-vapor-pressure, 10-centistoke L-45 silicone fluid obtained from Union Carbide was used. This was necessary to prevent the coolant from contaminating the distillation cuts.

The studies were made by installing the loaded cell in the pressure system, evacuating the system to remove traces of air and H_2O, and backfilling with argon to the desired pressure as

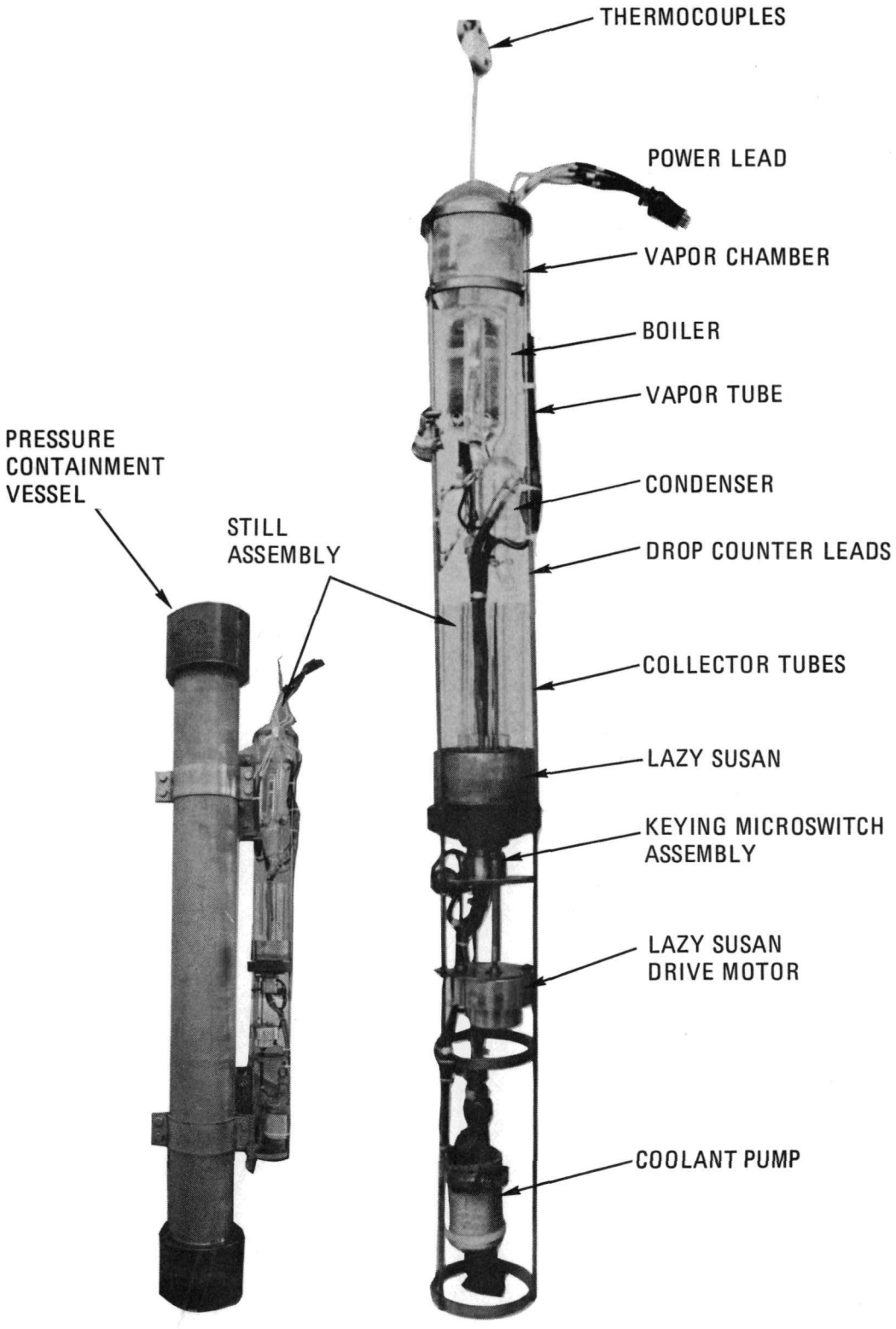

Fig. 39. High-pressure distillation apparatus

determined through the use of calibrated gauges. The still was then heated, pressures and temperatures were recorded (the pressure increased as the still was heated), and when distillation took place, the distillate flow was noted and the collection tubes were changed at appropriate times.

When the experiment was completed the still was cooled, the system was depressurized and disassembled, and the samples were protected as necessary. The composition of the samples was measured by titrimetric methods.

The vapor-liquid equilibrium data were constructed from the mass balances derived from the weights of the distillates and pot residue and the analyses.

Initially this technique was used to study the H_2SO_4-H_2O azeotrope. This work was performed early under an LANL subcontract (Ref. 27). Since that time the apparatus has been reconstructed so that thermocouple wires directly penetrate into the high-pressure apparatus and thus accurately measure the still temperatures. Previously these temperatures were underestimated due to chemical penetration temperature gradients where those penetrations carried the thermocouple voltages.

5.2.3. Rectification of the H_2O-HBr Solution

The HBr-H_2O solution resulting from the countercurrent extractor is highly superazeotropic in HBr. Thus, much of the HBr can be distilled out of this mixture without a large energy expenditure. Nevertheless, the distillation of HBr out of the 1 atm HBr-H_2O azeotrope (48% HBr) does involve energetic processes. Since the HCl-H_2O azeotrope was known to break in a high-pressure distillation, the HBr-H_2O was worth investigating. This was done utilizing the described high-pressure apparatus.

Charges above, below, and some quite near 25% HBr were distilled at ~200 atm, 350°C with the result that the pot composition moved toward 25% HBr. This composition is, thus, the 200 atm azeotrope. It is believed that this pressure is attainable and, thus, that a 25% HBr product can be obtained in a distillation column wherein HBr is the other product when above 25% HBr is distilled.* The data indicate that the HBr distillation can be done with a reasonable number of plates. It is expected that the efficiency of this distillation can be high. The problem then is how to recover or utilize this 25% HBr solution.

5.2.4. Treatment of the 25% HBr Solution

The result of the HBr treatment of $HI-I_2-H_2O$ solutions is that the water from this system contains about 25% HBr. Direct distillation techniques, without distilling water or adding agents such as H_3PO_4, will not result in reducing the HBr content of this mixture. The goal of this effort was to reduce the distillation of water from this product. In the present sulfur-iodine cycle all of the water in this product is distilled from H_3PO_4.

Clearly, there are ways of utilizing this solution and its relatively high water chemical potential. For instance, one could couple this solution osmotically with H_2SO_4 solutions like the 57% product of the H_2SO_4 boost reaction (Norman and others, 1980). In this case, for a water-only permeable membrane, water will pass from the HBr solution to the H_2SO_4 solution, diluting the H_2SO_4 product (countercurrently one could achieve an even more concentrated HBr solution). This HBr solution could be again treated by high-pressure distillation as recycle material. This process, however, requires a membrane stable in strong acids

*Tests at this same pressure on $HI-H_2O-I_2$ solution have resulted in a shift of the $HI-H_2O$ pseudoazeotrope from ~57 to ~45% HI--a shift, marginal at best, for treating $HI-H_2O-I_2$ solutions.

with specific high water transport. This membrane is not believed to be available in an economic sense. Other processes such as using the 57% H_2SO_4 to break the $HBr-H_2O$ azeotrope might also have a degree of success.

One process that has considerable merit has been studied. This is to use the 25% HBr solution directly in the $H_2O-I_2-SO_2$ reaction to produce H_2SO_4 and HI. This study was done using the same technique as employed previously to study the $H_2O-I_2-SO_2$ reaction itself (Ref. 5). A 25% HBr solution with added iodine was treated at 95°C with SO_2. The off-gases carried from the reaction product by transpiring SO_2 were used to determine the chemical activities of the volatile solution species. The results of the 25% HBr experiment (50% HBr solutions were also tested), where enough I_2 was used so that the phases were close to saturation with I_2 at 95°C, are given in Table 6. The high activity of I_2 was discerned from the closeness of the I_2 vapor pressure to that of pure I_2.

Table 6 demonstrates a considerable $H_2O-I_2-SO_2$ reaction. If one assumes the HBr surviving the reaction is azeotropic HBr (47.5%), then one arrives at the conclusion that essentially the yields of H_2SO_4 and HI are consistent with reacting normally with the water present in excess of that required to bring the HBr to azeotropic. This means that between 1/2 and 2/3 of the water from a 25% HBr solution can be reacted to form normal $H_2O-I_2-SO_2$ reaction products. Thus, this water does not have to be boiled in the cycle. The fraction of this water in the HI product solution is again recycled through the HBr treatment. Any HBr in this product is of no concern since more HBr is added in extracting the HI component. However, the system is complicated by having to process the $H_2SO_4-H_2O-HBr$ solution.

No experiments have been performed to determine the effect of the H_2SO_4 boost reaction (Ref. 5) on this product. However, a countercurrent I_2, SO_2 treatment will make more H_2SO_4 and HI and

TABLE 6

A STUDY OF THE SO_2-H_2O-I_2 REACTION IN 25% HBr SOLUTION AT 95°C

	Upper Phase (wt %)	Lower Phase (wt %)	Vapor Pressure (Atm)	Activity
HI	3.4	7.4	-0.004	(a)
HBr	25.0	2.4	0.016	(b)
I_2	3.3	82.5	0.042	0.86
H_2O	46.9	7.0	0.290	0.35
H_2SO_4	21.3	(0.6)	-	
SO_2	-	-	0.656	

(a) Result was negative due to errors in subtracting formed HI from the H_2O-SO_2-I_2 reaction based on amount of H_2SO_4 found.

(b) The HBr/H_2O molar ratio was 0.055, while the mole ratio for the HBr/H_2O atmospheric azeotrope is 0.204.

extract more HBr. In fact, it is projected from the experiment on 25% HBr solution that the boost reaction I_2 will extract nearly completely the HBr from the H_2SO_4. This being the case, the product of the boost reaction is expected to approach the 57% H_2SO_4 previously achieved without HBr present. In this case this HBr is returned to the main reactor with its accompanying H_2O.

It thus appears that the only water that will need to be boiled in the sulfur-iodine water-splitting cycle is that accompanying the 57% H_2SO_4. This is indeed a minimization of this quantity if one does not utilize solid sulfate techniques such as offered by, for example, $Bi_2(SO_3)_3$ techniques.

5.2.5. Rectification of the H_2SO_4-H_2O-HBr Solution

If HBr is not sufficiently removed by the boost reaction, then the question is what is its fate. The HBr-H_2SO_4-H_2O solution exhibits questions in common with the Ispra sulfur-bromine cycle: in particular, how does one separate HBr from H_2SO_4. The problem is far less difficult than the HI-H_2SO_4 separation. In this latter case, H_2SO_4 acts like an oxidizing agent toward HI at concentrations of H_2SO_4 around 50% to 60%. At these concentrations HBr is not oxidized. Moreover, at a concentration of about 60% H_2SO_4, the HBr-H_2O azeotrope is broken (Ref. 28). This means that dry HBr can be obtained from the HBr-H_2O-H_2SO_4 product by adding more concentrated H_2SO_4 and fractionally distilling. Concentrated H_2SO_4 is a necessary product of the operations of the sulfur-iodine cycle. A recycle of concentrated H_2SO_4 is within the normal scope of operations of the sulfur-iodine cycle. Thus, the selection of concentrated H_2SO_4 to act as an extractive agent for water in the extractive distillation is appropriate. Without adding extra H_2SO_4, it will be necessary to distill out the water contained in the product anyway. After adding the H_2SO_4 this same H_2O must be distilled. Of course, on the average, it is distilled from a deeper thermodynamic sink. That is, it takes

more energy per mole of water to distill 70% H_2SO_4 to azeotropic composition than it does 50% H_2SO_4. Nevertheless, this concentrated H_2SO_4 recycle results in obtaining the HBr in a dry form, which is a prerequisite for the treatment of the HI-H_2O-I_2 solution.

5.2.6. Conclusions

As a review of the revised sulfur-iodine cycle, a block diagram of this modification is presented in Fig. 40. The five additional and/or replacement sections are designated by stars. Three such blocks involving H_3PO_4 were replaced. The results presented in this report also indicate that the boiling of water in the cycle will be very substantially reduced (probably a factor of 3 or more). This savings does not come without cost, however. Distillation of HBr is an added task that has to be performed. At least 2.4 times the amount of HI in the form of HBr must be distilled also. The relative costs of equipment and operational costs as compared with the reference design H_3PO_4 process will determine whether this scheme is a true improvement in the sulfur-iodine cycle. At this point the HBr treatment is not clearly better, and an extensive evaluation is required. It is also true that the HBr system, aside from being not completely defined, is far from optimized. Thus, there is considerable work to be done on this modification, but at present it looks promising.

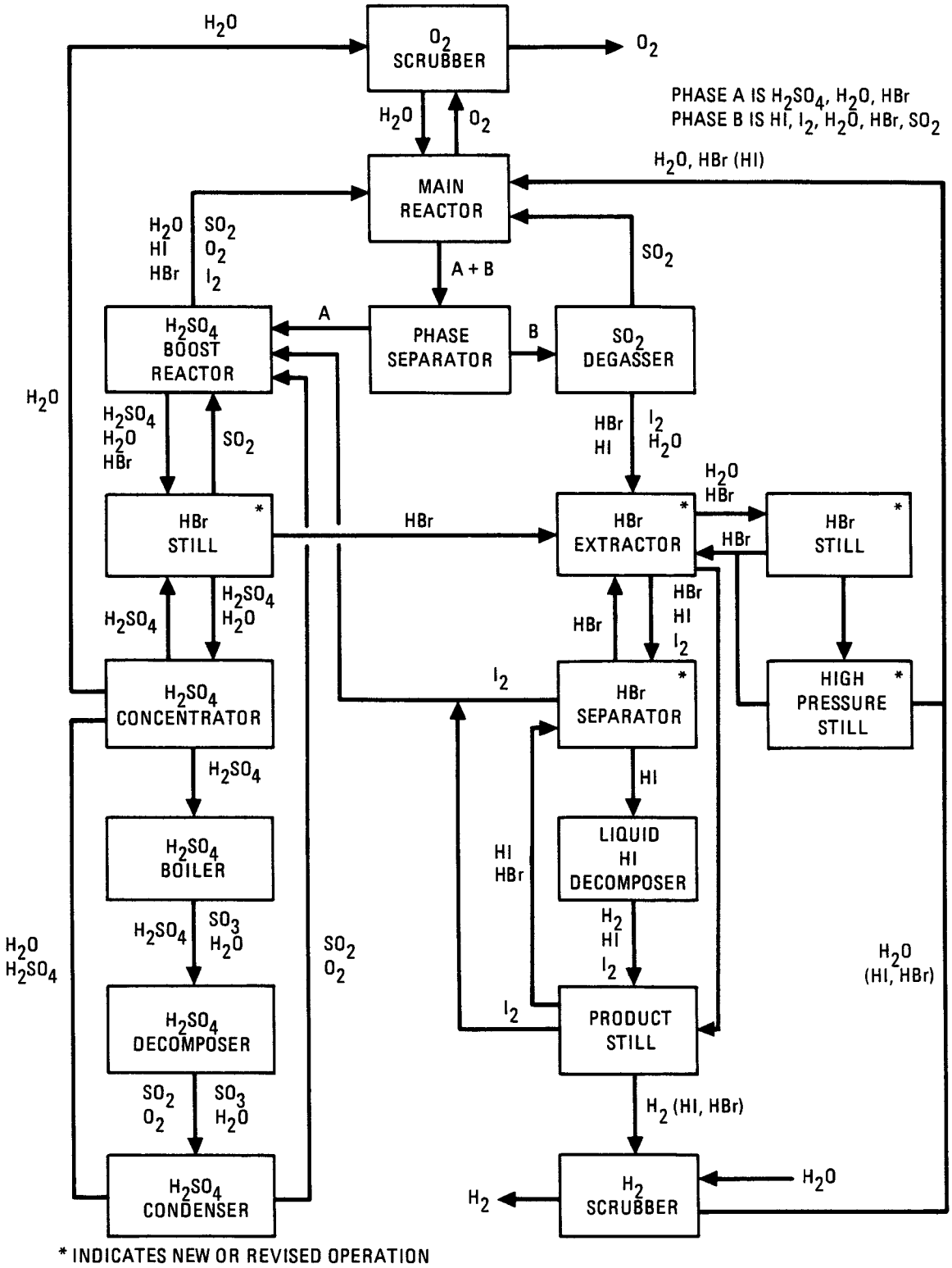

Fig. 40. Block diagram of the HBr modification of the GA sulfur-iodine cycle

5.3 HYDROGEN IODIDE DECOMPOSITION UTILIZING A HOMOGENEOUS CATALYTIC PROCESS

During the past few years, methods for improving the hydrogen-producing step of the GA sulfur-iodine water-splitting cycle, namely, the decomposition of HI, have been studied with support from the Gas Research Institute and the U.S. Department of Energy. The catalytic decomposition of gaseous HI was first investigated since a literature search revealed only a limited amount of available data in this area. Several gaseous catalytic studies were conducted at GA (Ref. 9), and a few systems were shown to be useful to the process. The National Chemical Laboratory for Industry in Japan is continuing such gaseous investigations (Ref. 29).

Subsequent work at GA has concentrated on enhanced HI decomposition concepts. Initially, an attempt was made to decompose gaseous HI in the presence of liquid iodine (I_2) (Ref. 3). This attempt failed because HI contact with the catalyst in the presence of liquid I_2 was greatly reduced, thereby depressing the reaction significantly.

Another enhanced conversion concept studied consists of decomposing HI in the liquid phase. Theoretical calculations indicate that high conversion levels are possible using such a scheme, and indeed high conversions were verified experimentally (Ref. 6). In addition, the same article reports that the magnitude of extrapolated rate data to high process temperatures appears sufficient to result in a viable process for HI decomposition. The above rate data were obtained by extrapolating measured rate data from lower temperatures and pressures in batch studies performed on supported platinum and ruthenium catalysts.

Recently, some data for a supported platinum catalyst at closer to actual engineering temperatures and pressures were

obtained in a new flowing liquid HI bench-scale system. The rate value obtained gave credence to the use of the extrapolated lower temperature data. When incorporated into the flowsheet for the overall sulfur-iodine cycle, the liquid HI decomposition process results in a considerable benefit to the cycle. The capital equipment cost is reduced, and overall thermal efficiency of the process is increased by an incremental 3% over that for the gaseous HI conversion case.

Further in-depth studies, however, revealed a problem associated with the use of heterogeneous catalysis to decompose liquid HI. This is associated with the finding that at least platinum, whether supported or not, does dissolve in the liquid HI to a non-negligible degree. This requires the use of some kind of catalyst recovery and remanufacture scheme. Catalyst recovery and remanufacture are commonplace in the chemical industry but add to the complexity and to the operational and capital costs of the overall process. It was due to the discovery of such an additional requirement of the process that some consideration was given to the use of homogeneous catalysis to decompose HI and to potential separation schemes inherent in the practical application of homogeneous catalysis.

This section describes a homogeneous catalyst concept in which there is an innate separation of the catalyst from the HI liquid, thereby allowing the catalyst to be totally recycled to the reactor. The concept is based on some unique findings surrounding the phase behavior of $HI-I_2-H_2O$ mixtures. For certain compositions of these three chemicals, two liquid phases in equilibrium can exist (Ref. 30). One phase is a very dry phase of HI and I_2; the other is an aqueous phase containing both I_2 and HI. It has been found that it is in this latter phase that certain homogeneous catalyst compounds tend to concentrate. This means that the aqueous phase acts essentially as the catalyst carrier and can be recycled to the HI decomposition reactor without having to recover the catalyst.

The potential advantages over a process employing heterogeneous catalysts with the need to recover and remanufacture 100% of the catalyst are worth investigating. The proposed homogeneous process has been conceptually flowsheeted and major areas requiring investigation have been identified. The needed information consists mainly in identifying the solubility and distribution of the catalyst in the fluids of the process train at engineering conditions, determining the best area of the $HI-I_2-H_2O$ phase diagram in which to work, and determining the best schemes for catalyst recycle.

The results of lower temperature surveys (<323 K) employing several catalyst compounds are reported. Included are compounds such as $Mo(CO)_6$, $H_2PtCl_6 \cdot 6H_2O$, PtI_2, $RhCl_3 \cdot 3H_2O$, $PdCl_2$, and PdI_2, listed in the order of increasing reaction rate for decomposition of HI. Also studied were compounds of PbI_2, FeI_2, and NiI_2 which displayed an undetectable activity level.

Solubility data, distribution coefficient data, and Arrhenius behavior for the most active catalyst, PdI_2, were studied in more detail. This promising catalyst candidate has been shown to have an activation energy higher than for all other homogeneous and heterogeneous catalysts studied. Furthermore, the extrapolated absolute rate on a per-gram active metal basis is significantly higher than the best candidate found to date (i.e., Pt/TiO_2). The conversion level, based on throughput of HI in the reactor, is about 48% for the design conditions chosen; and the reactor residence time is projected to be as small as 4 sec or less for the PdI_2 candidate. There is an expected decrease in conversion level based on reactor HI throughput compared to that for the heterogeneous case due to inherent recycle conditions associated with the process utilizing homogeneous catalysis. The effect of increased recycle of HI on the process must be weighed carefully against the anticipated savings in catalyst recovery and remanufacture processing. Complete flowsheeting of the proposed homogeneous catalysis process including mass and energy balance deter-

mination and capital equipment cost analysis is required for a valid comparison with the heterogeneous system.

5.3.1. Basis for the Homogeneous Catalysis Concept for Hydrogen Iodide Liquid Decomposition

5.3.1.1. Natural Separation Step for Homogeneous Catalysis Concept.

The basis for separation of the catalyst is reliant on carrying the catalyst in a separate liquid phase in contact with the liquid HI. Such a phase is inherently present for certain HI-H_2O-I_2 mixtures as shown in Fig. 37. The phase behavior of such mixtures has been researched at GA and will be reported in detail in a separate paper (Ref. 30). Therefore, only the information pertinent to making a homogeneous catalyst process work will be reported here.

Figure 37 illustrates that a two-liquid region exists over the temperature range 297 to 344 K in which an almost dry phase of HI-I_2 containing less than an estimated 0.5 mole % H_2O exists in equilibrium with an aqueous HI-H_2 phase. Some of the measured tie lines are shown in Fig. 37. Temperatures were restricted to below 344 K in the above study due to pressure limitations of the equipment used. However, it does appear that the boundary of the two-liquid region, at least above the apex of the triangular two-liquid/solid region, is very insensitive to temperature change. It is assumed that such an insensitivity will persist even for higher temperatures, perhaps even for temperatures close to the critical temperature for pure HI (424 K) and above. The presence of dissolved I_2 and H_2O is expected to increase the critical temperature.

Figure 41 shows what may be expected to occur as temperature is increased. This series of phase diagrams has been generated assuming no change in the location of the boundary of the two-

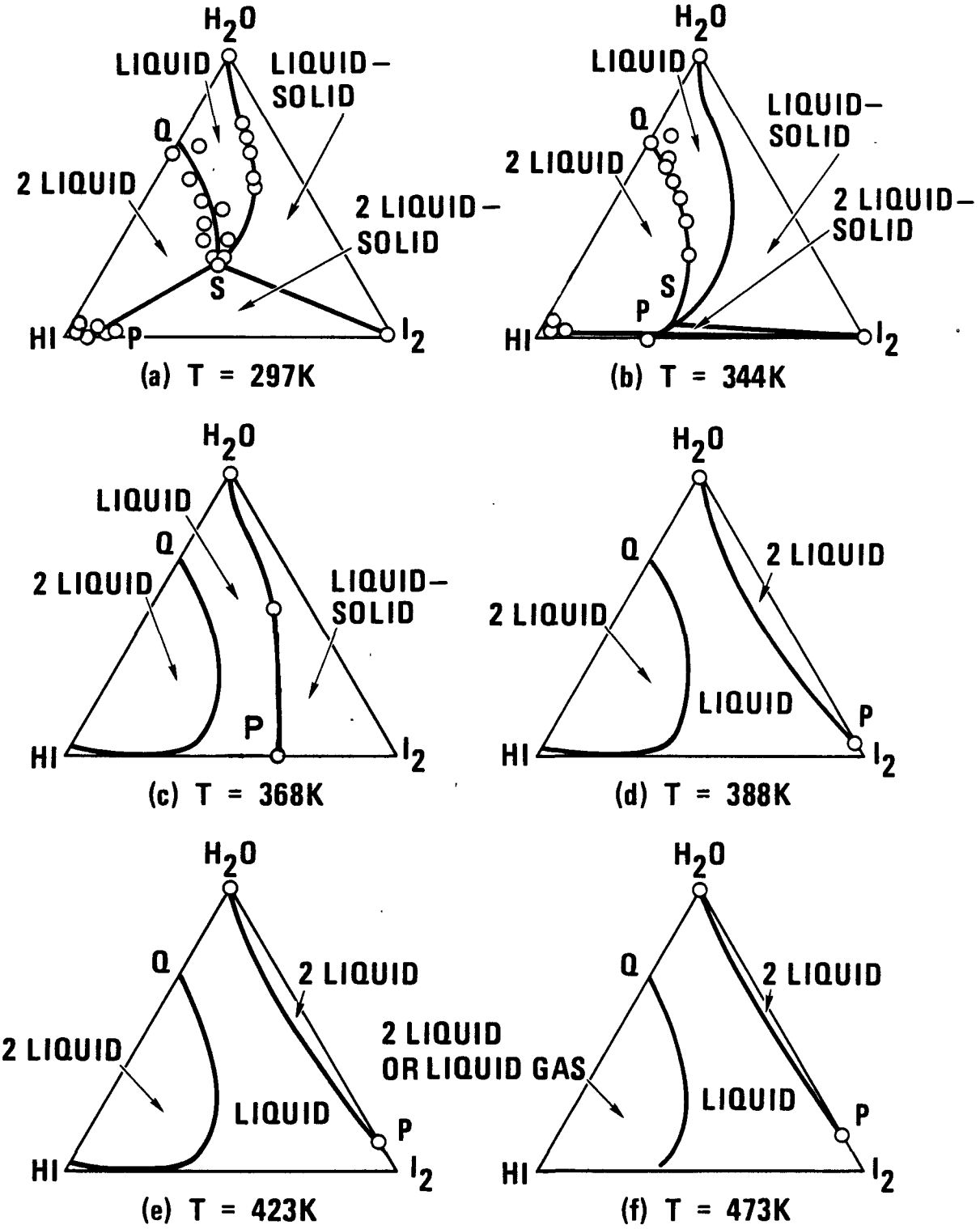

Fig. 41. Extrapolated data for HI-I_2-H_2O ternary system at various temperatures and mole % compositions (circles indicate reasonably secure points)

phase region above point S as the temperature is increased, a reduction in the size of the two-liquid/solid region as S moves down and P moves toward I_2, and an eventual disassociation of the liquidus line joining the H_2O apex and point S, thus leaving the two-liquid region as an isolated self-bounded area. In addition to following phase-rule behavior, pertinent information used in generating the diagrams of Fig. 41 are the measured I_2 solubility in HI at different temperatures (Ref. 25) and the solubility of I_2 in H_2O and H_2O in I_2 (Ref. 31).

A further detail can be added to the behavior of the two-liquid region of Fig. 41 with increasing temperature. The measurements made at 297 and 344 K show a tendency for the dry phase to continue to reject water even upon the addition of more I_2. This strongly implies the tendency for the lower boundary of the two-liquid region to remain close to the HI-I_2 axis even out to high I_2 values. The consequence of such behavior is for the two-liquid region to sharply rise near its closure point and provide the type of boundary sketched in Fig. 42. Another implied consequence from the observed behavior is a reversal of the tie line slopes as shown. Certainly, direct measurements of the actual boundary and position of the tie lines at the higher temperatures must be made eventually; a high-pressure sampling system is required to do so. Meanwhile, the assumed behavior has some credence based on the extrapolation of available data.

With the above judiciously chosen assumption it becomes possible to envisage a process to decompose liquid hydrogen iodide which operates using a tie line similar to that drawn as line AB in Fig. 42. The choice of such a line is important to the operation of a homogeneous catalysis system to decompose hydrogen iodide. The more concentrated the I_2 is at point A, the higher the conversion level which can be expected across the reactor. In addition, as verified experimentally, many very active catalyst compounds are carried almost entirely in the wet phase. Thus, it is equally important that point A not have much H_2O content, since

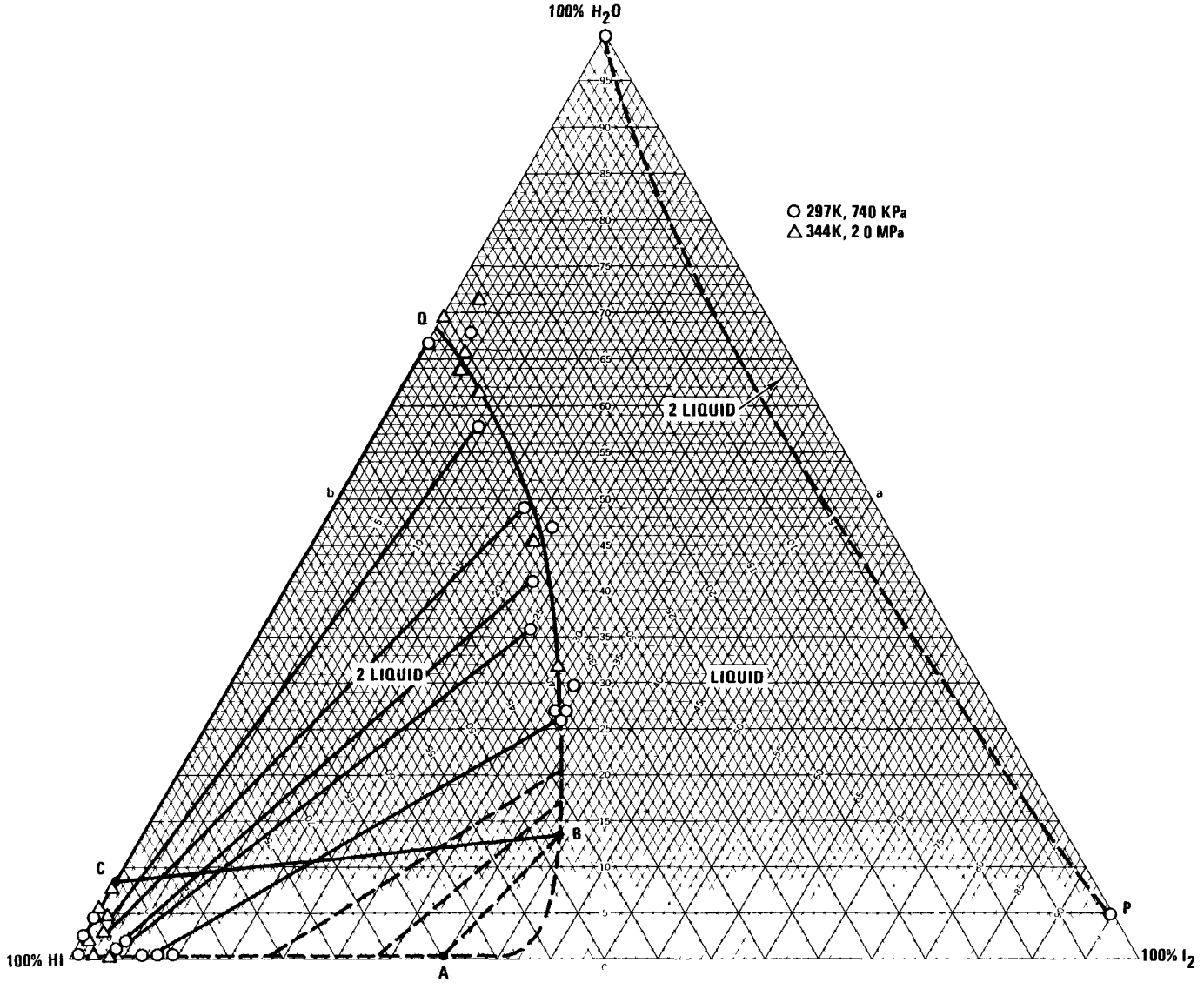

Fig. 42. Predicted mole % diagram for HI-I_2-H_2O mixtures at about 424 K

having such could mean a poorer separation of catalyst between the liquid phases and consequently more extensive catalyst recovery and recycle operations downstream.

5.3.1.2. Solubility of Catalyst in HI-H_2O and HI-H_2O-I_2 Mixtures.

Another criterion which must be met when employing a homogeneous concept for decomposing liquid HI concerns the solubility of the catalyst compound in the HI-H_2O-I_2 mixtures of the process. Since the aqueous phase is what carries the catalyst and allows separation and recycle of catalyst to the reactor, the chosen catalyst must be both active enough and soluble enough in this phase to lead to reasonable inventories. Too much recycle of the catalyst carrier phase necessitates larger reactor and recycle equipment, adding to catalyst and capital equipment costs.

5.3.1.3. Distribution of Catalyst Between Dry and Aqueous HI-I_2 Phases.

In order to use the envisaged homogeneous catalytic process discussed herein for liquid HI decomposition, a distribution of dissolved catalyst highly favoring the aqueous HI-I_2 phase is required. Any amount of catalyst carried in the dry phase must be recovered and recycled in additional process steps. There is obviously no major advantage over a heterogeneous system in which there is dissolution of the catalyst in the liquid HI if too much of the catalyst is carried in the dry phase of the proposed two-

5.3.2. Conceptual Homogeneous Catalytic Decomposition Process

A conceptual homogeneous catalytic decomposition process using the aqueous phase associated with the two-liquid region of the phase diagram is proposed. The flowsheet for such a process is shown in Fig. 43.

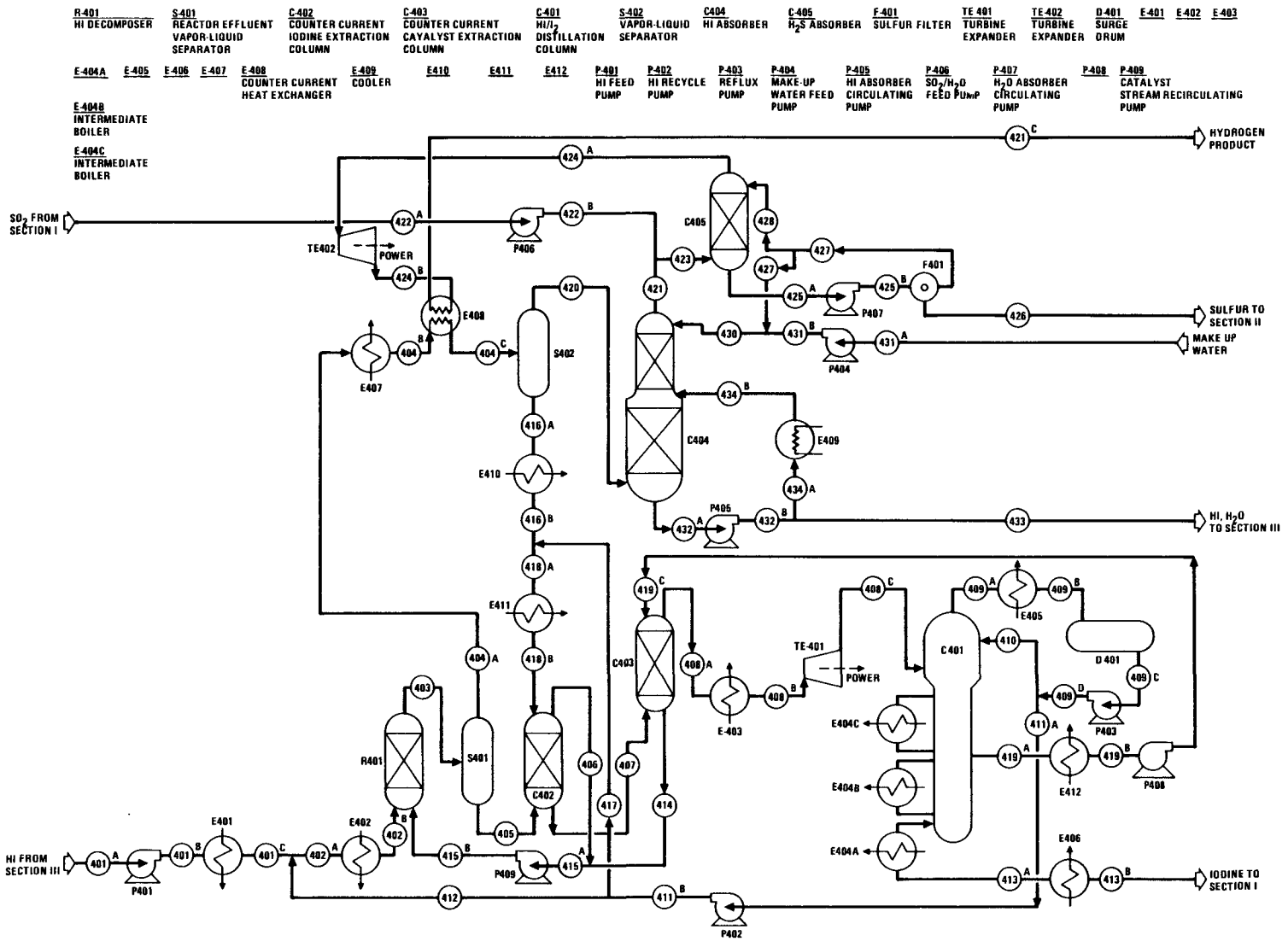

Fig. 43. Flowsheet for proposed homogeneous catalytic liquid hydrogen iodine decomposition process with integral catalyst recycle

Tables 7, 8, and 9 provide the estimated material balance, the power requirements of pumps, the expected output power for turbine expanders, and heat loads of the heat exchangers. Fluid flow streams are identified by stream numbers as indicated within circles in the diagram and in parentheses in the text. A brief description of the working of the process following the flowsheet (Fig. 43) is in order. The flowsheet is based on the production of 1 mole H_2.

Liquid HI, almost dry and free of I_2, at 5.0 MPa and 303 K comes to the proposed process from Section III (HI separation and purification) of the overall water-splitting process. The incoming HI from Section III (401A) is then pumped up to a pressure of 15.65 MPa accompanied by a small increase in temperature. The HI is then heat exchanged in E401 to a temperature of about 395 K; also returning to this point is stream (412) from the HI-I_2 distillation column C401, which is also at 395 K and 15.65 MPa. Heat exchanger E402 then boosts the combined almost pure HI stream to a temperature of 414 K before entering the reactor R401. A stream (415B) also enters the reactor cocurrently; it is an aqueous HI-I_2 phase carrying the dissolved catalyst to the reactor at 424 K.

The reactor R401 is a cocurrent plug flow reactor having internal baffling to assure intimate mixing of streams (402B) and (415B). Exiting from R401 is a two-phase (liquid-vapor) HI-I_2-H_2O-H_2 system stream (403). Within the reactor itself are three phases (liquid-liquid-vapor), all of which vary in composition along the length of the reactor, but conditions are chosen such that only a single aqueous liquid phase given by the composition at the point B in Fig. 42 exits the reactor in phase equilibrium with the gas phase. The liquid mixture composition actually changes from the entrance to exit of the reactor along the line CB drawn in Fig. 42. The end points of the tie lines which are crossed in going from C to B give the compositions of the liquid phases in equilibrium along with the relative magnitude of the

TABLE 7
MATERIAL BALANCE - SECTION IV: HOMOGENEOUS CATALYTIC PROCESS

Stream Number	Molar Flow Ratios									Phase	Pressure (MPA)	Temp. (K)	Comments
	HI	I_2	H_2O	H_2S	H_2	S	SO_2	Pd	Total				
401A	2.0343	0.0010	0.0020	0.0012	0	0	0	0	2.0385	L	5.07	303	HI from Sect. III
401B	2.0573	0.0010	0.0020	0.0012	0	0	0	0	2.0385	L	15.65	305	
401C	2.0573	0.0010	0.0020	0.0012	0	0	0	0	2.0385	L	15.65	395	
402A	3.6249	0.0015	0.0020	0.0012	0	0	0	0	3.6296	L	15.65	395	
402B	3.6249	0.0015	0.0020	0.0012	0	0	0	0	3.6296	L	15.65	414	
403	1.8296	1.0416	0.3328	0.0012	1.0000	0	0	0.002301	4.2052	L+G	15.65	424	
404A	0.5264	0.0013	0.0002	0.0012	1.0000	0	0	0	1.5291	G	15.65	424	
404B	0.5264	0.0013	0.0002	0.0012	1.0000	0	0	0	1.5291	L+G	15.65	303	
404C	0.5264	0.0013	0.0002	0.0012	1.0000	0	0	0	1.5291	L+G	15.65	291	
405	1.3032	1.0403	0.3326	0	0	0	0	0.002301	2.6784	L	15.65	424	
406	0.1565	0	0.3176	0	0	0	0	0.002287	0.4764	L	15.65	424	
407	1.9196	1.0417	0.0152	0	0	0	0	0.000014	2.9765	L	15.65	424	
408A	1.9193	1.0393	0.0152	0	0	0	0	0	2.9738	L	15.65	424	
408B	1.9193	1.0393	0.0152	0	0	0	0	0	2.9738	L	15.65	419.2	
408C	1.9193	1.0393	0.0152	0	0	0	0	0	2.9738	L	5.07	420.5	
409A	1.9605	0.0006	0	0	0	0	0	0	1.9611	G	5.07	393	
409B	1.9605	0.0006	0	0	0	0	0	0	1.9611	L	5.07	393	
409C	1.9605	0.0006	0	0	0	0	0	0	1.9611	L	5.07	393	
409D	1.9605	0.0006	0	0	0	0	0	0	1.9611	L	5.07	393	
410	0.0891	TRACE	0	0	0	0	0	0	0.0891	L	5.07	393	
411A	1.8714	0.0006	0	0	0	0	0	0	1.8720	L	5.07	393	(cont.)

TABLE 7
MATERIAL BALANCE - SECTION IV: HOMOGENEOUS CATALYTIC PROCESS (Cont.)

Stream Number	Molar Flow Ratios									Phase	Pressure (MPA)	Temp. (K)	Comments
	HI	I_2	H_2O	H_2S	H_2	S	SO_2	Pd	Total				
411B	1.8714	0.0006	0	0	0	0	0	0	1.8720	L	15.65	395	
412	1.5906	0.0005	0	0	0	0	0	0	1.5911	L	15.65	395	
413A	0	1.0010	0.0020	0	0	0	0	0	1.0030	L	5.07	713	
413B	0	1.0010	0.0020	0	0	0	0	0	1.0030	L	5.07	393	I_2 to Set 1
414	0.0482	0.0401	0.0132	0	0	0	0	0.000014	0.1015	L	15.65	424	
415A	0.2047	0.0401	0.3308	0	0	0	0	0.002301	0.5756	L	15.65	424	
415B	0.2047	0.0401	0.3308	0	0	0	0	0.002301	0.5756	L	15.65	424	
416A	0.4921	0.0013	0.0002	0	0	0	0	0	0.4936	L	15.65	291	
416B	0.4921	0.0013	0.0002	0	0	0	0	0	0.4936	L	15.65	395	
417	0.2808	0.0001	0	0	0	0	0	0	0.2809	L	15.65	395	
418A	0.7729	0.0014	0.0002	0	0	0	0	0	0.7745	L	15.65	395	
418B	0.7729	0.0014	0.0002	0	0	0	0	0	0.7745	L	15.65	424	
419A	0.0479	0.0377	0.0132	0	0	0	0	0	0.0988	L	5.07	500	
419B	0.0479	0.0377	0.0132	0	0	0	0	0	0.0988	L	5.07	422	
419C	0.0479	0.0377	0.0132	0	0	0	0	0	0.0988	L	15.65	424	
420	0.0343	0	0	0.0012	1.0000	0	0	0	1.0355	G	15.65	291	(cont.)
421	0	0	0.0003	0	0.0012	1.0000	0	0	1.0015	G	15.65	299	
422A	0	0	0.0289	0	0	0	0.0006	0	0.0295	L	0.195	298	SO_2 from Sect. 1
422B	0	0	0.0289	0	0	0	0.0006	0	0.0295	L	15.65	299	

TABLE 7
MATERIAL BALANCE - SECTION IV: HOMOGENEOUS CATALYTIC PROCESS (Cont.)

Stream Number	Molar Flow Ratios									Phase	Pressure (MPA)	Temp. (K)	Comments
	HI	I_2	H_2O	H_2S	H_2	S	SO_2	Pd	Total				
423	0	0	0.0292	0.0012	1.0000	0	0.0006	0	1.031	G	15.65	299	
424A	0	0	0.0005	0	1.0000	0	0	0	1.0005	G	15.65	299	
424B	0	0	0.0005	0	1.0000	0	0	0	1.0005	G	5.07	215	
424C	0	0	0.0005	0	1.0000	0	0	0	1.0005	G	5.07	303	
425A	0	0	0.5000	0	0	0.0018	0	0	0.5018	L	15.71	299	
425B	0	0	0.5000	0	0	0.0018	0	0	0.5018	L	15.65	299	
426	0	0	0.0210	0	0	0.0018	0	0	0.0228	L+S	0.520	299	S Slurry to Sect II
427	0	0.4790	0	0	0	0	0	0	0.4790	L	15.65	299	
428	0	0	0.4700	0	0	0	0	0	0.4700	L	15.65	299	
429	0	0	0.0090	0	0	0	0	0	0.0090	L	15.65	299	
430	0	0	0.0345	0	0	0	0	0	0.0345	L	15.65	299	
431A	0	0	0.0255	0	0	0	0	0	0.0255	L	0.101	298	Make-Up H_2O
431B	0	0	0.0255	0	0	0	0	0	0.0255	L	15.65	299	
432A	0.2613	0	0.2613	0	0	0	0	0	0.5226	L	15.65	323	
432B	0.2613	0	0.2613	0	0	0	0	0	0.5226	L	15.71	323	
433	0.0343	0	0.0343	0	0	0	0	0	0.0686	L	15.65	323	HI, H_2O, to Sect. III
434A	0.2270	0	0.2270	0	0	0	0	0	0.4540	L	15.65	323	
434B	0.2270	0	0.2270	0	0	0	0	0	0.4540	L	15.65	303	

TABLE 8
POWER DEVICES - SECTION IV: HOMOGENEOUS CATALYTIC PROCESS

Power Device Number	Energy Load (kJ)	Inlet Stream Number	Inlet Pressure (MPa)	Outlet Stream Number	Outlet Pressure (MPa)	Comments
P401	1.390	401A	5.07	401B	15.65	
P402	1.739	411A	5.07	411B	15.65	
P403	-----	409C	5.07	409D	5.07	Negligible Power Consumption
P404	0.009	431A	0.101	431B	15.65	
P405	-----	432A	15.65	432B	15.65	Negligible Power Consumption
P406	0.010	422A	0.195	422B	15.65	
P407	-----	425A	15.65	425B	15.65	Negligible Power Consumption
P408	0.077	419B	5.07	419C	15.65	
P409	-----	415A	15.65	415B	15.65	Negligible Power Consumption
TE401	1.639	408A	15.65	408B	5.07	
TE402	1.877	424A	15.65	424B	5.07	

TABLE 9
HEAT EXCHANGERS SECTION IV: HOMOGENEOUS CATALYTIC PROCESS

Heat Exchange Number	Heat Load (kJ)	Hot Side In		Hot Side Out		Cold Side In		Cold Side Out		Comments
		Stream Number	Temp. (Degree K)	Stream Number	Temp. (Degree K)	Stream Number	Temp. (Degree K)	Stream Number	Temp. (Degree K)	
E401	12.794	*	*	*	*	401B	305	401C	395	
E402	9.112	*	*	*	*	402A	395	402B	414	
E403	3.785	408A	424	408B	419	*	*	*	*	
E404A	6.690	*	*	*	*	----	713	----	713	
E404B	8.457	*	*	*	*	----	615.7	----	615.7	
E404C	26.792	*	*	*	*	----	521.8	----	521.8	
E405	18.062	409A	393	409B	393	*	*	*	*	
E406	24.702	413A	713	413B	393	*	*	*	*	
E407	11.381	404A	424	404B	303	*	*	*	*	
E408	0	404B	303	404C	291	*	*	*	*	Cooling from counter-current H_2 stream
E409	0.060	434A	323	434B	303	*	*	*	*	
E410	3.511	*	*	*	*	416A	291	416B	395	
E411	4.051	*	*	*	*	418A	395	418B	424	
E412	0.519	419A	500	419B	422	*	*	*	*	

* See heat match-up for Section IV in Appendix C for details.

volumes of each phase at each position in the reactor from entrance to exit points. Of course, accompanying the liquid mixture is produced H_2 gas. The exit temperature of the reactor is set at about 424 K, the critical temperature for pure HI. Higher temperatures could be run for a mixture of HI-I_2-H_2O since the pure HI critical temperature value is not expected to pertain upon the addition of H_2O and I_2 to HI. However, nearly pure liquid streams of HI, such as stream (402B), unless restricted to the 424 K maximum temperature would not be liquid above this temperature. For efficiency reasons, it seems best to avoid higher temperatures and the need for condensation and recompression of the pure liquid HI streams.

The gas composition in equilibrium with the liquid composition at point B in Fig. 42 and carried in stream (403) is obtained from the measured vapor pressures over HI-I_2 mixtures (Ref. 25) and the assumed ideal behavior of I_2 partial pressures above HI-I_2 mixtures using the values of pure I_2 vapor pressure from Ref. 32. The hydrogen pressure expected thermodynamically is then calculated from the equilibrium constant obtained from the JANAF Thermochemical Tables (Ref. 13), making certain to adjust for the phase change which occurs in I_2 at the temperatures studied. Reference 4 provides the details for such a calculation. The resulting calculated molar concentration is given in Table 7 for stream (404A). The pressure of 15.65 MPa is determined by addition of the partial pressures of HI, I_2, H_2, and H_2O at 424 K. The partial pressure of H_2O is estimated from the mole fraction of H_2O in the phase and the vapor pressure of H_2O at 424 K; it is small and contributes only an estimated 0.0024 MPa to the total pressure.

Following the process train for the gas, the vapor from S401 is cooled in E407 from 424 to 303 K. Stream (404B) is then further cooled in E408, a countercurrent heat exchanger using cool H_2 product gas from turbine expander TE402, to about 291 K. In separator S402, the H_2 gas is removed from the condensed almost-pure HI. The H_2 continues in a post-treatment stage as shown to remove

any remaining HI and I_2 (and H_2S should trace amounts of this gas enter from Section III). Depending on the reaction of the catalyst to trace contamination by H_2S, the H_2S may have to be removed prior to arrival at the reactor R401. The effect of trace quantities of H_2S on the prepared homogeneous catalysts has yet to be studied.

The details of the H_2 cleanup section will not be provided in this discussion except to point out that it is proposed that H_2S be removed by reaction with SO_2 from Section I to form elemental sulfur and that a gas turbine be used to drop the H_2 gas pressure from 15.65 MPa to pipeline quality gas at about 5 MPa. In addition, it is found that sufficient cooling of the H_2 results from the expansion to allow the final cooling of the predominantly HI-H_2 gas-liquid stream (404B) without additional equipment as in the old design. A countercurrent heat exchanger operation is proposed.

The condensed almost-pure HI liquid at 291 K exiting from S402 is then heated to about 395 K in E410 where it is joined by a side stream of almost-pure HI from (411B) at 395 K. Both streams are then heated to 424 K in E411 and put into the top end of a countercurrent I_2 extraction column C402. The purpose of this operation is to remove as best as possible the I_2 from the recycle stream to the reactor so that conversion levels can be kept high. The operation relies on the fact that treating the liquid of composition given by point B in Fig. 42 in a countercurrent fashion establishes at the bottom of the column a liquid stream (407) which is identical to point A in Fig. 42, i.e., an almost-dry HI-I_2 stream that can be easily distilled in normal fashion. In addition, the almost-pure HI stream (418B) upon entering the top of C402 is a point in the vicinity of C on the phase diagram (Fig. 42) but higher in HI content than C. The liquid phase in equilibrium with it is the phase at point Q in the diagram.

Stream (406) is found to carry about 99% of the dissolved catalyst on a mole basis, at least in the case of the most reactive catalyst PdI_2. Thus, stream (406) is recycled directly back to the reactor R401.

Meanwhile the dry $HI-I_2$ phase, stream (407) is brought to a countercurrent catalyst extraction column C403 where it is contacted with a $HI-H_2O-I_2$ mixture from distillation column C401. The aqueous HI/I_2 is temperature matched to column C403 in heat exchanger E412. The effect is the transfer of all of the dissolved catalyst which got through in stream (407) into stream (414) and the removal of a stream of HI-rich $HI-I_2$ in stream (412). All of the catalyst is returned to the reactor in a cyclic fashion without removal or handling or the processing of solids. H_2O is also internal to the distillation column recycle stream and does not have to be recycled or removed.

Theoretically, the above system does not require any catalyst recovery and remanufacture. In reality, countercurrent extraction columns are not 100% efficient in their operation, and there is some small throughput of catalyst expected into regions where recovery will be necessary. It seems certain, however, that the catalyst loss will be very small, and thus a great advantage over complete recovery and remanufacture of the catalyst is realized.

The $HI-I_2$ liquid mixture which comes out of the top of C403 in stream (408A) is first cooled and then put through turbine TE401 to reduce its pressure to about 5 MPa. The cooling stage is to prevent flashing in the turbine since the temperature of stream (408A) at the lower pressure is higher than its boiling point. The reduction in pressure is contingent on the fact that it is not beneficial to use high-grade heat and high temperatures in a distillation column such as C401. A column operated at 5 MPa requires temperatures of about 700 K in the still pot with condensation and extraction of heat in E405 at about 393 K. The extracted heat will provide most of the heat requirements of preheating HI in E401 and

E411. A portion of the resulting condensed HI(ℓ) is pumped to the top of C401 to meet reflux requirements of the column, and the rest is pumped to P402 where the pressure is again raised to 15.65 MPa for input to the incoming stream upstream of E402. Stream (413A), a pure I_2 stream at 5 MPa and 713 K, is cooled in E406 to 393 K (just above the melting point of I_2) and transferred to Section I (prime reaction).

5.3.3. Catalyst Survey Studies

Several dissolved catalysts have been studied in a batch liquid HI decomposition apparatus. (See Ref. 9 for the equipment description and procedure.) In the present case, dry HI liquid was added to various aqueous catalyst solutions, and the rates on the basis of moles H_2 produced per g active metal were measured. The above rate description would seem to be a much more valid way of presenting the data for homogeneous catalysis than for the heterogeneous cases since supposedly each molecular complex formed is an active center, whereas there is hardly a one-to-one correspondence between active site and metal atom in the heterogeneous case. With water present, a two-liquid system results.

The catalyst solutions employed included:

- PdI_2 in hydriodic acid
- $PdCl_2$ in hydrochloric acid
- $RhCl_3 \cdot 3H_2O$ in hydrochloric acid
- PtI_2 in hydriodic acid
- $H_2PtCl_6 \cdot 6H_2O$ in water
- $Mo(CO)_6$ in hydriodic acid
- PbI_2 in hydriodic acid
- FeI_2 in hydriodic acid
- NiI_2 in hydriodic acid
- $MoBr_2$ in hydriodic acid

The iodide and chloride equivalents of the same noble metal were used because initially only the chlorides were readily available

from laboratory stock. Later, the iodide equivalents were obtained. There was no discernible difference in the rates at a given temperature between the halide forms. Except for PdI_2 and $PdCl_2$ the compounds are listed in decreasing order of reactivity on a mole H_2 per g metal basis as determined at both 303 and 323 K. Below $Mo(CO)_6$ there was no measurable reactivity. PtI_2 and $H_2PtCl_6 \cdot 6H_2O$ are found to be about equivalent in reactivity. The palladium compounds, although lower in activity than the Rh and Pt compounds, especially at 303 K, do possess a significantly higher activation energy and thus a much higher rate at the projected engineering operation temperatures (up to 424 K). This makes Pd a prime candidate for the process. A higher temperature, higher pressure study of the reactivity of $PdCl_2$ conducted in an all-metal batch system did verify the existence of such a high rate at 348 K.

The $Mo(CO)_6$ candidate, although showing some activity, was not found to dissolve well in the aqueous phase. Instead, it dissolved in the almost "dry" phase. It has been shown that the measured activity did come from this phase but that the solubility of the $Mo(CO)_6$ was restricting to any possible use of this catalyst. In addition, it was found that this catalyst decomposed, making CO gas. It has been ruled out as a candidate for HI decomposition and also reflects potential problems with the use of other carbonyls for this chemical system.

All of the above compounds except for Pb, Fe, and Ni were studied in both dry (one-phase) and wet (two-phase) environments. In all cases, water was required in order to effect the correct complexing; there was no measurable activity without water present, indicating that the activity surely takes place in the aqueous catalyst carrying phase with HI replenishment taking place from the "dry" HI phase in equilibrium with it. The lower limit of the present measurement capability with the apparatus used is estimated at 1×10^{-6} mole/min·g metal. The reaction was found to be reaction limited rather than diffusion limited; stirring

the mixture did not show a measurable effect, at least for the temperature and pressure conditions of this study.

5.3.4. Results and Discussion

5.3.4.1 Characteristics of Proposed Homogeneous Catalytic Decomposition Process.

Some discussion of the characteristics of the proposed homogeneous catalytic decomposition process is in order. This is best achieved by looking once again at the flowsheet and Table 7. The major areas where further definition is required will be noted along with the assumptions used in the present iteration. In almost all cases the need for further definition involves the need for better experimental data. The attempt has been to employ reasonable extrapolations from existing data.

The first major area has already been addressed. It concerns the choice of operating tie line in Fig. 42. It is a critical input to the system since it affects the operation of the major steps, reaction, I_2 separation, Pd recovery, and HI,I_2 distillation. No data have yet been obtained for the phase behavior of HI-I_2-H_2O mixtures at near 424 K; but, as pointed out in the previous discussion, the choice of the line AB in Fig. 42 is much more than an arbitrary choice. The measured constancy of the two-liquid region with temperatures from 303 to 343 K suggests its existence at 424 K. In addition, the seeming proclivity of the dry phase to persist in rejecting water even when I_2 is added helps to judiciously make the choice of envelope as depicted in Fig. 42. The choice of tie line follows from this same reasoning. Of course, the effect of choosing a tie line in which the liquid at point A carries less I_2 will be to decrease the conversion level through the reactor. With the present choice, the conversion through the reactor (the ratio of total moles of HI out of the reactor to the total moles of HI into the reactor) is 48%. This is close to the theoretical maximum

expected (i.e., 50%) when operating without a recycle mode (see Ref. 6). It is believed that a judicious choice of the tie line has been made and that conversion levels will be high.

Another area of concern involves the operation of the countercurrent columns C402 and C403. It is known from the phase studies at 303 and 343 K that there is a density reversal at low I_2 values in the two-liquid region. This means that the two-liquid phases in equilibrium actually go from the top to bottom position on either side of a "gray" I_2 composition area near 5 to 10 mole % I_2 at the 303 to 343 K temperatures. This behavior is obviously not yet known at 424 K and will have to be measured and handled in some way under engineering conditions. Possible engineering solutions to the problem include splitting columns C401 and C402 at the appropriate positions and operating four columns in place of two or replacing each column by a mixer settler train. Pinch points caused by other effects are possible in the operation of such columns; thus, additional studies will be necessary before the design can be finalized.

A favorable behavior can be seen from a study of the mass balance for column C402. Not only is this countercurrent operation a good method for extracting I_2, but there is significant recovery in stream (407) of the HI being sent on to C403 and eventually to the HI-I_2 distillation column C401. Stream (407) is found to have about 2 moles of HI per mole of H_2 produced. This is again because of the predicted location of the tie line AB in Fig. 42; a fairly rich HI phase is expected to be in equilibrium with the aqueous phase. This assists in the recovery of HI from the process train, as any HI which goes with the aqueous phase has to be recycled in the mode of operation chosen.

Another favorable aspect of the proposed process is the high ratio of H_2 to HI generated in the gas stream (404). The ratio of H_2 to HI is about 2. This feature makes recovery of the HI from the H_2 less energy consuming from the point of view of

condensing the HI and scrubbing it out of the H_2. The only disadvantage would appear to be the requirement for equipment to withstand 15.65 MPa (i.e., ≈150 atm). Although a challenge, it would appear to be feasible. It is proposed that the pressure of H_2 be reduced to about 5 MPa (i.e., pipeline quality pressure) through turbine TE-402 and the power so generated used for in-plant needs. In addition, it is proposed that the 1.9 k/J of cooling energy available in the H_2 gas stream at 215 K be used to countercurrently cool the HI-H_2 gas-liquid stream (404B) in E408.

In the present design, a portion of the small amount of H_2S coming through in the fluid from Section III is allowed to pass through the reactor. The assumption, for the present, is that the H_2S does not affect the catalyst. In reality this H_2S might be incorporated into the catalyst in a complex chemical fashion to either aid or inhibit the reaction. Studies of HI(ℓ) decomposition using the proposed catalyst candidates are in order. In the event that such contact of H_2S with the catalyst compounds results in adverse poisoning effects, then this H_2S will have to be removed prior to entrance to the reactor.

An additional assumption made regarding H_2S in the present design is that all the H_2S stays with the H_2 gas and is treated downstream of the H_2 wash stage to remove HI. The vapor pressure of H_2S at 291 K, the temperature of the cooled gas stream, is 1.62 MPa compared to 0.64 MPa for HI at the same temperature. Thus, there is a separation toward H_2 when the gases are cooled, but it is not complete as assumed. The distribution coefficients for H_2S in the various mixtures of the flow train are required for complete definition of the flowsheet. In any case, H_2S which remains with the HI will be recycled back in the overhead from C401.

Also assumed in this design is zero solubility of H_2 in any of the liquids. Some data have been obtained for the solubility

of H_2 in both $HI(\ell)$ and $I_2(\ell)$ in Ref. 25. Although the solubilities or distribution coefficients for H_2 in the specific fluids are not yet known, the data available indicate that the effect will be small on the operation of the unit. Any H_2 which passes through to C401 will be concentrated in the overhead and recycled back to the reactor in stream (412).

One other noteworthy assumption regarding the present flowsheet is that a $HI-I_2-H_2O$ solution of appropriate composition, stream (419A), is taken off the distillation column C401 for use in recovery of the catalyst in C403. This solution will have to be obtained from a composite of separate extraction points on C401. For present purposes one extraction location has been assumed at a temperature of 500 K.

The entire flowsheet sketched in Fig. 43 assumes the use of a PdI_2 catalyst. The extrapolated solubility of this compound in $HI-H_2O$ mixtures from temperatures below 323 K is used to set the amount of water required in stream (406) and thus the entire recycle amounts.

The distribution coefficient of PdI_2 between dry and aqueous phases for $HI-H_2O$ mixtures is assumed to be constant with temperature and the same at 424 K as measured at 323 K regardless of the amount of I_2 present. This particular assumption needs verification.

It is possible to compare the present design with that derived previously (Ref. 7) for a heterogeneous catalyst with no catalyst recovery or remanufacture. Obviously, the latter design would appear to have less capital equipment than the present design, but only because the requirements for catalyst recovery and remanufacture have not been included. In addition, a comparison of the energy balance for each process does indicate about the same energy requirements. This would retain the same overall process efficiency of close to 47% quoted in Ref. 7. Thus, a

heterogeneous system which would require catalyst recovery and remanufacture would appear to be close to equivalent with the present built-in separation concept, both from the efficiency and capital equipment points of view.

The assumption in the present design that there will be zero recovery of catalyst is, of course, false. In actual fact, extremely small recovery will be necessary since countercurrent columns are never quite 100% efficient, and there are certain small losses just in the handling of fluids in such a process. The same applies, of course, to the other chemicals recycled in such plants.

The catalyst activity level has been assumed to be 1/3 of the initial extrapolated rate at 424 K. This assumption attempts to account for the expected depression of the forward rate due to back reaction at close to equilibrium conditions.

5.3.4.2. Catalyst Rate Behavior.

Figure 44 is the Arrhenius plot for the catalysts which demonstrated measurable reactivity for HI(ℓ) decomposition. $Mo(CO)_6$ is not included, although a measurable activity was obtained, because the $Mo(CO)_6$ also decomposed upon contact with HI(ℓ) and was not very soluble in the aqueous phase where the activity is found to be controlling.

All homogeneous catalytic activity recorded in Fig. 44 was obtained under the condition of unsaturated dissolution of the active component. This then provides an accurate measure of the activity irrespective of the solubility limit of the active species. The solubility becomes a consideration when water inventory for the process is required. As seen in Fig. 44 for those species other than PdI_2 for which at least two data points have been obtained, the activation energy appears to be like that of the previously measured Pt/TiO_2 heterogeneous case (Ref. 9),

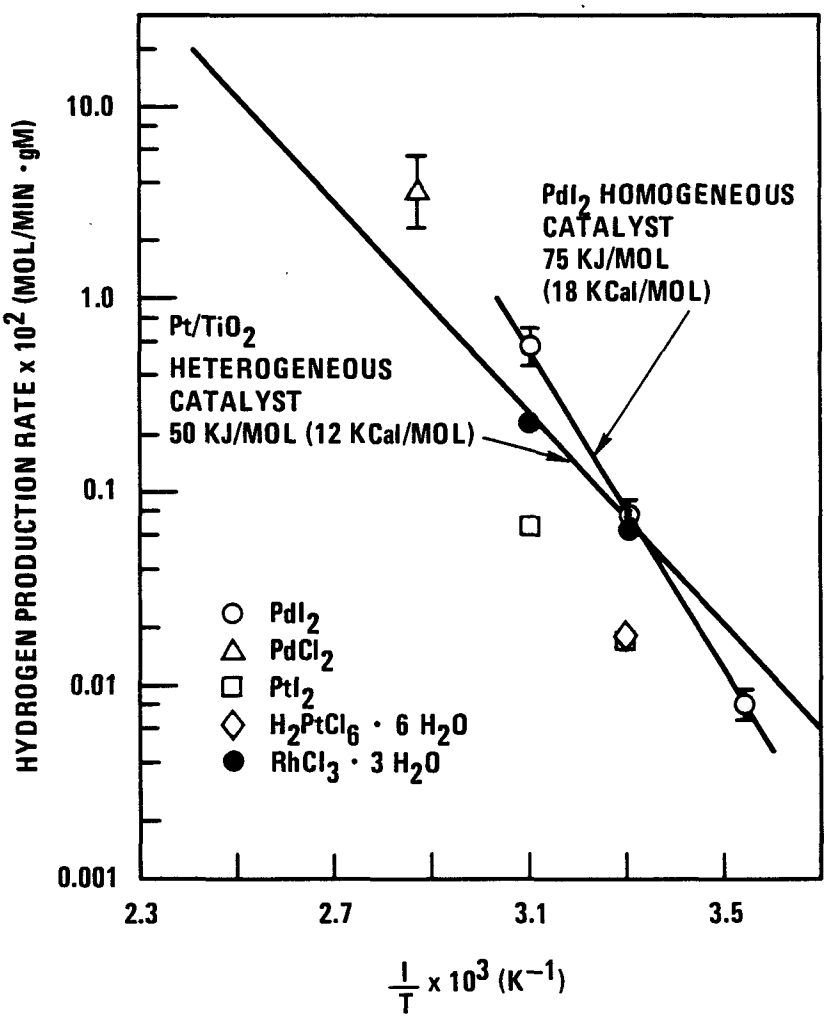

Fig. 44. Arrhenius plot for candidate homogeneous catalysts: comparison with heterogeneous Pt/TiO_2 catalyst

i.e., ≃50 kJ/mol (12 kcal/mol). The Pt/TiO_2 variation previously obtained is illustrated by a solid line as marked. The PdI_2 homogeneous catalyst on the other hand has an activation energy more like 75 kJ/mol (18 kcal/mol). At temperatures above 323 K, the PdI_2 rate is the highest of any found to date. $PdCl_2$ was shown to have about the same rate as PdI_2, but such comparisons were made under saturated conditions and not at the highest absolute rates and thus are not included in Fig. 44. Nevertheless, the comparison is valid and does indicate that the form of the halide does not matter. Rather, it is the active species that makes the difference.

Palladium, known as an effective hydrogenation catalyst in the chemical industry, does seem to be the best candidate. This was not found to be the case when using a heterogeneous palladium catalyst (Harshaw Pd-0501T 1/8") in the earlier studies. In that case, however, water was not added to the HI, and it has since been found that water is essential to obtaining high activity.

Included in Fig. 44 is the point for $PdCl_2$ measured in an unsaturated condition at 348 K There is more error in this measurement than in the others since the higher activity made it more difficult to obtain the H_2 gas production rates. The error on the PdI_2 results is indicated in the diagram and is the result of an estimated experimental error in determining the respective rates.

None of the above homogeneous species were active without water being present. A possible mechanism in support of this observation could be as depicted in Fig. 45. As shown, the proposed mechanism is drawn as the formation of a square planar form structure in which the OH radical and HI molecule are present. The palladium behaves as having a coordination of 4, and electron transfer takes place in the transfer of dative bonds supplied either by the OH radical or an I atom. The mechanism seems a

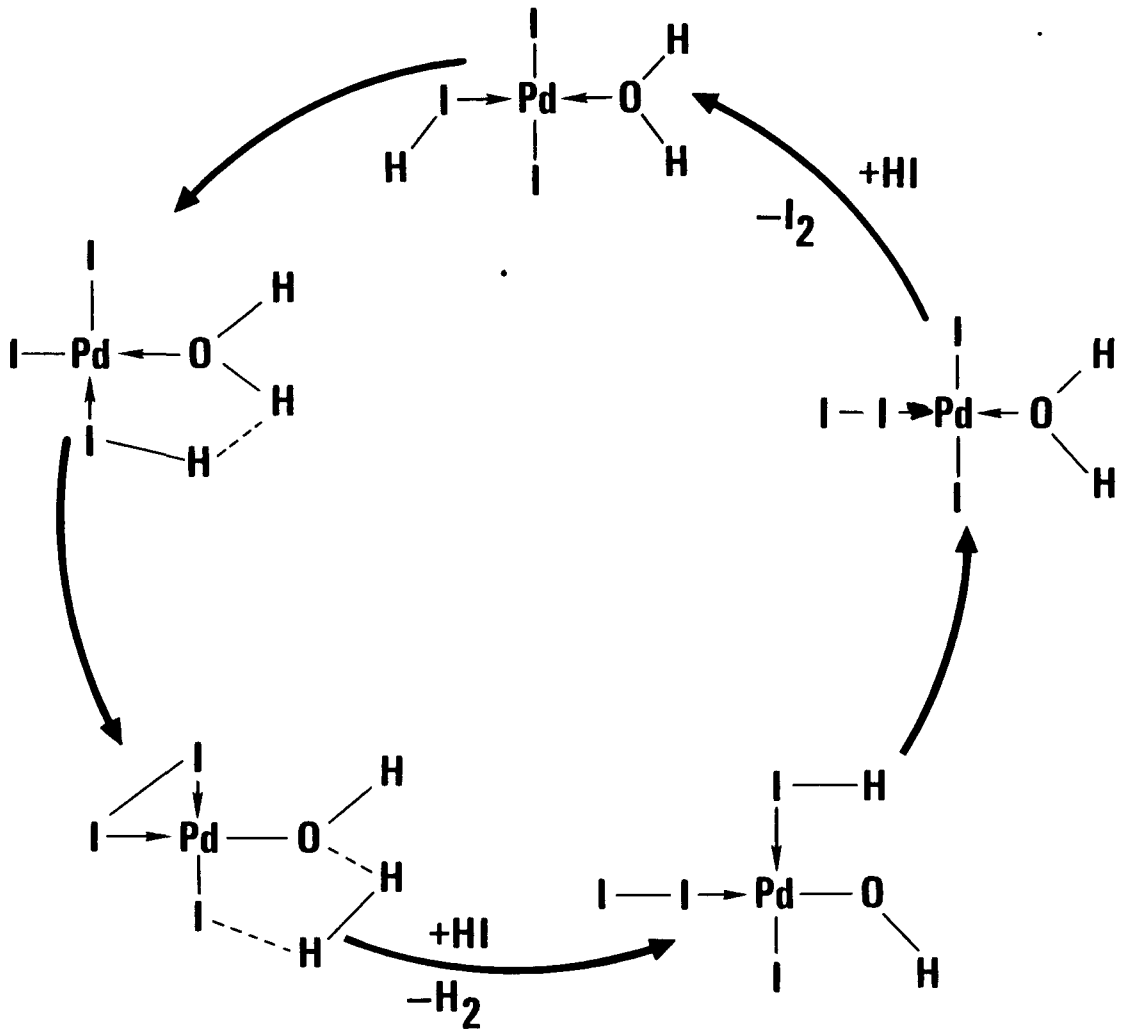

Fig. 45. Possible reaction mechanism to explain decomposition of HI(ℓ) by PdI_2 water complex (→ denotes dative bonding). Overall reaction is $2HI \rightarrow H_2 + I_2$

reasonable one, but certainly a much deeper investigation would be necessary to identify it with surety. It might even be speculated that the rate limiting step might be electron transfer required to "kick off" the I_2 molecule. This would seem to be correct thinking if one realizes that the propensity for I_2 to still coordinate (i.e., give up electrons) with other species is present, whereas H_2 has a filled electronic configuration. It is also obvious that for the case of homogeneous catalytic behavior, it is unreasonable to expect H or I atoms to be rejected since the required energetics would be too high to do without the assistance of a surface to allow the mobility of the atoms. The measured activation energy for the catalyzed reaction is much lower than the 147 kJ/mol (35 kcal/mol) measured for the uncatalyzed case.

A more detailed plot of the Arrhenius behavior of the PdI_2 homogeneous catalyst is shown in Fig. 46. In addition to the points plotted in Fig. 44, points are included giving the reaction rate after the catalyst induction period and for a case in which I_2 has been purposely added to the starting mixture. Also given are points for the situation in which there was no stirring of the HI/H_2O catalyst mixture.

All the PdI_2 experiments which were conducted indicated an induction period after which the initial rate of the catalyst for $HI(\ell)$ decomposition decreased by a factor of between 1.3 and 2. This change in rate due to induction was surprisingly abrupt and took place within a shorter period of time for the higher temperature cases than for the lower temperature ones. At 323 K, the rate change took place between 80 and 240 min. At 303 K the time for induction was found to be greater than 460 min as indicated by overnight runs. At 281 K the turnover point would appear to be at even longer times but again was not measured.

It should be noted as well that the one $PdCl_2$ experiment performed at 348 K (see Fig. 44) also showed an abrupt 1.7 factor

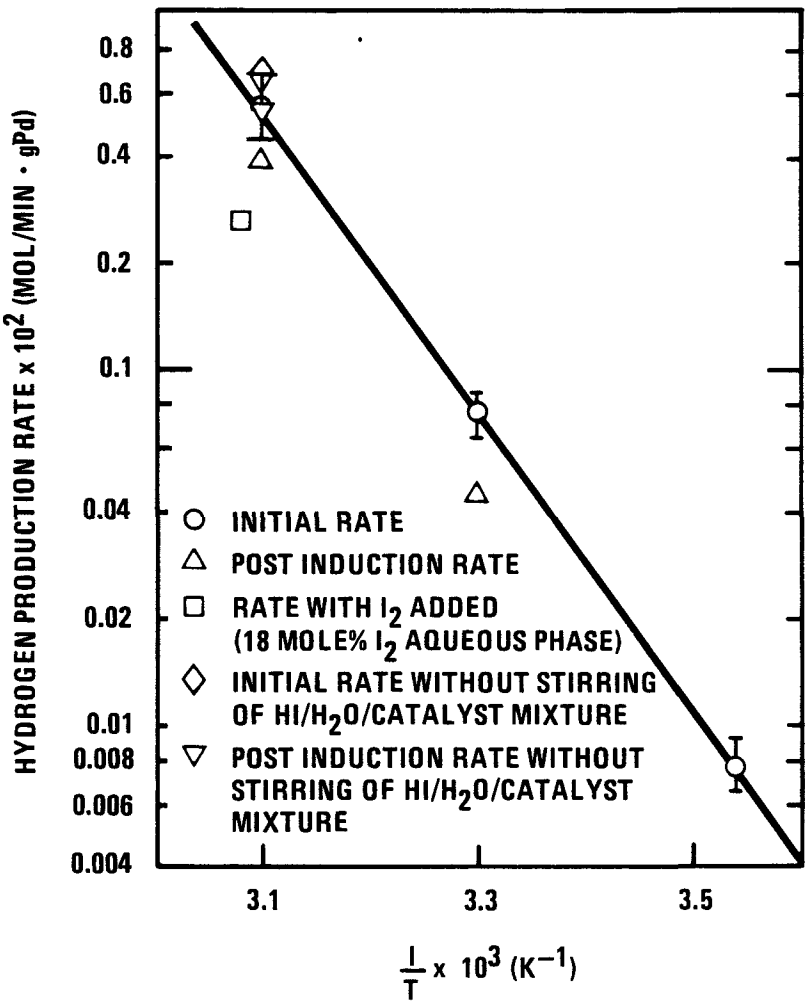

Fig. 46. Arrhenius plot for PdI_2 homogeneous catalyst for various experimental conditions

decrease in rate due to induction of the catalyst, this time within about 70 min of start of the experiment.

When I_2 was added to the initial charge of HI/H_2O to the equivalent of 18 mole % I_2 in the aqueous phase, a factor of 2 decrease in rate was observed over that of the initial rates without I_2 present. However, there was no indication in this case of an induction period for the catalyst at 323 K even out to 340 min. This might indicate that the induction period as seen for starting mixtures of only HI and H_2O might be due to the buildup of I_2 as the reaction proceeds. If so, it would appear that a reduction in rate of a factor of 2 would be the maximum expected even for higher loadings of I_2. Of course, the introduction of enough I_2 will result in lower rates due to the importance of back reaction effects. Figure 42 indicates that the chosen tie line AB will result in a mole fraction of I_2 in the aqueous phase (point B) of near 0.40, a factor of 2 greater than the test GA has performed with I_2. Higher temperatures and pressures involving the use of another apparatus would be required to test out to the maximum I_2 limit expected. However, there would not appear to be a large effect of I_2 beyond the factor of 2 decrease already measured. Nevertheless, such a study will have to be conducted in order to verify this hypothesis.

Also plotted in Fig. 46 are points indicating the rates at 323 K for mixtures of HI/H_2O/catalyst in which there was no stirring. These rates fall within the experimental error of rates measured with stirring. This would seem to indicate, at least for these lower temperature studies, that the rate is reaction rate limited rather than diffusion rate limited.

5.3.4.3. PdI_2 Homogeneous Catalyst Solubility Behavior.

The solubility of PdI_2 in HI/H_2O liquid mixtures was measured at <323 K in an identical manner to that described in Ref. 25 for

determining the solubility of I_2 in HI. In the present case, the amount of PdI_2 was measured by straightforward gravimetric means after identifying through emission spectrographic methods that Pd was the only metal present. Corrosion products such as Fe, Cr, and Ni from the stainless-steel parts of the apparatus were extremely low. Also it was verified that the resulting deposit after takeup in the HI/H_2O superazeotropic mixtures was really PdI_2 and not some higher or lower iodide.

Figure 47 is a depiction of the solubility of PdI_2 in the aqueous phase represented by point Q of Fig. 42 in an Arrhenius type plot. A straight line does not result, and it might be thought initially that the points are merely displaying scatter due to experimental error. However, the error in the measurement is not expected to be that great, and a plot of the available literature solubilities for $FeCl_2$ in hydrochloric acid, also plotted in Fig. 47, demonstrates the same kind of behavior (see Ref 33). Obvious from the $FeCl_2$ data in Ref. 33 is the complication due to the formation of different $FeCl_2$ hydrates in solution at different temperatures. This could account for the nonlinear behavior of both $FeCl_2$ and PdI_2 in Fig. 47. The form of the hydrate for PdI_2 is not known.

An extrapolation of the data for PdI_2 solubility out to 424 K, the proposed operational temperature for the flowsheet, is obtained by drawing the best straight line through the three points measured. In actual fact, it would appear that the solubility at 424 K will be greater than extrapolated and that less H_2O inventory will be required than designated in the material balances in Table 7. Even if the conservative value of PdI_2 is chosen, however, only 2.30×10^{-3} mole of Pd and 0.333 mole of H_2O are required per mole of H_2 produced. These values are obtained assuming about 1/3 the HI(ℓ) decomposition rate extrapolated from Fig. 46 in an attempt to account for the approach to equilibrium back reaction effect. A 3000 MWT high-temperature gas-cooled reactor plant is expected to produce about 3×10^5 moles H_2/min.

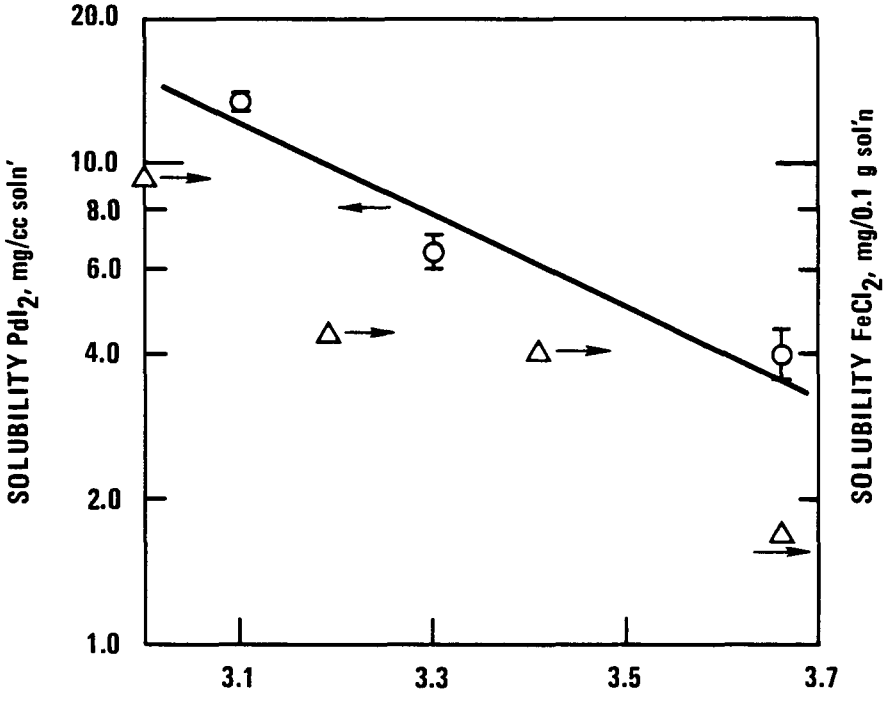

Fig. 47. Solubility of PdI_2 in 77 wt % solution. Trend compared to $FeCl_2$ solubility in 29 wt % HCl solution (Note: density factor must be included for absolute comparison purposes.)

The palladium inventory for such a plant therefore would be about 2400 troy ounces or about $200,000 at an assumed $87 per troy ounce cost for Pd (cost on 7/27/81). In addition, the H_2O inventory would be about 1800 liters (470 gal), not at all restrictive for such a large plant operation. Thus, neither the cost nor material inventories are prohibitive.

The solubility of PdI_2 was measured only in HI/H_2O mixtures at up to 323 K. In actual fact, in addition to being carried in stream (406), which is nearly pure HI/H_2O in nature, a small amount of the catalyst is being carried back to the reactor in stream (414), which has close to unit mole ratio of HI to I_2. Strictly speaking, measurements should be made at process temperatures and at the true stream compositions. For the present purposes the solubility is assumed the same in the HI/H_2O mixture containing I_2 as for the measured HI/H_2O case. Large differences are not expected to result from such changes.

5.3.4.4. PdI_2 Homogeneous Catalyst Distribution Coefficient Behavior in HI/H_2O Mixtures.

Equally important as the solubility of PdI_2 in the various mixtures of the flow train where catalyst exists is a knowledge of the distribution of this chemical species between the liquid phases in contact with one another. A measure of such a distribution coefficient was obtained at 303 K for an aqueous phase of composition 32 mole % HI, 18 mole % I_2, 50 mole % H_2O in contact with an almost dry phase of composition 98.25 mole % HI, 1.25 mole % I_2, and 0.5 mole % H_2O. The measurement was achieved by withdrawing a known amount of sample of the PdI_2 from the dry phase, evaporating off the HI and I_2 at low temperature, and detecting the amount of Pd in the remaining precipitate using emission spectrographic techniques. Unlike Pt, palladium can be detected quite reliably using such a technique. Thus, from a knowledge of the amount of Pd in the dry phase and the total amount of Pd added to known values of wet and dry phases, the distribution coefficient was derived.

The definition chosen for a distribution coefficient in this case was the ratio of the number of moles of Pd per mole of HI in the dry phase to the number of moles of Pd per mole of H_2O in the aqueous phase. The ratio so derived was 1/168 and is the number used in the flowsheet for defining the distribution of Pd between the dry and wet phases encountered there. In actual fact, the above number was not derived for the exact temperature and composition of the mixtures in the flowsheet. For the present purposes it has been assumed to be the same for the liquid phases A and B in equilibrium on the tie line AB of Fig. 42. The true number needs to be determined eventually through direct measurement. However, because of the retention of a very dry phase even out to point A of Fig. 42, it is not expected to vary significantly from the number obtained at the lower temperature and lower I_2 loading.

5.4. STUDIES OF COUNTERCURRENT TREATMENT OF HI-I_2-H_2O SOLUTIONS WITH H_3PO_4

An important portion of the current sulfur-iodine cycle is the treatment of HI-I_2-H_2O solutions with concentrated H_3PO_4, extracting the H_2O and HI while leaving the I_2 behind. Some laboratory batch studies have been performed on this concept and have established end conditions for this operation, but it is necessary to test a full countercurrent column to determine whether pinch points exist.

For this study, a staged countercurrent flow reactor column constructed for studying the H_2SO_4 boost reaction was utilized. This system (Fig. 48) consists of (1) a 10-stage stirred column in which the solutions passing from stage to stage are equilibrated by extraction, (2) an HI-I_2-H_2O solution feed system, (3) a H_3PO_4 feed system, and (4) appropriate reactant and product holding vessels. HI_x solution is added to the top of the column and flows down the column, where it is taken off as an iodine-rich phase. A

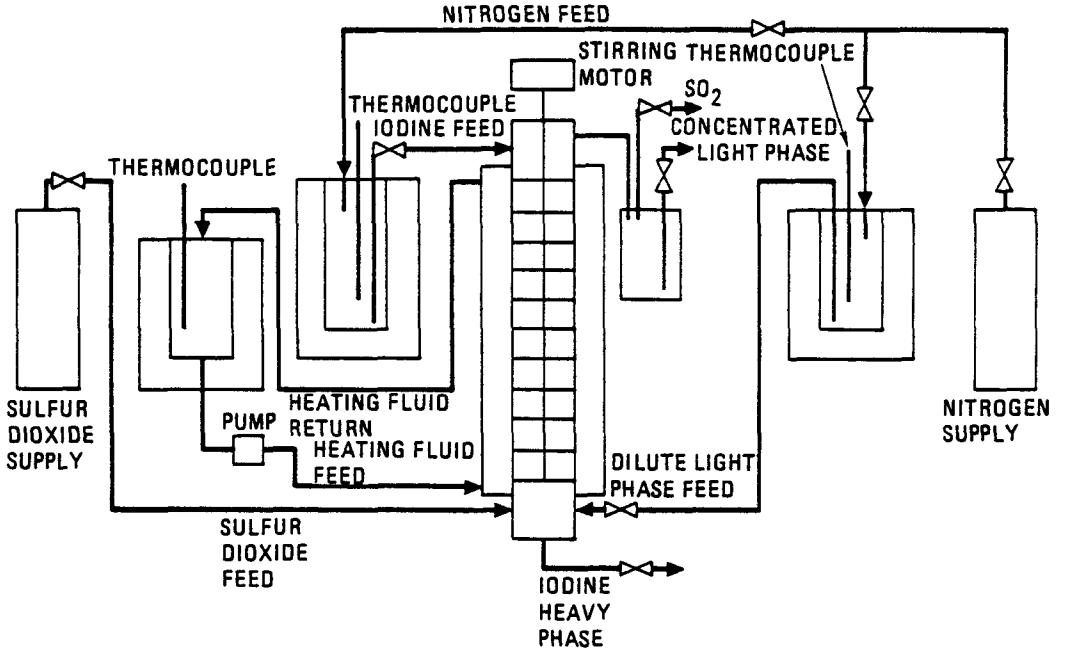

Fig. 48. Process flowsheet for reaction of iodine with upper-phase product

concentrated H_3PO_4 solution is fed to the bottom of the column, flowing up the column.

Figure 49 shows an individual stage of the column. The outer glass tube of this column, shown by diagonal cross hatching, has a precision inner bore internal diameter, and the glass support ring is of close-fitting explicit external dimensions. Between the glass support rings there are Teflon separators, which leave a small opening for phase flow. Stirring is accomplished by centrifugal pumping of liquid from the area of the opening between the separators to the spinning pump exit. A baffle in the lower portion of the cell reduces swirl. The stirrer/centrifugal pump is operated by a regulated variable-speed motor so that the stirring can be set at any desired rate. Stirring rates and torques are metered. Every stage of the column is expected to be operated in equilibrium.

All studies to date have been done isothermally at a few degrees above the melting point of iodine as a matter of convenience. A number of experiments have been performed. Some of these experiments have been done to establish flow control information and to test certain reactor modifications. Others have been done to produce metal data on the system. Manometric pressure difference measurements across an in-line orifice have been used to determine HI_x flow. Ball and float monitoring of H_3PO_4 was utilized. Both of the charged solutions were delivered from inert gas pressurized sources.

Two of these experiments which ran without equipment difficulties and were well characterized by analytical data are presented here. Both were run at a nominal 120°C. The solutions used in Experiment A were 97.74% H_3PO_4; and 82.73% I_2, 10.78% HI, and 6.49% H_2O. In Experiment B they were 96.74% H_3PO_4; 81.27% I_2, 10.94% HI, and 7.79% H_2O. The exiting products as a function of time for these two experiments are described in Figs. 50 and 51. In these experiments the column was prefilled with the concen-

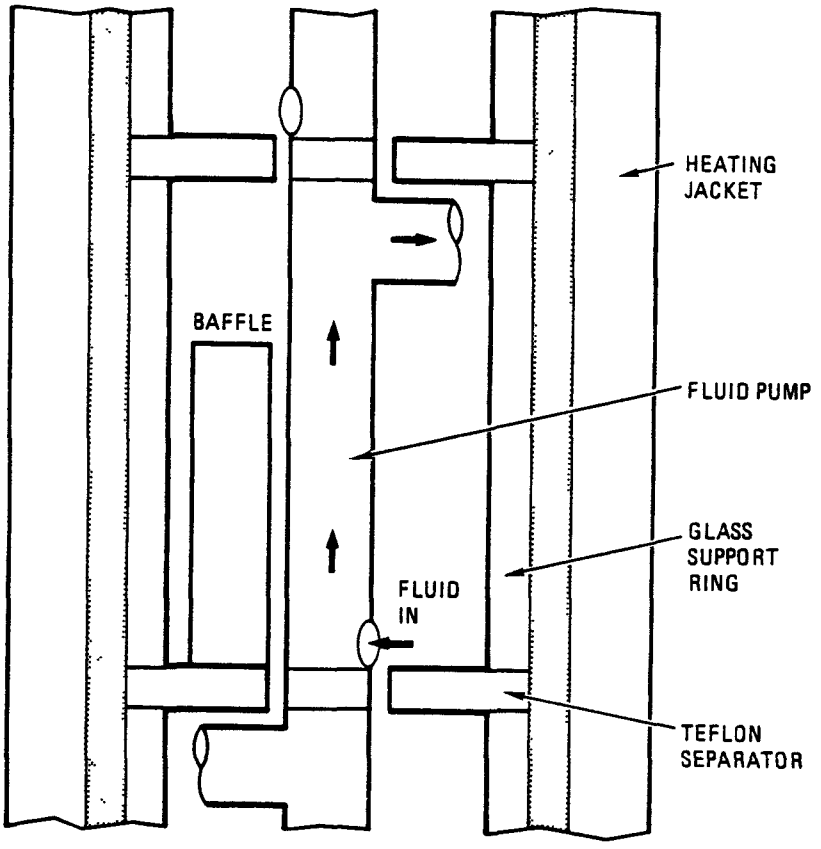

Fig. 49. Typical cell of H_2SO_4 boost column

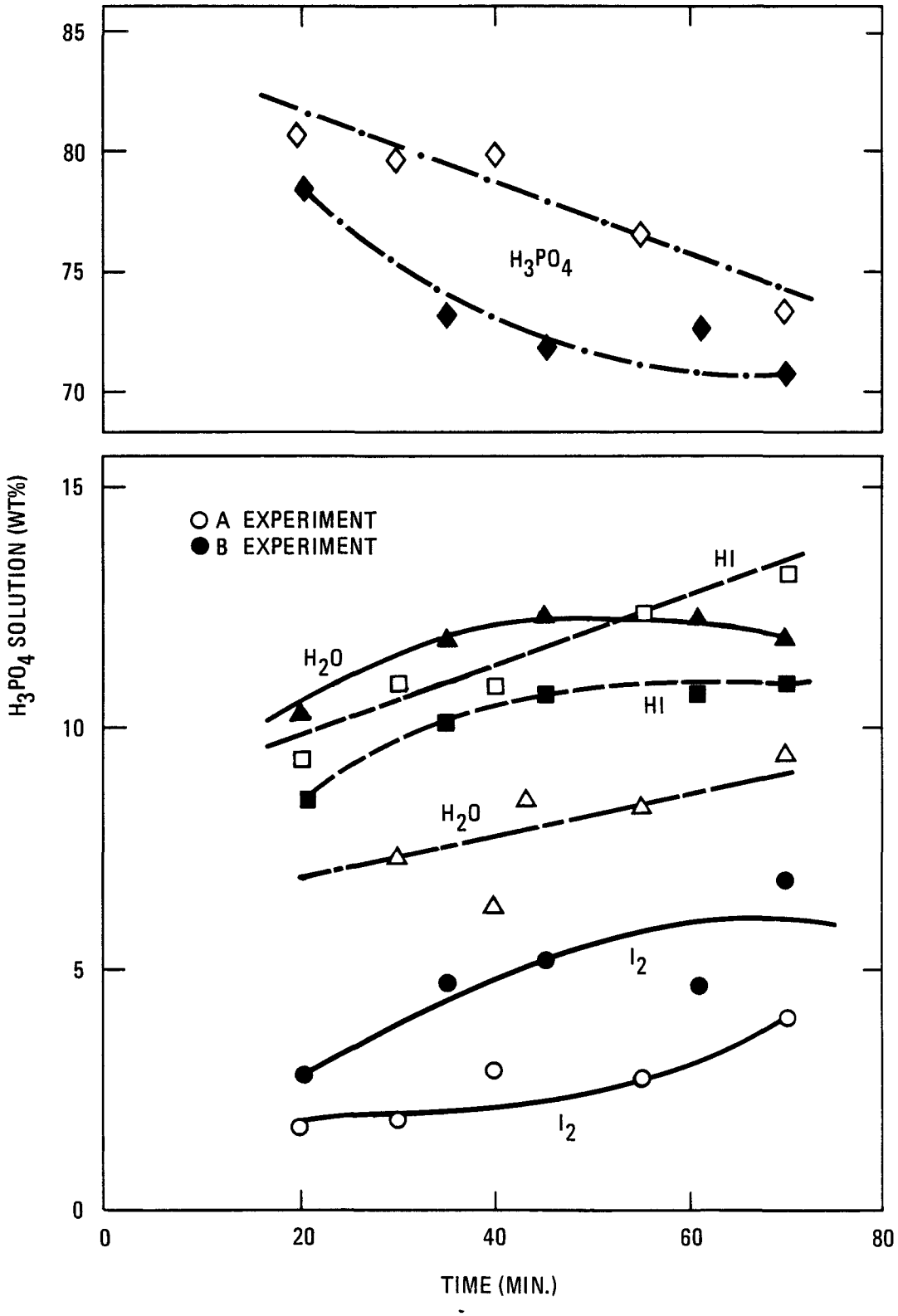

Fig. 50. Two countercurrent H_3PO_4-HI extraction experiments - H_3PO_4 solutions

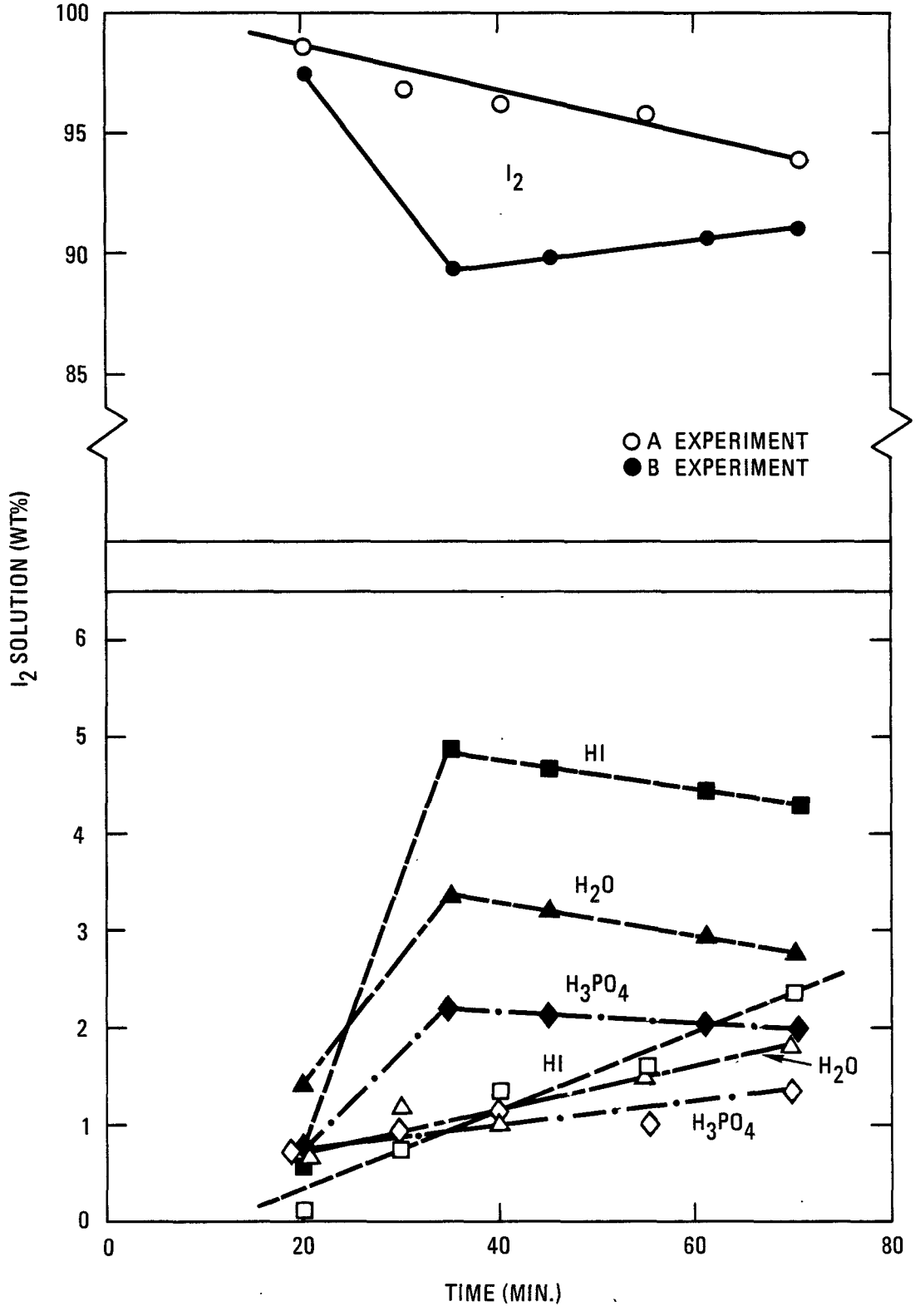

Fig. 51. Two countercurrent H_3PO_4-HI_x extraction experiments - I_2 solutions

trated H_3PO_4 and the HI_x solution delivered through the column. Flow of H_3PO_4 was stopped temporarily between the 20- and 35-min times in Experiment B.

The general characteristics of the column behavior are clear. At early times in the approach to steady state, the HI_x liquid is contacting very strong H_3PO_4 as it transverses the column. Figure 51 shows this iodine to emerge from the column with only minimal contamination. Steady state conditions might be represented to be between the A and B experiments at the end of the experiments. Thus, later in the experiments, the I_2 is more contaminated with HI, H_2O, and H_3PO_4 than early in the experiments. This correlates with the flow of less concentrated H_3PO_4 from the top of the column. Clearly, the column has to operate with stronger H_3PO_4 and/or more plates if product quality is to be maintained. On a HI- and I_2-free basis, the exiting H_3PO_4 is 87%. Thus, it would appear that using more plates is the only feasible approach. It is hoped that not too many more than the ten plates operable in this case will be required to perform the separation producing sufficiently clean I_2. It should be noted that the H_3PO_4 is close to satisfactory, but the iodine product is not sufficiently clean. More plates will accomplish the task, as evidenced by the initial quality of the iodine product, provided that there is not an extreme pinch point in the column operation.

More data of this quality for a column having a reasonably greater number of theoretical plates need to be obtained.

6. REFERENCES

1. Norman, J. H., G. E. Besenbruch, and D. R. O'Keefe, "Thermochemical Water-Splitting for Hydrogen Production, Final Report January 1975-December 1980," Gas Research Institute Report GRI-80/0105, General Atomic Company, March 1981 (GA-A16300).

2. Norman, J. H., et al., "Water Splitting - The Chemistry of the I_2-SO_2-H_2 Reaction and the Processing of H_2SO_4 and HI Products," General Atomic Report GA-A14746, December 1977. (Proceedings of the Miami International Conference on Alternative Energy Sources, Miami Beach, Florida, December 5-7, 1977, p. 537.)

3. Norman J. H., et al., "Chemical Studies on the General Atomic Sulfur-Iodine Thermochemical Water-Splitting Cycle," General Atomic Report GA-A14954, April 1978. (Paper presented at the 2nd World Hydrogen Energy Conference, Zurich, Switzerland, August 21-14, 1978.)

4. de Graaf, J. D., et al., "Engineering and Bench-Scale Studies on the General Atomic Sulfur-Iodine Thermochemical Water-Splitting Cycle," General Atomic Report GA-A14916, March 1978. (Paper presented at the 2nd World Hydrogen Energy Conference, Zurich, Switzerland, August 21-24, 1978.)

5. Norman, J. H., et al., "Studies of the Sulfur-Iodine Thermochemical Water-Splitting Cycle," General Atomic Report GA-A15757, February 1980. (Paper presented at the 3rd World Hydrogen Energy Conference, Tokyo, Japan, June 23-26, 1980.)

6. O'Keefe, D. R., and J. H. Norman, "The Liquid Hydrogen Iodide Decomposition Process Step for Water-Splitting Applications," General Atomic Report GA-A15750, February 1980. (Paper presented at the 3rd World Hydrogen Energy Conference, Tokyo, Japan, June 23-26, 1980.)

7. Besenbruch, G. E., "Hydrogen Production by the GA Sulfur-Iodine Process, A Progress Report," General Atomic Report GA-A15777 (Rev.), May 1980. (Paper presented at the 3rd World Hydrogen Energy Conference, Tokyo, Japan, June 23-26, 1980.)

8. O'Keefe, D. R., et al., "Preliminary Results from Bench-Scale Testing of a Sulfur-Iodine Thermochemical Water-Splitting Cycle," General Atomic Report GA-A15935, July 1980. (Paper presented at the 20th National Convention, Joint AIChE-IMIQ Meeting in Acapulco, Mexico, October 15-17, 1980. To be submitted in part to the International Journal of Hydrogen Energy.)

9. O'Keefe, D. R., J. H. Norman, and D. G. Williamson, "Catalysis Research in Thermochemical Water-Splitting Processes," Catalysis Rev. Sci. Eng. 22 (3), 325-369 (1980).

10. "Thermochemical Water-Splitting Cycle, Bench-Scale Investigations and Process Engineering, Annual Report for the Period February through December 31, 1977," DOE Report GA-A14950, General Atomic Company, April 1978.

11. "Thermochemical Water-Splitting Cycle, Bench-Scale Investigations and Process Engineering Annual Report for the Period October 1, 1978, through September 30, 1979," DOE Report GA-A15788, General Atomic Company, March 1980.

12. Proskouriakoff, K., "Oxidation of Halogen Acids by Sulphuric Acid," J. Phys. Chem. 33, 717 (1929).

13. JANAF Thermochemical Tables, Dow Chemical Company, Midland, Michigan, September 30, 1977.

14. Besenbruch, G. E., and K. H. McCorkle, "Thermochemical Water Splitting with Solar Thermal Energy, Final Report," General Atomic Report GA-A16022, February 1981.

15. Norman, J. H., G. Besenbruch, and L. Brown, "Solar Production of Hydrogen Using the Sulfur-Iodine Thermochemical Water-Splitting Cycle, Final Report," General Atomic Company, unpublished data, September 1981.

16. Warner, R. W., and S. L. Ribe, "Synfuels from Fusion Using the Tandem Mirror Reactor and a Thermochemical Cycle to Produce Hydrogen," Lawrence Livermore National Laboratory Report UCID-19311, February 1, 1982.

17. Perry, R. H., and C. H. Chilton, Chemical Engineering Handbook, 5th ed., McGraw Hill, New York, 1973, pp. 12-42.

18. Schulte, S. C., T. L. Willke, and J. R. Young, "Fusion Reactor Design Studies--Standard Accounts for Cost Estimates," Pacific Northwest Laboratory Report PNL-2648, May 1978.

19. Guthrie, K. M., "Capital Cost Estimating," Chem. Eng. 76 (6), 11, 4-142 (1969).

20. Guthrie, K. M., "Capital and Operating Costs for 54 Chemical Processes," Chem. Eng. 77 (13), 140-156 (1970).

21. Broggi, A., et al., "A Method for the Techno-Economic Evaluation of Chemical Processes. Improvement of the OPTIMO Code," in Proceedings of the 2nd World Hydrogen Energy Conference, Zurich, Switzerland, August 21-24, 1978, T. N. Veziroglu and W. Seifritz (eds.), Pergamon Press, p. 2205.

22. Knoche, K. F., University of Aachen, private communication.

23. Rupert, F. F., "A Study of the System Hydrogen Chloride and Water," J. Am. Chem. Soc. 31, 851 (1909).

24. Horsley, L. N., "Azeotropic Data III," Advances in Chemistry Series, Vol. 116, American Chemical Society, Washington, D. C., 1973.

25. Powell, C. F., and I. E. Campbell, "The Solubility of Iodine in Concentrated Hydriodic Acid Solutions," J. Am. Chem. Soc. 69, 1227 (1947).

26. O'Keefe, D. R., and J. H. Norman, "The Vapor Pressure, Iodine Solubility, and Hydrogen Solubility of Hydrogen Iodide-Iodine Solutions," J. Chem. Engr. Data 27, 77 (1982).

27. "Engineering Analyses of Thermochemical Hydrogen Processes, Final Report," General Atomic Report GA-A14188, November 1976.

28. Chevalier, J. E., and Y. H. Gaston-Bonhomme, "Vapor-Liquid Equilibrium Data for the Systems H_2O-H_2SO_4-HCl, H_2O-H_2SO_4-HBr, and H_2O-HBr at 780 mm Hg Pressure," J. Chem. Eng. Data 25, 271 (1980).

29. Kondo, W., et al., "The Magnesium-Iodine Cycle for the Thermochemical Decomposition of Water," in Proceedings of the 2nd World Hydrogen Energy Conference, Zurich, Switzerland, August 21-14, 1978, T. N. Veziroglu and W. Seifritz (eds.), Pergamon Press, p. 909.

30. O'Keefe, D. R., and J. H. Norman, to be published.

31. Kracek, F. C., "Solubilities in the System Water-Iodine to 200°C," J. Phys. Chem. 35, 417 (1931).

32. Nesmeyanov, A. N., Vapor Pressure of the Elements, translated and edited by J. I. Carasso, Academic Press, New York, 1963, p. 370 et seq.

33. O'Keefe, D. R., J. H. Norman, and G. E. Besenbruch, "HI Decomposition Catalyst Development Studies, Final Report for the Period January 1, 1980, through January 31, 1981," Gas Research Institute Report GRI-08/0060, April 1982 (General Atomic Report GA-A16261).

APPENDIX A
PROCESS SIMULATOR COMPUTER CODE

A.1. GENERAL

The evaluation of thermochemical water-splitting cycles in general and of process alternatives in one cycle in particular is difficult and time-consuming. The ultimate analysis should be based on a complete process engineering design which is based on experimentally proven results and which is optimized in such a way as to result in the lowest possible price for the hydrogen product. For the process engineer, this means trying to strike a balance between two usually counteracting characteristics of the chemical plant: (1) its thermal efficiency, which represents the cost of energy, and (2) its capital costs.

Such efforts may require many process design iterations. However, time and funding are limited, and therefore major iterations are not always possible. Because of this, it was decided to obtain a computer code that could be used to aid in process engineering design, and an investigation was initiated on the availability of computer codes for use in process engineering design work for thermochemical water splitting and process heat. It soon became apparent that due to the general nature of the process engineering designs, only the so-called process simulator codes would be of any value. Later the program OPTIMO, available from EEC-JRC Ispra, was evaluated and the same conclusion was reached.

A.2. SURVEY

A search for a suitable process simulator code was carried out in 1976. Table A.1 gives a list of codes which eventually emerged for evaluation. From these the package from the Chem-Share Corporation was chosen because it was the most comprehensive, complete, and versatile package with good service

TABLE A.1
LIST OF CODES INITIALLY INVESTIGATED

	Name	Company
1.	DESIGN/DISTILL/CHEMTRAN/REFINE	Chemshare Corporation
2.	SSI/100	Simulation Sciences Inc.
3.	Pacer-245	Digital Systems Corp.
4.	Flowtran	Monsanto
5.	Proslator	Nippon-Univac
6.	PDA	Phillips Petroleum Company
7.	PDS	General Electric
8.	Heat Exchange Network Simulator	Elshout & Assoc.

backing, and it could be operated at a reasonable cost. Chem-Share's most important features are:

1. To model a flowsheet, modules are used which describe a particular unit operation, e.g., pump, heat exchanger, distillation tower, chemical reactor, and process controller.

2. The user has the option of generating his own modules, for example, to describe a peculiar, possibly proprietary, operating step.

3. The system has a very extensive intrinsic property data bank. The user has the option of choosing from several types of enthalpy and phase equilibria calculation techniques.

4. There is an option which enables the user to correlate his own property data, in a preprocessing run, in such a way that the data is transformed in a format that can directly be accessed by the process simulator.

More recently Simulation Sciences, Inc. has began marketing an improved version of SSI/100 called PROCESS. It has the stated features of ChemShare, but it is much more flexible in being able to handle non-library components such as are encountered in the GA water-splitting cycle. In addition, it allows many more process streams. Since PROCESS allows both process units and streams to be given an alphanumeric designator, it is possible to tailor the computer output to the needs of the user. The DOE-sponsored ASPEN process simulator is now available but its special features, designed for simulating coal and hydrocarbon processing, are of little utility in simulating the GA water-splitting process.

A.3. EXAMPLE OF APPLICATION

Although GA is switching to PROCESS for its fusion-synfuel work, ChemShare was the only process simulator used in this work.

The only water-splitting application of ChemShare was on the H_2SO_4 concentration step in Section II. Even though this section was almost completed, it was felt that modeling would be attractive since in this section the largest amount of process heat is exchanged. As a first step, a part of the flowsheet consisting of a heat exchanger (E-11 in the heating mode) and the subsequent separator vessel (V-5) was modeled. For this system, it was necessary to create a so-called chemical data file with a preprocessor run in DISTILL, because H_2SO_4 and the heat of mixing for the system H_2SO_4-H_2O are not contained in the data bank.

Since H_2SO_4 at higher temperatures is partly decomposed into H_2O and SO_3, in effect three components in the gas phase are in phase equilibrium with two components in the liquid phase, and this condition cannot be described with the use of ordinary K values. Therefore, the DESIGN model of the flowsheet was modified as shown in Fig. A.1. It is assumed that H_2SO_4 does not decompose in the vapor phase in exchanger E-11 (named E-1 in DESIGN) and

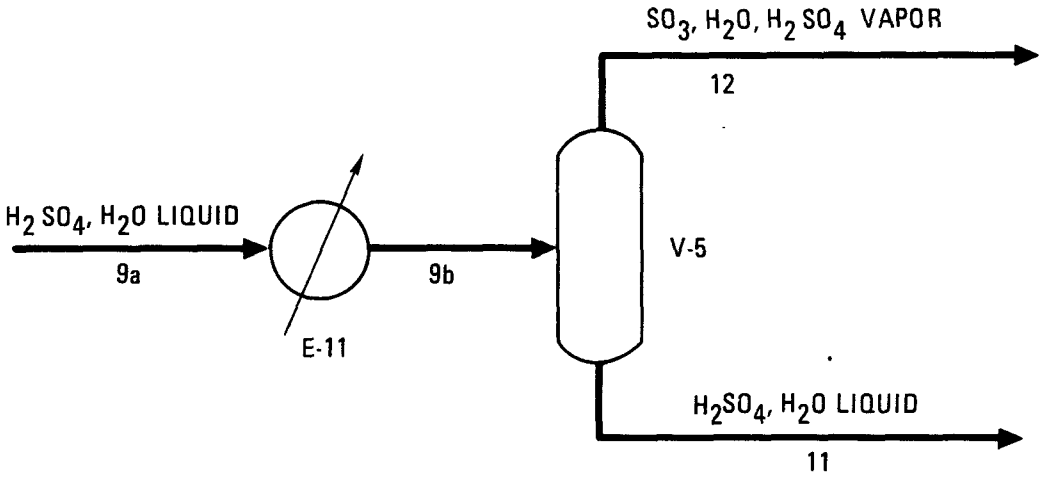

Process Engineering Flowsheet

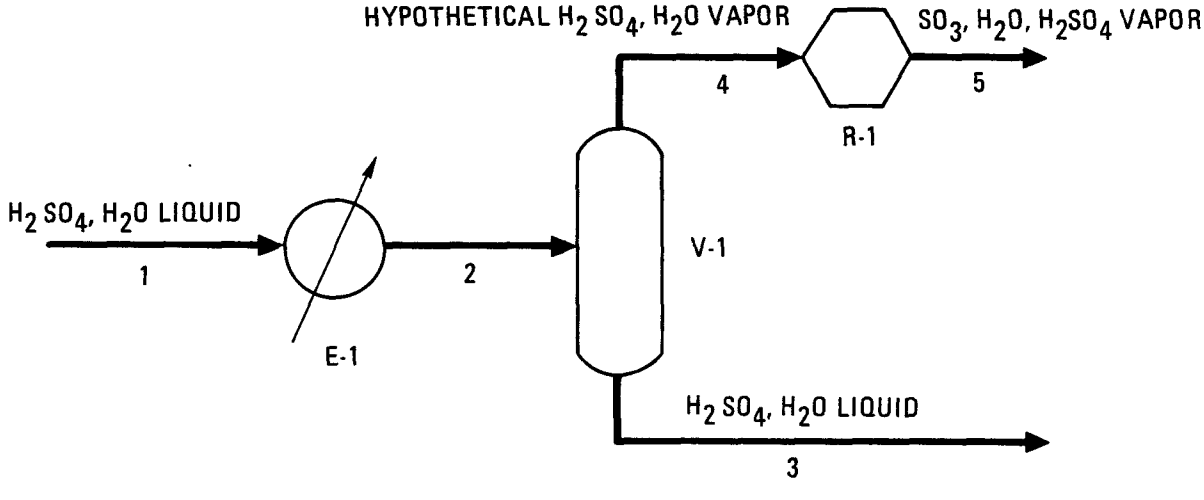

DESIGN Model

Fig. A-1. Modeling of H_2SO_4 concentration step with DESIGN code

therefore SO_3 does not exist in vessel V-5 (named V-1 in DESIGN), and the hypothetical reactor R-1 is introduced to do the partial decomposition of the H_2SO_4. The phase equilibrium in V-1 can then be described by defining apparent mole fractions as follows:

$$y^a_{H_2SO_4} = \frac{P^a_{H_2SO_4}}{P^a_T} = \frac{P_{H_2SO_4} + P_{SO_3}}{P_{H_2SO_4} + P_{H_2O}}$$

$$y^a_{H_2O} = \frac{P^a_{H_2O}}{P^a_T} = \frac{P_{H_2O} - P_{SO_3}}{P_{H_2SO_4} + P_{H_2O}}$$

where:

$y^a_{H_2SO_4}$ = apparent mole fraction of H_2SO_4 in vapor phase

$y^a_{H_2O}$ = apparent mole fraction of H_2O in vapor phase

$P^a_{H_2SO_4}$ = apparent partial pressure of H_2SO_4

$P^a_{H_2O}$ = apparent partial pressure of H_2O

P^a_T = apparent total pressure

$P_{H_2SO_4}$ = true partial pressure of H_2SO_4

P_{SO_3} = true partial pressure of SO_3

P_{H_2O} = true partial pressure of H_2O

Apparent K values then follow from:

$$K^a_{H_2SO_4} = \frac{y^a_{H_2SO_4}}{H_2SO_4}$$

$$K^a_{H_2O} = \frac{y^a_{H_2O}}{(1 - H_2SO_4)}$$

where:

$K^a_{H_2SO_4}$ = apparent K value of H_2SO_4

$K^a_{H_2O}$ = apparent K value of H_2O

H_2SO_4 = mole fraction of H_2SO_4 in liquid

In Table A.2, the input instructions for the simulator run with DESIGN are shown. Actually two parallel simulations were performed; the relevant statements for the simulation described here are indicated. The initial results of this H_2SO_4 concentration subunit showed that the apparent K-values and hypothetical reactor approach functioned well, giving a material balance which was more accurate than that for the hand calculations, and which enabled the calculations to be done in a reasonably short time. Table A.3 presents a comparison of the material balance obtained by hand and with the DESIGN code.

The results on the heat balance, however, given in Table A.4, are not sufficiently accurate. This is due to residual deviations in the curve fittings performed with the DISTILL preprocessor run on GA's enthalpy data, mainly on the heat of mixing, which for the moment has been accepted. GA is confident, however, that by choosing different curve fitting options it would be possible to decrease these residuals and thereby improve the accuracy.

TABLE A-2
INPUT INSTRUCTIONS FOR DESIGN SIMULATOR RUN
(Lines marked with → are relevant to example described in text)

```
          ECHO PRINT OF INPUT DATA          29DEC77          0: 4:24
→*H2SO4 CONCENTRATION * WATER SPLITTING *
→HXE1=E-1,1,-2,TEM OUT9KO=613.15
→FLA2=V-1,2,-4,-3
→REA3=R-1,4,-5,STO COE=-1,1,1,CON=0.158223,HEA(CAL/GMOL)=-24176,LIM=201,
→ISO
 REA50=R-50,44,-50,STO COE=1,-1,-1,CON=1.0,HEA(CAL/GMOL)=-24176,LIM=1068,
 ISO
 HXE41=E-10,50-45,TEM OUT(K)=573.15
 FLA42=V-8,45,-46,-35
 REA43=R-8,46,-47,STO COE=-1,1,1,CON=3.76046E-2,HEA(CAL/GMOL)=-24277,
 LIM=201,ISO
→GENERAL
→COM=201,62,1068
→CHE FIL='SULF','IS42','WSGA'
→FLO(KGMOL/SEC)1=1.6175,0.8333,0.0000
→TP(K,ATM)1=573,15,2.0
 FLO(KGMOL/SEC)44=0.2146,0.7189,0.0404
 TP(K,ATM)44=613.15,2.0
→KKEY=1
→EXC TAB
→MAS UNI=3,TIM UNI=2,TEM UNI=2,PRE UNI=4,DUTY UNI=7
→END

 THERMO DATA FILE OPENED FOR READ
 FILE NAME IS;  SULF/IS42(WSGA)
```

TABLE A-3
COMPARISON OF MATERIAL BALANCE

	Eng. Flowsheet	DESIGN	Eng. Flowsheet	DESIGN	Eng. Flowsheet	DESIGN	Eng. Flowsheet	DESIGN
Stream No.	9a	1	9b	2	11	3	12	5
Temp., K	573.16	573.16	613.16	613.16	613.16	613.16	613.16	613.16
Press., 10^5 Pa	2.027	2.027	2.027	2.027	2.027	2.027	2.027	2.027
H_2SO_4, kMol/s	1.6175	1.6175	1.5858	1.6175	1.4172	1.4031	0.1686	0.1805
H_2O, kMol/s	0.8333	0.8333	0.8650	0.8333	0.3004	0.2973	0.5646	0.5699
SO_3, kMol/s	0.0000	0.0000	0.0317	0.0000	0.0000	0.0000	0.0317	0.0339
TOTAL, kMol/s	2.4508	2.4508	2.4825	2.4508	1.7176	1.7004	0.7649	0.7843

TABLE A.4

COMPARISON OF HEAT DUTIES OF E-11 BASED ON DESIGN'S MATERIAL BALANCE

	Design	Hand Calc.
Heating 573.16K to 613.16K, MJ/S	13.95	14.51
Vaporization at 613.16K, MJ/S	26.94	27.05
Decomposition at 613.16K, MJ/S	3.45	3.45
Mixing, MJ/S	13.19	16.16
Total, MJ/S	57.53	61.17

APPENDIX B

THE 1981 PRELIMINARY CAPITAL COSTS FOR FOR SECTIONS I, III, AND IV FOR A 3000 MW HEAT SUPPLY

Table B-1 - Preliminary Capital Costs for Section I - M$

Item No.		Parallel Units	Diameter Meters	Length Meters	Equivalent Mild Steel FOB Cost	Actual FOB Cost Plus Adders	Installed Direct Capital Cost	Total Plant Investment Basis
C101	Primary scrubbing reactor	6	3.8	9.0	0.326	1.353*+	2.211	2.934
C102	Lower phase SO_2 scrubber	6	5.1	19.5	0.847	3.868*+	6.096	8.027
C103	Boost reactor	6	5.1	19.5	0.847	3.868*+	6.096	8.027
C104	Secondary scrubbing reactor	6	4.5	8.6	0.381	1.651*+	2.653	3.508
S101	High pressure flash drum	6	3.6	13.5	0.489	1.743+	2.929	3.956
S102	Low pressure flash drum	6	4.2	12.0	0.452	1.692+	2.875	3.849
S103	SO_2-H_2O knockout drum	6	4.7	3.9	0.184	0.192+	0.564	0.868
S104	Primary water knockout drum	6	3.0	3.9	0.113	0.113	0.337	0.505
S105	Secondary water knockout drum	1	3.0	3.9	0.019	0.019	0.056	0.084
R101	Heat exchanger reactor	6	1.8	7.5	1.175	20.171	22.206	26.518
E101	SO_2 heat exchanger	6	1.7	12.0	0.713	1.084	2.023	2.945
E102	Sec. III water heat exchanger	2	1.1	12.0	0.174	0.174	0.403	0.615
E103	Sec. II water heat exchanger	3	1.2	12.0	0.275	0.275	0.638	0.972
P101	Water feed pump	6+1	-	-	0.002	0.002	0.008	0.012
P103	Reactor feed pump from C101	6+1	-	-	0.009	0.017	0.031	0.042
P104	Iodine feed pump	6+1	-	-	0.018	0.036	0.065	0.090
P105	Reactor feed pump from C103	6+1	-	-	0.033	0.066	0.118	0.163
P106	Reactor feed pump from C104	6+1	-	-	0.046	0.092	0.169	0.233
P107	Reactor feed pump from S103	6+1	-	-	0.007	0.007	0.016	0.024
TE101	O_2 power recovery turbine	1	-	-	0.971	0.971	2.095	3.157
TE103	Iodine power recovery turbine	1	-	-	0.057	0.165	0.244	0.321
TC101	SO_2 turbine compressor	6	-	-	7.059	7.059	15.233	22.960

*Adder includes the field installation of packing.

+Adder includes the field installation of liner.

Table B-2 - Preliminary Capital Costs for Section III - M$

Item No.		Parallel Units	Diameter Meters	Length Meters	Equivalent Mild Steel FOB Cost	Actual FOB Cost Plus Adders	Installed Direct Capital Cost	Total Plant Investment Basis
C301	Iodine wash column	3	4.5	18.0	0.339	2.700*+	3.263	4.036
C302	Iodine knockout column	10	7.7	24.0	3.059	28.537*+	33.618	41.220
C303	HI distillation	3	6.9	21.6	0.889	21.642*	24.394	28.745
S301	Surge drum - C303 reflux	3	2.7	10.2	0.125	0.413*	0.737	0.945
S303	Flash drum - 1st H_3PO_4 stage	6	6.0	9.0	0.487	1.619+	2.876	3.686
S304	Flash drum - 2nd H_3PO_4 stage	5	3.6	16.2	0.348	1.162+	2.061	2.641
S305	Flash drum - 3rd H_3PO_4 stage	4	6.6	10.7	0.451	3.156	5.653	6.852
S306	S-H_3PO_4 separator	3	5.9	22.2	0.544	3.810	6.620	8.037
E301	Dilute H_3PO_4 cooler	48	1.5	12.0	5.098	51.486	58.025	70.859
E302	Intermediate condenser on C303	3	1.6	12.0	0.144	1.459	2.029	2.450
E303	Reboiler on C303	6	1.1	12.0	0.881	3.853	4.983	6.444
E304	Condenser on C303	6	1.6	12.0	0.800	3.962	5.344	6.794
E305	Iodine cooler	1	1.4	12.0	0.099	0.998	1.388	1.676
E306	Heater - 1st H_3PO_4 stage	48	1.5	12.0	4.964	46.083	63.000	77.019
E307	Heater - 2nd H_3PO_4 stage	28	1.5	12.0	3.124	24.758	33.644	41.249
E308	Heater - 3rd H_3PO_4 stage	22	1.5	12.0	2.203	16.713	22.697	27.874
E309	Concentrated H_3PO_4 cooler	6	1.8	12.0	0.794	8.023	11.154	13.471
E310	Water cooler - 1st H_3PO_4 stage	1	1.7	12.0	0.125	0.923	1.250	1.539
E311	Water cooler - 2nd H_3PO_4 stage	1	1.8	12.0	0.134	0.987	1.337	1.646
E312	Water cooler - 3rd H_3PO_4 stage	1	1.7	12.0	0.139	1.027	1.391	1.713
P301	Lower phase feed pump	10+1	-	-	0.207	0.414	0.794	1.084
P302	Iodine wash water pump	3+1	-	-	0.006	0.006	0.013	0.020
P304	Feed pump - C303	10+1	-	-	0.724	1.449	2.653	3.656
P305	Concentrated H_3PO_4 pump	10+1	-	-	0.202	0.404	0.739	1.017
TE301	Dilute H_3PO_4 PR turbine	1	-	-	0.684	1.368	2.314	3.139
TE302	1st H_3PO_4 stage PR turbine	1	-	-	0.618	0.618	1.322	1.946
TE303	2nd H_3PO_4 stage PR turbine	1	-	-	0.618	0.618	1.322	1.946
TE304	3rd H_3PO_4 stage PR turbine	1	-	-	0.548	0.548	1.173	1.727
TE305	Iodine power recovery turbine	1	-	-	0.597	0.995	1.821	2.505
TC301	1st H_3PO_4 stage steam comp.	6	-	-	25.791	25.791	55.657	83.891
TC302	2nd H_3PO_4 stage steam comp.	5	-	-	21.492	21.492	46.381	69.909
TC303	3rd H_3PO_4 stage steam comp.	4	-	-	17.194	17.194	37.105	55.927

*Adder includes field installation of packing.
+Adder includes field installation of liner.

Table B-3 - Preliminary Capital Costs for Section IV - M$

Item No.		Parallel Units	Diameter Meters	Length Meters	Equivalent Mild Steel FOB Cost	Actual FOB Cost Plus Adders	Installed Direct Capital Cost	Total Plant Investment Basis
C401[1]	HI-I_2 Distillation column	1	4.7[1]	15.0[1]	0.170	1.749*	2.143	2.597
C402	HI Absorber	6	4.1	9.6	1.050	1.301*+	4.301	5.704
C403	H_2S Scrubber	2	3.8	27.3	0.700	1.023*+	2.828	3.981
S401	Reactor effluent V-L separator	1	2.9	13.2	0.162	0.293+	0.710	0.984
S402	H2-HI vapor liquid separator	1	2.4	9.6	0.121	0.201+	0.514	0.717
D401	Reflux surge drum - C401	1	3.3	15.0	0.075	0.248+	0.364	0.497
R401	HI decomposition reactor	4	4.5	27.0	1.750	3.688*+	8.202	11.245
E400	Misc. integrated heat exch.	13	-	-	1.300	6.461	9.222	11.799
E4XX[2]	Absorption refrigeration unit	1	-	-	1.689	1.689	2.819	4.562
P401	Reactor feed pump	4+1	-	-	0.638	1.845	2.906	3.876
P402	HI recycle feed pump	1+1	-	-	0.287	1.406	2.215	2.954
P403	Reflux pump - C401	1+1	-	-	0.013	0.037	0.058	0.075
P404	Make-up water feed pump	6+1	-	-	0.020	0.020	0.048	0.072
P405	Recycle pump - C402	6+1	-	-	0.024	0.069	0.109	0.145
P406	SO_2-H_2O pump to C403	6+1	-	-	0.018	0.018	0.042	0.063
P407	Recycle pump -C403	2+1	-	-	0.015	0.015	0.035	0.052
TE401	HI-I_2 power recovery turbine	1	-	-	0.348	1.007	1.483	1.997
TE402	Hydrogen power recovery turbine	1	-	-	1.625	1.625	3.507	5.286

*Adder includes field installation of packing.

+Adder includes field installation of liners.

[1]The HI-I_2 distillation column is 2.7M dia. for the bottom 12M and 4.7M dia. for the remaining 3M.

[2]The absorption refrigerator includes heat exchangers E408, E410 and E411.

APPENDIX C

THE 1981 FLOWSHEETS FOR SECTIONS I, III, AND IV

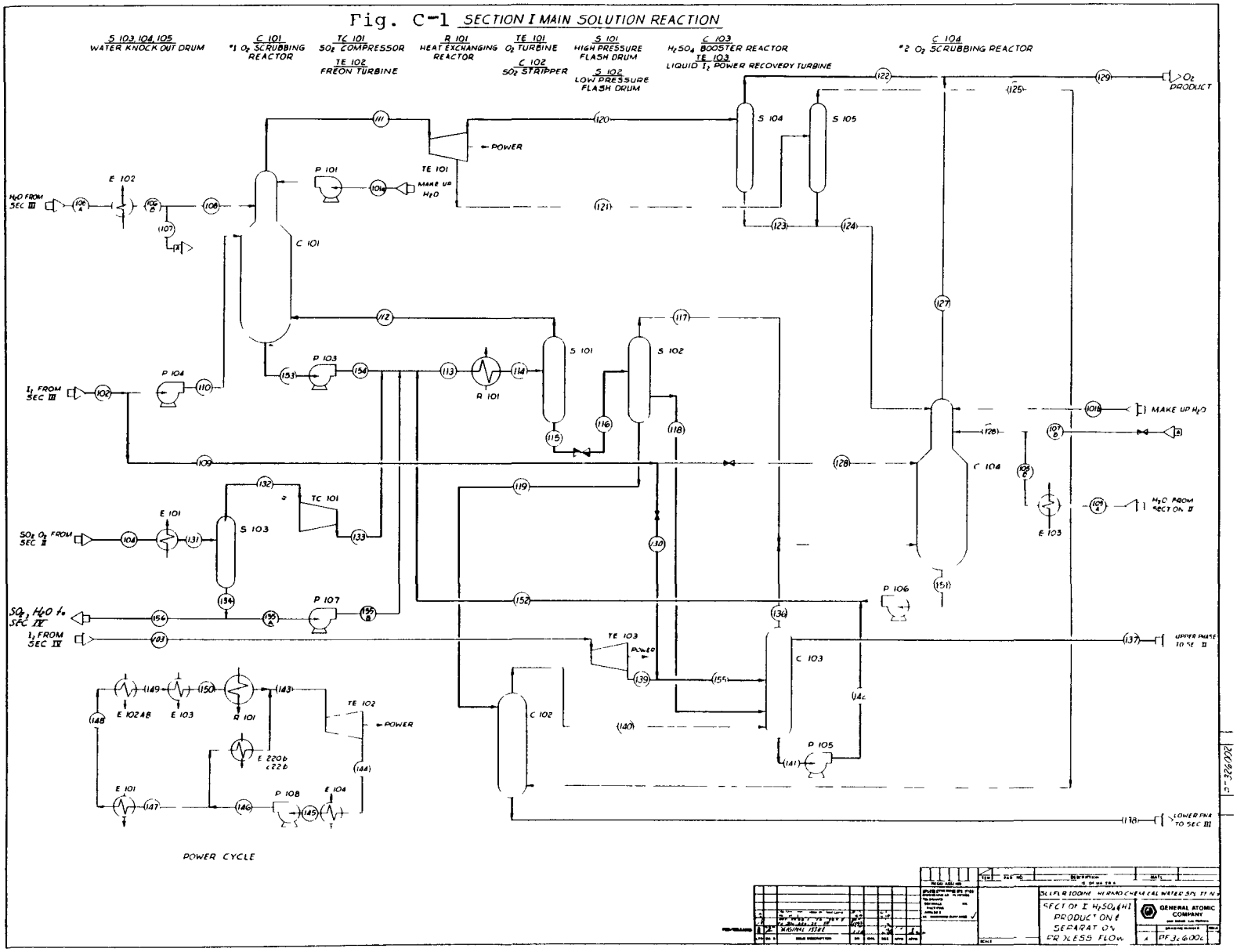
Fig. C-1 SECTION I MAIN SOLUTION REACTION
S 103, 104, 105 WATER KNOCK OUT DRUM
C 101 *1 O2 SCRUBBING REACTOR
TC 101 SO2 COMPRESSOR
TE 102 FREON TURBINE
R 101 HEAT EXCHANGING REACTOR
TE 101 O2 TURBINE
C 102 SO2 STRIPPER
S 101 HIGH PRESSURE FLASH DRUM
S 102 LOW PRESSURE FLASH DRUM
C 103 H2SO4 BOOSTER REACTOR
TE 103 LIQUID I2 POWER RECOVERY TURBINE
C 104 *2 O2 SCRUBBING REACTOR
O2 PRODUCT
POWER
MAKE UP H2O
H2O FROM SEC III
I2 FROM SEC III
SO2 O2 FROM SEC II
SO2 H2O Io SEC IX
I2 FROM SEC IX
H2O FROM SECTION II
UPPER PHASE TO SE II
LOWER PHA TO SEC III
E 102
P 101
P 103
P 104
P 105
P 106
P 107
P 108
E 101
E 103
E 104
E 102A
E 102B
E 220A
E 220B
S 103
S 104
S 105
C 101
C 102
C 103
C 104
R 101
TC 101
TE 101
TE 102
TE 103
POWER CYCLE
SCALE 1:100 IN. HEIGHT CHEMICAL WATER SPLITTING
EFFECT OF E H2SO4 CONCENTRATION ON PRODUCTION RATE FOR LESS FLOW
GENERAL ATOMIC COMPANY
DF 3, 6002

Fig. C-2. SECT III HI CONCENTRATION

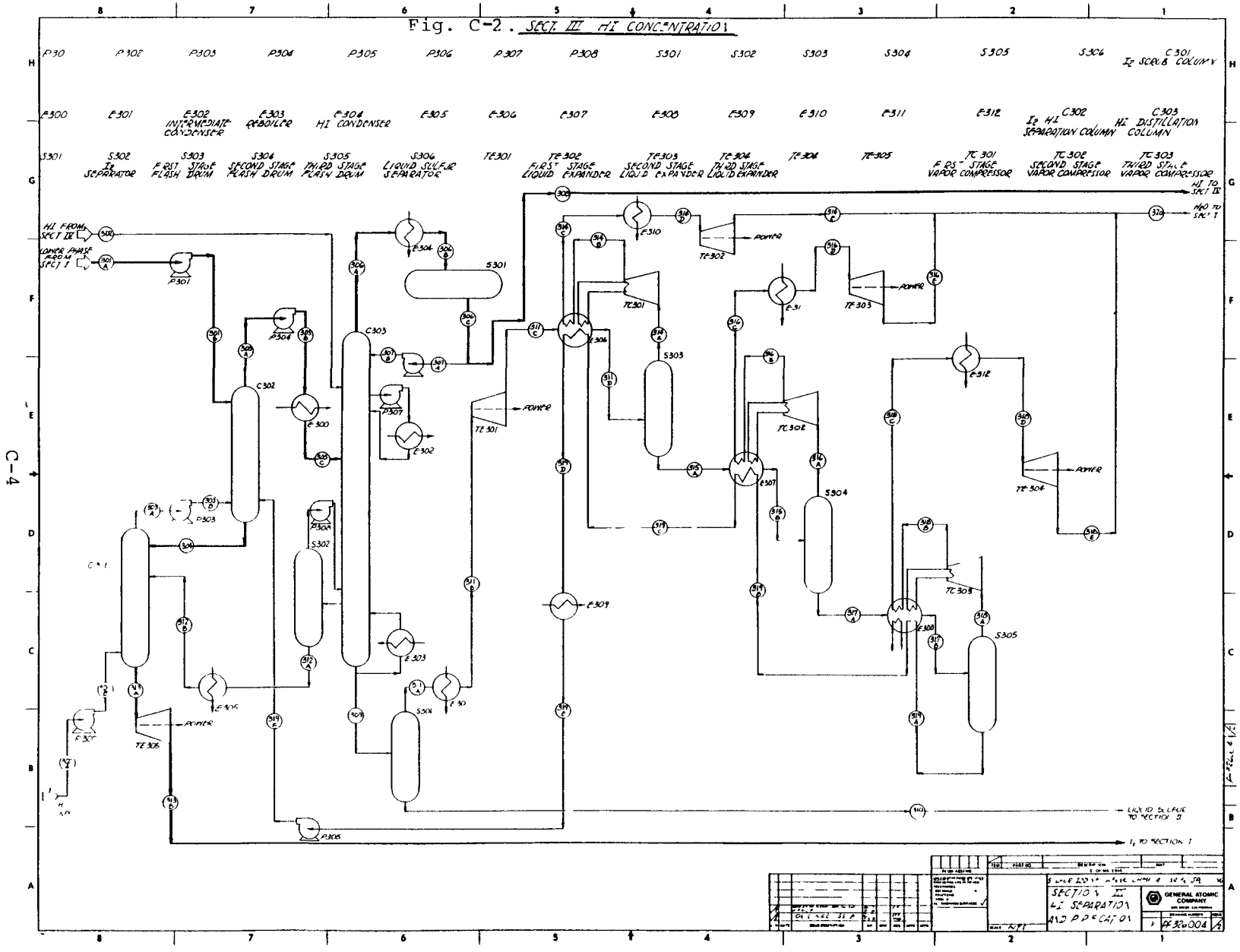

C-4

Fig. C-3. SECTION IV HI CRACKING

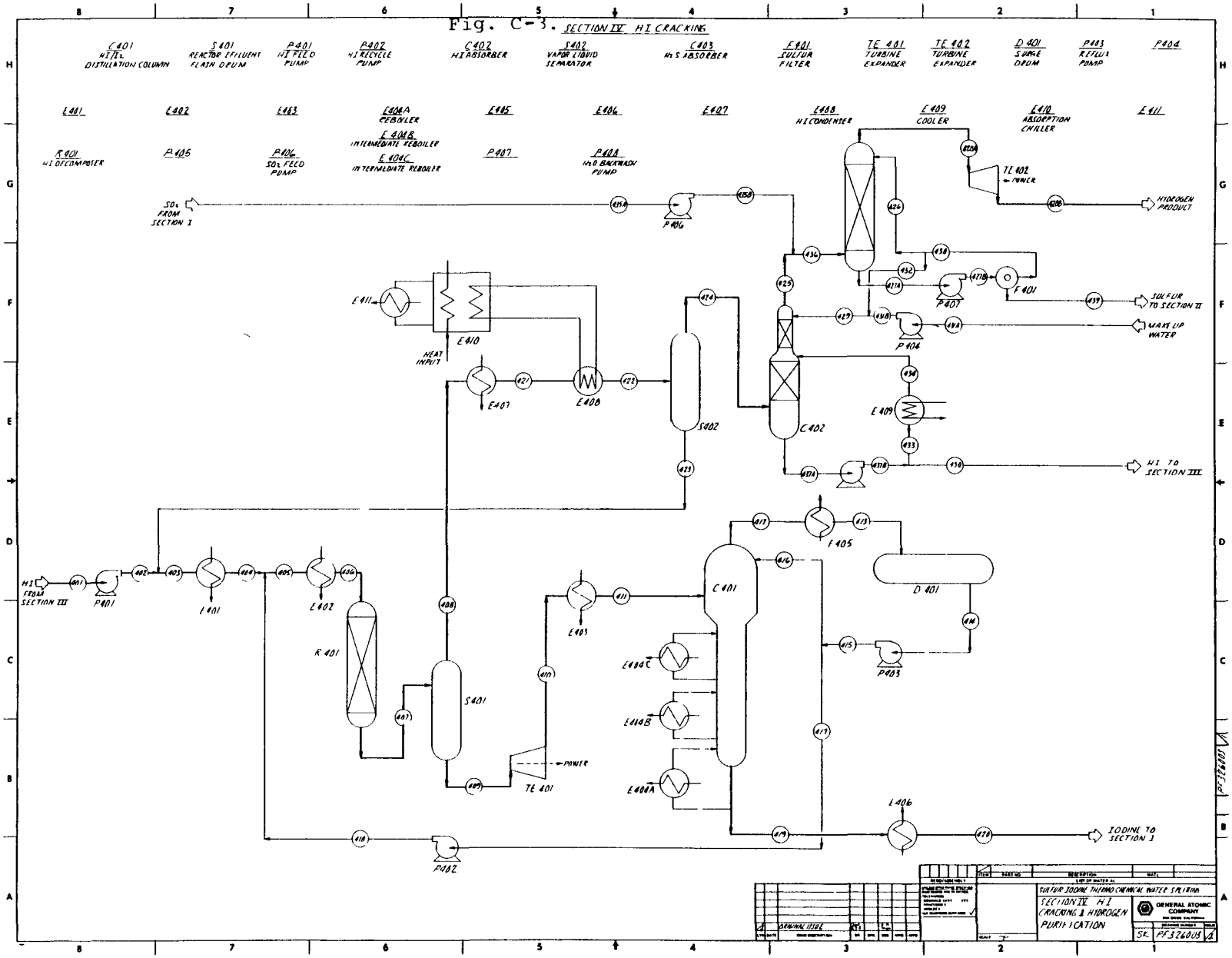

TABLE C-1

MATERIAL BALANCE SECTION I - MAIN SOLUTION

Stream Number	Molar Flow Ratios H_2SO_4	HI	I_2	H_2O	SO_2	O_2	R-11	Total	Phase	Pres MPa	Temp K	Comments
101a	0	0	0	0.4580	0	0	0	0.4580	L	0.101	298	Make up water
101b	0	0	0	0.4144	0	0	0	0.4144	L	0.101	298	Make up water
102	0	0	12.1686	0.1327	0	0	0	12.3013	L	0.185	393	I_2 from Section III
103	0	0	1.0010	0.0020	0	0	0	1.0030	L	5.066	393	I_2 from Section IV
104	0	0	0	0.4257	1.0129	0.5000	0	1.9054	G	0.200	418	SO_2, O_2 from Section II
105A	0	0	0	4.7446	0	0	0	4.7446	L	0.502	422	H_2O from Section II
105B	0	0	0	4.7446	0	0	0	4.7446	L	0.101	359.6	
106A	0	0	0	10.7178	0	0	0	10.7178	L	0.450	368	
106B	0	0	0	10.7178	0	0	0	10.7178	L	0.420	359.6	
107	0	0	0	2.8488	0	0	0	2.8488	L	0.420	359.6	
108	0	0	0	7.8690	0	0	0	7.8690	L	0.420	359.6	
109	0	0	8.8322	0.0964	0	0	0	8.9286	L	0.185	393	
110	0	0	3.3364	0.0364	0	0	0	3.3728	L	0.430	393	
111	0	0	0	0.0151	0	0.5000	0	0.5151	G	0.420	323	
112	0	0	0.0154	0.1951	0.1963	0.5000	0	0.9068	G	0.440	393	
113	0.4143	0.9754	12.7303	17.3722	1.0275	0.5000	0	33.0197	L+G	0.500	-	
114	0.9356	2.0181	12.2090	16.3295	0.5061	0.5000	0	32.4983	L+G	0.440	393	
115	0.9356	2.0181	12.1936	16.1344	0.3099	0	0	31.5916	L	0.440	393	
116	0.9356	2.0181	12.1936	16.1344	0.3099	0	0	31.5916	L+G	0.110	384.5	
117	0	0	0.0281	0.3603	0.1790	0	0	0.5674	G	0.110	384.5	
118	0.9336	0	0	5.0382	0.0054	0	0	5.9772	L	0.110	384.5	
119	0.0020	2.0181	12.1655	10.7360	0.1255	0	0	25.0471	L	0.110	384.5	
120	0	0	0	0.0136	0	0.4499	0	0.0516	L+G	0.101	286.0	
121	0	0	0	0.0015	0	1.0501	0	0.0516	L+G	0.110	289.	

TABLE C.1 (cont.)
MATERIAL BALANCE SECTION I - MAIN SOLUTION

Stream Number	Molar Flow Ratios H_2SO_4	HI	I_2	H_2O	SO_2	O_2	R-11	Total	Phase	Pres MPa	Temp K	Comments
122	0	0	0	0.0066	0	0.4499	0	0.4565	G	0.101	286.0	
123	0	0	0	0.0069	0	0	0	0.0069	L	0.101	286	
124	0	0	0	0.0077	0	0	0	0.0077	L	0.101	286	
125	0	0	0	0.0008	0	0.0501	0	0.0509	G	0.110	289.1	
126	0	0	0	7.5935	0	0	0	7.5935	L	0.101	359.6	
127	0	0	0	0.0039	0	0.0501	0	0.0540	G	0.101	313	
128	0	0	3.2288	0.0352	0	0	0	3.2640	L	0.101	393	
129	0	0	0	0.0106	0	0.5000	0	0.5106	G	0.103	288.7	O_2 product
130	0	0	5.6034	0.0611	0	0	0	5.6641	L	0.105	393	
131	0	0	0	0.3925	1.0129	0.5000	0	1.9054	L+G	0.195	313	
132	0	0	0	0.0595	1.0052	0.5000	0	1.5718	G	0.195	313	
133	0	0	0	0.0595	1.0052	0.5000	0	1.5718	G	0.500	395.1	
134	0	0	0	0.3327	0.0069	0	0	0.3396	L	0.195	313	
135A	0	0	0	0.3038	0.0063	0	0	0.3327	L	0.195	313	
135B	0	0	0	0.3038	0.0063	0	0	0.3327	L	0.500	313	
136	0	0	0.0133	0.1568	0.0391	0.0501	0	0.2092	G	0.105	393	
137	1.0060	0	0	4.1224	0.0038	0	0	5.1322	L	0.105	393	Upper phase to Sec. II
138	0.0020	2.0161	12.1615	10.6842	0.0004	0	0	24.8642	L	0.110	381.4	Lower phase to Sec. III
139	0	0	1.0010	0.0020	0	0	0	1.0030	L	0.105	393	
140	0	0.0020	0.0039	0.0526	0.1251	0.0501	0	0.2337	G	0.105	384.5	
141	0	0.1469	6.5227	0.7299	0.0152	0	0	7.4147	L	0.105	384.5	

TABLE C-1 (cont.)
MATERIAL BALANCE SECTION I - MAIN. SOLUTION

Stream Number	Molar Flow Ratios H_2SO_4	HI	I_2	H_2O	SO_2	O_2	R-11	Total	Phase	Pres MPa	Temp K	Comments
142	0	0.1516	6.5227	0.7299	0.0152	0	0	7.4194	L	0.500	384.5	
143	0	0	0	0	0	0	5.8942	5.8942	G	0.818	373	Power recovery cycle
144	0	0	0	0	0	0	5.8942	5.8942	G	0.113	300	" " "
145	0	0	0	0	0	0	5.8942	5.8942	L	0.113	300	" " "
146	0	0	0	0	0	0	5.8942	5.8942	L	0.880	300	" " "
147	0	0	0	0	0	0	5.7125	5.7125	L	0.880	300	" " "
148	0	0	0	0	0	0	5.7125	5.7125	L	0.865	327.3	" " "
149	0	0	0	0	0	0	5.7125	5.7125	L	0.860	342.3	" " "
150	0	0	0	0	0	0	5.7125	5.7125	L	0.850	373	" " "
151	0.2180	0.4361	3.0522	8.1279	0	0	0	11.8342	L	0.101	-	
152	0.2180	0.5828	9.5748	8.8578	0	0	0	19.2334	L	0.500	-	
153	0.1963	0.3926	3.1555	8.1508	0	0	0	11.8952	L	0.440	-	
154	0.1963	0.3926	3.1555	8.1508	0	0	0	11.8952	L	0.500	-	
155	0	0	6.6044	0.0631	0	0	0	6.6675	L	0.105	393	
156	0	0	0	0.0289	0.0006	0	0	0.0295	L	0.195	313	SO_2, H_2O to Sec. IV

TABLE C-2

MATERIAL BALANCE - SECTION III - HI SEPARATION AND PURIFICATION

Stream No.	Molar Flow Ratios H_2SO_4	HI	I_2	H_2O	SO_2	H_3PO_4	Other	Total	Phase	Pressure MPa	Temp K	Comments
300A	0	0	0	0.0777	0	0	0	0.0777	1	0.101	298.15	Water input from environ.
300B	0	0	0	0.0777	0	0	0	0.0777	1	0.304	298.15	
301A	0.0020	2.0151	12.1615	10.6842	0.0004	0	0	24.8642	1	0.110	381.40	Input from Sec. I.
301B	0.0020	2.0161	12.1615	10.6842	0.0004	0	0	24.8642	1	0.304	381.40	
302	0	0.0818	0	0.0818	0	0	0	0.1636	1	8.309	298.15	Input from Sec. IV.
303A	0	0.0217	0.0080	0.1212	0	0.0869	0	0.2378	1	0.304	393.15	
303B	0	0.0217	0.0080	0.1212	0	0.0869	0	0.2378	1	0.304	393.15	
304	0	0.0213	11.7847	0.1327	0	0.0869	0	12.0256	1	0.304	393.15	
305A	0.0020	2.0165	0.3848	14.8090	0.0004	18.2352	0	35.4479	1	0.304	393.15	
305B	0.0020	2.0165	0.3848	14.8090	0.0004	18.2352	0	35.4479	1	0.912	393.15	
305C	0.0020	2.0165	0.3848	14.8090	0.0004	18.2352	0	35.4479	1	0.912	514.0	
306A	0	2.2197	0.0011	0.0022	0	0	*0.0013	2.2243	g	0.912	303.15	(* H_2S)
306B	0	2.2197	0.0011	0.0022	0	0	*0.0013	2.2243	1	0.912	303.15	(* H_2S)
306C	0	2.2197	0.0011	0.0022	0	0	*0.0013	2.2243	1	0.912	303.15	(* H_2S)
307A	0	0.1379	0.0001	0.0002	0	0	*0.0001	0.1383	1	0.912	303.15	(* H_2S)
307B	0	0.1379	0.0001	0.0002	0	0	*0.0001	0.1383	1	0.912	303.15	(* H_2S)
308	0	2.0818	0.0010	0.0020	0	0	*0.0012	2.0860	1	0.912	303.15	(* H_2S) HI output, Sec.IV.
309	0	0	0	14.8541	0	18.2352	*0.0012	33.0905	1	0.962	523.0	(* S)
310	0	0	0	0	0	0	*0.0012	0.0012	1	0.962	523.0	(* S) Liq. sulfur output
311A	0	0	0	14.8541	0	18.2352	0	33.0893	1	0.962	523.0	
311B	0	0	0	14.8541	0	18.2352	0	33.0893	1	0.962	436.15	
311C	0	0	0	14.8541	0	18.2352	0	33.0893	1	0.101	436.15	
311D	0	0	0	14.8541	0	18.2352	0	33.0893	1+g	0.101	453.15	

TABLE C-2 (cont.)

MATERIAL BALANCE - SECTION III - HI SEPARATION AND PURIFICATION

Stream No.	Molar Flow Ratios H_2SO_4	HI	I_2	H_2O	SO_2	H_3PO_4	Other	Total	Phase	Pressure MPa	Temp K	Comments
312A	0	0.0004	0.3918	0.0435	0	0	0	0.4357	l	0.962	520.0	
312B	0	0.0004	0.3918	0.0435	0	0	0	0.4357	l	0.962	393.15	
313A	0	0	12.1685	0.1327	0	0	0	12.3012	l	0.304	393.15	
313B	0	0	12.1685	0.1327	0	0	0	12.3012	l	0.185	393.15	Iodine, output to Sec. I.
314A	0	0	0	5.0438	0	0	0	5.0438	g	0.101	453.15	
314B	0	0	0	5.0438	0	0	0	5.0438	g	1.165	460.15	
314C	0	0	0	5.0438	0	0	0	5.0438	l	1.165	460.15	
314D	0	0	0	5.0438	0	0	0	5.0438	l	1.165	368.15	
314E	0	0	0	5.0438	0	0	0	5.0438	l	0.185	368.15	
315A	0	0	0	9.8103	0	18.2352	0	28.0455	l	0.101	453.15	
315B	0	0	0	9.8103	0	18.2352	0	28.0455	l+g	0.101	471.15	
316A	0	0	0	3.4788	0	0	0	3.4788	g	0.101	471.15	
316B	0	0	0	3.4788	0	0	0	3.4788	g	1.722	478.15	
316C	0	0	0	3.4788	0	0	0	3.4788	l	1.722	478.15	
316D	0	0	0	3.4788	0	0	0	3.4788	l	1.722	368.15	
316E	0	0	0	3.4788	0	0	0	3.4788	l	0.185	368.15	
317A	0	0	0	6.3315	0	18.2352	0	24.5667	l	0.101	471.15	
317B	0	0	0	6.3315	0	18.2352	0	24.5667	l+g	0.101	484.15	
318A	0	0	0	2.1953	0	0	0	2.1953	g	0.101	484.15	
318B	0	0	0	2.1953	0	0	0	2.1953	g	2.279	491.15	
318C	0	0	0	2.1953	0	0	0	2.1953	l	2.279	491.15	
318D	0	0	0	2.1953	0	0	0	2.1953	l	2.279	368.15	
318E	0	0	0	2.1953	0	0	0	2.1953	l	0.185	368.15	

TABLE C-2 (cont.)
MATERIAL BALANCE - SECTION III - HI SEPARATION AND PURIFICATION

Stream No.	Molar Flow Ratios H_2SO_4	HI	I_2	H_2O	SO_2	H_3PO_4	Other	Total	Phase	Pressure MPa	Temp K	Comments
319A	0	0	0	4.1362	0	18.2352	0	22.3714	1	0.101	484.15	
319B	0	0	0	4.1362	0	18.2352	0	22.3714	1	0.101	481.15	
319C	0	0	0	4.1362	0	18.2352	0	22.3714	1	0.101	466.22	
319D	0	0	0	4.1362	0	18.2352	0	22.3714	1	0.101	445.02	
319E	0	0	0	4.1362	0	18.2352	0	22.3714	1	0.101	405.26	
319F	0	0	0	4.1362	0	18.2352	0	22.3714	1	0.304	405.26	
320	0	0	0	10.7178	0	0	0	10.7178	1	0.185	368.15	H_2O output to Sec. I.

TABLE C-3

MATERIAL BALANCE SECTION IV - HYDROGEN IODIDE CRACKING AND HYDROGEN PURIFICATION

Stream	Molar Flow Ratios									Pres	Temp	Comments
Number	HI	I_2	H_2O	H_2S	H_2	S	SO_2	Total	Phase	MPa	K	
401	2.0818	0.0010	0.0020	0.0012	0			2.0860	L	0.912	303	HI from Section III
402	2.0818	0.0010	0.0020	0.0012	0			2.0860	L	8.309	313.6	
403	3.2557	0.0028	0.0021	0.0012	0.0339			3.2957	L	8.309	305.5	
404	3.2557	0.0028	0.0021	0.0012	0.0339			3.2957	L	8.309	393	
405	4.2573	0.0034	0.0021	0.0012	0.0369			4.3009	L	8.309	393	
406	4.2573	0.0034	0.0021	0.0012	0.0369			4.3009	L	8.309	415.2	
407	2.2573	1.0034	0.0021	0.0012	1.0369			4.3009	L+G	8.309	424	
408	1.2257	0.0018	0.0001	0.0012	1.0339			2.2927	G	8.309	424	
409	1.0016	1.0016	0.0020	0	0.0029			2.0081	L	8.309	424	
410	1.0016	1.0016	0.0020	0	0.0029			2.0081	L	5.066	424	
411	1.0016	1.0016	0.0020	0	0.0029			2.0081	L	5.066	439	
412	1.0517	0.0006	0	0	0.0030			1.0553	G	5.066	393	
413	1.0517	0.0006	0	0	0.0030			1.0553	L	5.066	393	
414	1.0517	0.0006	0	0	0.0030			1.0553	L	5.066	393	
415	1.0517	0.0006	0	0	0.0030			1.0553	L	5.066	393	
416	0.0501	T	0	0	0.0001			0.0502	L	5.066	393	
417	1.0016	0.0006	0	0	0.0029			1.0051	L	5.066	393	
418	1.0016	0.0006	0	0	0.0029			1.0051	L	8.309	393.6	
419	0	1.0010	0.0020	0	0			1.0030	L	5.066	713	
420	0	1.0010	0.0020	0	0			1.0030	L	5.066	393	Iodine to Section I
421	1.2557	0.0018	0.0001	0.0012	1.0339			2.2927	L+G	8.309	303	
422	1.2557	0.0018	0.0001	0.0012	1.0339			2.2927	L+G	8.309	291	

TABLE C-3 (cont.)

MATERIAL BALANCE SECTION IV - HYDROGEN IODIDE CRACKING AND HYDROGEN PURIFICATION

Stream	Molar Flow Ratios									Pres	Temp	Comments
Number	HI	I_2	H_2O	H_2S	H_2	S	SO_2	Total	Phase	MPa	K	
423	1.1739	0.0018	0.0001	0	0.0339	0	0	1.2097	L	8.309	291	
424	0.0818	0	0	0.0012	1.0000	0	0	1.0818	G	8.309	291	
425	0	0	0.0004	0.0012	1.0000	0	0	1.0016	G	8.309	298	
426	0	0	0.4700	0	0	0	0	0.4700	L	8.309	298	
427A	0	0	0.5000	0	0	0.0018	0	0.5018	L	8.309	298	
427B	0	0	0.5000	0	0	0.0018	0	0.5018	L	8.343	298	
428A	0	0	0.0005	0	1.0000	0	0	1.0005	L	8.309	298	
428B	0	0	0.0005	0	1.0000	0	0	1.0005	G	5.066	294	Hydrogen product
429	0	0	0.0822	0	0	0	0	0.0822	L	8.309	298	
430	0.0818	0	0.0818	0	0	0	0	0.1636	L	8.309	323	HI_2, H_2O to Section III
431A	0	0	0.0609	0	0	0	0	0.0609	L	0.101	298	Make-up water
431B	0	0	0.0609	0	0	0	0	0.0609	L	8.309	298	
432	0	0	0.0213	0	0	0	0	0.0213	L	8.309	298	
433	0.3792	0	0.3792	0	0	0	0	0.7584	L	8.309	323	
434	0.3792	0	0.3792	0	0	0	0	0.7584	L	8.309	305	
435A	0	0	0.0289	0	0	0	0.0006	0.0295	L	0.202	313	SO_2 from Section I
435B	0	0	0.0289	0	0	0	0.0006	0.0295	L	8.309	298	
436	0	0	0.0293	0.0012	1.0000	0	0.0006	1.0311	G	8.309	298	
437A	0.4610	0	0.4610	0	0	0	0	0.9220	L	8.309	323	
437B	0.4610	0	0.4610	0	0	0	0	0.9220	L	8.343	323	
438	0	0	0.4913	0	0	0	0	0.5000	L	8.309	298	
439	0	0	0.0087	0	0	0.0018	0	0.0105	L+S	0.520	298	S slurry to Section II

TABLE C-4

HEAT MATCH-UP SECTION III - HYDROGEN IODIDE SEPARATION AND PURIFICATION

Heat Exch Number	Hot Side Temp In Deg K	Temp Out Deg K	Heat Exch Number	Cold Side Temp In Deg K	Temp Out Deg K	Heat Load kJ	Comments
E301A	522.90	520.00	E300A	509.26	512.00	12.009	
E301B	520.00	510.00	E300B1	499.74	509.26	41.409	
E305A	520.00	510.00	E300B2	499.74	509.26	0.351	
E305C	510.00	491.15	E300C1	481.23	499.74	78.057	
E305B	510.00	491.15	E300C2	481.23	499.74	0.679	
E302A	510.00	491.15	E300C3	481.23	499.74	2.495	
E301D	491.15	478.15	E300D1	467.85	481.23	53.833	
E305C	491.15	478.15	E300D2	467.85	481.23	0.457	
E302B	491.15	478.15	E300D3	467.85	481.23	1.722	
E312A	491.15	478.15	E300D4	467.85	481.23	2.700	
E301E	478.15	460.15	E300E1	448.43	467.85	74.537	
E305D	478.15	460.15	E300E2	448.43	467.85	0.632	
E302C	478.15	460.15	E300E3	448.43	467.85	2.384	
E312B	478.15	460.15	E300E4	448.43	467.85	2.707	
E311A	478.15	460.15	E300E5	448.43	467.85	4.941	
E301F	460.15	444.99	E300F1	430.63	448.43	62.777	
E305E	460.15	444.79	E300F2	430.63	448.43	0.533	
E302D	460.15	444.79	E300F3	430.63	448.43	2.007	
E312C	460.15	444.79	E300F4	430.63	448.43	2.644	
E311B	460.15	444.79	E300F5	430.63	448.43	4.161	
E310A	460.15	444.79	E300F6	430.63	448.43	5.968	

TABLE C-4 (cont.)

HEAT MATCH-UP SECTION III - HYDROGEN IODIDE SEPARATION AND PURIFICATION

Heat Exch Number	Hot Side Temp In Deg K	Temp Out Deg K	Heat Exch Number	Cold Side Temp In Deg K	Temp Out Deg K	Heat Load kJ	Comments
E301G	444.99	436.15	E300G1	412.62	430.63	36.606	
E305F	444.99	436.15	E300G2	412.62	430.63	0.310	
E302E	444.99	436.15	E300G3	412.62	430.63	1.191	
E312D	444.99	436.15	E300G4	412.62	430.63	3.372	
E311C	444.99	436.15	E300G5	412.62	430.63	2.427	
E310B	444.99	436.15	E300G6	412.62	430.63	3.499	
E309A	444.99	436.15	E300G7	412.62	430.63	31.617	
E305G1	436.15	416.72	E300H1	393.15	412.62	0.683	
E305G2	416.72	393.15	Sec. V	-	-	0.828	Heat avail. for Sec. V Power Bottoming Cycle
E302F1	436.15	416.72	E300H2	393.15	412.62	2.552	
E302F2	416.72	410.00	Sec. V	-	-	0.883	Heat avail. for Sec. V Power Bottoming Cycle
E312E1	436.15	416.72	E300H3	393.15	412.62	2.029	
E312E2	416.72	368.15	Sec. V	-	-	7.750	Heat avail. for Sec. V Power Bottoming Cycle
E311D1	436.15	416.72	E300H4	393.15	412.62	5.333	
E311D2	416.72	368.15	Sec. V	-	-	13.016	Heat avail. for Sec. V Power Bottoming Cycle
E310C1	436.15	416.72	E300H5	393.15	412.62	7.662	
E310C2	416.72	368.15	Sec. V	-	-	18.851	Heat avail. for Sec. V Power Bottoming Cycle
E309B1	436.15	416.72	E300H6	393.15	412.62	67.211	
E309B2	416.72	412.33	Sec. V	-	-	17.042	Heat avail. for Sec. V Power Bottoming Cycle

TABLE C-5

HEAT MATCH-UP SECTION IV - HYDROGEN IODIDE DECOMPOSITION AND HYDROGEN PURIFICATION

Heat Exch Number	Hot Side Temp In Deg K	Temp Out Deg K	Heat Exch Number	Cold Side Temp In Deg K	Temp Out Deg K	Heat Load kJ	Comments
E406E	403	393	E401A1	381.3	393	0.681	
E407B	403	393	E401A2	381.3	393	2.190	
E405B	393	393	E401B	356.4	381.3	8.290	
E407C	393	347.8	E401C	305.5	356.4	9.890	
E407A	421	403	E402A	393	415.2	4.599	
E406D	497.1	403	E402B	393	415.2	7.354	
Sec. V	555	555	E402C	393	415.2	2.159	Thermal energy from Section V, steam
E405A	393	393	E410	373	373	2.434	
E406C	531.8	497.1	E403	424	439	2.597	
Sec. V	875	784	E404A	713	713	6.690	Thermal energy from Sec. V, helium
E406A	713	625.7	E404B1	615.7	615.7	6.778	
Sec. V	875	784	E404B2	615.7	615.7	1.679	Thermal energy from Sec. V, helium
E406B	625.7	531.8	E404C1	521.8	521.8	7.296	
Sec. V	555	555	E404C2	521.8	521.8	7.373	Thermal energy from Sec. V, steam
E407D	347.8	308	Sec. V	303	-	8.700	To Section V Power Bottoming Cycle
E407E	308	303	C. W.	293		1.220	

TABLE C-6
HEAT EXCHANGERS SECTION I - MAIN SOLUTION REACTION

Heat Exch No.	Heat Load kJ	Hot Side In Stream No.	Hot Side In Temp Deg K	Hot Side Out Stream No.	Hot Side Out Temp Deg K	Cold Side In Stream No.	Cold Side In Temp Deg K	Cold Side Out Stream No.	Cold Side Out Temp Deg K	Comments
R101	110.551	113	393	114	393	*	*	*	*	Heat Avail. for Sec. V Power Recovery
E101	18.303	104	368	131	313	*	*	*	*	"
E102	6.873	107	368	108	359.6	*	*	*	*	"
E103	23.933	105A	425	105B	342.3	*	*	*	*	"

* Cold Side in Section V for waste heat recovery.

TABLE C-7
HEAT EXCHANGERS SECTION III - HYDROGEN IODIDE SEPARATION AND PURIFICATION

Heat Exch No.	Heat Load kJ	Hot Side In Stream No.	Hot Side In Temp Deg K	Hot Side Out Stream No.	Hot Side Out Temp Deg K	Cold Side In Stream No.	Cold Side In Temp Deg K	Cold Side Out Stream No.	Cold Side Out Temp Deg K	Comments
E300	521.478	*	*	*	*	305B	393.15	305C	512.00	
E301	359.228	311A	522.90	311B	436.15	*	*	*	*	
E302	13.234	-	510.00	-	410.10	*	*	*	*	
E303	72.412	Sec.V	555.00	Sec.V	555.00	-	523	-	523	Thermal energy from Sec. V, steam
E304	39.685	306A	303.15	306B	303.15	*	*	*	*	
E305	4.456	312A	520.00	312B	393.15	*	*	*	*	
E306A	77.568	319C	466.22	319D	466.22	311C	436.15	-	447.39	
E306B	179.797	314B	460.15	314C	460.15	-	447.39	-	453.15	
E306C	59.177	-	511.15	-	460.15	-	453.15	311D	453.15	TC301 Interstage Cooler
E307A	54.578	319B	481.15	319C	466.22	315A	453.15	-	466.66	
E307B	120.361	316B	478.15	316C	478.15	-	466.66	-	471.15	
E307C	49.826	-	515.15	-	478.15	-	471.15	315B	471.15	TC302 Interstage Cooler
E308A	10.964	319A	484.15	319B	481.15	317A	471.15	-	474.02	
E308B	34.934	-	550.0	-	491.15	-	474.02	-	482.25	TC303 Interstage Cooler
E308C	73.669	318B	491.15	318C	491.15	-	482.25	-	484.25	
E308D	21.197	Sec.V	555.00	Sec.V	555.00	-	484.25	317B	484.25	Thermal energy from Sec. V, steam
E309	115.865	319D	444.99	319E	412.33	*	*	*	*	
E310	35.980	314C	460.15	314D	368.15	*	*	*	*	
E311	29.878	316C	478.15	316D	368.15	*	*	*	*	
E312	21.202	318C	491.15	316D	368.15	*	*	*	*	

* See Heat Match-up Section III for details.

TABLE C-8

HEAT EXCHANGERS SECTION IV - HYDROGEN IODIDE DECOMPOSITION AND HYDROGEN PURIFICATION

Heat Exch No.	Heat Load kJ	Hot Side In Stream No.	Hot Side In Temp Deg K	Hot Side Out Stream No.	Hot Side Out Temp Deg K	Cold Side In Stream No.	Cold Side In Temp Deg K	Cold Side Out Stream No.	Cold Side Out Temp Deg K	Comments
E401	21.051	*	*	*	*	403	305.5	404	393	
E402	14.113	*	*	*	*	405	393	406	415.2	
E403	2.597	*	*	*	*	410	415.2	411	439	
E404A	6.690	*	*	*	*	-	713	-	713	
E404B	8.457	*	*	*	*	-	615.7	-	615.7	
E404C	14.664	*	*	*	*	-	521.8	-	521.8	
E405	10.724	412	393	413	393	*	*	*	*	
E406	24.702	419	713	420	393	*	*	*	*	
E407	26.499	408	424	421	303	*	*	*	*	
E408	1.704	421	303	422	291	*	*	*	*	
E409	0.100	433	323	434	303	C. W.	293			
E410	2.434	*	*	*	*	-	373	-	373	
E411	4.138	-	303	-	303	C. W.	293	-	-	Cooling water on cold side

* See Heat Match-up Section IV for details.

TABLE C- 9

POWER DEVICES SECTION I - MAIN SOLUTION REACTOR

Power Device Number	Energy Load kJ	Inlet Stream Number	Inlet Pres MPa	Outlet Stream Number	Outlet Stream MPa	Comments
P101	0.0019	101A	0.101	-	0.420	
P102	0.0167	-	0.185	-	0.430	
P103	0.2185	153	0.440	154	0.500	
P104	0.0625	-	0.185	110	0.430	
P105	0.2134	141	0.105	142	0.500	
P106	0.1419	151	0.101	-	0.500	
P107	0.0017	134	0.195	135	0.500	
P108	0.5582	145	0.113	146	0.886	
TC101	4.3666	132	0.195	133	0.500	
TE101	-0.8902	111	0.420	121	0.110	Intermediate pressure outlet of TE101
				120	0.101	Low pressure outlet of TE101
TE102	-25.9392	143	0.818	144	0.113	
TE103	-0.2046	132	0.195	133	0.500	

TABLE C-10

POWER DEVICES SECTION III - HYDROGEN IODIDE SEPARATION AND PURIFICATION

Power Device Number	Energy Load kJ	Inlet Stream Number	Inlet Pres MPa	Outlet Stream Number	Outlet Pres MPa	Comments
P301	0.2537	301A	0.110	301B	0.304	
P302	0.0029	300A	0.101	300B	0.304	
P303	0	303A	0.304	303B	0.304	Negligible Power Consumption
P304	0.9942	305A	0.304	305B	0.912	
P305	0.2392	319E	0.101	319F	0.304	
P306	-	307A	0.912	307B	0.912	Negligible Power Consumption
P307	-	-	0.922	-	0.922	Negligible Power Consumption, Recycle Stream
P308	-	-	0.950	-	0.950	Negligible Power Consumption, Recycle Stream
TC301	53.5690	314A	0.101	314B	1.165	
TC302	45.7492	316A	0.101	316B	1.722	
TC303	31.6103	318A	0.101	318B	2.279	
TE301	-0.9044	311B	0.962	311C	0.101	
TE302	-0.0841	314D	1.165	314E	0.185	
TE303	-0.0902	316D	1.772	316E	0.185	
TE304	-0.0759	318D	2.279	318E	0.185	
TE305	-0.1828	313A	0.304	313B	0.185	

TABLE C-11

POWER DEVICES SECTION IV - HI CRACKING

Power Device Number	Energy Load kJ	Inlet Stream Number	Inlet Pres MPa	Outlet Stream Number	Outlet Pres MPa	Comments
P401	0.996	401	0.912	402	8.309	
P402	0.258	417	5.066	418	8.309	
P403	-	414	5.066	415	5.066	Negligible Power Consumption
P404	0.015	431	0.101	429	5.066	
P405	-	437A	8.309	437B	8.309	Negligible Power Consumption
P406	0.004	435A	0.202	435B	8.309	
P407	-	427A	8.309	427B	8.309	Negligible Power Consumption
TE401	-0.482	409	8.309	410	5.066	
TE402	-1.194	426	8.309	428	5.066	

APPENDIX D
DETAILED FLOWSHEETS, INCLUDING MASS AND ENERGY BALANCES, FOR SECTIONS I THROUGH V

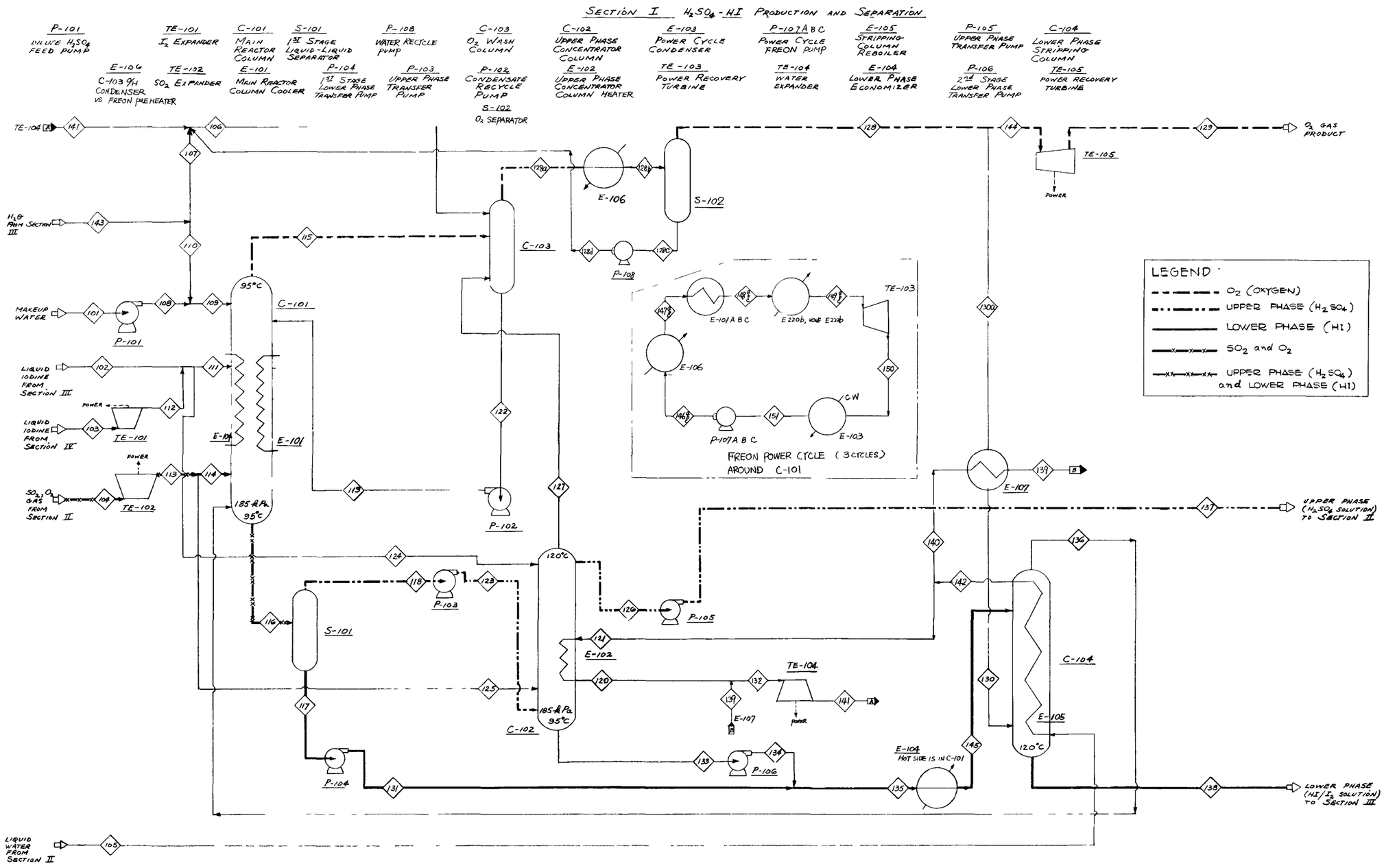

Fig. D-1. Section I - H_2SO_4-HI production and separation; O_2 purification

P-201 Feed Pump
V-212 1st Stage H_2SO_4 Separator
E-202 1st Stage H_2SO_4 Condenser
V-211 2nd Stage H_2SO_4 Separator
E-204 2nd Stage H_2SO_4 Condenser
V-210 3rd Stage H_2SO_4 Separator
E-206 3rd Stage H_2SO_4 Condenser
V-209 4th Stage H_2SO_4 Separator
E-208 4th Stage H_2SO_4 Condenser
V-208 5th Stage H_2SO_4 Separator
E-210 5th Stage H_2SO_4 Condenser
V-207 6th Stage H_2SO_4 Separator
E-212 6th Stage H_2SO_4 Condenser
P-202 Con H_2SO_4 Pump
C-201 First Stage Steam Compressor
E-222 Precooler
C-202 Second Stage Steam Compressor
E-223, 5, 8 After Cooler
E-224 6, 9. Condenser
C-203 Third Stage Steam Compressor
E-227, 230 Sub Cooler
V-214 SO_2 Separator

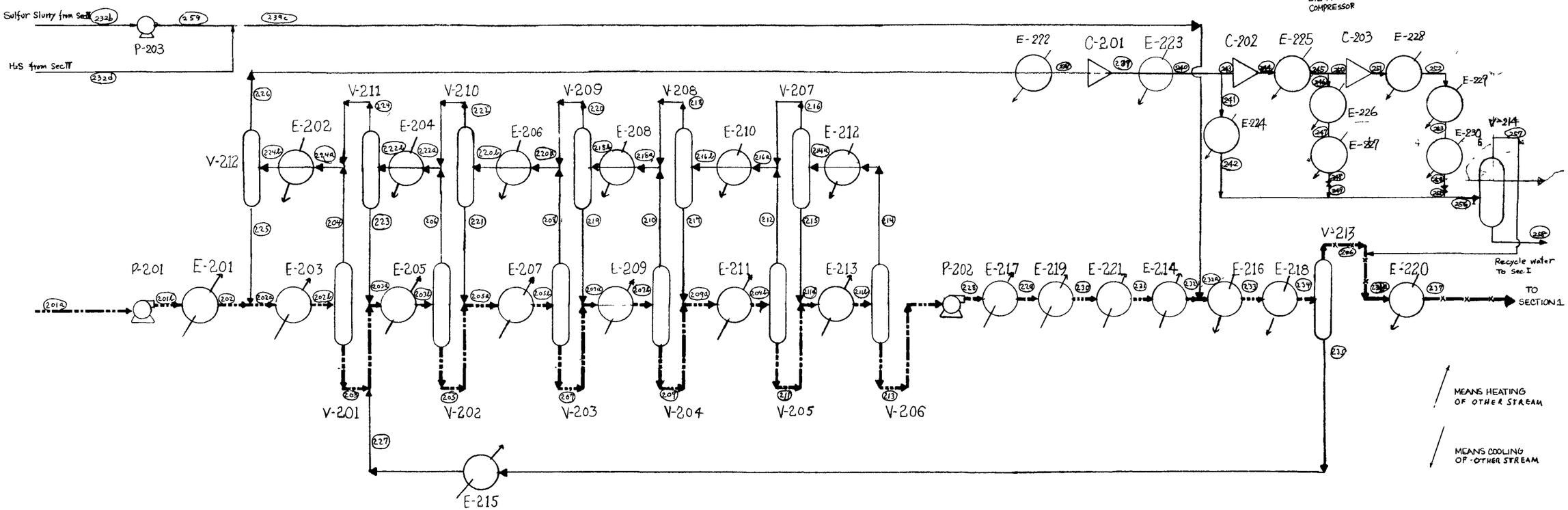

E-201 1st Stage H_2SO_4 Flash Preheater
E-203 1st Stage H_2SO_4 Flash Heater
V-201 1st Stage H_2SO_4 Flash Drum
E-205 2nd Stage H_2SO_4 Flash Heater
V-202 2nd Stage H_2SO_4 Flash Drum
E-207 3rd Stage H_2SO_4 Flash Heater
V-203 3rd Stage H_2SO_4 Flash Drum
E-209 4th Stage H_2SO_4 Flash Heater
V-204 4th Stage H_2SO_4 Flash Drum
E-211 5th Stage H_2SO_4 Flash Heater
V-205 5th Stage H_2SO_4 Flash Drum
E-213 6th Stage H_2SO_4 Flash Heater
V-206 6th Stage H_2SO_4 Flash Drum
E-217 Concentrated H_2SO_4 Preheater
E-221 H_2SO_4 Decomposer
E-216 SO_3 Decomposer Product Cooler
V-213 SO_3 Decomposer Product Separator
P-203 Sulfer Slurry Pump
E-215 Recycle H_2SO_4 Preheater
E-219 Concentrated H_2SO_4 Boiler
E-214 SO_3 Decomposer
E-218 SO_3 Decomposer Product Condenser
E-220 SO_2-O_2 Cooler

LEGEND :
- UPPER PHASE (H_2SO_4)
- SO_2 and O_2 (OXYGEN)

Fig. D-2. Section II - H_2SO_4-H_2O separation and H_2SO_4 decomposition

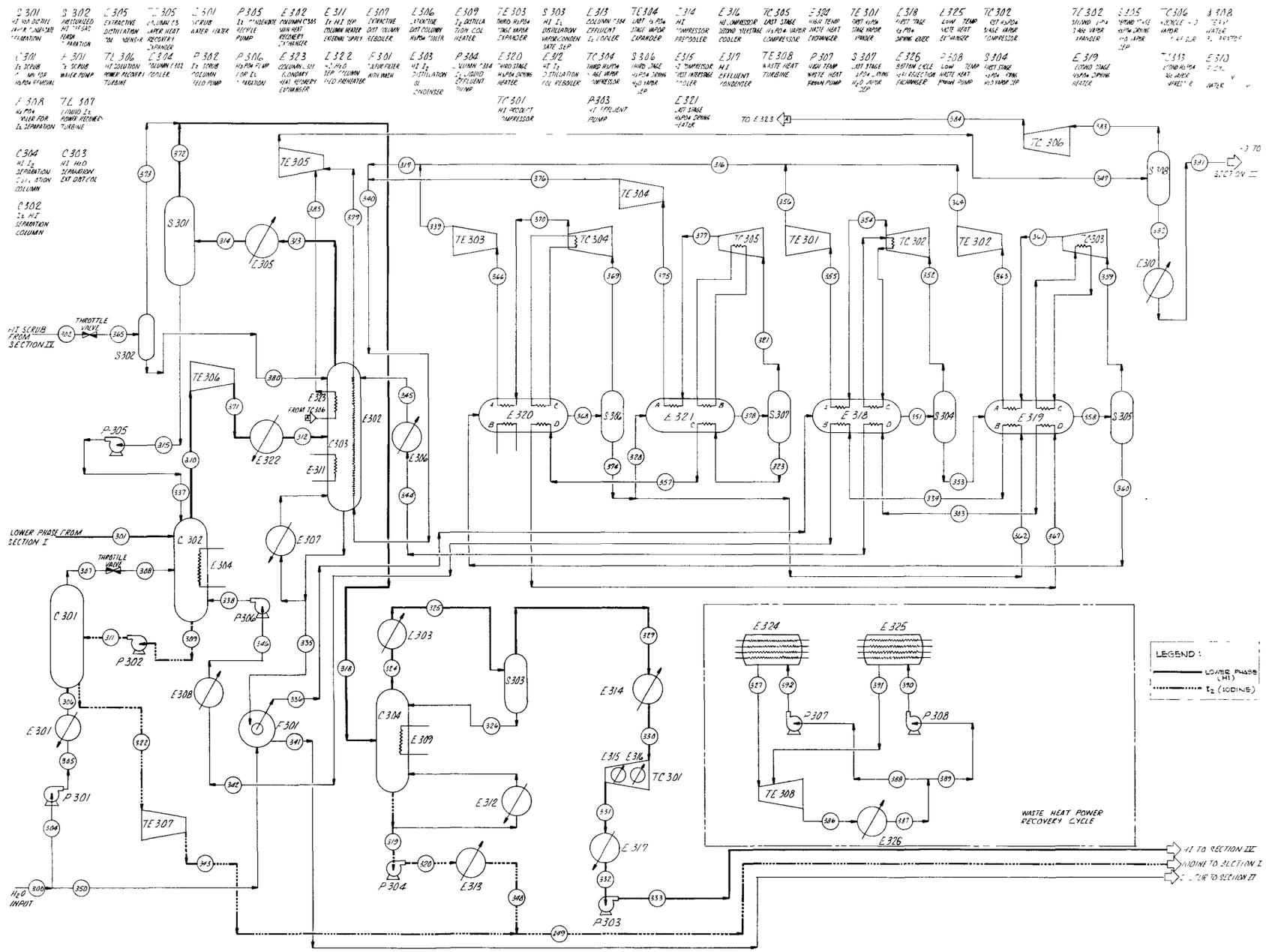

Fig. D-3. Section III - HI separation

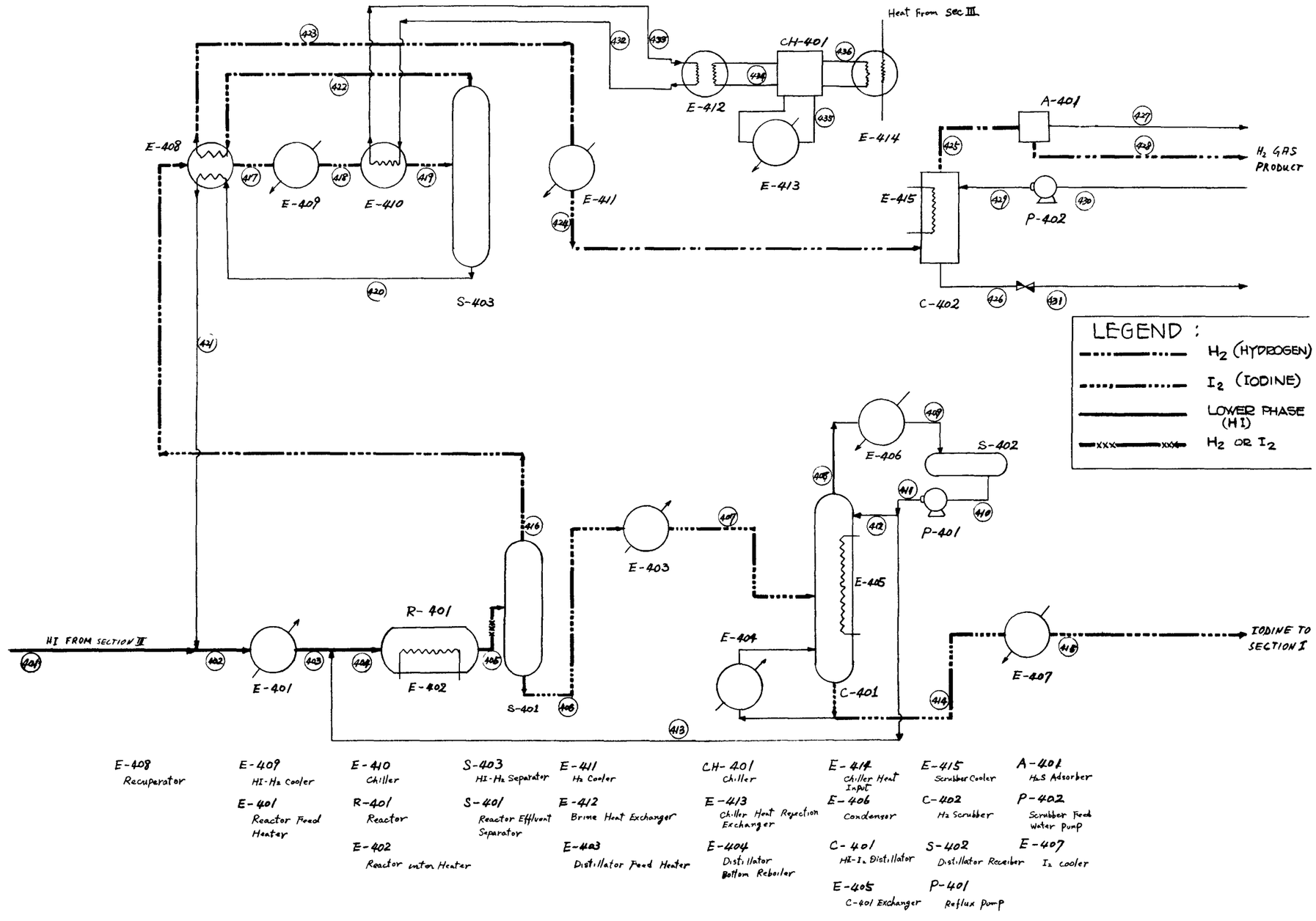

Fig. D-4. Section IV - HI decomposition

TE-500
PRIMARY HE EXPANDER

TC-500
PRIMARY HE COMPRESSOR

TE- 505
SECOND STEAM CYCLE FIRST EXPANDER

E-500
HIGH TEMP SECONDARY HE HEAT EXCHANGER

E-501
LOW TEMP SECONDARY HE HEAT EXCHANGER

TE-506
SECOND STEAM CYCLE SECOND EXPANDER

E-502
INTERMEDIATE TEMP SEC HE HEAT EXCHANGER

P-500
FIRST STEAM CYCLE CONDENSATE PUMP

TE-509
SECOND STEAM CYCLE THIRD EXPANDER

TE 501
INTERMEDIATE TEMP SEC HE 1ST EXPANDER

E-504
FIRST STEAM CYCLE SEC HE TO H_2O HEAT EXCHANGER

TE-508
SECOND STEAM CYCLE FOURTH EXPANDER

E-505
FIRST STEAM CYCLE BOILER FEEDWATER HEAT EXCHANGER

E-506
FIRST STEAM CYCLE CONDENSER

E-507
SECOND STEAM CYCLE CONDENSER

TE 502
INTERMEDIATE TEMP SEC HE EXPANDER

TE 503
FIRST STEAM CYCLE FIRST EXPANDER

TE 504
FIRST STEAM CYCLE SECOND EXPANDER

E-503
HIGH TEMP PROCESS HEAT EXCHANGER

E 508
INTERMEDIATE TEMP PROCESS HEAT EXCHANGER

TC 501
FIRST STEAM CYCLE FIRST RECOMPRESSOR

TC-502
FIRST STEAM CYCLE SECOND RECOMPRESSOR

E 510
SECOND STEAM CYCLE HIGH TEMP SEC HE HEAT EXCHANGER

E 511
SECOND STEAM CYCLE BOILER FEEDWATER HEAT EXCHANGER

P-501
SECOND STEAM CYCLE FOURTH LOOP BOILER FEEDWATER PUMP

P-502
SECOND STEAM CYCLE THIRD LOOP BOILER FEEDWATER PUMP

P-503
SECOND STEAM CYCLE SECOND LOOP BOILER FEEDWATER PUMP

TC 503
INTERMEDIATE TEMP SECONDARY HE RECOMPRESSOR

TE-509
INTERMEDIATE TEMP SECONDARY HE 5 CWD EXPANDER

P-504
SECOND STEAM CYCLE FIRST LOOP BOILER FEEDWATER PUMP

E 509
LOW TEMP PROCESS HEAT EXCHANGER

TC 504
INTERMEDIATE TEMP SECONDARY HE FIRST RECOMPRESSOR

TC-505
INTERMEDIATE TEMP SECONDARY HE FIRST RECOMPRESSOR

TC-506
INTERMEDIATE TEMP SECONDARY HE THIRD RECOMPRESSOR

TC-50A
INTERMEDIATE TEMP SECONDARY HE FOURTH RECOMPRESSOR

TE 510
AUXILIARY POWER LOOP EXPANDER

E-513
AUXILIARY POWER LOOP CONDENSER

P-505
AUXILIARY POWER LOOP PUMP

E 512
SECONDARY HE WASTE HEAT TO STEAM CYCLE HEAT EXCHANGER

E-514
AUXILIARY POWER BOILER FEEDWATER HEAT EXCHANGER

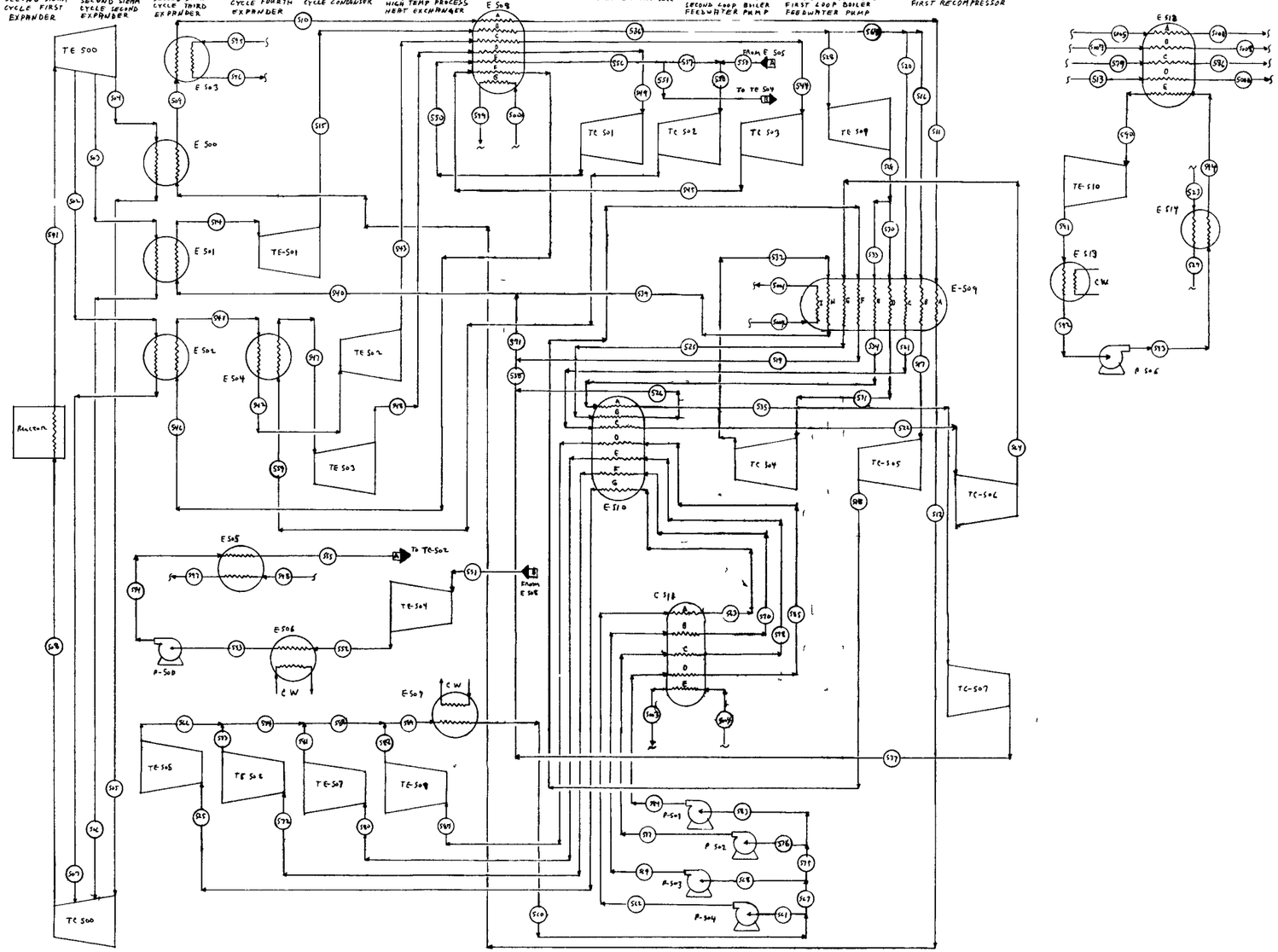

Fig. D-5. Section V - power generation and heat transfer

TABLE D-1

ENERGY BALANCE

kJ/0.993 mole H_2	Section I	Section II	Section III	Section IV	Process Sections Subtotal	Section V *	Overall Total
Gross Power Load	0.50	31.32	126.53	0.01	158.79	239.27	-
Power Recovery	23.53	0	22.90	0	46.43	351.97	-
Net External Power Demand	-23.03	31.32	104.06	0.01	112.36	112.70	-
Gross Heat Load	191.24	792.47	1087.18	98.26	2169.15	558.29	608.47
Heat Recovery	186.19	512.74	944.20	77.39	1720.52	33.70	-
Heat from Other Sections	5.05	0	151.43	8.45	164.93	0	-
Net External Heat Demand	0	421.29	0	27.34	448.63	495.54	608.47
Net External Energy Demand	-23.03	452.61	104.06	27.35	560.99	608.47	608.61
Heat to Other Sections	0	141.56	8.45	14.92	164.93	461.05	285.63
Reject Heat	116.18	0	140.86	18.18	275.22	81.89	322.98
Enthalpy Δ	-134.16	311.05	106.18	2.70	285.77	608.47	608.47

* The redesign of Section V needs to be completed since Section I has recently been modified. The given values in this table will change only slightly and the effect on the overall process efficiency will be insignificant.

Thermal efficiency $= \left[\Delta H - \left(\frac{\Delta H}{\Delta G}\right) W\right] / Q = [285.77 - 1.2 \times 0]/608.47 = 0.47\ (47\%)$

TABLE D-2

SECTION I
MAIN SOLUTION REACTION
MATERIAL BALANCE

Basis: 0.993 Mole H_2

Stream Number	Component Molar Flow Ratios							Total Flow Ratios		Phase	Pressure $Pa \times 10^5$	Temp °K	Comments
	H_2SO_4	HI	I_2	H_2O	SO_2	O_2	R-11	Mole	Weight				
101	0	0	0	0.84806	0	0	0	0.84806	7.6321	ℓ	1.01	298	H_2O input from environment
102	0	0.01000	7.75966	0.13180	0	0	0	7.90146	985.75	ℓ	1.85	393	I_2 from Section III
103	0	0	0.99400	0.00200	0	0	0	0.99600	126.06	ℓ	50.66	393	I_2 from Section IV
104	0	0	0	0.38953	1.00515	0.49650	0	1.89118	43.607	g	2.00	368	SO_2, O_2 from Section II
105	0	0	0	4.71137	0	0	0	4.71137	42.400	ℓ	5.02	425	
106	0	0	0	7.69382	0	0	0	7.69382	69.241	ℓ	1.85	370	
107	T	0	0	2.49854	0	0	0	2.49854	22.486	ℓ	1.85	368	
108	0	0	0	0.84806	0	0	0	0.84806	7.6321	ℓ	1.85	298	
109	0	0	0	8.99232	0	0	0	8.99232	80.926	ℓ	1.85	361	
110	T	0	0	8.14426	0	0	0	8.14426	73.294	ℓ	1.85	368	
111	0	0.00923	8.11102	0.12399	0	0	0	8.24424	1030.2	ℓ	1.85	393	
112	0	0	0.99400	0.00200	0	0	0	0.99600	126.06	ℓ	1.85	393	
113	0	0	0	0.38953	1.00515	0.49650	0	1.89118	43.607	g	1.85	362	
114	0	0	0	0.34496	0.89139	0.44100	0	1.67735	38.678	g	1.85	362	
115	0	0	0.02455	0.40816	0	0.46717	0	0.89988	14.254	g	1.85-	368	
116	0.92899	1.86924	7.19908	14.89721	0.21605	0	0	25.11057	1218.8	ℓ	1.85	368	
117	0.00186	1.86924	7.11908	9.89430	0.20118	0	0	19.16566	1127.9	ℓ	1.85-	368	
118	0.92713	0	0	5.00291	0.01487	0	0	5.94491	90.921	ℓ	1.85-	368	
119	0.03773	0.07546	0	7.57446	0	0	0	7.68765	74.837	ℓ	1.85+	379.5	
120	0	0	0	3.40455	0	0	0	3.40455	30.639	ℓ	5.02	377.5	
121	0	0	0	3.40455	0	0	0	3.40455	30.639	ℓ	5.02	400	
122	0.03773	0.07546	0	7.57446	0	0	0	7.68765	74.837	ℓ	1.85	379.5	
123	0.92713	0	0	5.00291	0.01487	0	0	5.94491	90.921	ℓ	1.85+	368	
124	0	0.00073	0.64265	0.00983	0	0	0	0.65321	81.623	ℓ	1.85	393	
125	0	0	0	0.04457	0.11376	0.05629	0	0.21462	4.9412	g	1.85	362	
126	0.99900	0	0	4.09350	0.00375	0	0	5.09625	85.902	ℓ	1.85-	393	
127	0	0	0.01318	0.05360	0.03773	0.05629	0	0.16080	4.2607	g	1.85-	393	
128	0	0	0	0.02175	0	0.52267	0	0.54442	8.5506	g	1.85-	313	
128a	0	0	0	0.50566	0	0.52267	0	1.02833	12.906	g	1.85	370	
128b	0	0	0	0.50566	0	0.52267	0	1.02833	12.906	g+ℓ	1.85	313	
128c	0	0	0	0.48391	0	0	0	0.48391	4.3550	ℓ	1.85-	313	
128d	0	0	0	0.48391	0	0	0	0.48391	4.3550	ℓ	1.85+	313	
129	0	0	0	0.02066	0	0.49650	0	0.51716	8.1224	g+ℓ	1.01	290.7-	O_2 output-H_2O vapor 0.01000
130	0	0	0	0.00109	0	0.02617	0	0.02726	0.42813	g	1.85-	378	H_2O liquid 0.01066

TABLE D-2

SECTION I
MAIN SOLUTION REACTION
MATERIAL BALANCE
(Continued)

Stream Number	Component Molar Flow Ratios							Total Flow Ratios		Phase	Pressure Pa×10^5	Temp °K	Comments
	H_2SO_4	HI	I_2	H_2O	SO_2	O_2	R-11	Mole	Weight				
130a	0	0	0	0.00109	0	0.02617	0	0.02726	0.42813	g	1.85	313	
131	0.00186	1.86924	7.19908	9.89430	0.20118	0	0	19.16566	1127.9	g	1.85+	368	
132	0	0	0	4.71137	0	0	0	4.71137	42.400	ℓ	5.02	377.5	
133	0.00014	0.14476	0.55746	0.76618	0.01514	0	0	1.48368	87.323	ℓ	1.85-	368	
134	0.00014	0.14476	0.55746	0.76618	0.01514	0	0	1.48368	87.323	ℓ	1.85+	368	
135	0.00200	2.01400	7.75654	10.66048	0.21632	0	0	20.64934	1215.2	ℓ	1.85+	368	
136	0	0.00200	0.00388	0.05217	0.21592	0.02617	0	0.30014	8.4170	g	1.85	393	
137	0.99900	0	0	4.0935	0.00375	0	0	5.09625	85.902	ℓ	1.85+	393	Upper phase to Section II
138	0.00200	2.01200	7.75266	10.60940	0.00040	0	0	20.37646	1207.2	ℓ	1.85	393	Lower phase to Section III
139	0	0	0	1.30682	0	0	0	1.30682	11.761	ℓ	5.02	377.5	
140	0	0	0	1.30682	0	0	0	1.30682	11.761	ℓ	5.02	400	
141	0	0	0	4.71137	0	0	0	4.71137	42.400	ℓ	1.85	377.5	
142	0	0	0	4.71137	0	0	0	4.71137	42.400	ℓ	5.02	400	
143	0	0	0	10.64280	0	0	0	10.64280	95.780	ℓ	1.85	368	H_2O from Section III
144	0	0	0	0.02066	0	0.49650	0	0.51716	8.1224	g	1.85-	313	
145	0.00200	2.01400	7.75654	10.66048	0.21632	0	0	20.64934	1215.2	ℓ	1.85	390.8	
146a	0	0	0	0	0	0	1.36462	1.36462	93.648	ℓ	7.00	300	R-11 MW=137.38 (c cl_3F)
146b	0	0	0	0	0	0	1.28574	1.28574	88.234	ℓ	8.80	300	
146c	0	0	0	0	0	0	2.05860	2.05860	141.27	ℓ	10.60	300	
147a	0	0	0	0	0	0	1.36462	1.36462	93.648	ℓ	7.00	340.1	R-11
147b	0	0	0	0	0	0	1.28574	1.28574	88.234	ℓ	8.80	340.1	Power cycle
147c	0	0	0	0	0	0	2.05860	2.05860	141.27	ℓ	10.60	340.1	
148a	0	0	0	0	0	0	1.36462	1.36462	93.648	g+ℓ	6.42	363.1	
148b	0	0	0	0	0	0	1.28574	1.28574	88.234	g	8.18	373.1	
148c	0	0	0	0	0	0	2.05860	2.05860	141.27	g+ℓ	10.12	383.1	
149a	0	0	0	0	0	0	1.36462	1.36462	93.648	g	6.39	363.1	
149b	0	0	0	0	0	0	1.28574	1.28574	88.234	g	8.18	373.1	
149c	0	0	0	0	0	0	2.05860	2.05860	141.27	g	10.08	383.1	
150	0	0	0	0	0	0	4.70896	4.70896	323.15	g	1.13	300	
151	0	0	0	0	0	0	4.70896	4.70896	323.15	ℓ	1.13	300	

TABLE D-3
SECTION I
MAIN SOLUTION REACTION
HEAT LOADS

Heat Exch. Number	Energy Load, kJ	Hot-Side In		Hot-Side Out		Cold-Side In		Cold-Side Out		Comments
		Stream Number	Stream Temp.,°K	Stream Number	Stream Temp.°K	Stream Number	Stream Temp.°K	Stream Number	Stream Temp.°K	
E-101A	29.409	-	379	-	368	147a	340.1	148a	363.1	Hot side is in C-101
B	31.231	-	389	-	368	147b	340.1	148b	373.1	Hot side is in C-101
C	49.010	-	398	-	368	147c	340.1	148c	383.1	Hot side is in C-101
E-102	5.880	121	400	120	377.5	-	368	-	393	Cold side is in C-102
E-103	116.178	150	300	151	300	C.W.	-	-	-	
E-104	36.403	-	398	-	383	135	368	145	390.8	Hot side is in C-101
E-105	9.103	105	425	142	400	-	390.8	-	393	Cold side is in C-104
E-106	22.903	128a	370	128b	313	146 a,b,c	300	147 a,b,c	340.1	
E-107	2.257	140	400	139	377.5	130a	313	130	378	
E-220b	2.974	-	410	-	368	148a	363.1	149a	363.1	
E-222b	2.071	-	405	-	393	148c	383.1	149c	383.1	

TABLE D-4

SECTION I

MAIN SOLUTION REACTION
POWER LOADS

Power Device Number	Energy Load kJ	Input Stream No.	Input Stream Pressure, Pax10^5	Output Stream No.	Output Stream Pressure, Pa x 10^5	Comments
P-101	0.001	101	1.01	108	1.85	
P-102	negligible	122	1.85$^-$	119	1.85+	
P-103	negligible	118	1.85$^-$	123	1.85+	
P-104	negligible	117	1.85$^-$	131	1.85+	
P-105	negligible	126	1.85$^-$	137	1.85+	
P-106	negligible	133	1.85$^-$	134	1.85+	
P-107A	0.108	151	1.13	146a	7.00	
107B	0.127	151	1.13	146b	8.80	
107C	0.262	151	1.13	146C	10.60	
P-108	negligible	128c	1.85$^-$	128d	1.85+	
TE-101	0.287	103	50.66	112	1.85	
TE-102	0.497	104	2.00	113	1.85	
TE-103	21.916	149a,b,c	6.39,8.18,10.08	150	1.13	
TE-104	0.023	132	5.02	141	1.85	
TE-105	0.809	144	1.85$^-$	129	1.01	

TABLE D-5

SECTION II
H_2SO_4 CONCENTRATION AND DECOMPOSITION
MATERIAL BALANCE

Basis: .0993 mole H_2 Product

Stream No.	Component Molar Flow Ratios							Total Flow Ratio		Phase	Pressure $Pa \times 10^5$	Temp. °K	Comments
	H_2SO_4	SO_3	SO_2	H_2O	O_2	S	H_2S	Mole	Weight				
201a	0.9990	0	0.0038	4.0935	0	0	0	5.0963	85.194	ℓ	1.85	393	
201b	0.9990	0	0.0038	4.0935	0	0	0	5.0963	85.194	ℓ	2.00	393	
202	0.9990	0	0.0038	4.0935	0	0	0	5.0963	85.194	ℓ	2.00	425	
202a	0.9999	0	0.0038	4.0973	0	0	0	5.1010	85.992	ℓ	2.00	425	
202b	0.9999	0	0.0038	4.0973	0	0	0	5.1010	85.992	ℓ+g	2.00	470	
203	0.9995	0	0	2.1161	0	0	0	3.1156	68.017	ℓ	2.00	470	
203a	1.3688	0	0	2.9024	0	0	0	4.2712	93.189	ℓ	2.00	470	
203b	1.3688	0	0	2.9024	0	0	0	4.2712	93.189	ℓ+g	2.00	502	
204	0.0004	0	0.0038	1.9812	0	0	0	1.9854	17.975	g	2.00	470	
205	1.3660	0	0	1.8608	0	0	0	3.2268	83.676	ℓ	2.00	502	
205a	1.3983	0	0	1.9048	0	0	0	3.3031	85.654	ℓ	2.00	502	
205b	1.3982	0.0001	0	1.9049	0	0	0	3.3032	85.654	ℓ+g	2.00	536	
206	0.0028	0	0	1.0416	0	0	0	1.0444	9.513	g	2.00	502	
207	1.3838	0	0	1.2263	0	0	0	2.6101	78.836	ℓ	2.00	536	
207a	1.4704	0	0	1.3031	0	0	0	2.7735	83.770	ℓ	2.00	536	
207b	1.4683	0.0021	0	1.3052	0	0	0	2.7756	83.770	ℓ+g	2.00	573	
208	0.0144	0.0001	0	0.6786	0	0	0	0.6931	6.818	g	2.00	536	
209	1.4157	0	0	0.7294	0	0	0	2.1451	75.926	ℓ	2.00	573	
209a	1.6362	0	0	0.8430	0	0	0	2.4792	87.752	ℓ	2.00	573	
209b	1.6019	0.0343	0	0.8773	0	0	0	2.4792	86.380	ℓ+g	2.00	613	
210	0.0526	0.0021	0	0.5758	0	0	0	0.6305	7.844	g	2.00	573	
211	1.4193	0	0	0.3009	0	0	0	1.7202	72.245	ℓ	2.00	613	
211a	1.6561	0	0	0.3510	0	0	0	2.0071	84.298	ℓ	2.00	613	
211b	1.5578	0.0983	0	0.4493	0	0	0	2.1054	84.298	ℓ+g	2.00	634	
212	0.1826	0.0343	0	0.5764	0	0	0	0.7933	15.506	g	2.00	613	
213	1.3610	0	0	0.1547	0	0	0	1.5157	68.073	ℓ	2.00	634	
214	0.1968	0.0983	0	0.2946	0	0	0	0.5897	16.225	g	2.00	634	
214a	0.2859	0.0092	0	0.2055	0	0	0	0.5006	16.225	ℓ+g	2.00	613	
215	0.2368	0	0	0.0501	0	0	0	0.2869	12.053	ℓ	2.00	613	
216	0.0491	0.0092	0	0.1554	0	0	0	0.2137	4.173	g	2.00	613	
216a	0.2317	0.0435	0	0.7318	0	0	0	1.0070	19.679	g	2.00	613	
216b	0.2731	0.0021	0	0.6904	0	0	0	0.9656	19.679	ℓ+g	2.00	573	
217	0.2205	0	0	0.1136	0	0	0	0.3341	11.826	ℓ	2.00	573	
218	0.0526	0.0021	0	0.5768	0	0	0	0.6315	7.853	g	2.00	573	
218a	0.1052	0.0042	0	1.1526	0	0	0	1.2620	15.697	g	2.00	573	
218b	0.1092	0.0002	0	1.1486	0	0	0	1.2580	15.697	ℓ+g	2.00	536	

TABLE D-5

SECTION II
H_2SO_4 CONCENTRATION AND DECOMPOSITION
MATERIAL BALANCE
(CONTINUED)

Stream No.	Component Molar Flow Ratios							Total Flow Ratio		Phase	Pressure $Pa \times 10^5$	Temp. °K	Comments
	H_2SO_4	SO_3	SO_2	H_2O	O_2	S	H_2S	Mole	Weight				
219	0.0866	0	0	0.0768	0	0	0	0.1634	4.934	ℓ	2.00	536	
220	0.0226	0.0002	0	1.0718	0	0	0	1.0946	10.763	g	2.00	536	
220a	0.0370	0.0003	0	1.7504	0	0	0	1.7877	17.581	g	2.00	536	
220b	0.0372	0.0001	0	1.7502	0	0	0	1.7875	17.581	ℓ+g	2.00	502	
221	0.0323	0	0	0.0440	0	0	0	0.0763	1.979	ℓ	2.00	502	
222	0.0049	0.0001	0	1.7042	0	0	0	1.7092	15.584	g	2.00	502	
222a	0.0077	0.0001	0	2.7478	0	0	0	2.7556	25.116	g	2.00	502	
222b	0.0078	0	0	2.7477	0	0	0	2.7555	25.116	ℓ+g	2.00	470	
223	0.0073	0	0	0.0137	0	0	0	0.0210	0.481	ℓ	2.00	470	
224	0.0005	0	0	2.7340	0	0	0	2.7345	24.635	g	2.00	470	
224a	0.0009	0	0.0038	4.7152	0	0	0	4.7199	42.610	g	2.00	470	
224b	0.0009	0	0.0038	4.7152	0	0	0	4.7199	42.610	ℓ+g	2.00	425	
225	0.0009	0	0	0.0038	0	0	0	0.0047	0.078	ℓ	2.00	425	
226	0	0	0.0038	4.7114	0	0	0	4.7152	42.531	g	2.00	425	
227	0.3620	0	0	0.7726	0	0	0	1.1346	24.690	ℓ	2.00	470	
228	1.3610	0	0	0.1547	0	0	0	1.5157	68.073	ℓ	8.60	635	
229	1.3610	0	0	0.1547	0	0	0	1.5157	68.073	ℓ	8.60	686	
230	0.8269	0.5341	0	0.6888	0	0	0	2.0498	68.073	g	8.60	686	
231	0.1966	1.1644	0	1.3191	0	0	0	2.6801	68.073	g	7.80	800	
232	0.0005	0.3615	0.9990	1.5152	0.4995	0	0	3.3757	68.073	g	5.20	1144	
232a	0.0005	0.3615	1.0014	1.5236	0.4965	0	0	3.3835	68.183	g	5.20	1144	
232b	0	0	0	0.0072	0	0.0012	0	0.0084	0.084	ℓ+s	1.013	303	Slurry pump.
232c	0	0	0	0.0072	0	0.0012	0	0.0084	0.084	ℓ+s	5.2	303	
232d	0	0	0	0	0	0	0.0012	0.0012	0.020	g	5.2	400	
233	0.3484	0.0136	1.0014	1.1757	0.4965	0	0	3.0356	68.183	g	2.40	579	
234	0.3620	0	1.0014	1.1621	0.4965	0	0	3.0220	68.183	ℓ+g	2.00	418	
235	0.3620	0	0	0.7726	0	0	0	1.1346	24.690	ℓ	2.00	418	
236	0	0	1.0014	0.3895	0.4965	0	0	1.8874	43.492	g	2.00	418	
236a	0	0	1.0052	0.3895	0.4965	0	0	1.8912	43.614	g	2.00	418	
237	0	0	1.0052	0.3895	0.4965	0	0	1.8912	43.614	g	2.00	368	
238	0	0	0.0038	4.7114	0	0	0	4.7152	42.531	g	2.00	425	
239	0	0	0.0038	4.7114	0	0	0	4.7152	42.531	g	5.02	499	
240	0	0	0.0038	4.7114	0	0	0	4.7152	42.531	g	5.02	425	
241	0	0	0.0011	1.3163	0	0	0	1.3174	11.884	g	5.02	425	
242	0	0	0.0011	1.3163	0	0	0	1.3174	11.884	ℓ	5.02	425	
243	0	0	0.0027	3.3951	0	0	0	3.3978	30.648	g	5.02	425	

TABLE D-5

SECTION II
H_2SO_4 CONCENTRATION AND DECOMPOSITION
MATERIAL BALANCE
(Continued)

Stream No.	Component Molar Flow Ratios							Total Flow Ratio		Phase	Pressure $Pa \times 10^5$	Temp. °K	Comments
	H_2SO_4	SO_3	SO_2	H_2O	O_2	S_2	H_2S	Mole	Weight				
244	0	0	0.0027	3.3951	0	0	0	3.3978	30.648	g	9.35	496	
245	0	0	0.0027	3.3951	0	0	0	3.3978	30.648	g	9.35	450	
246	0	0	0.0012	1.4459	0	0	0	1.4471	13.054	g	9.35	450	
247	0	0	0.0012	1.4459	0	0	0	1.4471	13.054	ℓ	9.35	450	
248	0	0	0.0012	1.4459	0	0	0	1.4471	13.054	ℓ	9.35	425	
249	0	0	0.0012	1.4459	0	0	0	1.4471	13.054	ℓ	5.02	425	
250	0	0	0.0015	1.9492	0	0	0	1.9507	17.594	g	9.35	450	
251	0	0	0.0015	1.9492	0	0	0	1.9507	17.594	g	17.95	533	
252	0	0	0.0015	1.9492	0	0	0	1.9507	17.594	g	17.95	480	
253	0	0	0.0015	1.9492	0	0	0	1.9507	17.594	ℓ	17.95	480	
254	0	0	0.0015	1.9492	0	0	0	1.9507	17.594	ℓ	17.95	425	
255	0	0	0.0015	1.9492	0	0	0	1.9507	17.594	ℓ	5.02	425	
256	0	0	0.0038	4.7114	0	0	0	4.7152	42.531	ℓ	5.02	425	
257	0	0	0.0038	0	0	0	0	0.0038	0.121	g	5.02	425	
258	0	0	T	4.7114	0	0	0	4.7114	42.409	ℓ	4.90	425	

TABLE D-6

SECTION II

H_2SO_4 CONCENTRATION AND DECOMPOSITION

HEAT AND POWER LOADS

Heat Exch. Number	Energy Load, kJ	Hot-Side Input		Hot-Side Output		Cold-Side Input		Cold-Side Output		Comments
		Stream Number	Stream Temp, °K	Stream Number	Stream Temp, °K	Stream Number	Stream Temp, °K	Stream Number	Stream Temp, °K	
E-201	15.113	(a)	(a)	(a)	(a)	201b	393	202	425	
E-202	3.854	224a	470	224b	425	(a)	(a)	(a)	(a)	
E-203	103.162	(a)	(a)	(a)	(a)	202a	425	202b	470	
E-204	4.632	222a	502	222b	470	(a)	(a)	(a)	(a)	
E-205	63.546	(a)	(a)	(a)	(a)	203a	470	203b	502	
E-206	6.979	220a	536	220b	502	(a)	(a)	(a)	(a)	
E-207	49.390	(a)	(a)	(a)	(a)	205a	502	205b	536	
E-208	12.303	218a	573	218b	536	(a)	(a)	(a)	(a)	
E-209	48.984	(a)	(a)	(a)	(a)	207a	536	207b	573	
E-210	26.195	216a	613	216b	573	(a)	(a)	(a)	(a)	
E-211	61.130	(a)	(a)	(a)	(a)	209a	573	209b	613	
E-212	26.113	214a	634	214b	613	(a)	(a)	(a)	(a)	
E-213	44.058	(a)	(a)	(a)	(a)	211a	613	211b	614	
E-214	172.119	(a)	(a)	(a)	(a)	231	800	232	1144	
E-215	6.120	(a)	(a)	(a)	(a)	235	418	227	470	
E-216	123.561	232	1144	233	579	(a)	(a)	(a)	(a)	
E-217	13.531	(a)	(a)	(a)	(a)	228	635	229	686	
E-218	93.326	233	579	234	418	(a)	(a)	(a)	(a)	
E-219	132.401	(a)	(a)	(a)	(a)	229	686	230	686	
E-220	3.591	236	418	237	368	(a)	(a)	(a)	(a)	
E-221	81.540	(a)	(a)	(a)	(a)	230	686	231	800	
E-222	5.518	226	425	238	393	(b)	(b)	(b)	(b)	Heat generated by compression of steam.
E-223	13.805	239	499	240	425	(b)	(b)	(b)	(b)	
E-224	50.001	241	425	242	425	(b)	(b)	(b)	(b)	
E-225	6.653	244	496	245	450	(b)	(b)	(b)	(b)	
E-226	52.775	246	450	247	450	(b)	(b)	(b)	(b)	
E-227	2.843	247	450	248	425	(b)	(b)	(b)	(b)	
E-228	4.849	251	533	252	480	(b)	(b)	(b)	(b)	
E-229	67.193	252	480	253	480	(b)	(b)	(b)	(b)	
E-230	8.544	253	480	254	425	(b)	(b)	(b)	(b)	

(a): See Table - 4 for first heat load match up

(b): See Table - 5 for heat load match up (utilization of heat generated by compression of steam)

TABLE D-6

SECTION II
H_2SO_4 CONCENTRATION AND DECOMPOSITION
HEAT AND POWER LOADS
(Continued)

Power Device	Energy Load kJ	Input Stream Number	Input Stream Pressure, Pax 10^5	Output Stream Number	Output Stream Pressure, Pax 10^5	Comments
P-201	0.003	201a	1.85	201b	2.00	
P-202	0.067	213	2.00	228	8.60	
P-203	Negligible	232b	1.013	232c	5.20	Slurry pump.
C-201	17.362	238	2.00	239	5.02	
C-202	8.280	243	5.02	244	9.35	
C-203	5.608	250	9.35	251	17.95	

TABLE D-7

SECTION II
H_2SO_4 CONCENTRATION AND DECOMPOSITION
HEAT LOAD MATCHUP

BASIS: 0.993 mole H_2 Product

Hot - Side			Cold - Side			Heat Load	Comments
Heat Exch. Number	Input Temp. °K	Output Temp. °K	Heat Exch. Number	Input Temp. °K	Output Temp. °K	k_J	
(a)	(a)	(a)	E214a	1130	1144	7.005	
E-216a	1144	810	E214b1	800	1130	73.043	E214 load total 172.119
(a)	(a)	(a)	E214b2	800	1130	92.071	
E-216b	810	706.9	E221A	686	800	22.553	E221 load total 81.540
(a)	(a)	(a)	E221B	686	800	58.987	
(a)	(a)	(a)	E219	686	686	132.401	
E-216C	706.9	645	E217	635	686	13.531	
E-216d	645	628	E213A	613	634	3.718	E213 load total 44.058
(a)	(a)	(a)	E213B	613	634	40.340	
E-216e	628	579	E211A	573	613	10.716	
E-212	634	613	E211B	573	613	26.113	E211 load total 61.130
(a)	(a)	(a)	E211C	573	613	24.301	
E-210	613	573	E209A	536	573	26.195	
E-218a	579	546	E209B	536	573	19.129	E209 load total 48.984
(a)	(a)	(a)	E209C	536	573	3.660	
E-208	573	536	E207A	502	536	12.303	
E-218b	546	512	E207B	502	536	19.709	E207 load total 49.390
(a)	(a)	(a)	E207C	502	536	17.378	
(a)	(a)	(a)	E205a	497	502	9.929	
E-206	536	502	E205b	493.49	497	6.979	
E-218C	512	495	E205C	488.5	493.49	9.854	E205 load total 63.546
E-218d	495	480	E205d1	470	488.5	8.695	
(a)	(a)	(a)	E205d2	473.6	488.5	22.584	
(b)	(b)	(b)	E205e	470	473.6	5.505	
E-204a	502	485.7	E203A	425	470	2.366	
E-218e	480	435	E203B	425	470	26.085	E203 load total 103.162
(b)	(b)	(b)	E203C	425	470	63.455	
(a)	(a)	(a)	E203D	425	470	11.256	
E-218f	435	418	E201a	404.1	425	9.854	
E-220a	418	410	E201b	402.8	404.1	0.617	E201 load total 15.113
(b)	(b)	(b)	E201c	393	402.8	4.642	
E-204b	485.7	470	E215a	450.7	470	2.266	E215 load total 6.120
E-202	470	425	E215b	418	450.7	3.854	
E-220b	410	368	-	-	-	2.974	~~Cold side is in power cycle~~ of Section I

(a): Heat supplied from Section V (Helium Section)
(b): See Table - 5 for heat load match up (Heat generated by steam compression)

TABLE D-7

SECTION II
H_2SO_4 CONCENTRATION AND DECOMPOSITION
HEAT LOAD MATCHUP
(Continued)

Hot - Side			Cold - Side				
Heat Exch. Number	Input Temp. °K	Output Temp. °K	Heat Exch. Number	Input Temp. °K	Output Temp. °K	Heat Load k_J	Comments
E-228	533	480	E205e1	470.4	473.6	4.849	
E-225a	496	491.5	E205e2	470	470.4	0.656	
E-223a	499	480	E203C1	467.5	470	3.545	
E-225b	491.5	480	E203C2	466.3	467.5	1.658	
E-229A	480	480	E203C3	449.3	466.3	23.946	
E-225C	480	450	E203C41	438.98	449.3	4.339	
E-223b	480	450	E203C42	438.98	449.3	5.596	
E-230a	480	450	E203C43	438.98	449.3	4.660	
E-226A	450	450	E203C5	425	438.98	19.711	
E-229B	480	480	E320	461.38	465	38.567	
E-229C	480	480	E312	457.5	457.5	2.375	
E-229D	480	480	E309B	430.85	457.5	2.305	
E-226B	450	450	E307	430.85	430.85	5.061	
E-226C	450	450	E311A11	423.17	430.85	28.003	
E-223C	450	432.55	E311A12	422.28	423.17	3.225	
E-230b	450	445.23	E309B1	422.28	430.85	0.742	
E-230C	445.23	441.92	E309C12	407.16	413.09	0.513	
E-227A	450	425	E322A121	412.79	413.09	1.306	
E-227B	450	425	E311B21	412.79	413.09	1.537	
E-230C1	441.92	425	E322A122	412.51	412.79	1.207	
E-230C2	441.92	425	E311B22	412.51	412.79	1.422	
E-223d1	432.55	425	E322A123	412.36	412.51	0.647	
E-223d2	432.55	425	E311B23	412.36	412.51	0.762	
E-224A	425	425	E322A124	407.16	412.36	22.415	
E-224B	425	425	E311B24	407.16	412.36	26.391	
E-224C	425	425	E201C1	399.7	402.8	1.195	
E-222a	425	405	E201C2	393	399.7	3.447	
E-222b	405	393	-	-	-	2.071	Cold side is in power cycle in Section 1

Basis: 0.99300 g-mole H_2 Product
T = "Trace"

TABLE D-8

SECTION III
HI Separation
Material Balance

Stream Number	Component Molar Flow Ratios								Total Flow Ratio		Phase	Pressure k $Pa^{x}10^{-2}$	Temp. °K	Comments
	H_2SO_4	HI	I_2	H_2O	SO_2	S	H_2S	H_3PO_4	Moles	Weight				
300	0	0	0	0.08440	0	0	0	0	0.08440	0.076	ℓ	1.013	298.15	Net input from the environment
301	0.00200	2.01200	7.75266	10.60940	0.00040	T	T	0	20.46646	1207.204	ℓ	1.850	393.15	Input from Sec. I, H_2SO_4-HI Synthesis
302	0	0.08120	T	0.08120	0	0	T	0	0.16240	5.920	ℓ	50.663	303.00	Input from Section IV, HI Decomposition
303	T	0	0	T	0	T	0	1.06604	1.06604	52.186	ℓ	1.013	457.75	
304	0	0	0	0.07000	0	0	0	0	0.07000	0.630	ℓ	1.013	298.15	
305	0	0	0	0.07000	0	0	0	0	0.07000	0.630	ℓ	2.026	298.15	
306	0	0	0	0.07000	0	0	0	0	0.07000	0.630	ℓ	2.026	381.57	
307	T	0.01240	0.01240	0.03100	0	0	0	0.06200	0.11780	5.679	ℓ	2.026	393.15	
308	T	0.01240	0.01240	0.03100	0	0	0	0.06200	0.11780	5.679	ℓ	1.850	393.15	
309	T	0.01240	7.56836	0.02480	0	0	0	0.06200	7.66756	963.721	ℓ	1.850	393.15	
310	0.00200	2.02450	0.53970	14.72583	0.00040	T	T	14.26942	31.65185	1028.978	ℓ	1.850	393.15	
311	T	0.01240	0.01240	0.02480	0	0	0	0.06200	7.66756	963.721	ℓ	2.026	393.15	
312	0.00200	2.02450	0.53970	14.72583	0.00040	T	T	14.26942	31.65185	1028.978	ℓ	1.013	418.00	
313	0	2.08535	0.54770	0.09500	T	T	0.00120	0	2.72925	203.585	g	1.013	401.00	
314	0	2.08535	0.54770	0.09500	T	T	0.00120	0	2.72925	203.586	g&ℓ	1.013	387.00	[0.01250 HI·0.34300 I_2· 0.02500 H_2O] (ℓ) plus a trace of S(s).
315	0	0.01250	0.34300	0.02500	T	T	T	0	0.38050	44.516	ℓ	1.013	387.00	
316	0	0	0	7.74113	0	0	0	0	7.74113	69.666	g&ℓ	6.786	436.85	1.14003 H_2O (g)
317	0	0	0	10.33761	0	0	0	0	10.33761	93.033	g&ℓ	6.786	436.85	1.39315 H_2O (g)
318	0	2.07720	0.20470	0.07000	T	0	0.00120	0	2.35310	159.347	g	1.013	387.00	
319	0	0.01000	0.20370	0.06800	0	0	0	0	0.28170	2.708	ℓ	1.013	457.50	
320	0	0.01000	0.20370	0.06800	0	0	0	0	0.28170	2.708	ℓ	1.850	457.51	
321	0	0	0	0.30519	0	0	0	0	0.30519	2.747	g	1.013	534.15	
322	0	T	7.55596	0.06380	0	0	0	0	7.61976	958.672	ℓ	2.026	393.15	
323	T	0	0	T	0	0	0	1.06604	1.06604	52.186	ℓ	1.013	534.15	
324	0	2.21820	0.05140	0.26900	0	0	0.00120	0	2.53980	150.710	g	1.013	377.60	
325	0	2.21820	0.05140	0.26900	0	0	0.00120	0	2.53980	150.710	g&ℓ	1.013	368.15	[2.06720 HI+0.00100 I_2+ 0.00200 H_2O+0.00120 H_2S](g)
326	0	0.15100	0.05040	0.26700	0	0	T	0	0.46840	18.443	ℓ	1.013	368.15	

TABLE D-8

SECTION III
HI Separation
Material Balance
(Continued)

Stream Number	Component Molar Flow Ratios								Total Flow Ratio		Phase	Pressure k $Pa^{\times}10^{-2}$	Temp. °K	Comments
	H_2SO_4	HI	I_2	H_2O	SO_2	S	H_2S	H_3PO_4	Moles	Weight				
327	0	0	0	0	0	0	0	3.05102	3.05102	419.15	g	9.480	380.00	
328	T	0	0	0.30519	0	T	0	1.06604	1.37123	52.186	ℓ	1.013	476.65	
329	0	2.06720	0.00100	0.00200	0	0	0.00120	0	2.07140	132.267	g	1.013	368.15	
330	0	2.06720	0.00100	0.00200	0	0	0.00120	0	2.07140	132.267	g	1.013	300.00	
331	0	2.06720	0.00100	0.00200	0	0	0.00120	0	2.07140	132.267	g	8.268	373.24	
332	0	2.06720	0.00100	0.00200	0	0	0.00120	0	2.07140	132.267	ℓ	8.268	300.00	
333	0	2.06720	0.00100	0.00200	0	0	0.00120	0	2.07140	132.267	ℓ	50.663	300.41	HI output to Section IV.
334	T	0	0	4.08523	0	T	0	14.26942	18.35465	735.300	ℓ	1.013	457.75	
335	T	0	0	14.72083	0	0.00120	0	15.33546	30.05749	883.221	ℓ	1.013	430.85	
336	T	0	0	14.72803	0	T	0	15.33546	30.06349	883.266	ℓ	1.013	430.85	
337	0	0.01250	0.34300	0.02500	T	T	T	0	0.38050	44.516	ℓ	1.850	387.01	
338	T	0	0	4.08523	0	T	0	14.26942	18.35465	735.300	ℓ	1.850	393.15	
339	0	0	0	2.59648	0	0	0	0	2.59648	23.367	g&ℓ	6.786	436.85	0.25312 H_2O(g)
340	0	0	0	10.64280	0	0	0	0	10.64280	95.780	g&ℓ	6.786	436.85	1.45639 H_2O(g)
341	0	0	0	0.00720	0	0.00120	0	0	0.00840	0.084	ℓ&s	1.013	300.00	0.00120 S(s) Output to Section II.
342	T	0	0	4.08523	0	T	0	14.26942	18.35465	735.300	ℓ	1.013	438.85	
343	0	T	7.55596	0.06380	0	0	0	0	7.61976	958.672	ℓ	1.850	393.15	
344	T	0	0	T	0	0	0	1.06604	1.06604	52.186	ℓ	1.013	438.85	
345	T	0	0	T	0	0	0	1.06604	1.06604	52.186	ℓ	1.013	401.00	
346	T	0	0	4.08523	0	T	0	14.26942	18.35465	735.00	ℓ	1.013	393.15	
347	0	0	0	11.14230	0	0	0	0	11.14230	100.275	g&ℓ	1.850	391.01	0.49950 H_2O(g)
348	0	0.01000	0.20370	0.06800	0	0	0	0	0.28170	2.708	ℓ	1.850	389.80	
349	0	0.01000	7.75966	0.13180	0	0	0	0	7.90146	985.752	ℓ	1.850	393.15	Iodine Output to Section I
350	0	0	0	0.01440	0	0	0	0	0.01440	0.130	ℓ	1.013	298.15	
351	T	0	0	14.72803	0	T	0	15.33546	30.06349	883.266	g&ℓ	1.013	446.11	4.33285 H_2O(g)
352	0	0	0	4.33285	0	0	0	0	4.33285	38.994	g	1.013	446.11	
353	T	0	0	10.39518	0	T	0	15.33546	25.73064	844.272	ℓ	1.013	446.11	
354	0	0	0	4.33285	0	0	0	0	4.33285	38.994	g	10.252	454.11	
355	0	0	0	4.33285	0	0	0	0	4.33285	38.994	g&ℓ	10.252	454.11	0.31583 H_2O(g)
356	0	0	0	4.33285	0	0	0	0	4.33285	38.994	g&ℓ	6.786	436.85	0.45110 H_2O(g)
357	T	0	0	T	0	T	0	1.06604	1.06604	52.186	ℓ	1.013	488.65	
358	T	0	0	10.39518	0	T	0	15.33546	25.73064	844.272	g&ℓ	1.013	461.38	3.40828 H_2O(g)
359	0	0	0	3.40828	0	0	0	0	3.40828	30.673	g	1.013	461.38	
360	T	0	0	6.98690	0	T	0	15.33546	22.32236	813.600	ℓ	1.013	461.38	

TABLE D-8

SECTION III
HI Separation
Material Balance
(continued)

Stream Number	Component Flow Molar Ratios								Total Flow Ratio		Phase	Pressure k Pax10^{-2}	Temp. °K	Comments
	H_2SO_4	HI	I_2	H_2O	SO_2	S	H_2S	H_3PO_4	Moles	Weight				
361	0	0	0	3.40828	0	0	0	0	3.40828	30.673	g	14.348	469.38	
362	T	0	0	4.08523	0	T	0	14.26942	18.35465	735.300	ℓ	1.013	476.65	
363	0	0	0	3.40828	0	0	0	0	3.40828	30.673	g&ℓ	14.348	469.38	0.52105 H_2O(g)
364	0	0	0	3.40828	0	0	0	0	3.40828	30.673	g&ℓ	6.786	436.85	0.68893 H_2O(g)
365	0	0.08120	T	0.08120	0	0	T	0	0.16240	5.920	g&ℓ	1.013	288.94	[0.00435 HI+trace H_2O](g)
366	0	0	0	2.59648	0	0	0	0	2.59648	23.367	ℓ	19.666	484.65	
367	T	0	0	T	0	0	0	1.06604	1.06604	52.186	ℓ	1.013	469.38	
368	T	0	0	6.98690	0	T	0	15.33546	22.32236	813.600	g&ℓ	1.013	476.65	2.59648 H_2O(g)
369	0	0	0	2.59648	0	0	0	0	2.59648	23.367	g	1.013	476.65	
370	0	0	0	2.59648	0	0	0	0	2.59648	23.367	g	19.666	484.65	
371	0	2.02450	0.53970	14.72583	0.00040	T	T	14.26942	31.65185	1028.978	ℓ	1.013	393.15	
372	0	2.07285	0.20470	0.07000	T	T	0.00120	0	2.34875	15.907	g	1.013	387.00	
373	0	0.00435	0	T	0	0	T	0	0.00435	0.278	g	1.013	288.94	
374	T	0	0	4.39042	0	T	0	15.33546	19.72588	790.233	ℓ	1.013	476.65	
375	0	0	0	0.30519	0	0	0	0	0.30519	2.747	ℓ	52.519	540.15	
376	0	0	0	0.30519	0	0	0	0	0.30519	2.747	g&ℓ	6.786	436.85	0.06324 H_2O(g)
377	0	0	0	0.30519	0	0	0	0	0.30519	2.747	g	52.519	540.15	
378	T	0	0	0.30519	0	T	0	1.06604	1.37123	54.933	ℓ	1.013	534.15	0.30519 H_2O(g)
379	0	0	0	10.64280	0	0	0	0	10.64280	95.780	ℓ	1.850	415.00	
380	0	0.07685	T	0.08120	0	0	T	0	0.15805	5.642	ℓ	1.013	288.94	
381	0	0	0	10.64280	0	0	0	0	10.64280	95.780	ℓ	1.850	368.15	H_2O Output to Section I
382	0	0	0	10.64280	0	0	0	0	10.64280	95.780	ℓ	1.850	391.01	
383	0	0	0	0.49950	0	0	0	0	0.49950	4.495	g	1.850	391.01	
384	0	0	0	0.49950	0	0	0	0	0.49950	4.495	g	3.396	463.92	
385	0	0	0	0.49950	0	0	0	0	0.49950	4.495	ℓ	3.396	413.00	
								R-11*						
386	0	0	0	0	0	0	0	3.96034	3.96034	544.07	g	1.130	300	
387	0	0	0	0	0	0	0	3.96034	3.96034	544.07	ℓ	1.130	300	
388	0	0	0	0	0	0	0	3.05102	3.05102	419.15	ℓ	1.130	300	
389	0	0	0	0	0	0	0	0.90932	0.90923	124.92	ℓ	1.130	300	
390	0	0	0	0	0	0	0	0.90932	0.90932	124.92	ℓ	7.000	300	
391	0	0	0	0	0	0	0	0.90932	0.90932	124.92	g	6.390	363.1	
392	0	0	0	0	0	0	0	3.05102	3.05102	419.15	ℓ	10.000	300	

*FREON-11

TABLE D-9

Section III
HI Separation
Heat Exchanger Loads and Operating Temperatures

Basis: 0.993 g-mole H_2

Heat Exch. Number	Energy Load, kJ	Hot-Side In		Hot-Side Out		Cold-Side In		Cold-Side Out		Comments
		Stream Number	Stream Temp, K	Stream Number	Stream Temp, K	Stream Number	Stream Temp, K	Stream Number	Stream Temp, K	
E-301	0.4400	[Heat Recovered with Section III]				305	298.15	306	381.57	
E-302	72.2842	340	436.85	379	415.00	(C-303)	401.00	(C-303)	430.85	54.2347 kJ is isothermal at 436.85K on warm side
E-303	21.5858	324	377.60	325	368.15	[See Section III Heat Recovery Table]				
E-304	41.2642	(C-302)	393.15	(C-302)	393.15	[See Section III Heat Recovery Table]				
E-305	4.5295	313	401.00	314	387.00	[See Section III Heat Recovery Table]				
E-306	8.0996	344	438.85	345	401.00	[See Section III Heat Recovery Table]				
E-307	5.0611	[Heat from Section II]				-	430.85(-)	-	430.85(+)	See Section II for heat supply temperature
E-308	136.2974	342	438.85	346	393.15	[See Section III Heat Recovery Table]				
E-309	6.9204	[See Comments]				(C-304)	377.50	(C-304)	457.50	3.5605 kJ demand is supplied from Section II; the remainder is recovered within Section III.
E-310	18.4793	382	391.00	381	368.15	[See Section III Heat Recovery Table]				
E-311	108.8309	[See Comments]				(C-303)	405.78	(C-303)	430.85	61.3702 demand is supplied from Section II; the remainder is recovered within Section III.
E-312	2.3750	[Heat from Section II]				-	457.50(-)	-	457.50(+)	See Section II for heat supply temperature.
E-313	1.5130	320	457.51	348	389.80	[See Section III Heat Recovery Table]				
E-314	4.1025	329	368.15	330	300.00	[See Section III Heat Recovery Table]				
E-315	4.1975	(TC-301)	373.23	(TC-301)	300.00	[See Section III Heat Recovery Table]				
E-316	4.1975	(TC-301)	373.23	(TC-301)	300.00	[See Section III Heat Recovery Table]				
E-317	41.1935	331	373.23	332	300.00	[See Section III Heat Recovery Table]				36.9960 kJ is isothermal at 300.00K on warm side
E-318A	145.2961	354	454.11	355	454.11	Shell Side	430.85	Shell Side	446.11	
E-318B	60.2526	334	457.75	342	438.85	Shell Side	430.85	Shell Side	446.11	
E-318C	42.8573	(TC-302)	454.11	(TC-302)	454.11	Shell Side	430.85	Shell Side	446.11	
E-318D	4.0444	303	457.75	344	438.85	Shell Side	430.85	Shell Side	446.11	
E-319A	101.5068	361	469.38	363	469.38	Shell Side	446.11	Shell Side	461.38	
E-319B	60.3627	362	476.65	334	457.75	Shell Side	446.11	Shell Side	461.38	
E-319C	41.1041	(TC-303)	469.38	(TC-303)	469.38	Shell Side	446.11	Shell Side	461.38	
E-319D	0.5706	367	469.38	303	457.75	Shell Side	446.11	Shell Side	461.38	
E-320A	88.4231	370	484.65	366	484.65	Shell Side	465.01	Shell Side	476.65	
E-320B	38.5672	[Heat from Section II]				Shell Side	465.01	Shell Side	461.38	See Section II for heat supply temperature
E-320C	35.4359	(TC-304)	484.65	(TC-304)	484.65	Shell Side	465.01	Shell Side	476.65	
E-320D	4.1236	357	488.65	367	469.38	Shell Side	461.38	Shell Side	476.65	
E-321A	8.9001	377	540.15	375	540.15	Shell Side	499.17	Shell Side	519.76	
E-321B	6.2228	(TC-305)	540.15	(TC-305)	540.15	Shell Side	519.76	Shell Side	534.15	
E-321C	9.7365	323	534.15	357	488.65	Shell Side	476.65	Shell Side	499.17	

TABLE D-9

Section III
HI Separation
Heat Exchanger Loads and Operating Temperatures
(Continued)

Heat Exch. Number	Energy Load, kJ	Hot-Side In		Hot-Side Out		Cold-Side In		Cold-Side Out		Comments
		Stream Number	Stream Temp, K	Stream Number	Stream Temp, K	Stream Number	Stream Temp, K	Stream Number	Stream Temp, K	
E-322	107.0491	[Heat Recovered within Section III]				371	393.15	312	418.00	See Section III Heat Recovery Table
E-323	20.7363	384	463.92	385	413.00	(C-303)	401.00	(C-303)	405.78	
E-324	90.0754	[Heat Recovered within Section III&IV]				392	300.00	327	380.00	See Section III Heat Recovery Table
E-325	26.0012	[Heat Recovered within Section III]				390	300.00	391	363.10	See Section III Heat Recovery Table
E-326	97.7397	386	300.00	387	300.00	CW				

TABLE D-10

Section III
Detailed Heat Matchup

	Heat Exch. No.	Max. Temp. K	Min. Temp. K	Heat Exch. No.	Max. Temp K	Min. Temp. K	Heat Load kJ	Comments
1	E-301 A_1	381.57	377.50	E-313S	398.09	397.98	0.0001	
2	E-301 A_2	381.57	377.50	E-308Q	398.09	397.98	0.0198	
3	E-301 A_3	381.57	377.50	E-305E	398.09	397.98	0.0016	
4	E-301 B_1	377.50	298.15	E-313T	397.98	397.85	0.0029	
5	E-301 B_2	377.50	298.15	E-308R	397.98	397.85	0.3857	
6	E-301 B_3	377.50	298.15	E-305F	397.98	397.85	0.0297	
7	E-303 A	377.60	376.94	E-325B_1	363.15	363.15	1.5112	
8	E-303 B	376.94	373.23	E-414	-	-	8.4480	
9	E-303 C_1	373.23	371.15	E325B_2	363.15	363.15	4.7605	
10	E-303 C_2	371.15	368.15	E-324E_2	363.07	338.00	6.8661	
11	E-304	393.15	393.15	E-324G_4	380	380	41.2642	
12	E-305 A	401.00	393.39	E-309J_3	395.13	393.13	0.0121	
13	E-305 B	401.00	398.39	E-322F_3	395.13	393.15	0.6056	
14	E-305 C	398.39	398.09	E-309K_3	393.15	381.57	0.0712	
15	E-305 D	398.09	397.98	E-309L_3	381.57	377.50	0.0251	
16	E-305 E	398.09	397.98	E-301A_3	381.57	377.50	0.0016	
17	E-305 F	397.98	397.85	E-301B_3	377.50	298.15	0.0297	
18	E-305 G	397.85	393.15	E-324C	380.00	380.00	41.2642	
19	E-305 H	393.15	387.00	E-325B	365.00	365.00	1.9897	
20	E-306 A	438.85	419.59	E-309D_3	426.28	418.00	0.4432	
21	E-306 B	438.85	419.59	E-311B_3	426.28	418.00	22.2371	
22	E-306 C	438.85	419.59	E-309E_3	418.00	413.71	0.3441	
23	E-306 D	438.85	419.59	E-322A_3	418.00	413.71	17.1376	
24	E-306 E	438.85	419.59	E-311D_3	418.00	413.71	17.2699	
25	E-306 F	419.59	415.54	E-309G_3	407.27	405.78	0.0092	
26	E-306 G	419.59	415.54	E-322C_3	407.27	405.78	0.4570	
27	E-306 H	419.59	415.54	E-311F_3	407.27	405.78	0.4606	
28	E-306 I	415.54	409.02	E-309H_3	405.78	401.00	0.0293	
29	E-306 J	415.54	409.02	E-322D_3	405.78	401.00	1.4633	
30	E-306 K	409.02	401.00	E-309I_3	401.00	395.13	0.0361	
31	E-306 L	409.02	401.00	E-323E_3	401.00	395.13	1.7975	
32	E-307	430.85	430.85	-	-	-	5.0611	Heat Supplied from Section II. See Section II Heat Exchanger Tables for Matchup
33	E-308 A	438.85	419.59	E-309D_2	426.28	418.00	0.0318	
34	E-308 B	438.85	419.59	E-311B_2	426.28	418.00	1.5955	
35	E-308 C	438.85	419.59	E-309E_2	418.00	413.71	0.0247	

TABLE D-10

Section III
Detailed Heat Matchup
(Continued)

	Heat Exch. No.	Max. Temp. K	Min. Temp. K	Heat Exch. No.	Max. Temp. K	Min. Temp. K	Heat Load kJ	Comments
36	E-308 D	438.85	419.59	$E\text{-}322A_2$	418.00	413.71	1.2296	
37	E-308 E	438.85	419.59	$E\text{-}311D_2$	418.00	413.71	1.2392	
38	E-308 F	419.59	415.54	$E\text{-}309G_2$	407.27	405.78	0.1190	
39	E-308 G	419.59	415.54	$E\text{-}322C_2$	407.27	405.78	5.9297	
40	E-308 H	419.59	415.54	$E\text{-}311F_2$	407.27	405.78	5.9755	
41	E-308 I	415.54	409.02	$E\text{-}309H_2$	405.78	401.00	0.3813	
42	E-308 J	415.54	409.02	$E\text{-}322D_2$	405.78	401.00	18.9857	
43	E-308 K	409.02	401.00	$E\text{-}309I_2$	401.00	395.13	0.4684	
44	E-308 L	409.02	401.00	$E\text{-}322E_2$	401.00	395.13	23.3216	
45	E-308 M	401.00	398.39	$E\text{-}309J_2$	395.13	393.15	0.1578	
46	E-308 N	401.00	398.39	$E\text{-}322F_2$	395.13	393.15	7.8580	
47	E-308 O	398.39	398.09	$E\text{-}309K_2$	393.15	381.57	0.9236	
48	E-308 P	398.09	397.98	$E\text{-}309L_2$	381.57	377.50	0.3246	
49	E-308 Q	398.09	397.98	$E\text{-}301A_2$	381.57	377.50	0.0198	
50	E-308 R	397.98	397.85	$E\text{-}301B_2$	377.50	298.15	0.3859	
51	E-308 S	397.85	393.15	$E\text{-}324G_3$	380.00	380.00	14.0146	
52	E-309 A	457.50	430.85	-	-	-	2.3053	Heat Supplied from Section II. See Section II Heat Exchanger Tables for Matchup.
53	E-309 B	430.85	426.62	-	-	-	0.6252	Heat Supplied from Section II. See Section II Heat Exchanger Tables for Matchup.
54	E-309 C	426.62	426.28	E-313A	457.51	438.85	0.0081	
55	$E\text{-}309D_1$	426.28	418.00	E-313C	438.85	419.59	0.0033	
56	$E\text{-}309D_2$	426.28	418.00	E-308A	438.85	419.59	0.0318	
57	$E\text{-}309D_3$	426.28	418.00	E-306A	438.85	419.59	0.4432	
58	$E\text{-}309E_1$	418.00	413.71	E-313E	438.85	419.59	0.0026	
59	$E\text{-}309E_2$	418.00	413.71	E-308C	438.85	419.59	0.0247	
60	$E\text{-}309E_3$	418.00	413.71	E-306C	438.85	419.59	0.3441	
61	E-309F	413.71	407.27	-	-	-	0.5566	Heat Supplied from Section II. See Section II Heat Exchanger Tables for Matchup.
62	$E\text{-}309G_1$	407.27	405.78	E-313H	419.59	415.54	0.0009	
63	$E\text{-}309G_2$	407.27	405.78	E-308F	419.59	415.54	0.1190	
64	$E\text{-}309G_3$	407.27	405.78	E-306F	419.59	415.54	0.0092	
65	$E\text{-}309H_1$	405.78	401.00	E-313K	415.54	409.02	0.0029	
66	$E\text{-}309H_2$	405.78	401.00	E-308I	415.54	409.02	0.3813	
67	$E\text{-}309H_3$	405.78	401.00	E-306I	415.54	409.02	0.0293	
68	$E\text{-}309I_1$	401.00	395.13	E-313M	409.02	401.00	0.0035	

TABLE D-10

Section III
Detailed Heat Matchup
(Continued)

	Heat Exch. No.	Max. Temp. K	Min. Temp. K	Heat Exch. No.	Max. Temp. K	Min. Temp. K	Heat Load kJ	Comments
69	E-309I$_2$	401.00	395.13	E-308K	409.02	401.00	0.4684	
70	E-309I$_3$	401.00	395.13	E-306K	409.02	401.00	0.0361	
71	E-309J$_1$	395.13	393.15	E-313O	401.00	398.39	0.0012	
72	E-309J$_2$	395.13	393.15	E-308M	401.00	398.39	0.1578	
73	E-309J$_3$	395.13	393.15	E-305A	401.00	398.39	0.0121	
74	E-309K$_1$	393.15	381.57	E-313Q	398.39	398.09	0.0069	
75	E-309K$_2$	393.15	381.57	E-308O	398.39	398.09	0.9236	
76	E-309K$_3$	393.15	381.57	E-305C	398.39	398.09	0.0712	
77	E-309L$_1$	381.57	377.50	E-313R	398.09	397.98	0.0024	
78	E-309L$_2$	381.57	377.50	E-308P	398.09	397.98	0.3246	
79	E-309L$_3$	381.57	377.50	E-305D	398.09	397.98	0.0251	
80	E-310A	391.00	389.21	E-324G$_1$	380.00	380.00	1.4455	
81	E-310B	389.21	386.08	E-324F$_1$	380.00	363.07	2.5275	
82	E-310C	386.08	370.30	E-325B$_3$	363.15	363.15	12.7565	
83	E-310D	370.30	368.15	E-324E$_1$	363.07	338.00	1.7498	
84	E-311A	430.85	426.26	-	-	-	31.3748	Heat Supplied from Section II. See Section II Heat Exchanger Tables for Matchup.
85	E-311B	426.62	426.28	E-313B	457.51	438.85	0.4089	
86	E-311C$_1$	426.28	418.00	E-313D	438.85	419.59	0.1666	
87	E-311C$_2$	426.28	418.00	E-308B	438.85	419.59	1.5955	
88	E-311C$_3$	426.28	418.00	E-306B	438.85	419.59	22.2371	
89	E-311D$_1$	418.00	413.71	E-313G	438.85	419.59	0.1294	
90	E-311D$_2$	418.00	413.71	E-308E	438.85	419.59	1.2392	
91	E-311D$_3$	418.00	413.71	E-306E	438.85	419.59	17.2699	
92	E-311E	413.71	407.27	-	-	-	27.9286	Heat Supplied from Section II. See Section II Heat Exchanger Tables for Matchup.
93	E-311F$_1$	407.27	405.78	E-313J	419.59	415.54	0.0448	
94	E-311F$_2$	407.27	405.78	E-308H	419.59	415.54	5.9755	
95	E-311F$_3$	407.27	405.78	E-306H	419.59	415.54	0.4606	
96	E-312	457.50	457.50	-	-	-	2.3750	Heat Supplied from Section II. See Section II Heat Exchanger Tables for Matchup.
97	E-313A	457.51	438.85	E-309C	426.62	426.28	0.0081	
98	E-313B	457.51	438.85	E-311B	426.62	426.28	0.4089	
99	E-313C	438.85	419.59	E-309D$_1$	426.28	418.00	0.0033	
100	E-313D	438.85	419.59	E-311B$_1$	426.28	418.00	0.1666	
101	E-313E	438.85	419.59	E-309E$_1$	418.00	413.71	0.0026	
102	E-313F	438.85	419.59	E-322A$_1$	418.00	413.71	0.1284	
103	E-313G	438.85	419.59	E-311D$_1$	418.00	413.71	0.1294	
104	E-313H	419.59	415.54	E-309G$_1$	407.27	405.78	0.0009	

TABLE D-10

Section III
Detailed Heat Matchup
(Continued)

	Heat Exch. No.	Max. Temp. K	Min. Temp. K	Heat Exch. No.	Max. Temp. K	Min. Temp. K	Heat Load kJ	Comments
105	E-313I	419.59	415.54	$E\text{-}322C_1$	407.27	405.78	0.0444	
106	E-313J	419.59	415.54	$E\text{-}311F_1$	407.27	405.78	0.0448	
107	E-313K	415.54	409.02	$E\text{-}309H_1$	405.78	401.00	0.0029	
108	E-313L	415.54	409.02	$E\text{-}322D_1$	405.78	401.00	0.1423	
109	E-313M	409.02	401.00	$E\text{-}309I_1$	401.00	395.13	0.0035	
110	E-313N	409.02	401.00	$E\text{-}322E_1$	401.00	395.13	0.1747	
111	E-313O	401.00	398.39	$E\text{-}309J_1$	395.13	393.15	0.0012	
112	E-313P	401.00	398.39	$E\text{-}322F_1$	395.13	393.15	0.0589	
113	E-313Q	398.39	398.09	$E\text{-}309K_1$	393.15	381.57	0.0069	
114	E-313R	398.09	397.98	$E\text{-}309L_1$	381.57	377.50	0.0024	
115	E-313S	398.09	397.98	$E\text{-}301A_1$	381.57	377.50	0.0001	
116	E-313T	397.98	397.85	$E\text{-}301B_1$	377.50	298.15	0.0029	
117	E-313U	397.85	389.80	$E\text{-}324G_6$	380.00	380.00	0.1798	
118	E-314A	368.23	335.00	$E\text{-}324D_1$	338.00	325.82	1.9975	
119	E-314B	335.00	313.00	$E\text{-}324C_2$	325.82	300.00	1.3224	
120	E-314C	313.00	300	C.W.	-	-	0.7826	
121	E-315A	373.23	335.00	$E\text{-}324D_3$	338.00	325.82	2.1913	
122	E-315B	335.00	313.00	$E\text{-}324C_3$	325.82	300	1.2610	
123	E-315C	313.00	300.00	C.W.	-	-	0.7452	
124	E-316A	373.23	312.4	$E\text{-}325A_1$	363.15	300.00	3.4865	
125	E-316B	312.4	300.00	C.W.	-	-	0.7110	
126	E-317A	373.23	312.4	$E\text{-}325A_2$	363.15	300.00	3.4865	
127	E-317B	312.4	300.00	C.W.	-	-	37.7070	
128	E-320B	465.01	461.38	-	-	-	38.5672	Heat Supplied from Section II. See Section II Heat Exchanger Tables for Matchup.
129	$E\text{-}322A_1$	418.00	413.71	E-313F	438.85	419.59	0.1284	
130	$E\text{-}322A_1$	418.00	413.71	E-308D	438.85	419.59	1.2296	
131	$E\text{-}322A_2$	418.00	413.71	E-306D	438.85	419.59	17.1376	
132	$E\text{-}322A_3$	413.71	407.27	-	-	-	27.7148	Heat Supplied from Section II. See Section II Heat Exchanger Tables for Matchup.
133	$E\text{-}322C_1$	407.27	405.78	E-313I	419.59	415.54	0.0444	
134	$E\text{-}322C_2$	407.27	405.78	E-308G	419.59	415.54	5.9297	
135	$E\text{-}322C_3$	407.27	405.78	E-306G	419.59	415.54	0.4570	
136	$E\text{-}322D_1$	405.78	401.00	E-313L	415.54	409.02	0.1423	
137	$E\text{-}322D_2$	405.78	401.00	E-308J	415.54	409.02	18.9857	
138	$E\text{-}322D_3$	405.78	401.00	E-306J	415.54	409.02	1.4633	

TABLE D-10

Section III
Detailed Heat Matchup
(Continued)

	Heat Exch. No.	Max. Temp. K	Min. Temp. K	Heat Exch. No.	Max. Temp. K	Min. Temp. K	Heat Load kJ	Comments
139	$E-322E_1$	401.00	395.13	E-313N	409.02	401.00	0.1747	
140	$E-322E_2$	401.00	395.13	E-308L	409.02	401.00	23.3216	
141	$E-322E_3$	401.00	395.13	E-306L	409.02	401.00	1.7975	
142	$E-322F_1$	395.13	393.15	E-313P	401.00	398.39	0.0589	
143	$E-322F_2$	395.13	393.15	E-308N	401.00	398.39	7.8580	
144	$E-322F_3$	395.13	393.15	E-305B	401.00	398.39	0.6056	
145	E-324A	373.00	300.00	E-411A	383.00	315.00	2.2577	
146	E-324B	380.00	373.00	E-305G	397.85	387.00	0.2165	
147	$E-324C_1$	325.82	300.00	E-409A	335.70	313.00	6.2920	
148	$E-324C_2$	325.82	300.00	E314B	335.00	313.00	1.3224	
149	$E-324C_3$	325.82	300.00	E-315B	335.00	313.00	1.2610	
150	$E-324D_1$	338.00	325.82	E314A	368.23	335.00	1.9975	
151	$E-324D_2$	338.00	325.82	E-315A	373.33	335.00	2.1913	
152	$E-324E_1$	363.07	338.00	E-310D	370.30	368.15	1.7498	
153	$E-324E_2$	363.07	338.00	$E-303C_2$	371.15	368.15	6.8661	
154	$E-324F_1$	380.00	363.07	E-310B	389.21	386.08	2.5275	
155	$E-324F_2$	380.00	363.07	E-305H	397.85	387.00	3.2935	
156	$E-324G_1$	380.00	380.00	E-310A	391.00	389.21	1.4455	
157	$E-324G_2$	380.00	380.00	E-407A	403.00	393.00	0.8120	
158	$E-324G_3$	380.00	380.00	E-308S	397 85	393.15	14.0146	
159	$E-324G_4$	380.00	380.00	E-304	393.15	393.15	41.2642	
160	$E-324G_5$	380.00	380.00	E-406C	393.90	393.00	2.3840	
161	$E-324G_6$	380.00	380.00	E-313U	397 85	389.80	0.1798	
162	$E-325A_1$	363.15	300.00	E-316A	373.23	312.40	3.4865	
163	$E-325A_2$	363.15	300.00	E-317A	373.23	312.40	3.4865	
164	$E-325B_1$	363.15	363.15	E-303A	377.60	376.94	1.5112	
165	$E-325B_2$	363.15	363.15	$E-303C_1$	373.23	371.15	4.7605	
166	$E-325B_3$	363.15	363.15	E-310C	386.08	370.30	12.7565	
167	E-406C	393.9	393.00	$E-324G_5$	380.00	380.00	2.3840	
168	E-407C	403.00	393.00	$E-324G_2$	380.00	380.00	0.8120	
169	E-409A	335.70	313.00	$E-324C_1$	325.82	300.00	6.2920	
170	E-409B	313.00	300.00	C.W.			2.7720	
171	E-411A	383.00	315.00	E-324A	373.00	300.00	2.2577	
172	E-411B	315.00	300.00	C.W.			0.4003	
173	E-414	-	-	E-303B	376.94	373.23	8.4480	
174	E-326	300.00	300.00	C.W.			97.7397	

TABLE D-11

SECTION III
Power Machinery

Basis: 0.993 g-moles H_2 Product

Power Equipment Number	Work Load k J	Input		Output	
		Stream Number	Pressure k Pa$\times 10^{-2}$	Stream Number	Pressure k Pa$\times 10^{-2}$
P-301	0.0001	304	1.013	305	2.026
P-302	0.0093	309	1.850	311	2.026
P-303	0.5464	332	8.268	333	50.663
P-304	0.0014	319	1.013	320	1.850
P-305	0.0021	315	1.013	337	1.850
P-306	0.0844	346	1.013	338	1.850
P-307	0.3633	388	1.13	392	10.00
P-308	0.0718	389	1.13	390	7.00
TC-301	12.5925	330	1.013	331	8.268
TC-302	39.4051	352	1.013	354	10.252
TC-303	35.8200	359	1.013	361	14.348
TC-304	31.3214	369	1.013	370	19.666
TC-305	5.0616	321	1.013	377	52.519
TC-306	1.6831	383	1.850	384	3.396
TE-301	-0.5630	355	10.252	356	6.786
TE-302	-1.4768	363	14.348	364	6.786
TE-303	-0.5435	366	19.666	339	6.786
TE-304	-0.2746	375	52.519	376	6.786
TE-305	-1.1723	379	6.786	347	1.850
		385	3.396		
TE-306	-0.0945	310	1.850	371	1.013
TE-307	-0.0074	322	2.026	343	1.850
TE-308	-18.7719	327	9.480		
		391	6.390	386	1.13

TABLE D-11

Basis: 0.993 g mole H_2 product
T = "Trace"

SECTION IV
HI DECOMPOSITION
Material Balance

Stream Number	Component Molar Flow Ratios					Total Flow Ratios		Phase	Pressure Pa x 10^5	Temp. °K	Comments
	HI	I_2	H_2O	H_2S	H_2	Mole	Weight				
401	2.0672	0.0010	0.0020	0.0012	0	2.0714	132.24	ℓ	(a)	300.41	
402	3.1776	0.0045	0.0021	0.0012	0.0252	3.2106	203.65	ℓ	(a)	342.2	
403	3.1776	0.0045	0.0021	0.0012	0.0252	3.2106	203.65	ℓ	(a)	393	
404	3.9914	0.0051	0.0021	0.0012	0.0281	4.0279	255.73	ℓ	(a)	393	
405	2.0054	0.9981	0.0021	0.0012	1.0211	4.0279	255.73	ℓ	(a)	393	
406	0.8138	0.9946	0.0020	0	0.0029	1.8133	178.11	ℓ	(a)	393	
407	0.8138	0.9946	0.0020	0	0.0029	1.8133	178.11	ℓ	(a)	420	
408	1.9531	0.0014	0	0	0.0069	1.9614	124.97	g	(a)	403	
409	1.9531	0.0014	0	0	0.0069	1.9614	124.97	ℓ	(a)	393	
410	1.9531	0.0014	0	0	0.0069	1.9614	124.97	ℓ	(a)	393	
411	1.9531	0.0014	0	0	0.0069	1.9614	124.97	ℓ	51.663	393	
412	1.1393	0.0008	0	0	0.0040	1.1441	72.895	ℓ	(a)	393	
413	0.8138	0.0006	0	0	0.0029	0.8173	52.075	ℓ	(a)	393	
414	T	0.9940	0.0020	0	0	0.9960	126.04	ℓ	(a)	713	
415	T	0.9940	0.0020	0	0	0.9960	126.04	ℓ	(a)	393	
416	1.1916	0.0035	0.0001	0.0012	1.0182	2.0527	77.621	g	(a)	393	
417	1.1916	0.0035	0.0001	0.0012	1.0182	2.0527	77.621	g&ℓ	(a)	335.7	
418	1.1916	0.0035	0.0001	0.0012	1.0182	2.0527	77.621	g&ℓ	(a)	303	
419	1.1916	0.0035	0.0001	0.0012	1.0182	2.0527	77.621	g&ℓ	(a)	273	
420	1.1104	0.0035	0.0001	0	0.0252	1.1392	71.413	ℓ	(a)	273	
421	1.1104	0.0035	0.0001	0	0.0252	1.1392	71.413	ℓ	(a)	383	
422	0.0812	0	0	0.0012	0.9930	1.0754	6.2081	g	(a)	273	
423	0.0812	0	0	0.0012	0.9930	1.0754	6.2081	g	(a)	383	
424	0.0812	0	0	0.0012	0.9930	1.0754	6.2081	g&ℓ	(a)	303	
425	0	0	0.0008	0.0012	0.9930	0.9950	1.0276	g	(a)	303	
426	0.0812	0	0.0812	0	0	0.1624	5.9189	ℓ	(a)	303	
427	0	0	0	0.0012	0	0.0012	0.0205	g	(a)	400	
428	0	0	0.0008	0	0.9930	0.9938	1.0070	g	(a)	303	
429	0	0	0.0812	0	0	0.0812	0.7308	ℓ	(a)	298.15	
430	0	0	0.0812	0	0	0.0812	0.7308	ℓ	1.01325	298.15	
431	0.0812	0	0.0812	0	0	0.1624	5.9189	ℓ	1.01325	303	
432	0	--	--	--	--	--	--	ℓ	--	275.74(b)	Brine loop output from chiller.
433	0	--	--	--	--	--	--	g&ℓ	--	275.74(b)	Brine loop input to chiller.
434	0	--	--	--	--	--	--	g&ℓ	--	263.74(b)	
435	0	--	--	--	--	--	--	g&ℓ	--	303(b)	
436	0	--	--	--	--	--	--	g&ℓ	--	361.15(b)	

(a) Pressure is 50.663 x 10^5 Pa. (50 atm)
(b) These are mean temperatures.

TABLE D-13

SECTION IV
HI DECOMPOSITION
HEAT AND POWER LOADS

Basis: 0.993 g mole H_2 Product

Heat Exch. Number	Energy Load kJ	Hot Side In		Hot Side Out		Cold Side In		Cold Side Out		Comments
		Stream Number	Temp.°K	Stream Number	Temp. °K	Stream Number	Temp. °K	Stream Number	Temp. °K	
E-401	16.151	(a)	(a)	(a)	(a)	402	342.2	403	393	
E-402	8.075	(a)	(a)	(a)	(a)	--	393	--	393	
E-403	4.619	(a)	(a)	(a)	(a)	406	393	407	420	
E-404	4.786	(a)	(a)	(a)	(a)	--	713	--	713	
E-405	43.079	(a)	(a)	(a)	(a)	--	403	--	713	
E-406	26.610	408	403	409	393	(a)	(a)	(a)	(a)	
E-407	25.960	414	713	415	393	(a)	(a)	(a)	(a)	
E-408	13.103	416	393	417	335.7	420 & 422	273 & 273	421 & 423	383 & 383	
E-409	9.064	417	335.7	418	303	--	--	--	--	Cold side is in power cycle in Section III
E-410	6.758	418	303	419	273	432	~275.74	433	~275.74	Cold side temperature is a log mean average for heat transfer.
E-411	2.658	423	383	424	303	--	--	--	--	Cold side is in power cycle Section III
E-412	6.758	433	~275.74	432	~275.74	434(b)	~263.74	434(b)	~263.74	Temperatures are log mean average.
E-413	15.206	435	~303	435	~303	--	C.W.	--	C.W.	
E-414	8.448	--	377	--	373	436(b)	361.5	436(b)	361.5	Heat source is Sec. III.
E-415	2.979	--	303	--	303	--	C.W.	--	C.W.	

(a) See Table 3 for heat match up.

(b) Flow direction, amount and composition are not defined.

TABLE D-14

SECTION IV
HI DECOMPOSITION
HEAT AND POWER LOADS

Power Device Number	Energy Load	Input Stream Number	Input Pressure Pa x 10^5	Output Stream Number	Output Pressure Pa x 10^5	Comments
P-401	Negligible	410	50.663	411	51.663	
P-402	0.008	430	1.01325	429	50.663	

Special Equipment Number	Heat Effect kJ	Power Demand kJ	Comment
A-401	0.0004 in	0	Isothermal at 393°F

TABLE D-15

SECTION IV
HI DECOMPOSITION
HEAT RECUPERATION MATCH-UP

Basis: 0.993 g mole H_2 Product

Hot Side			Cold Side			Heat Load kJ	Comments
Heat Exch. Number	Input Temp. °K	Output Temp. °K	Heat Exch. Number	Input Temp. °K	Output Temp. °K		
Sec. V	-	-	E-404	713	713	4.786	
Sec. V	-	-	E-405A	705	713	1.112	Total 27.336 kjoul should be applied from Sec. V
Sec. V	-	-	E-405B	403	705	21.438	
E-407A	713	459.95	E-405C	403	705	20.529	
E-407B	459.95	403	E-403	393	420	4.619	
E-406A	403	400	E-402	393	393	8.075	
E-406B	400	393.9	E-401	342.2	393	16.151	
E-406C	393.9	393	-	-	-	2.384	Cold side is in power power cycle in Sec. III
E-407C	403	393	-	-	-	0.812	

TABLE D-16

SECTION V

Power Generation and Helium Heat Transfer Material Balance

Basis: 0.993 g-mol H_2 Product

Stream Number	Molar Flow Ratio		Mass Flow Ratio	Temp. K	Pressure Pa x 10^5	Phase	Comments
	Helium	H_2O					
500	-	-	-	686.00	-	-	Intermediate temperature process heat lowest temperature stream input; see detailed matchup table of Section V.
501	60.71023	-	121.3969	1255.40	49.041	g	
502	21.11470	-	42.2212	1226.86	46.000	g	
503	23.51088	-	47.0126	934.29	21.245	g	
504	16.08465	-	32.1631	1214.56	44.726	g	
505	16.08465	-	32.1631	742.27	44.726	g	
506	23.51088	-	47.0126	536.51	21.245	g	
507	21.11470	-	42.2212	751.56	46.000	g	
508	60.71023	-	121.3969	773.20	49.041	g	
509	16.08465	-	32.1631	1159.00	51.676	g	
510	16.08465	-	32.1631	728.00	51.676	g	
511	16.08465	-	32.1631	696.00	51.676	g	
512	16.08465	-	32.1631	686.71	51.675	g	
513	-	-	-	368.15	-	-	Waste heat from Section III input; see detailed matchup table of Section V.
514	23.51088	-	47.0126	878.73	51.675	g	
515	23.51088	-	47.0126	728.00	30.445	g	
516	7.42623	-	14.8496	696.00	30.445	g	
517	7.42623	-	14.8496	480.95	30.445	g	
518	7.42623	-	14.8496	606.79	51.675	g	
519	7.42623	-	14.8496	480.95	51.675	g	
520	7.42622	-	14.8496	696.00	30.445	g	
521	7.42622	-	14.8496	606.79	30.445	g	
522	7.42622	-	14.8496	544.30	30.445	g	
523	-	-	-	368.15	-	-	Waste heat from Section III input; see detailed matchup table of Section V.

TABLE D-16

SECTION V
Power Generation and Helium Heat Transfer
Material Balance
(Continued)

Stream Number	Molar Flow Ratio		Mass Flow Ratio	Temp. K	Pressure Pa x 10^5	Phase	Comments
	Helium	H_2O					
524	7.42622	-	14.8496	686.71	51.675	g	
525	7.42622	-	14.8496	616.73	51.675	g	
526	7.42622	-	14.8496	480.95	51.675	g	
527	-	-	-	311.00	-	-	Waste heat from Section III output; see detailed matchup table of Sec. V.
528	8.65483	-	29.6992	696.00	30.455	g	
529	8.65483	-	29.6992	686.71	29.328	g	
530	8.04233	-	16.0815	686.71	29.328	g	
531	8.04233	-	16.0815	480.95	29.328	g	
532	8.04233	-	16.0815	616.73	51.675	g	
533	0.61610	-	1.2320	686.71	29.328	g	
534	0.61610	-	1.2320	616.73	29.328	g	
535	0.61610	-	1.2320	375.07	29.328	g	
536	23.51088	-	47.0726	696.00	30.445	g	
537	0.61610	-	1.2328	480.95	51.675	g	
538	8.04232	-	16.0815	480.95	51.675	g	
539	8.04233	-	16.0815	480.95	51.675	g	
540	23.51088	-	47.0126	480.95	51.675	g	
541	21.11470	-	42.2212	1171.30	51.675	g	
542	21.11470	-	42.2212	755.00	51.675	g	
543	21.11470	-	42.2212	728.00	46.691	g	
544	21.11470	-	42.2212	696.00	46.691	g	
545	21.11470	-	42.2212	728.00	51.675	g	
546	21.11470	-	42.2212	696.00	51.675	g	
547	-	7.05705	63.5099	1159.30	379.210	g	
548	-	7.05705	63.5099	976.94	156.945	g	
549	-	7.05705	63.5099	696.00	156.945	g	
550	-	7.05705	63.5099	728.00	189.510	g	
551	-	1.01643	2.0325	696.00	189.510	g	
552	-	1.01643	2.0325	300.00	0.035	g+ℓ	0.28664 $H_2O(\ell)$
553	-	1.01643	2.0325	300.00	0.035	ℓ	

TABLE D-16

SECTION V
Power Generation and Helium Heat Transfer
Material Balance
(Continued)

Stream Number	Molar Flow Ratio		Mass Flow Ratio	Temp. K	Pressure Pa x 10^5	Phase	Comments
	Helium	H_2O					
554	-	1.01643	2.0325	300.85	189.510	ℓ	
555	-	1.01643	2.0325	391.00	189.510	ℓ	
556	-	7.05705	63.5099	696.00	189.510	g	
557	-	6.04062	12.0789	696.00	189.510	g	
558	-	7.05705	63.5099	644.02	189.510	g	
559	-	7.05705	63.5099	743.00	379.210	g	
560	-	0.79590	7.1627	300.00	0.035	ℓ	
561	-	0.07007	0.6306	300.00	0.035	ℓ	
562	-	0.07007	0.6306	300.10	24.978	ℓ	
563	-	0.07007	0.6306	368.00	24.978	ℓ	
564	14.85245	-	29.6992	696.00	30.455	g	
565	-	0.07007	0.6306	524.82	24.978	g	
566	-	0.07007	0.6306	300.00	0.035	g+ℓ	0.01536 $H_2O(\ell)$
567	-	0.72583	6.5321	300.00	0.035	ℓ	
568	-	0.17772	1.5994	300.00	0.035	ℓ	
569	-	0.17772	1.5994	300.15	40.906	ℓ	
570	-	0.17772	1.5994	368.00	24.978	ℓ	
571	15.46855	-	30.9311	480.95	51.675	g	
572	-	0.17772	1.5994	552.59	40.906	g	
573	-	0.17772	1.5994	300.00	0.035	g+ℓ	0.04242 $H_2O(\ell)$
574	-	0.24779	2.2300	300.00	0.035	g+ℓ	0.05778 $H_2O(\ell)$
575	-	0.54811	4.9327	300.00	0.035	ℓ	
576	-	0.27343	2.4607	300.00	0.035	ℓ	
577	-	0.27343	2.4607	300.26	63.652	ℓ	
578	-	0.27343	2.4607	368.00	63.652	ℓ	
579	-	-	-	383.00	-	-	Waste heat from Section IV input; see detailed matchup table of Section V.
580	-	0.27343	2.4607	580.73	63.652	g	
581	-	0.27343	2.4607	300.00	0.035	g+ℓ	0.07053 $H_2O(\ell)$
582	-	0.52122	4.6907	300.00	0.035	g+ℓ	0.12831 $H_2O(\ell)$
583	-	0.27468	2.4720	300.00	0.035	ℓ	

TABLE D-16

SECTION V
Power Generation and Helium Heat Transfer
Material Balance
(Continued)

Stream Number	Molar Flow Ratio		Mass Flow Ratio	Temp. K	Pressure Pa x 10^5	Phase	Comments
	Helium	H_2O					
5002	-	-	-	403	-	-	Low temperature process heat lowest temperature input; see detailed matchup table of Section V.
5003	-	-	-	311.00	-	-	Waste heat recovery from Sec. II & III
5004	-	-	-	410.00	-	-	Waste heat recovery from Sec. II & III
5005	-	-	-	378.00	-	-	Waste heat from Section
5006	-	-	-	368.00	-	-	Waste heat from Section
5007	-	-	-	394.90	-	-	Waste heat from Section
5008	-	-	-	393.00	-	-	Waste heat from Section

TABLE D-16

SECTION V
Power Generation and Helium Heat Transfer
Material Balance
(Continued)

Stream Number	Molar Flow Ratio		Mass Flow Ratio	Temp. K	Pressure Pa x 10^5	Phase	Comments
	Helium	H_2O					
584	-	0.27468	2.4720	300.28	94.989	ℓ	
585	-	0.27468	2.4720	360.00	94.989	ℓ	
586	-	-	-	358.00	-	-	Waste heat from Section IV output; see detailed matchup table of Section V.
587	-	0.27468	2.4720	608.15	94.989	g	
588	-	0.27468	2.4720	300.00	0.035	g+ℓ	0.07630 H_2O(g)
589	-	0.79590	7.1627	300.00	0.035	g+ℓ	0.20461 H_2O(ℓ)
590	-	0.25096	2.2585	350.00	0.411	g	
591	-	0.25096	2.2585	300.00	0.035	g+ℓ	0.02311 H_2O(ℓ)
592	-	0.25096	2.2585	300.00	0.035	ℓ	
593	-	0.25096	2.2585	300.00	0.411	ℓ	
594	-	0.25096	2.2585	350.00	0.411	ℓ	
595	-	-	-	713	-	-	High temperature process heat lowest temperature input; see detailed matchup table of Section V.
596	-	-	-	1144	-	-	High temperature process heat highest temperature output; see detailed matchup table of Sec. V.
597	-	-	-	311.00	-	-	Waste heat recovery from Sec. II & III.
598	-	-	-	410.00	-	-	Waste heat recovery from Sec. II & III.
599	-	-	-	713	-	-	Intermediate temperature process heat highest temperature output; see detailed matchup table of Section V.
5000	-	-	-	358.00	-	-	Waste heat from Section III output; see detailed table of Section V.
5001	-	-	-	686	-	-	Low temperature process heat highest temperature output; see detailed matchup table of Sec. V.

TABLE D-17

SECTION V

Power Generation and Helium Heat Transfer
Energy Transfer, Overall Table

Basis: 0.993 g-mol H_2 Product

Heat Exchanger No.	Heat Load, kJ	Warm Side				Cool Side				Comments
		Inlet Stream No.	Inlet Stream Temp., K	Outlet Stream No.	Outlet Stream Temp., K	Inlet Stream No.	Inlet Stream Temp., K	Outlet Stream No.	Outlet Stream Temp., K	
E-500	157.896	504	1214.56	505	742.27	512	686.71	509	1159.00	
E-501	194.385	503	934.29	506	536.51	540	480.95	514	878.73	
E-502	208.595	502	1226.86	507	751.56	546	696.00	541	1171.30	
E-503	144.092	509	1159.00	510	728.00	-	713.00	-	1144.00	High temperature process heat loads; see detailed matchup table of Section V.
E-504	182.701	541	1171.30	542	755.00	559	743.00	547	1159.30	
E-505	6.844	598	410.00	597	311.00	554	368.15	555	311.00	Waste heat from Sec. II and III see detailed matchup table for Section V.
E-506	32.052	552	300.00	553	300.00	CW	-	-	-	
E-507	25.948	589	300.00	560	300.00	CW	-	-	-	
E-508	169.612	-	728.00	-	696.00	-	686.00	-	713.00	Intermediate temperature process heat loads; see heat exchangers matchup summary table.
E-509	138.281	-	696.00 to 606.79		480.95	-	403.00	-	686.00	Low temperature process head heat loads, see heat exchanger matchup summary table.
E-510	33.697	-	696.00	-	686.71 to 480.95	-	686.71 to 606.79	-	616.73 to 480.95	See heat exchanger matchup summary table.
E-511	5.962	5003	410.00	5004	311.00	-	~300.00	-	368.00	See heat exchangers matchup table for warm side and see detailed matchup table for cool side.
E-512	10.464	-	410 to 378	-	394.9 to 368.00	594		590		
E-513	9.999	591	300.00	592	300.00	CW	-	-	-	
E-514	0.994	523	311.00	527	350.00	593	300.00	594	350.00	Waste heat from Section III, see detailed matchup table for Section V.

TABLE D-17

SECTION V

Power Generation and Helium Heat Transfer
Energy Transfer, Overall Table
(Continued)

Power Equipment No.	Work Load kJ	Inlet Stream No.	Inlet Stream Pressure Pa x 10^5	Outlet Stream No.	Outlet Stream Pressure Pa x 10^5	Comments
P-500	0.385	553	0.035	554	189.510	
P-501	0.052	583	0.035	584	94.989	
P-502	0.035	576	0.035	577	63.652	
P-503	0.015	568	0.035	569	40.906	
P-504	0.004	561	0.035	562	24.978	
P-505	negligible	592	0.035	593	0.6212	
TC-500	135.503	*	*	508	49.041	*Streams 505 (44.726x10^5Pa), 506(21.245x10^5Pa) and 507(46.000x10^5Pa)
TC-501	6.830	549	156.945	550	189.510	
TC-502	16.938	558	189.510	559	379.210	
TC-503	14.044	544	46.619	545	51.675	
TC-504	22.696	531	29.328	532	51.675	
TC-505	19.423	517	30.445	518	51.675	
TC-506	21.982	522	30.445	524	51.675	
TC-507	1.356	535	29.328	537	51.675	
TE-500	183.100	501	49.041	+	+	+streams 502(46.000x10^5Pa), 503(21.245x10^5Pa) and 504(44.726x10^5Pa)
TE-501	73.660	514	51.675	515	30.445	
TE-502	11.850	542	51.679	543	46.691	
TE-503	45.964	547	379.210	548	156.945	
TE-504	20.494	551	189.510	552	0.035	
TE-505	1.094	565	24.978	566	0.035	
TE-506	2.965	572	40.906	573	0.035	
TE-507	4.788	580	63.652	581	0.035	
TE-508	4.970	587	94.989	588	0.035	
TE-509	1.672	528	30.455	529	29.328	
TE-510	1.313	590	0.621	591	0.035	

TABLE D-18

SECTION V

Power Generation and Heat Transfer
Heat Exchangers Matchup Summary Table

Basis: 0.993 g-mole H_2 Product

			Warm Side				Cool Side				
		Heat Load, kJ	Inlet Stream No.	Inlet Stream Temp., K	Outlet Stream No.	Outlet Stream Temp., K	Inlet Stream No.	Inlet Stream Temp., K	Outlet Stream No.	Outlet Stream Temp., K	Comments
E-508	A	10.698	510	728.00	511	696.00	-	-	-	-	
	B	15.638	515	728.00	536	696.00	-	-	-	-	
	C	14.044	543	728.00	544	696.00	-	-	-	-	See detailed matchup table for cool side heat exchangers.
	D	99.574	548	976.94	549	696.00	-	-	-	-	
	E	15.614	550	728.00	556	696.00	-	-	-	-	
	F	14.044	545	728.00	546	696.00	-	-	-	-	
	G	169.612	-	-	-	-	500	686	599	713	Intermediate temperature process heat demand.
E-509	A	3.106	511	696.00	512	686.71	-	-	-	-	
	B	33.193	516	696.00	517	480.95	-	-	-	-	
	C	13.770	520	696.00	521	606.97	-	-	-	-	
	D	34.395	530	686.71	531	480.95	-	-	-	-	See detailed matchup table for cool side heat exchangers.
	E	0.896	533	686.71	534	616.73	-	-	-	-	
	F	19.423	518	606.79	519	480.95	-	-	-	-	
	G	10.802	524	686.71	525	616.73	-	-	-	-	
	H	22.696	532	616.73	539	480.95	-	-	-	-	
	I	138.281	-	-	-	-	5002	403	5001	686	Low temperature power heat demand.
E-510	A	3.095	534	616.73	535	375.07	-	-	-	-	
	B	20.957	525	616.73	526	480.95	-	-	-	-	
	C	9.645	521	606.97	522	544.30	-	-	-	-	
	D	11.985	-	-	-	-	585	360.00	587	608.15	
	E	11.368	-	-	-	-	578	410.00	580	580.73	
	F	7.395	-	-	-	-	570	410.00	572	552.59	
	G	2.949	-	-	-	-	563	410.00	565	524.82	
E-511	A	0.543	562	300.10	563	410.00	-	-	-	-	
	B	1.493	569	300.15	570	410.00	-	-	-	-	See detailed matchup table for cool side exchangers.
	C	2.289	577	300.26	578	410.00	-	-	-	-	
	D	1.638	584	300.28	585	360.00	-	-	-	-	
	E	5.963	5003	410.00	5004	311.00	-	~ 300	-	360.00	Waste heat recovery for second steam cycle.

TABLE D-18

SECTION V

Power Generation and Heat Transfer
Heat Exchangers Matchup Summary Table
(Continued)

	Heat Load, kJ	Warm Side				Cool Side				Comments
		Inlet Stream No.	Inlet Stream Temp., K	Outlet Stream No.	Outlet Stream Temp., K	Inlet Stream No.	Inlet Stream Temp., K	Outlet Stream No.	Outlet Stream Temp., K	
E-512 A	3.566	5005	378.00	5006	368.00	-	-	-	-	Higher temperature waste heat recovery for auxiliary power cycle.
B	4.982	5007	394.90	5008	393.00	-	-	-	-	
C	0.831	578	383.00	586	358.00	-	-	-	-	
D	1.085	513	368.15	5000	358.00	-	-	-	-	
E	10.464	-	-	-	-	594	350.00	590	350.00	Auxiliary power cycle heat demand

TABLE D-19

Detailed Matchup of Processing Sections
High Temperature Heat Demand
from Section V

Basis: 0.993 g-mol H_2 Product

Cool Side				Warm Side		
Heat Exchanger No.	Heat Load kJ	Input Temperature, K	Output Temperature, K	Heat Exchanger No.	Input Temperature, K	Output Temperature K
E-205 a_1	2.379	499.00	502.00	E-509B$_{21232}$	542.28	526.33
E-205 a_2	2.573	499.00	502.00	E-509D$_{2232}$	542.28	526.33
E-205 a_3	2.377	499.00	502.00	E-509F$_{232}$	542.28	526.33
E-205 a_4	2.563	499.00	502.00	E-509G$_{232}$	542.28	526.33
E-205 d_{21}	5.411	473.60	488.50	E-509B$_{21252}$	525.39	488.73
E-205 d_{22}	5.853	473.60	488.50	E-509D$_{2252}$	525.39	488.73
E-205 d_{23}	5.406	473.60	488.50	E-509F$_{252}$	525.39	488.73
E-205 d_{24}	5.853	473.60	488.50	E-509H$_{252}$	525.39	488.73
E-207 c_1	4.207	502.00	530.00	E-509B$_{21221}$	573.25	542.28
E-207 c_2	4.550	502.00	530.00	E-509D$_{2222}$	573.25	542.28
E-207 c_3	4.203	502.00	530.00	E-509F$_{222}$	573.25	542.26
E-207 c_4	4.550	502.00	530.00	E-509H$_{222}$	573.25	542.28
E-209 c_1	0.877	530.00	573.00	E-509B$_{21212}$	582.90	573.25
E-209 c_2	0.949	530.00	573.00	E-509D$_{2212}$	582.90	573.25
E-209 c_3	0.876	530.00	573.00	E-509G$_{212}$	582.90	573.25
E-209 c_4	0.949	530.00	573.00	E-509H$_{212}$	582.90	573.25
E-211 c_1	5.389	573.00	613.00	E-509B$_{2111}$	625.21	582.90
E-211 c_2	2.519	573.00	613.00	E-509C$_{21}$	625.21	606.97
E-211 c_3	6.324	573.00	613.00	E-509D$_{211}$	625.21	582.90
E-211 c_4	0.107	573.00	613.00	E-509E$_{21}$	625.21	616.73
E-211 c_5	1.171	573.00	613.00	E-509G$_{21}$	625.21	616.73
E-211 c_6	3.288	573.00	613.00	E-509F$_{11}$	606.77	582.90
E-211 c_7	5.053	573.00	613.00	E-509H$_{11}$	616.73	582.90

TABLE D-19

Detailed Matchup of Processing Sections
High Temperature Heat Demand
from Section V
(Continued)

Cool Side				Warm Side		
Heat Exchanger No.	Heat Load kJ	Input Temperature, K	Output Temperature, K	Heat Exchanger No.	Input Temperature, K	Output Temperature K
E-213 B_1	3.106	613.00	636.00	E-509A	696.00	625.21
E-213 B_2	5.742	613.00	636.00	E-509B$_{11}$	662.43	625.21
E-213 B_3	10.952	613.00	636.00	E-509C$_{11}$	696.00	625.21
E-213 B_4	10.275	613.00	636.00	E-509D$_1$	686.71	625.21
E-213 B_5	0.776	613.00	636.00	E-509E$_1$	686.71	625.21
E-213 B_6	9.489	613.00	636.00	E-509G$_1$	686.71	625.21
E-214 a	7.005	1300.00	1144.00	E-503 I	1159.00	1138.05
E-214 b_2	92.071	800.00	1130.00	E-503 II	1138.05	862.49
E-219 A	78.356	686.00	686.00	E-508 DVI	917.08	696.00
E-219 B_1	10.698	686.00	686.00	E-508 A	728.00	696.00
E-219 B_2	15.638	686.00	686.00	E-508 B	728.00	696.00
E-219 B_3	14.044	686.00	686.00	E-508 C	728.00	696.00
E-219 B_4	15.614	686.00	686.00	E-508 E	728.00	696.00
E-219 B_5	14.044	686.00	686.00	E-508 F_2	728.00	696.00
E-221 B_1	45.017	713.00	800.00	E-503 III	862.49	728.00
E-221 B_2	4.139	705.00	713.00	E-508 DII	963.37	951.76
E-221 B_3	9.831	686.00	705.00	E-508 DIV	948.62	920.88
E-404	4.786	713.00	713.00	E-508 DI	976.54	963.37
E-405 A	1.112	705.00	713.00	E-508 DIII	951.76	948.62
E-405 B_1	1.349	686.00	705.00	E-508 DV	920.88	917.08
E-405 B_2	3.691	634.00	686.00	E-509 B_1 I	696.00	672.08
E-405 B_3	1.491	613.00	634.00	E-509 B_1 II	672.08	662.43
E-405 B_{41}	0.682	573.00	613.00	E-509 B_{2112}	625.21	582.90
E-405 B_{42}	0.294	573.00	613.00	E-509 C_{22}	625.21	606.97

TABLE D-19

Detailed Matchup of Processing Sections
High Temperature Heat Demand
from Section V
(Continued)

Cool Side				Warm Side		
Heat Exchanger No.	Heat Load kJ	Input Temperature, K	Output Temperature, K	Heat Exchanger No.	Input Temperature, K	Output Temperature K
E-405 B_{43}	0.739	573.00	613.00	E-509D_{2112}	625.21	582.90
E-405 B_{44}	0.119	573.00	613.00	E-509E_{2}	625.21	616.73
E-405 B_{45}	0.137	573.00	613.00	E-509D_{212}	625.21	616.73
E-405 B_{46}	0.384	573.00	613.00	E-509F_{12}	606.77	582.90
E-405 B_{47}	0.590	573.00	613.00	E-509H_{12}	616.73	582.90
E-405 B_{51}	0.629	530.00	573.00	E-509B_{21211}	582.90	573.25
E-405 B_{52}	0.680	530.00	573.00	E-509D_{2211}	582.90	573.25
E-405 B_{53}	0.628	530.00	573.00	E-509F_{211}	582.90	573.25
E-405 B_{54}	0.680	530.00	573.00	E-509H_{211}	582.90	573.25
E-405 B_{61}	0.578	502.00	530.00	E-509B_{21221}	573.25	542.28
E-405 B_{62}	0.625	502.00	530.00	E-509D_{2221}	573.25	542.28
E-405 B_{63}	0.578	502.00	530.00	E-509F_{221}	573.25	542.28
E-405 B_{64}	0.626	502.00	530.00	E-509H_{221}	573.25	542.28
E-405 B_{71}	0.085	499.00	502.00	E-509B_{21231}	542.28	526.33
E-405 B_{72}	0.092	499.00	502.00	E-509D_{2231}	542.28	526.33
E-405 B_{73}	0.085	499.00	502.00	E-509F_{231}	542.28	526.33
E-405 B_{74}	0.092	499.00	502.00	E-509H_{231}	542.28	526.33
E-405 B_{81}	0.144	488.50	499.00	E-509B_{2124}	526.33	525.39
E-405 B_{82}	0.156	488.50	499.00	E-509D_{224}	526.33	525.39
E-405 B_{83}	0.145	488.50	499.00	E-509F_{24}	526.33	525.39
E-405 B_{84}	0.156	488.50	499.00	E-509H_{24}	526.33	525.39
E-405 B_{91}	0.253	473.60	488.50	E-509B_{21251}	525.39	488.73
E-405 B_{92}	0.274	473.60	488.50	E-509D_{2251}	525.39	488.73
E-405 B_{93}	0.253	473.60	488.50	E-509F_{251}	525.39	488.73
E-405 B_{94}	0.274	473.60	488.50	E-509H_{251}	525.39	488.73
E-405 B_{101}	1.201	403.00	473.60	E-509B_{2126}	488.73	480.95
E-405 B_{102}	1.299	403.00	473.60	E-509D_{226}	488.73	480.95
E-405 B_{103}	1.201	403.00	473.60	E-509F_{26}	488.73	480.95
E-405 B_{104}	1.299	403.00	473.60	E-509H_{26}	488.73	480.95

TABLE D-20

Detailed Matchup of Processing Sections Waste Heat
in Section V

Basis: 0.993 g-mol H_2 Product

Warm Side						Cool Side				
Heat Exchanger No.	Heat Load kJ	Input Strean No.	Input Temperature K	Output Stream No.	Output Temperature K	Heat Exchanger No.	Input Stream No.	Input Temperature K	Output Stream No.	Output Temperature K
E-106	3.566	5005	378.00	5006	368.00	E-512 A	594	350.00	590	350.00
E-220 b_1	2.000	5004(A)	410.00	5003(A)	368.00	E-511-I	-	300.00	-	360.00
E-220 b_2	0.974	598(A)	410.00	597(A)	368.00	E-505-I	554	300.00	555.00	391.00
E-222 b_1	1.909	598(B)	405.00	597(B)	311.00	E-505-II	554	300.00	555.00	391.00
E-222 b_2	0.162	-	311.00	-	300.00	CW	-		-	-
E-314 A	3.365	5004(B)	368.15	5003(B)	311.00	E-511-II	-	300.00	-	360.00
E-314 B	0.738	-	311.00	-	300.00	CW	-	-	-	-
E-315 B_1	0.598	5004(C)	368.15	5003(C)	311.00	E-511-III	-	300.00	-	360.00
E-315 B_2	2.677	598(C)	368.15	597(C)	311.00	E-505-III	554	300.00	555.00	391.00
E-315 B_3	0.630	-	311.00	-	300.00	CW	-	-		-
E-316 B_1	0.406	598(D)	368.15	597(D)	311.00	E-505-IV	554	300.00	555.00	391.00
E-316 B_2^1	0.503	513(A)	368.15	5000(A)	358.00	E-512D-I	594	350.00	590.00	350.00
E-316 B_3^2	0.944	-	368.15	-	311.00	E-514	593	300.00	594	350.00
E-316 B_4	1.422	-	368.15	-	311.00	CW	-	-	-	-
E-316 B_5	0.630	-	311.00	-	300.00	CW	-	-	-	-
E-317 B_1^5	0.582	513(B)	368.15	5000(B)	358.00	E-512D-II	594	350.00	590.00	350.00
E-317 B_2^1	3.324	-	358.00	-	303.00	CW	-	-	-	-
E-406 C_1^2	0.066	598(E)	394.90	597(E)	393.00	E-505-V	554	300.00	555	391.00
E-406 C_2	0.498	5007	394.90	5008	393.00	E-512 B	594	350.00	590	350.00
E-407 C	0.812	598(F)	403.00	597 (F)	393.00	E-505-VI	554	300.00	555	391.00
E-411 A	0.831	597	383.00	586	358.00	E-512 C	594	350.00	590	350.00
E-411 B	1.827	-	358.00	-	303.00	CW	-	-	-	-

APPENDIX E

COST SENSITIVITY OF THERMOCHEMICAL HYDROGEN PRODUCTION

The cost of hydrogen from a thermochemical hydrogen plant is a strong function of the capital cost of the thermochemical plant and the capital cost of the heat source. The total capital cost per gigawatt (GW) of hydrogen, C, is given by

$$C = A + B/\varepsilon \qquad \text{(E-1)}$$

where A is the capital cost of the thermochemical plant per GW of hydrogen, B is the capital cost of the heat source per GW of thermal energy produced, and ε is the thermal efficiency of the thermochemical plant.

The capital cost of the thermochemical plant will be a strong function of its thermal efficiency. As the efficiency, ε, approaches the maximum theoretical efficiency, η, the capital cost of the thermochemical plant per GW of hydrogen must approach infinity. Some reasons for this are given in Table E-1. Some would argue that the capital cost of the thermochemical plant must also approach infinity as the efficiency approaches theoretical because of the large amount of heat that is transported into and out of the thermochemical plant. A mathematical form which, in the asymptotic limits, properly relates the capital cost of the thermochemical plant to its thermal efficiency is:

$$A = \frac{K}{\varepsilon^m (1-\varepsilon/\eta)^n} \qquad \text{(E-2)}$$

Thus, the ratio of the total plant cost per GW of hydrogen to the heat source cost per GW of thermal energy may be given by:

$$\frac{C}{B} = \frac{K/B}{\varepsilon^m (1-\varepsilon/\eta)^n} + \frac{1}{\varepsilon} \qquad \text{(E-3)}$$

TABLE E-1

EFFECT OF APPROACHING MAXIMUM THEORETICAL EFFICIENCY

Variable	Result
Heat exchanger T approaches zero	Heat exchanger area approaches infinity.
Distillation separations approach 100%.	Distillation column height approaches infinity.
Distillation separations approach thermodynamic efficiency.	Distillation column height approaches infinity, and integral heat exchangers are required with areas approaching infinity.
Chemical reactions approach equilibria.	Chemical reactor size approaches infinity.

This equation form is proposed as a representation of how the relative cost of an integrated water-splitting plant might vary as the primary design of a particular water-splitting process is refined to achieve even higher efficiency. The parameter K/B is a measure of the inherent capital cost of the water-splitting process relative to the heat source cost.

Figure E-1 shows plots of Eq. (E-3) for various values of the parameters n and m using a theoretical efficiency, η, of 0.8, which is typical of the GA sulfur-iodine water-splitting process. In each case, the parameter K/B has been chosen so that the graph describes the point representing the fusion-powered water-splitting plant, for which a complete cost estimate is available (Ref. E-1). Also shown are the locus of the minima as K/B is varied.

Several qualitative statements may be made concerning Fig. E-1. First, within the range of parameters investigated, the minimum in capital cost is relatively broad, so there may be little gain from extensive optimization. Second, efficiencies approaching the theoretical efficiency can be appropriate only when the thermochemical plant cost is negligible compared with that of the heat source. Finally, if the parameter n is greater than m (which appears reasonable since there are many factors leading to an infinite plant cost as the efficiency approaches theoretical), the optimum efficiency for the GA water-splitting cycle may be less than 47%.

REFERENCE

E-1. Werner, R. W., O. H. Krikorian, and S. L. Ribe, "Conceptual Design Study FY 1981, Synfuels from Fusion Using the Tandem Mirror Reactor and a Thermochemical Cycle to Produce Hydrogen," Lawrence Livermore National Laboratory Report UCID-19311, February 9, 1982.

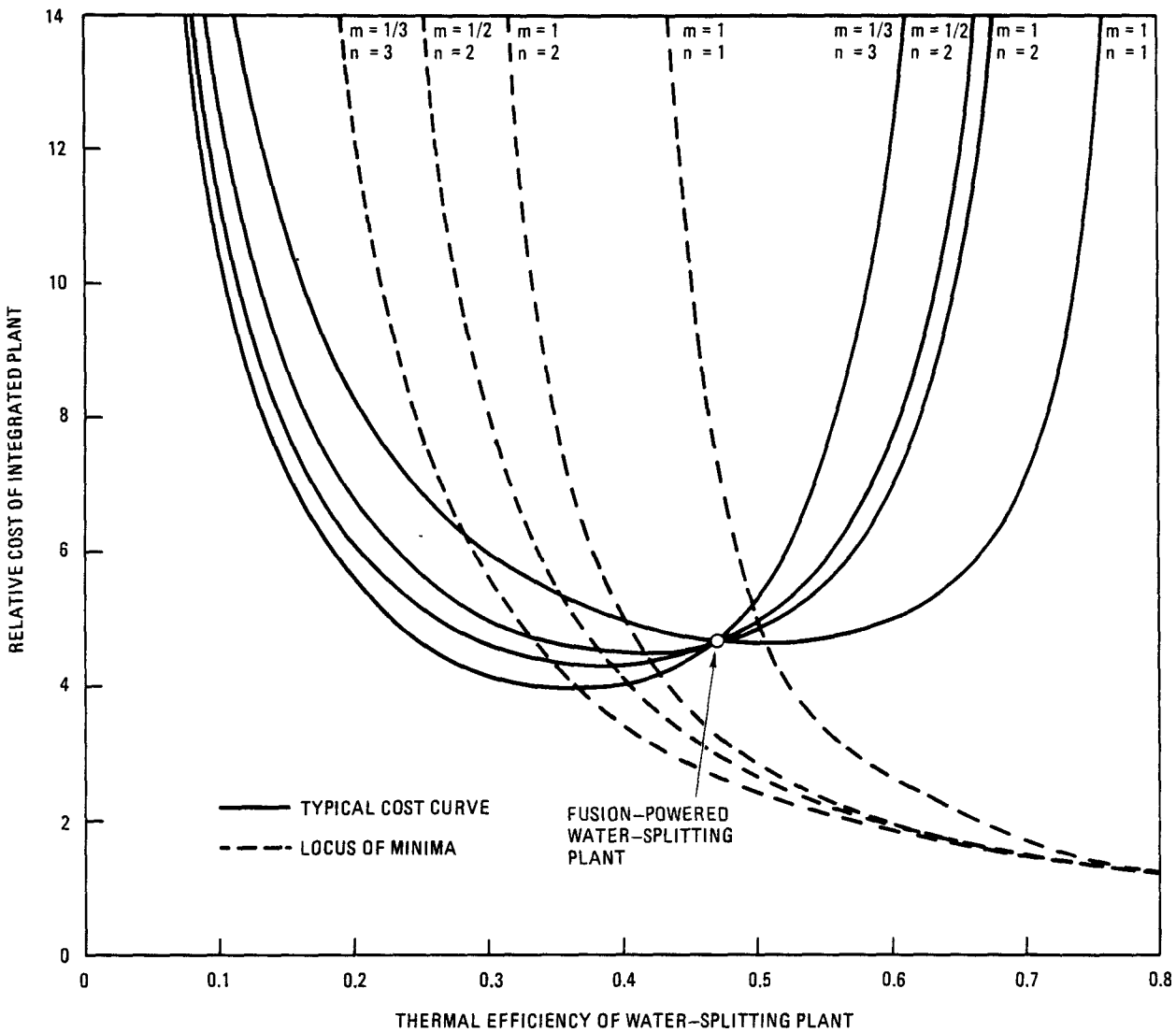

Fig. E-1. Thermal efficiency of water-splitting plant